CONTROL TECHNIQUES APPLIED TO INTEGRATED SHIP MOTION CONTROL

by

MOHAMMED TARIQ SHARIF

A thesis submitted to the University of Plymouth
in partial fulfilment for the degree of

DOCTOR OF PHILOSOPHY

Control Engineering Section
Royal Naval Engineering College

May 1995

ABSTRACT

Control Techniques Applied to Integrated Ship Motion Control

by

Mohammed Tariq Sharif

Fins stabilisers are devices which are fitted to the hull of a ship and utilised to ameliorate its rolling motions. They apply a regulated moment about the ship's axis of roll in order to oppose the sea induced disturbances. Recognising their unsurpassed performance, the Royal Navy, since the 1950's, equips all its vessels with fin stabilisers. It can be shown that the rudders, in vessels of appropriate size, also have the potential to be harnessed as roll stabilisers Rudder Roll Stabilisation (RRS) without degrading the ship's course-keeping. Thus creating a more stable platform for the human operators and equipment.

The reported success of RRS imparted an impetus to the Royal Navy to initiate this study. The objectives are to ascertain whether RRS is possible without rudder modifications and to establish whether enhanced levels of stabilisation would accrue if the fins and RRS were operated in congress. The advantages in this novel approach being: avoidance of redesign and refit of rudders, three modes of operation (fins alone, RRS alone and combined RRS and fins), reduced fin activity and by implication self-generated noise, and amenability to be retrofitted by simple alteration of any existing ship's autopilot software.

The study initially examined the mathematical models of the ship dynamics, defining deficiencies and evaluating sources of uncertainty. It was postulated that the dual purpose of the rudder can be separated into non-interacting frequency channels for controller design purposes. An integrated design methodology is adopted to the roll stabilisation problem.

Investigating the capabilities of the rudder servomechanism, a new scheme, the Anti-Saturation Algorithm (ASA) was proposed which can eliminate slew rate saturation. Application of the ASA is generic to any servomechanism.

The effects of lateral accelerations of the ship on human operators was examined. This resulted in an unique contribution to the Lateral Force Estimator problem in terms of generating time domain models and defining the limitations of the applicability of a control design strategy.

Linear Quadratic Guassian and two types of classical controllers were constructed for the RRS and fins. A novel application of linear robust control theory to the ship roll stabilisation problem resulted in H_∞ controllers whose performance was superior to the other design methods. This required the development of weight functions and the identification and quantification of possible sources of uncertainty. The structured singular value utilised this information to give comparable measures of robustness.

The sea trials conducted represent the first experience of the integrated ship roll stabilisation approach. Experimental results are detailed. These afforded an invaluable opportunity to validate the software employed to predict ship motion. The data generated from the sea trials concurs with the simulations data in predicting that enhanced levels of roll stabilisation are possible without any modification to the rudder system. They also confirm that when the RRS is acting in congress with the fin stabilisers the activity of both actuators diminishes.

CONTENTS

LIST of FIGURES

CHAPTER 7

LIST of TABLES

NOMENCLATURE

A_F	Fin area
C_L	Planform lift coefficient
D	Fin drag force
e_m	Maximum slew error
g	gravitational acceleration
$\overline{GM}$	Metacentric height
$\overline{GZ}$	Restoring lever arm
H_W	Significant wave height
I_{xx}	Moment of inertia about x-axis
I_{yy}	Moment of inertia about y-axis
I_{zz}	Moment of inertia about z-axis
k	Wave number
k_A	Acceleration gain
k_R	Rate gain
K	Roll moment
$K_{w\phi}$	Sea induce roll moment
K_α	Fin induced roll moment
K_δ	Rudder induced roll moment
$\overline{KG}$	Keel to CoG
L	Fin lift force
m	Mass of ship
M	Pitch moment
N	Yaw moment
Oxyz	Tracking axis
$O_B x_B y_B z_B$	Body-fixed axis
$O_G x_G y_G z_G$	Location of centre of gravity
$O_o x_o y_o z_o$	Earth-fixed axis
p	Roll rate
P	Location on ship
q	Pitch rate
Q	Control effort weighting
r	Yaw rate
r_F	Fin lever arm
R	Output weight
T	Draft
T_W	Significant wave period
U	Ship speed
V	Sway velocity
W	Heave velocity
x	Surge
X	Surge force
y	Sway
y_m	Maximum slew rate
Y	Sway force
z	Heave
Z	Heave force

α	Fin deflection angle
β	Fin dihedral angle
χ	Ship and wave encounter angle
δ	Rudder deflection angle
δI_{xx}	Added mass roll inertia
ϕ	Roll angle
ϕ_v	Sway velocity induced roll angle
θ	Pitch angle
ρ	Density of sea water
τ	Time constant
α	Fin angle
ω_e	Wave encounter frequency
ω_n	Natural roll frequency
ω_o	Wave frequency
ψ	Yaw angle
ξ	Wave slope
ζ_{ss}	Ship damping ratio

GLOSSARY

ADC	Analogue to Digital Converter
ASU	Auto Steering Unit
CoG	Centre of Gravity
DAC	Digital to Analogue Converter
GTR	Gas Turbine Room
HPU	Hydraulic Power Units
LFE	Lateral Force Estimator
LQG	Linear Quadratic Guassian
MIF	Motion Induced Fatigue
MII	Motion Induced Interruptions
MIMO	Multi-Input Multi-Output
MSI	Motion Sickness Incidence
PID	Proportional Integral Derivative
rhp	Right Hand Plane
RMS	Root Mean Square
RRS	Rudder Roll Stabilisation
SISO	Single-Input Single-Output
SCC	Ship Control Centre

ACKNOWLEDGEMENTS

The author wishes to express sincerest gratitude to his supervisor, Dr. G. N. Roberts, who initially gave the opportunity to embark upon a PhD programme and without whose continual encouragement and stimulation it, simply, would not have been completed. Similar, thanks are extended to Dr. R. Sutton for many fruitful suggestions and constructive criticisms.

The author is indebted to the Dean of the College, Commander P. C. Gregory, Royal Navy, Head of the Control Engineering Department, and the Departmental staff, in general, who generously gave constant assistance and made the environment at the Royal Naval Engineering College an extremely pleasant one in which to work.

The continual support of the MoD (ES251) is gratefully acknowledged. The author extends thanks to the Captain, Officers and ship's company of the Royal Navy trials vessel, for their assistance, generous co-operation, hospitality and flexibility in accommodating the requirements during the trials.

Due acknowledgement is made to the Defence Research Agency at Haslar and Brown Brothers of Edinburgh who, obligingly provided access to sophisticated simulation software and comprehensively furnished technical information respectively. Many enlightening discussions were conducted with Paul Crossland (DRA Haslar), from which the author gained insight into ship hydrodynamics.

Finally, the author wishes to express unaffected and profound gratitude to his wife, Robina, for her patience and support, and to his parents for their inspiration and countless sacrifices.

AUTHOR'S DECLARATION

At no time during the registration for the degree of Doctor of Philosophy has the author been registered for any other University award.

The programme of study was financed by the Ministry of Defence (Royal Navy). Sea trials were sponsored by Naval Procurement Department (ES251), Foxhill, Bath. To whom the results and recommendations of the complete investigation were submitted. Technical advice regarding the ship's relevant mechanical systems was furnished by Brown Brothers of Edinburgh. The Defence Research Agency at Haslar provided access to advanced ship motion prediction software. The course of study also included attending a one week advanced control engineering course.

Results from the study were subject to the critical scrutiny of peers and established practitioners when participating in relevant scientific conferences and symposia.

The following publications in the public domain resulted as a direct consequence of the study, and are included in Appendix I:

Journal Papers:

M.T. Sharif, G.N. Roberts, R. Sutton
"Sea Trials Experimental Results of Fin/Rudder Roll Stabilisation", *Control Engineering Practice (IFAC), May 1995,* 703-708

M.T. Sharif, G.N. Roberts, R. Sutton
"Automatic Saturation Prevention of Servomechanisms", *Trans. Inst. Measurement and Control (submitted for publication)*

Conference Papers

M.T. Sharif, G.N. Roberts, R. Sutton
"Lateral Force Stabilisation: A Comparison of Controller Designs", *Proc. 10th Ship Control Systems Symposium, Ottawa, October 1993, Vol. 5, 149-169*

M.T. Sharif, G.N. Roberts, R. Sutton
"Integrated Robust Ship Roll Stabilisation", *Proc. IEE Control '94, Coventry, March 1994, 1566-1571*

M.T. Sharif, G.N. Roberts, R. Sutton
"Robust Fin/Rudder Roll Stabilisation", *Proc. 3rd IEEE Conference on Control Applications, Glasgow, Aug. 1994, 1107-1112*

M.T. Sharif, G.N. Roberts, R. Sutton
"Full-Scale Experimental Results of Fin/Rudder Roll Stabilisation", *Proc. Manoeuvring and Control of Marine Craft (IFAC), Southampton, Sept. 1994, 127-135*

M.T. Sharif, G.N. Roberts, R. Sutton
"Final Experimental Results of Full-Scale Fin/Rudder Roll Stabilisation Sea Trials", *Proc. Control Applications in Marine Systems (IFAC), Trondheim, May 1995, 247-254*

The following restricted reports was submitted to Naval Procurement (ES251) detailing the sea trials results and recommending a strategy for the Future Frigate design:

M.T. Sharif, G.N. Roberts
"Integrated Ship Roll Stabilisation Study: Work to Date and Proposed", *Interim Report to ES251, Jan. 1994, Restricted*

M.T. Sharif, G.N. Roberts
"Final Results of Integrated Fin/Rudder Roll Stabilisation Trials", *Report No. RR94021 to ES251, Dec. 1994, Restricted*

Signed M.T. Sharif

Date 26th May 1995.

CHAPTER 1
INTRODUCTION

1.1 BACKGROUND

Since the advent of shipping a major source of concern has always been the inclement forces of nature. These induce seemingly unpredictable perturbations in the vessel which are not conducive to effective ship operation. The pernicious aspect of the environment can be appreciated even by those who seldom, or never, travel by sea. In particular, the rolling motion of a ship contributes significantly to degrade a ship's operability.

Consider the particular role of warships in such an environment. The launching systems of modern weapons, although possess independent motion dampers, their accuracy would be facilitated if the ship's motions can be further reduced. It will also afford the ship's sensors to function with increased reliability. Most frigate size warships are equipped with helicopters. In recovery mode when it lands the ship which may have been induced by the sea to accelerate upwards will cause possible damage to the fuselage. Therefore, if the ship's motions are excessive it will curtail helicopter excursions. Hence, amelioration of a warship's rolling motion would not only increase its potency, but also allow it to operate in a wider environmental envelope.

For ships in general, violent motions and excessive roll may pose a risk to the secure fastening of cargo, for example, if the load of a container ship moves it will imperil the flotation stability of the vessel. The accelerations and inertia created by the ship's motion may undermine the effective operation of machinery. An alarming consideration is from marine history's abundant examples of ships' hulls cracking under the intolerable stresses and strains provoked by sea induced motions. Perhaps the most serious repercussions are on the human operators in terms of their ability to perform routine manual tasks in the presence of these ship motions, for example, radar and sonar monitoring, weapons loading and firing and engine maintenance work. Indeed, in severe conditions, personnel may be reduced to simply 'hanging-on' to a deck-secured object in order to maintain balance rendering the accomplishment of even the simplest task impossible. Constantly adopting a pre-emptive stance to counter incessant ship motions leads to fatigue, is devoid of comfort, generally unsafe and precipitates nausea and sea sickness. The human aspect will be further elaborated in context of the lateral force estimator (LFE), in which this work is a unique contribution is made with a time domain model and outlining a controller synthesis methodology.

All these factors, amongst others, conspire in conglomeration to produce an inherent degradation in ship operability. Therefore any device to stabilise the ship would be a most desirable feature.

Researchers have dissipated considerable effort, over innumerable years, to invent effective devices which will reduce the rolling of mono-hull ships. Some devices ostensibly possess these desirable qualities but on closer examination were proved to be spurious. Other, more fanciful, contrivances were impractical and destined to failure. To date, fin stabilisers have been the most propitious device which delivers an unparalleled degree of roll stabilisation.

Their relative position on a typical ship is illustrated in Figure 1.1. Recognising their advantages the Royal Navy, as early as the 1950's, specified the installation of fins stabilisers to every class of ship which can accommodate them. In retrospect, with the introduction of helicopter bearing ships and general advances in radar and weapons technology, the decision has proven to be a judicious one.

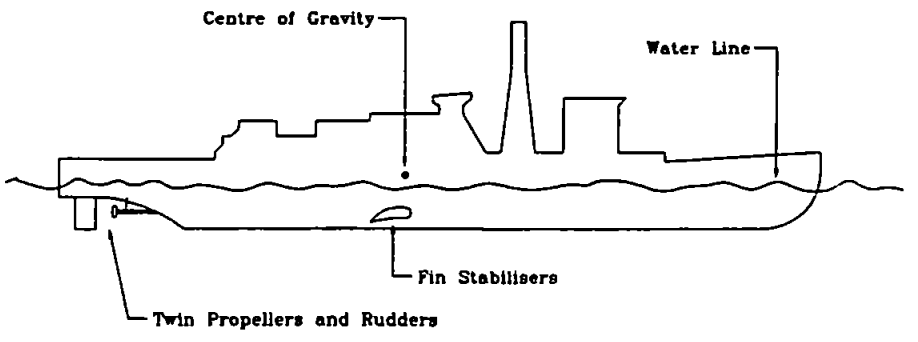

Figure 1.1 : Relative location of appendages of ship under investigation

The principles of operation of fin stabilisers are identical to and inspired by the wings of an aircraft. A forward velocity induces lift forces on the aerofoil surfaces. These qualities are not violated in a different medium such as water. Indeed, on account of the viscosity of the water, the magnitude of the forces generated is considerably greater at comparable speeds. By regulation of the angle of incidence of the fin to the water flow a regulated moment can be imparted to a ship's axis of roll in order to oppose the sea induced roll disturbances. Hence, the net roll motion of the ship will diminish. In essence the control problem from their inception has been to formulate a control strategy which minimises the rolling.

Normally, the rudders of a ship are utilised for course-keeping. When the rudder is first 'put-over' large ships will, peculiarly, roll inwards before adopting the expected outward steady-state heel angle as it enters the turn. This phenomenon may be explained by consideration of the attendant hydrodynamic forces. Since, no appreciable yaw motion

occurs during the inward heel phase, the rudders may also be harnessed (Rudder Roll Stabilisation, RRS) in congress with the fins to achieve enhanced roll stabilisation without any detriment to the ship's course.

The navies of the Netherlands, Sweden and USA are actively pursuing RRS which has resulted in its successful implementation on many classes of warship. This approach has rendered the fin stabilisers obsolete being in complete accordance with their objectives. Similar levels of roll reduction to the fins stabilisers are expected with the RRS system. The results of these studies are generally not available in literature owing to the classified nature of the work.

An often cited advantage of removing the fins is that a major source of noise which degrades sonar operations and emanates a large noise signature is eliminated. Since, it is imperative that the ship should be able to steer a course, noise in the vicinity of the stern cannot be avoided. Therefore, any additional noise generated by an RRS system will be irrelevant. However, implementation of dedicated RRS to the exclusion of fin stabilisers has incurred the significant expense of redesign and construction of the rudder assembly and its peripherals in order to accommodate the added stresses and the requirements to increase the rudder slew rate typically by trebling it.

Although, preliminary studies conducted at the behest of the Royal Navy (Lloyd, 1975, and Cowley and Lambert, 1975) revealed that RRS systems have a propensity to become unstable in following seas, the success of foreign navies has enticed a re-examination of this approach. Therefore, the Royal Navy initiated this study with the object of quantifying the roll stabilisation capabilities of the rudders currently installed on frigate size warships. Another aim was to establish that enhanced levels of roll stabilisation can be achieved with

both the fins and rudders acting in congress. Furthermore, it is imperative that these objectives are adhered to without the requirement for upgrading any aspect of the rudder system.

There are several advantages to this integrated and pragmatic approach. Primarily, greater levels of roll stabilisation are envisaged when the fins and RRS are functioning simultaneously. The activity of both the rudders and the fins will diminish as compared with when operating individually. Therefore, expensive redesign and refit costs can be avoided since it will be neither necessary to increase the slew rate of the rudder servomechanism, nor will RRS impose additional stresses on the rudder bearings. However, since, the current rudders of a typical frigate warship move approximately three times slower than the fins, slew rate saturation remains a source of concern. This aspect is discussed and a novel algorithm proposed which is shown to be an affective contingency against such a scenario.

Another advantage resulting from pursuing an integrated approach is that, since a portion of the stabilisation is being performed by the rudders, the resultant decrease in fin activity accrues in reduced noise levels. Since, the integrated method affords three modes of operation viz. fins alone, RRS alone and fins and RRS in congress, there is an element of redundancy inherent in the system. For example should a malfunction in the fins occur the ship will not be completely devoid of roll stabilisation capabilities, thus permitting many of the operations which otherwise would have been abandoned. Finally, it is a simple matter to retrofit an RRS system on existing ships by modification to the autopilot software algorithms.

To these ends the Royal Navy allocated two sea trials periods in a frigate size warship's schedule to this investigation. On account of the ever increasing demands and

responsibilities imposed on the Royal Navy and coupled with its diminishing resources it was not possible to countenance more than these trial sessions. Furthermore, the specific dates could only be confirmed a few weeks in advance, depending on the impending operational duties of the selected vessel.

Considering the control engineering aspect of designing RRS and fin stabiliser controllers. The controllers which are most commonly implemented to activate a ship's fins and rudder motions are derived from linear classical and LQG control techniques. These are designed for a specific set of expedient environmental and ship conditions. However, the operational envelope of any ship is extremely broad, for example the waves of the sea are constantly changing in magnitude and frequency in an apparently irrational manner, there are often strong currents and winds associated with particular regions, the loading condition of a ship may change which has profound ramifications on its behaviour and the ship's speed and orientation with the prevalent sea conditions is rarely constant.

The foundation of controller syntheses relies on accurate mathematical models of the plant dynamics being studied. By the virtue of the requirements for linear representations, these models cannot accommodate the highly complex and non-linear behaviour ship dynamics and at best remain a crude approximation to reality. Therefore, the performance of classical and LQG type controllers is optimised when the ship's physical environment reflects the appropriate conditions for which they were envisaged. Fluctuations in any environmental factor results in severe degradation in the controllers' roll stabilisation abilities. The thesis initially proceeds to construct these mathematical models of ship dynamics and to subsequently identify and quantify these sources of uncertainty. The models are then utilised for linear classical and LQG controller design.

Recently linear robust control theory has been promulgated in literature which generates controllers that can accommodate these uncertainties at the outset of the design stage and adhere to specified performance levels. A novel application of this advanced technique to the fin and RRS problem reveals that the levels of roll stabilisation do not diminish in the presence of unstructured uncertainty and explicit perturbations which may impinge on the system. Unlike the LQG and classical controller the robust controllers also maintain internal stability when these uncertainties impinge on the closed-loop system. These assertions are subject to the inclemency of reality in full-scale sea trials, the results of which will be presented. The sea trials also afford an invaluable opportunity to validate the mathematical models and the simulations software.

1.2 LITERATURE REVIEW

A plethora of devices have been conceived to stabilise the rolling motions of ships with diverging degrees of success. An oscillating weight system was proposed by the Thornycroft Company of Southampton in 1891 and tested on board a ship named Cecile. The concept was later adopted by Hort (Germany) in 1929. Although at a cursory examination the principle appears to be suitable, its implementation has severe limitations on account of the requirement to move immense masses in a restricted environment. It is now of historical interest only.

A more successful proposition was the anti-rolling tank and U-tube systems which are still in active service on many ships. They can be either passive types, in which case the 'free-surface effect' (Saunders, 1965) is utilised, by altering the volume of water in the tanks, located on the port and starboard sides of the vessel in order to counter the sea induced roll disturbance.

Examples of the former were manufactured by Frahm (Germany, 1912), whilst the latter were constructed by Hort in 1929. Both systems have some inherent disadvantages: installation, maintenance and power requirement costs are significant, and they occupy valuable space in the ship's hull. Perhaps the simplest device has been the bilge keel, invariably fitted to every class of ship. These constitute two appendages incorporated along the length of the hull surface. They have a profile similar to an aircraft wing incident with the direction of air flow. The ship's forward speed engenders specific forces on the bilge keel resulting in an increase in the total hydrodynamic damping. Thus the sea is compelled to overcome the effect of the bilge keels in order to perturb the ship. Hence, the roll on the ship is reduced when compared with the case of a ship devoid of bilge keels. The performance of these devices is dependet on the ship speed.

The most propitious device invented to stabilise the roll of a ship has been active fin stabilisers. These were first introduced by Motora (Japan, 1925). Initially they were operated manually; until Denny-Brown in 1936 introduced a hydraulic control scheme.

Amongst the first to investigate the possibility of fin stabilisers being exploited commercially was the Chief of Experimental Tank, Allen (1945), at Denny-Brown. He gives a comprehensive insight to the mechanical construction of the devices and elaborates on the hydrodynamic characteristics of fins in general. The paper summarises the development of the previous ten years and contributes by examining the effectiveness of incorporating flaps into the fin structure. From sea trials data, which were not as optimistic as was expected, it was conjectured that cavitation may be responsible for the deterioration in performance. These effects were systematically evaluated by Lloyd (1974) and Cox and Lloyd (1977) with the tremendous advances in hydrodynamics theory in general. They also gave empirical methods for degradation calculations due to cavitation, boundary layer and trailing fin

effects. By modern standards the controller proposed by Allen (1945) was primitive, utilising simple roll rate feedback from a velocity gyro.

In the same era Bode (1950) was enlightening the field of control engineering in the context of general feedback and frequency domain theory. Application of these techniques produced a series of publications by Bell (1957a and 1957b) and Chadwick (1955). Their papers contain a formidable amount of detail regarding selection of the controller coefficients and operation of the fin stabilisation system. The controllers derived were essentially variations of proportional-integral-derivative (PID) controllers from sufficiently promulgated theory. They also conducted extensive sea trials on board the Hunt class destroyers and scale-model trials. The results of which were favourable. Approaching the roll stabilisation problem from a novel perspective Bell (1965) proposed to reformulate it by analogy of the ship acting as a weight at the end of a pendulum. However, this endeavour proved futile to be amenable for fin stabilisers. It did yield intuition for the subsequent ramifications of lateral force acceleration in context of human performance as elaborated in Chapter 4.

A significant advance was secured when Conolloy (1969) simplified the ship roll to a dominant second order transfer function. Vindicating this hypothesis from sea trials data which correlated adequately with the linear predictions. This lead him to examine the controller from a new perspective and the conduction of further sea trials with various permutations of roll rate feedback. A method was illustrated to calculate the approximate roll reduction envisaged for the given geometry of a pair of fins by consideration of relative phases. Finally, in order to accurately describe the roll motions, an analysis was attempted to predict the non-linear nature of the damping ratio of the mathematical model. This facet of the second order ship system is investigated comprehensively in section 2.2.

Lloyd (1972, 1974) and Schmitke (1978) contributed to development by refining the fin to ship roll model by hydrodynamic and experimental considerations. Lloyd (1974) outlines a design procedure for ship designers in the construction and hydrodynamic ramifications of fin stabilisers. These researchers postulated that the unexpected degradation in fin performance often reported, can be attributed to boundary layer, fin/hull interactions and yaw and sway induced roll motions.

The performance of fin stabilisers in active service was assessed by Baitis and Cox (1972), Gunsteren (1974), Davies and Chase (1987) and Clarke (1981). These were essentially evaluations of commercially available fin stabilisers conducted by their respective research employees. In terms of control engineering, the predominant control techniques utilised were classical (Tinn, 1970). With the development of LQG theory a design study of roll stabilisation was performed by Whyte (1977) and Katebi and Wong (1987). The experiences of roll stabilisers for small ships is given in Martin (1994). A comprehensive study of the cost benefits analysis from a financial perspective in selection of a stabiliser system for a ship is presented in Sellars and Martin (1992).

The advances in the application of control technology to fin stabilisers stagnated since the early 1970's, until a determined effort was initiated to exploit the rudders as stabilisers. This thesis being a study of the application of the latest control techniques in fin and RRS in an integrated approach. The state of current research in this field is now outlined.

Taggart (1970) at the behest of the owners of the container ship SS American Resolute, acting on the crews' complaints of excessive roll motions induced by the rudder, was engaged to determine it causes. He conducted the investigation during her voyage across the Atlantic. It was discovered that at high speed and in a following sea it was possible to

achieve synchronism between the wave encounter and ship roll resonance frequency. Under autopilot control, the rudder exacerbated the roll when attempting to correct yaw. Taggart reasoned that the forces which generate such large motions could be harnessed to reduce roll motions. This is the first instance of RRS.

The concept was demonstrated as a reality by practical and theoretical studies by Cowley and Lambert (1972, 1975) and Cowley (1974) in sea trials on board the container ship Manchester Concord and scale-model tests. Broome (1979) describes the experiences of fin and RRS roll stabilisation on the same vessel. This ship has low damping and a long roll period, hence, it was immanently suited to RRS. Roll reductions of 20% were reported at sea state 4 with no increase in rudder activity or yaw error.

The Ministry of Defence (Mod, Navy) in the U.K. initiated theoretical studies which resulted in the publication by Carley and Duberley (1972) and Carley (1975) who considered the problem form a yaw/roll interference perspective. Lloyd (1975) utilised these results in combination with hydrodynamic realities in attempting to predict the possible repercussions of RRS. Transfer function models were verified by their derivation of the motions induced by the rudder on several classes of Royal Navy ships and stabilisation trials performed by Marshfield (1981a). On account of these studies revealing that instability may occur at low encounter frequencies and that there may be yaw interference, the MoD decided not to implement RRS on any Royal Navy vessel.

Studies in France, the Netherlands, America and Sweden have, in general, arrived at positive conclusions regarding the viability of RRS as a cost effective alternative to fin stabilisers and which achieves moderate levels of roll stabilisation. The study in the Netherlands has the support of Van Rietchoten and Houwens and the Royal Netherlands

Navy (RNN) with a view as to whether to specify RRS or fin stabilisers in their new M-class frigates. The protagonists in this work have been Amerongen (1984), Amerongen and Haarman (1975), Amerongen and Lemke (1982), Amerongen *et al* (1983), Amerongen *et al* (1984 and 1987) and his co-researcher Klugt (1987, 1990a and 1990b). Their earlier work consisted of utilising adaptive Linear Quadratic Gaussian (LQG) controller for the RRS.

The results confirm that the dual purpose of the rudder, viz. steering and roll stabilisation, can be regarded as independent control problems on account of the frequency separation between the motions. In order to ensure that the motions do not interact they postulate the inclusion of appropriate filters. Full-scale sea trials from Amerongen *et al* (1984 and 1987) indicate that roll reduction of between 4% and 69% with RRS, as compared with 30% to 80% with fin stabilisers, can be achieved. On the basis of these trials it is envisaged that RRS would provide comparable roll stabilisation if the rudder slew rate was increased from $7^{0}s^{-1}$ to $15^{0}s^{-1}$. This is perhaps not justified since the available moment capacity of the rudder for the class of ship considered is 75% of the fin stabilisers and, in addition, the slew rate is much slower than the fins. Despite this, from the evidence presented the RNN has specified RRS on its M-class frigates. The results from this installation have not be divulged (Klugt, 1987, 1990a and 1990b). The RNN's decision was also influenced by the advantage that rendering the fins obsolete with RRS would eliminate noise generated by the fins which is an impediment to effective sonar operation. Since, it is imperative that the ship have rudders for steering then noise considerations in this vicinity are irrelevant. However, the redundancy of fins has probably not accrued any fiscal advantage. RRS has necessitated the stern of the ship and rudder assembly to be modified in order to contend with the extra stresses expected. Also it has required the installation of enhanced hydraulic machinery.

A parallel development of RRS was in progress in Sweden. Following the identification of the yaw dynamics of a roll-on roll-off (RO-RO) ferry by maximum likelihood methods (Astrom and Kallstrom, 1976), Kallstrom (1981) presented the results of LQG controller design study of yaw and RRS in conjunction with the fins. In contrast with the assertions of the Netherlands study he concludes that the controller yields better results if the ship is treated as a mulitvariable system.

An unfortunate combination of changes in metacentric height due to loading conditions and strong winds resulted in disaster for the RO-RO ferry, MS Zenobia, in 1980 when it capsized outside the port of Larnaca. This lead to an investigation of the causes. Kallstrom and Ottosson (1982) conducted the study of the applicability of RRS to this type of vessel with respect to metacentric heights and wind/wave interactions with the ship. The inference being that RO-RO ferries are readily susceptible to instability. The Swedish company SSPA Maritime Consulting, of which Kallstrom is the technical director, initiated a project to develop RRS controllers which culminated in a commercial product named Roll-Nix. The controller design strategy adopted was based on LQG methods. The technical results of its efficacy were published in Kallstrom and Schultz (1990) which gave general results of achieving roll stabilisation of 40% to 60% for many classes of ship. These results are achieved with the rudder slew rate restricted to 6^0s^{-1}.

The US Navy traditionally does not have fin or RRS stabilisation capacity implemented on any of its vessels. However, the experience of the RNN enticed them to conduct a feasibility study for the Hamilton class vessels (Baitis, 1980). The scope of this study was also to assess the implications of ship motions on human operators which is discussed in Chapter 4. The results are presented in these terms in further research by Baitis *et al* (1983) and Baitis and Schmidt (1989).

There have been very few researchers outside these environments who have examined this aspect of marine control: Zhou *et al* (1990), Burns (1991) and Wibrans and Klugt (1991) being the exception.

The Royal Navy has again expressed a pragmatic interest in RRS. However, the objective is to retain the fin stabilisers and implement RRS without modifications on the rudder assembly and peripheral systems. This approach has several advantages as compared with dedicated RRS systems. The expenses incurred in redesigning and refit of the rudders can be avoided. This aspect will be examined in Chapter 3. It is envisaged that enhanced levels of roll stabilisation will be achieved on account of some of the stabilisation being performed by the rudders. By the same virtue endowed by this approach the fin generated noise will diminish. Since, there are three modes of operation the integrated stabilisation provides a degree of redundancy. For example should the fin stabilisers fail the ship will not be completely without roll reducing abilities, thus permitting operations which might have been curtailed to be countenance. The primary objective of any prospective RRS system for the Royal Navy must not require any modifications to the rudder assembly. Therefore, the controller can be retrofitted on any vessel by the simple alteration of the autopilot software algorithm. This facet of the proposed study has not been previously evaluated and affords the greatest advantage over the other RRS implementations.

To these ends Roberts and Braham (1990 and 1991), utilising models of frigate size warships derived by Whalley and Westcott (1981), have conducted studies to assess the viability of utilising the rudders in this additional capacity. They have examined the ramifications on yaw interference and designed classical type controllers which are arranged to avoid saturation of the rudders. This thesis is a significant progression of that work, adopting a integrated ship motion control philosophy. It exhaustively explores many

avenues of controller design, defines the limitations of the mathematical models, proposes an algorithm to avoid the slew rate saturation of the servomechanisms and examines the roll stabilisation problem for the human operators' perspective in the context of lateral accelerations.

1.3 OUTLINE OF THESIS

The remainder of the thesis takes the following format. Chapter 2 proceeds to derive the linear mathematical models of the ship's roll, yaw and LFE dynamics. Sources of uncertainty in these models are identified and quantified which will be required in subsequent controller analysis. The ramifications of utilising the rudder in a dual capacity is also investigated. Finally, an evaluation is made of the possible design techniques which may be most conducive to successful controller synthesis.

A mechanical examination of the rudder servomechanism capabilities is detailed in Chapter 3 with respect to slew rate saturation. This results in the proposal of a novel algorithm which inhibits the device from encroaching into non-linear regions of operation.

Chapter 4 is concerned with the human operator's limitations in the ship's environment in terms of lateral forces. Very few researchers have analysed this aspect of ship motion and a contribution is made with proposals for time domain simulation models and defining the limitations of control action applicability.

The next two Chapters develop linear controllers for the fins and rudders. Chapter 5 stipulates two classical domain techniques, and describes the generation of LQG controllers. The motivations and a brief development of the theory of linear robust H_∞ controller design is presented in Chapter 6. All the controllers are then analysed in the presence of the

uncertainties extracted from Chapter 2, by employing the structured singular value. The penultimate Chapter details the results from exhaustive simulations studies. Following a description of the preparations for the sea trials, the actual results are presented and compared with the predictions.

Finally, in Chapter 8 the salient inferences are derived from the study and presented along with suitable discussion and recommendations for further work.

CHAPTER 2
SHIP MOTION MODELLING

2.1 INTRODUCTION

Successful design of a controller, based on linear theory, and its evaluation by means of simulation, requires an adequate mathematical representation of the dynamics of the system, which describes its function. The actual level of complexity which is embedded in the models depend upon the application. Comprehensive and complete models, encapsulating every aspect of the system, from non-linearities, mutual interactions, frequency and causal dependencies, demand detailed knowledge of the operation of the dynamics of the plant based upon physical laws and human experience. Such a model would be invaluable in predicting the effects of a controller, the environment, changes in operating conditions, perturbations and any other phenomena which impinge upon the system. Thus affording a formidable advantage to the ship designer in assessing the performance of an ocean vessel with various permutations in hull geometry, loading conditions and control appendages. The PAT91, (Crossland, 1991) ship motion prediction software at DRA Haslar, developed over many years, allows the designer this opportunity. The accuracy of the strip theory models encoded in the software have been extensively validated with full-scale and model-scale sea trials by Lloyd and Crossland, (1989). Access was granted to utilise the

software throughout the duration of the project. Nevertheless, establishing complex models, to accurately emulate the real world, necessitates a considerable amount of full-scale and scale-model trials. Unfortunately, to undertake such studies is an extremely expensive business which has to be repeated for each ship type.

Utilising a more accurate mathematical model, in general, results in better controller synthesis. The robust controller design methodology, to be presented in Chapter 5, permits controllers to be designed using relatively simple models which describe the dominant dynamics of a system, since, if the magnitude of variation in its parameters are known, it is possible to accommodate this from the inception of the controller design. It will be shown that the resulting controllers possess relatively better robustness and performance properties than those derived by traditional techniques.

This chapter proceeds with the modelling of the various ship subsystems; both linear and non-linear models being presented and in particular the variations in their parameters are assessed. It has three constituents namely; vessel dynamics, environmental disturbances, and finally, an overview of the proposed control scheme.

2.2 SHIP DYNAMICS

The dynamics of a ship can be analysed by considering it as a six degree-of-freedom body in space, and is permitted to have angular and linear velocities about theses perpendicular axis. The complete equations of motion can be established by using two axis of reference as shown in Figure 2.1. The body-fixed axis system, Oxyz, is located in the ship, not necessarily coincident with the centre of gravity, CoG, (Lloyd, 1989) and moves with it in a longitudinal direction. The inertial axis, $O_o x_o y_o z_o$ is fixed at a location on earth. At some initial condition the two axis system will be coincident.

For navigational purposes the earth axis is invoked. In terms of local navigation this centre, O_o, is located relative to the earth by means of co-ordinates on a chart. To study the motions experienced on the ship the terms, surge, sway, heave, roll, pitch and yaw are commonly employed. These are motions in which the first three quantities refer to linear translations along, Ox, Oy and Oz respectively and the second three correspond to angular rotations about the same axis.

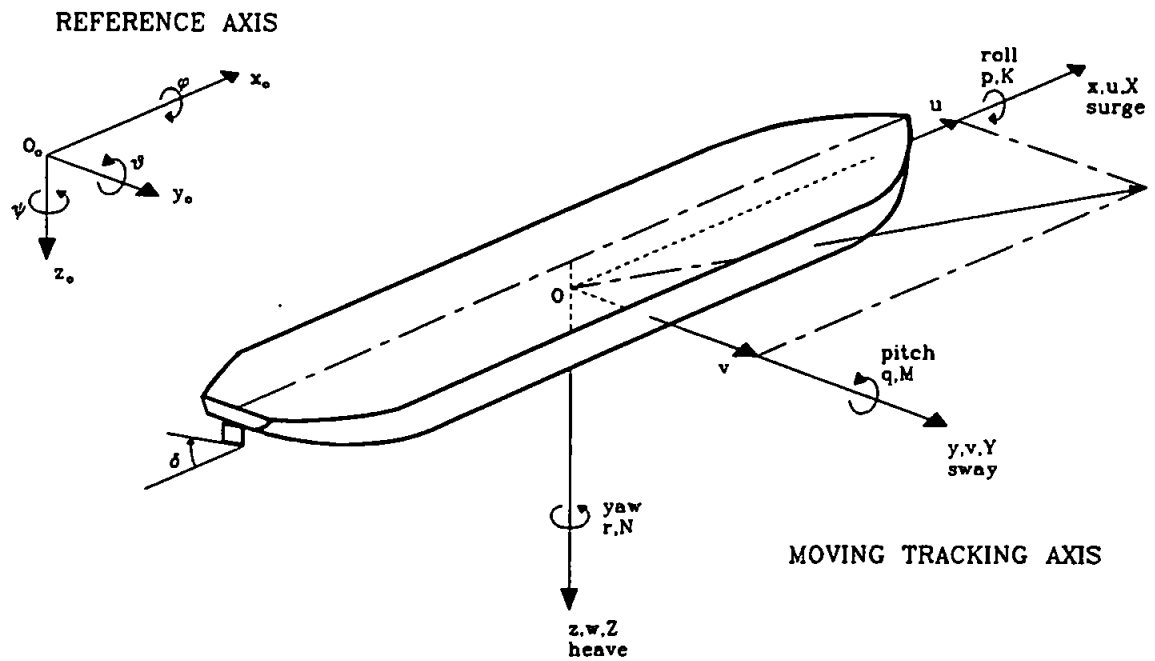

Figure 2.1 : Tracking and reference axis system

The following notation refers to Figure 2.1, and is reproduced from the nomenclature for convenience,

ϕ	roll angle, radian	p	roll rate, $rads^{-1}$	K	roll moment, kgm^2
θ	pitch angle, radian	q	pitch rate, $rads^{-1}$	M	pitch moment, kgm^2
ψ	yaw angle, radian	r	yaw rate, $rads^{-1}$	N	yaw moment, kgm^2
x	surge, m	u	ship velocity, ms^{-1}	X	surge force, Nm
y	sway, m	v	sway velocity, ms^{-1}	Y	sway force, Nm
z	heave, m	w	heave velocity, ms^{-1}	Z	heave force, Nm
δ	rudder angle, radian	α	fin angle, (not shown)		

The constituents of ship motion may be divided into two classes. Vertical plane motions are those which do not possess components in the y-direction; surge, pitch and heave. Lateral plane motions include roll, sway and yaw, since these have velocities in the y-direction. The various motions which form a class of motions may be coupled in a variety of permutations. However, it is assumed, (Abkowitz, 1972 and Lloyd, 1989) , that for motions of small amplitudes, there is no coupling between the two classes of motion.

The basic relevant equations of motion for a rigid body, may be ascertained by Newton's laws of considering rates of changes of force and moments. Given that the co-ordinate of the CoG is $R_G=ix_G+jy_G+kz_G$, where *i*, *j*, and *k* are perpendicular unit vectors in the co-ordinate system, the equations are then:

$$X = m[\dot{u} + qw - rv - x_G(q^2 + r^2) + y_G(pq - \dot{r}) + z_G(pr + \dot{q})] \quad (2.1)$$

$$Y = m[\dot{v} + ru - pw - y_G(r^2 + p^2) + z_G(qr - \dot{p}) + x_G(qp + \dot{r})] \quad (2.2)$$

$$Z = m[\dot{w} + pv - qw - z_G(p^2 + q^2) + x_G(rp - q^2) + y_G(rq + \dot{p})] \quad (2.3)$$

$$K = I_{xx}\dot{p} + (I_{zz} - I_{yy})qr + m[y_G(\dot{w} + pv - qu) - z_G(\dot{v} + ru - pw)] \quad (2.4)$$

$$M = I_{yy}\dot{q} + (I_{xx} - I_{zz})rp + m[z_G(\dot{u} + qw - rv) - x_G(\dot{w} + pv - qu)] \quad (2.5)$$

$$N = I_{zz}\dot{r} + (I_{yy} - I_{xx})pq + m[x_G(\dot{v} + ru - pw) - y_G(\dot{u} + qw - rv)] \quad (2.6)$$

where

m	is the mass of the ship, kg
I_{xx}	is the moment of inertia about the x axis, kgm^2s^{-2}
I_{yy}	is the moment of inertia about the y axis, kgm^2s^{-2}
I_{zz}	is the moment of inertia about the z axis, kgm^2s^{-2}

The terms $\dot{u}, \dot{v}, \dot{w}, \dot{p}, \dot{q}$ and $\dot{r}$ are the acceleration components within the moving axis system. The additional terms qw-rv, ru-pw, pv-qu and qr, rp, pq arise from the moving co-ordinate system and represent components of centripetal accelerations. All the remaining terms

involving the co-ordinates of the CoG describes centrifugal and reaction forces and the moments acting at the origin due to the acceleration of CoG relative to the origin.

Consider the motions in the lateral plane with rolling and invoking the following assumptions:

i. Origin of the rectangular system is on the line of lateral symmetry going through the CoG, i.e. $y_G=0$

ii. No pitching motion

Then

$$X = m(\dot{u} - rv - x_G r^2 + z_G pr) \tag{2.7}$$

$$Y = m(\dot{v} + ru + x_G \dot{r} - z_G p) \tag{2.8}$$

$$K = I_{xx}\dot{p} + mx_G(\dot{v} + ru) \tag{2.9}$$

$$N = I_{zz}\dot{r} + mx_G(\dot{v} + ru) \tag{2.10}$$

The force Y is the resultant of all the forces which act on the ship in the y-direction, similarly for the X force. K and N are the roll and yaw moments which are consequently generated. The forces may be attributed to various factors according to its origin. Those contributing to hydrodynamic effects are generated by control surfaces such as fins, rudders and the bilge keel, Y_{hydro}. Propeller excitation imparts a velocity to the ship, Y_{prop}. The ship is perturbed from its equilibrium by a number of external factors such as wind, current and sea-waves. These forces which engender the resultant motions, taking the Y force as an example, may be expressed.

$$Y = Y_{hydro} + Y_{prop} + Y_{ext} \tag{2.11}$$

Each component is now considered.

Hydrodynamic Forces

The hydrodynamic forces which act on the ship are a complicated function of ship motions, for example, loading conditions, speed, and hull geometry. A mathematically expedient approach is to express these as functions of small perturbations in velocities as expressed in equation (2.12):

$$Y_{hydro} = f(\phi, \theta, \psi, u, \dot{u}, v, \dot{v}, r, \dot{r}, p, \dot{p}, \delta, \dot{\delta}, \alpha, \dot{\alpha}, u^2, \dot{u}^2, v^2 .....) \qquad (2.12)$$

Provided that the forces, X and Y, and the moments, K and N, are continuous functions of the set of the above independent variables and their derivatives then the Taylor expansion can be employed to express, ΔY_{hydro}, a small perturbation in force, in a precise form around some nominal operating point where, $u=U_o$, $v = r = p = \dot{v} = \dot{r} = \dot{p} = ... = 0$, and the CoG is coincident with the origin of the body-fixed axis. Therefore, neglecting second order, and higher, terms ΔY_{hydro}, reduces to (2.13);

$$\Delta Y_{hydro} = Y_\phi \phi + Y_p p + Y_{\dot{p}} \dot{p} + Y_\psi \psi + Y_r r + Y_{\dot{r}} \dot{r} + Y_v v + Y_{\dot{v}} \dot{v} + Y_u mu + Y_{\dot{u}} \dot{u} + Y_\delta \delta + Y_\alpha \alpha + Y_W \qquad (2.13)$$

where for example,

$$Y_v = \frac{\partial Y}{\partial v}\Big|_{v=0} \qquad Y_{\dot{v}} = \frac{\partial Y}{\partial \dot{v}}\Big|_{\dot{v}=0} \quad ....\text{etc}$$

are called the "slow motion derivatives" and are dependent upon ship speed and loading conditions. The parameter, Y_W, represents the external excitation. Similar expressions may be generated for X, K and N, i.e.

$$m(\dot{u} - rv) = X_\phi \phi + X_\psi \psi + X_r r + X_{\dot{r}} \dot{r} + X_v v + X_{\dot{v}} \dot{v} + X_u mu + X_{\dot{u}} \dot{u} + X_\delta \delta + X_\alpha \alpha + X_W \qquad (2.14)$$

$$I_{xx} \dot{p} = K_\phi \phi + K_p p + K_{\dot{p}} \dot{p} + K_\psi \psi + K_r r + K_{\dot{r}} \dot{r} + K_{\dot{v}} \dot{v} + K_\delta \delta + K_\alpha \alpha + K_W \qquad (2.15)$$

$$I_{zz}\dot{r} = N_\phi\phi + N_p p + N_{\dot{p}}\dot{p} + N_\psi\psi + N_r r + N_{\dot{r}}\dot{r} + N_v v + N_{\dot{v}}\dot{v} + N_u mu + N_{\dot{u}}\dot{u} + N_\delta\,\delta + N_\alpha\alpha + N_W \tag{2.16}$$

It is possible to represent this system in terms of a state space equation (2.17)

$$\begin{bmatrix} -Y_{\dot{p}} & -Y_{\dot{r}} & -Y_{\dot{u}} & (m-Y_{\dot{v}}) & 0 & 0 \\ -X_{\dot{p}} & -X_{\dot{r}} & (m-X_{\dot{u}}) & -X_{\dot{v}} & 0 & 0 \\ -N_{\dot{p}} & (I_{zz}-N_{\dot{r}}) & -N_{\dot{u}} & -N_{\dot{v}} & 0 & 0 \\ (I_{xx}-K_{\dot{p}}) & -K_{\dot{r}} & -K_{\dot{u}} & -K_{\dot{v}} & 0 & 0 \\ 0 & 0 & 0 & 0 & 1 & 0 \\ 0 & 0 & 0 & 0 & 0 & 1 \end{bmatrix} \begin{pmatrix} \dot{p} \\ \dot{r} \\ \dot{u} \\ \dot{v} \\ \dot{\phi} \\ \dot{\psi} \end{pmatrix} =$$

$$\begin{bmatrix} Y_p & (Y_r+mu) & Y_u & Y_v & Y_\phi & Y_\psi \\ X_p & (X_r-mv) & X_u m & X_v & X_\phi & X_\psi \\ N_p & N_r & N_u m & N_v & N_\phi & N_\psi \\ K_p & K_r & K_u m & K_v & K_\phi & K_\psi \\ 1 & 0 & 0 & 0 & 0 & 0 \\ 0 & 1 & 0 & 0 & 0 & 0 \end{bmatrix} \begin{pmatrix} p \\ r \\ u \\ v \\ \phi \\ \psi \end{pmatrix} + \begin{bmatrix} Y_\alpha & Y_\delta \\ X_\alpha & X_\delta \\ N_\alpha & N_\delta \\ K_\alpha & K_\delta \\ 0 & 0 \\ 0 & 0 \end{bmatrix} \begin{pmatrix} \alpha \\ \delta \end{pmatrix} + \begin{bmatrix} Y_W \\ X_W \\ N_W \\ K_W \\ 0 \\ 0 \end{bmatrix} \tag{2.17}$$

This state space description embodies the linear motion of the ship in the lateral plane. However, some of the parameters are not only speed dependent but also vary with encounter frequency. If all the variables generated by the Taylor expansion were permitted in the state space description (2.17), a much more complex and accurate model would be produced such as suggested by (Abkowitz, 1972). This would be a very desirable model in ship motion prediction studies.

In order to determine and identify these complex parameters, sophisticated manipulation techniques, and full-scale and model-scale sea trials are imperative. Thus rendering this approach to modelling an extremely expensive and impracticable proposition. Perhaps this explains the reason for a dearth of hydrodynamic data released in academic literature. However, researchers have extensively endeavoured to comprehend, capture and evaluate these hydrodynamic parameters (Eda and Crane, 1965; Lloyd, 1972; Lloyd and Crossland, 1989; Kallstrom and Ottosson, 1982; Roberts, 1983; Yamasaki and Fasataka, 1985;

Troesch, 1981). The relative importance of each parameter is expounded by these authors. Despite these efforts, it is still not normally possible to isolate every quantity.

Generally, many of the linear parameters may be considered negligible under certain circumstances and it may be assumed that lateral plane motions have no coupling with each other. However, for example, in aircraft carriers the roll induced sway and yaw motions are insignificant. Therefore, for such large vessels, the terms containing p and $\dot{p}$ may be eliminated from the appropriate equations. For smaller vessels, for example, yachts, these coupling must be accounted in developing the equations of motion. In this thesis both scenarios will be considered and justified when considering the roll and yaw models.

Having removed the terms which are negligible and eliminated others through decoupling the motions, the resultant model may still not be amenable to control design. Researchers have with considerable success attempted to simplify the models even further by means of estimation and representing only the dominant dynamics.

The purpose of this project is to design advanced controllers for the regulation of roll via the stabilising fins and rudders, minimisation of yaw error and reducing the Lateral Force Estimator. Therefore, mathematical modelling is restricted to these motions. However, interaction amongst the lateral plane motions are also examined where appropriate.

Each model is now discussed and the variations in their parameter values established for stability analysis in Chapter 5.

2.2.1 Yaw Models

The turning characteristics of a ship may be succinctly divided into three distinctive phases. The first phase commences with the initial deflection of the rudder in this example to starboard for a starboard turn. During this period the rudder force, $Y_\delta \delta$, and the rudder moment, $N_\delta \delta$, develop accelerations. The opposing forces arise solely from the inertia of the ship since drift and rotation, r, have not had sufficient opportunity to increase. From equation (2.13) it is noted that the transverse acceleration, $\dot{v}$, hence the CoG, begins to move towards port whereas the turn will eventually be to starboard. Despite this proclivity, the bow of the ship remains to starboard throughout. The second phase now initiates with the introduction of a drift angle, and a rotation, r, and all the terms co-exist in (2.13). The significant event in this phase is the creation of a $Y_v v$ force on the hull directed towards starboard. When this magnitude exceeds that of $Y_\delta \delta$, which was directed to port, the ship's CoG tends to move to starboard. This phase ceases with the establishment of an equilibrium in forces, after some transients, and the ship enters the third phase: a steady-state turn with constant radius. From (2.13), v and r, become non-zero however the accelerations, $\dot{v}$ and $\dot{r}$, diminish to zero. Further details and illustrations may be found in (Bhattacharya, 1978 and Saunders, 1965).

The approach pursued here, in order to develop the yaw models required, is to review the established research work of various authors which will be summarised and the relevant information regarding parameter variation extracted and refined.

The development of a simple linear model is of concern such as that suggest by (Davidson and Schiff, 1946 and Gerritsma, 1980), for yaw and sway, by removing the dependence on roll, are :

$$m(\dot{v} + ur) = Y_r r + Y_{\dot{r}} \dot{r} + Y_v v + Y_{\dot{v}} \dot{v} + Y_\delta \delta \qquad (2.18)$$

$$I_{zz}\dot{r} = N_r r + N_{\dot{r}}\dot{r} + N_v v + N_{\dot{v}}\dot{v} + N_\delta \delta \tag{2.19}$$

The Nomoto Model

Nomoto *et al*, (1957), combined the equations (2.18) and (2.19), to form a second order differential equation (2.20), where the coefficients are functions of the hydrodynamic derivatives and will be given presently,

$$\tau_1\tau_2\ddot{r} + (\tau_1 + \tau_2)\dot{r} + r = K(\delta + \tau_3\dot{\delta}) \tag{2.20}$$

Taking the Laplace transforms of (2.20) yields a transfer function relating ship yaw rate to rudder angle.

$$\frac{r(s)}{\delta(s)} = \frac{K(1 + s\tau_3)}{(1 + s\tau_1)(1 + s\tau_2)} \tag{2.21}$$

The parameters of (2.21) may be expressed as functions of the hydrodynamic derivatives (2.18) and (2.19)

$$\tau_1\tau_2 = \frac{(m - Y_{\dot{v}})(I_{zz} - N_{\dot{r}}) - N_{\dot{v}}Y_{\dot{r}}}{D} \qquad K\tau_3 = \frac{Y_v N_\delta - N_v Y_\delta}{D}$$

$$K\tau_3 = \frac{-N_\delta (m - Y_{\dot{v}}) - N_{\dot{v}}Y_\delta}{D} \qquad D = N_v(mu - Y_r) + N_r Y_v$$

and

$$\tau_1 + \tau_2 = \frac{-Y_v(I_{zz} - N_{\dot{v}}) - N_r(m - Y_{\dot{v}}) + (mu - Y_r)N_{\dot{v}} - Y_{\dot{r}}N_r}{D}$$

Nomoto further reduces this model to

$$\frac{r(s)}{\delta(s)} = \frac{K}{(1 + s\tau)} \tag{2.22}$$

or in terms of a differential equation;

$$\tau\dot{r} + r = K\delta \qquad \text{where} \qquad \tau = \tau_1 + \tau_2 - \tau_3$$

Nomoto acknowledges that, despite its accurate response in predicting ship yaw for a large class of vessels, it is invalid for large rudder angles and manoeuvres and "directionally unstable ships", where non-linearities dominate. Figure 2.2 illustrates this concept. A course stable ship is one in which there is a constant heading on the application of a temporary rudder angle. In a course unstable ship, there is no new constant heading, but a constant rate of turn. To achieve the correct new heading and opposite sense moment must be introduced by the rudder. This phenomena may be determined by measuring the static relationship between rate of turn, r, and rudder angle, δ .

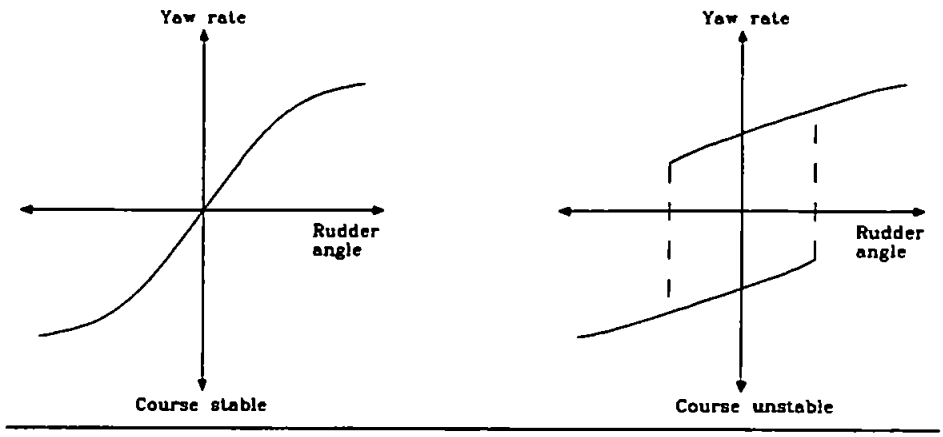

Figure 2.2 : Course stability

The Norbin Model

Considering the disadvantages of the Nomoto model, Norbin, (1963), extends (2.19) by introducing a non-linear term. Thus enabling it to accommodate large heading and rudder deflections and course instability (2.23)

$$T\dot{r} + H(r) = K\delta \qquad (2.23)$$

Under steady-state conditions all the derivatives disappear then $H(r)=K\delta$. And the non-linear approximation of H(r) may be given as

$$H(r) = \alpha_3 r^3+\alpha_2 r^2+\alpha_1 r+\alpha_0$$

$\alpha_1 = +1$ for course stable ships

and $\alpha_2 = -1$ for course unstable ships

The parameter α_0 assumes a zero value caused by asymmetric hull or by flow conditions due to single screw propulsion. By introducing non-linear feedback, as shown in Figure 2.3, a set of parameters may be deduced for various rudder angles.

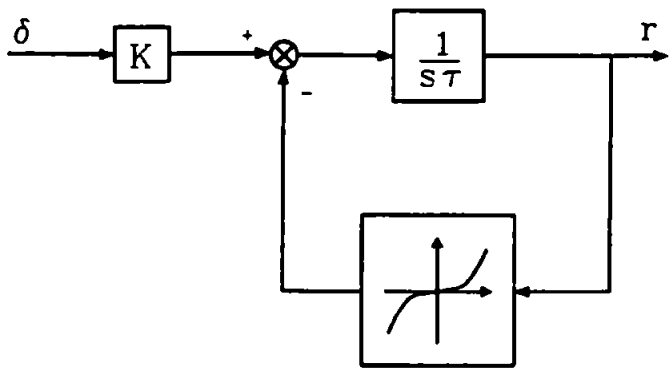

Figure 2.3 : Norbin's non-linear model for yaw (Norbin, 1963)

For simulation purposes this model would be adequate given the limited availability of hydrodynamic data, since the inherent non-linearities are encapsulated by the five parameters. It is utilised in simple simulation studies. For the frigate size warships considered here, the non-linearity can successfully be described by α_3 alone and are course stable. Amerongen *et al* (1982), Mort (1983) and Marshfield, (1981c) have derived values for these parameters, at various ship speeds, from sea trials, listed in Table 2.1.

Table 2.1 : Parameters for Norbin model

Ship Speed (ms^{-1})	α_3	K	τ (secs)
6.2	0.4	0.08	20
9.2	0.6	0.18	27
13.4	0.3	0.23	21

The Roberts Approach

Roberts (1989), and Whalley and Westcott, (1981), regard the ship as a "black-box" in order to construct the yaw model. By measuring the input/ouput response of an known system and using identification techniques it is possible to represent the dominant dynamics by means of a transfer function. During full-scale sea trials they passed various test signals to the rudder and by measuring the yaw response generated the transfer function (2.24).

$$\frac{r(s)}{\delta\ (s)} = g22(s) = \frac{k_{22}}{(12s^3 + 32.25s^2 + 11.2s + 1)} \qquad (2.24)$$

Where k_{22} is a speed dependent term to account for the increasing moment generating capabilities of the rudder. It varies by ±40% and shall be considered in the robustness assessment of the controllers in Chapter 5. The g22(s) will be placed in context when describing the multivariable models in section 2.4.

Figure 2.4, shows the corresponding time responses of the Nomoto and Roberts models for a frigate size warship. These responses are at a nominal rudder excitation of $\pm 1^0$.

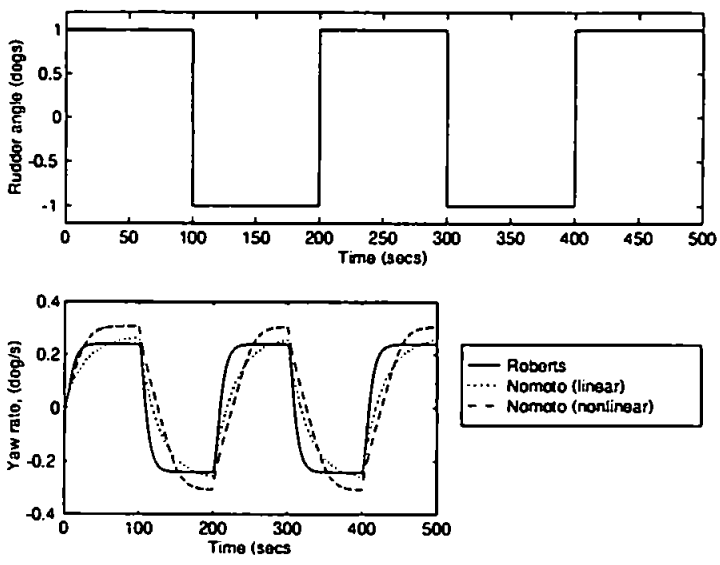

Figure 2.4 : Yaw rate responses

2.2.2 Roll Models

The roll of a ship is a lateral-plane motion, it therefore has couplings with sway and yaw (Lloyd, 1972). However, a single degree-of-freedom model is most amenable to control design which will be pursued here. Several authors have theoretically justified this approach (Troesch, 1981 and Haddara and Nassar, 1986) and others by experimentation (Amerongen *et al*, 1983, Amerongen *et al*, 1987 and Kallstrom 1981).

A similar method is adopted here as with the yaw models development; established results from researchers are presented and refined in order to extract information regarding magnitudes of variations in the parameters values.

The Conolloy Model

With the yaw and sway terms neglected the roll motion may be expressed by (2.25).

$$(I_{xx} + \delta\ I_{xx})\dot{p} - K_p p + mg\overline{GM}\phi = K_w \xi \tag{2.25}$$

where $\delta\ I_{xx}$ is the added mass inertia to describe motion imparted to the surrounding water by the hull, which may contribute as much as 30% to the total moment of inertia about the x-axis, ξ is the wave slope, and $\overline{GM}$ the metacentric height.

Unlike yaw and sway motions the roll behaves as a classic "damped-spring-mass" system, where $mg\overline{GM}$ is the restoring force. This provides damping action which makes the system oscillatory. Taking the Laplace transform of (2.25) a transfer function relating roll angle to wave slope is derived (2.26).

$$\frac{\phi(s)}{\xi(s)} = \frac{K_{w\phi}}{s^2 + 2\zeta_s \omega_n s + \omega_n^2} \tag{2.26}$$

where $\omega_n^2 = \dfrac{mg\overline{GM}}{I_{xx} + \delta\ I_{xx}}$ $\qquad$ $K_{w\phi} = \dfrac{K_w}{I_{xx} + \delta\ I_{xx}}$, Nm

$$\zeta_s = \frac{-K_p}{2}\sqrt{\frac{I_{xx} + \delta\, I_{xx}}{mg\overline{GM}}}$$

The natural roll frequency, ω_n, essentially a measure of restoring moment, and damping ratio, ζ_s, may be measured from full-scale trials by establishing a roll motion oscillation with the stabilising fins. The fins are then placed in a neutral position and the typical roll decay results in a response as shown by Figure 2.5.

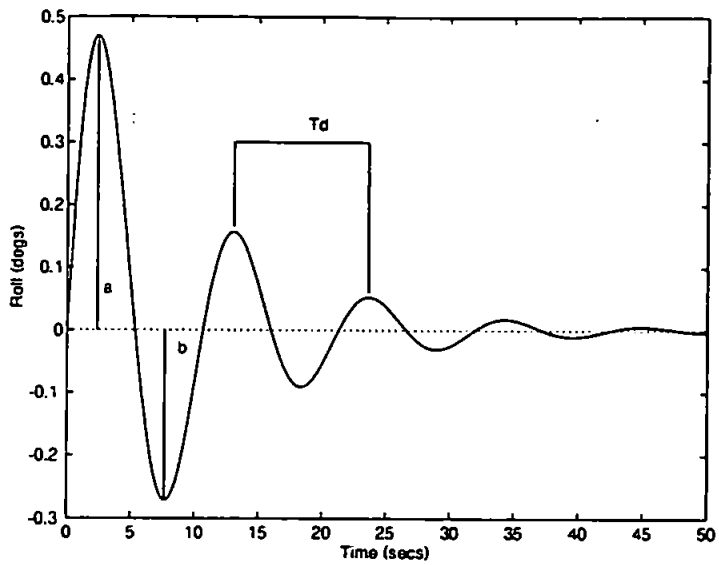

Figure 2.5 : Typical roll response

The parameters can be readily ascertained by the log-decrament method:

$$\zeta_s = \frac{\ln(\frac{a}{b})}{\sqrt{\pi^2 + 1}} \qquad \omega_n = \frac{2\pi}{T_d\sqrt{1-\zeta_s^2}}\ rads^{-1} \qquad (2.27)$$

It is seen from (2.26) that the natural frequency of oscillation is dependent upon the inertial moment about the x-axis and the metacentric height. These parameters are, in turn, dependent upon ship hull geometry and loading conditions and remain unchanged irrespective of ship speed. For the vessel under consideration, DRA Haslar, in a private communication (Crossland, 1992) informed that ω_n=0.598 rads^{-1}. Since, added mass inertia, $\delta\ I_{xx}$, is dependent upon the roll angle, ω_n will vary. However, it is assumed that this is

negligible providing the roll angle remains small thus ensuring a linear restoring lever arm, $\overline{GZ} = \overline{GM}\sin(\phi)$, (De Heere and Bakker, 1970).

The damping ratio is a function of the hydrodynamic derivative K_p, which results from the Taylor expansion about a nominal ship speed, therefore, it is assumed that this parameter is speed dependent. Froude first realised that the damping is not only related to ship speed but also, equally significantly, to roll velocity and ship heading (to be defined in the next section). Thus (2.25) may be simplified to

$$\dot{p} + (a + n|p|)p + \omega_n^2 = K_w\xi \tag{2.28}$$

where the roll damping is now in a 'linear-plus-quadratic' term. The solution of a linear roll equation such as (2.26) takes the form,

$$y(t) = \frac{1}{\sqrt{1-\zeta_s}} \exp^{-\zeta_s\omega_n t}\sin(\omega_n\sqrt{1-\zeta_s^2}\, t) \tag{2.29}$$

If the envelope of the response from (2.29) is plotted against a natural logarithmic scale a straight line will result. This is shown in Figure 2.6. The curve of the simulated non-linear decay is apparent. Using data for a frigate warship from Marshfield, (198b) it can be seen that there is very little non-linearity manifest.

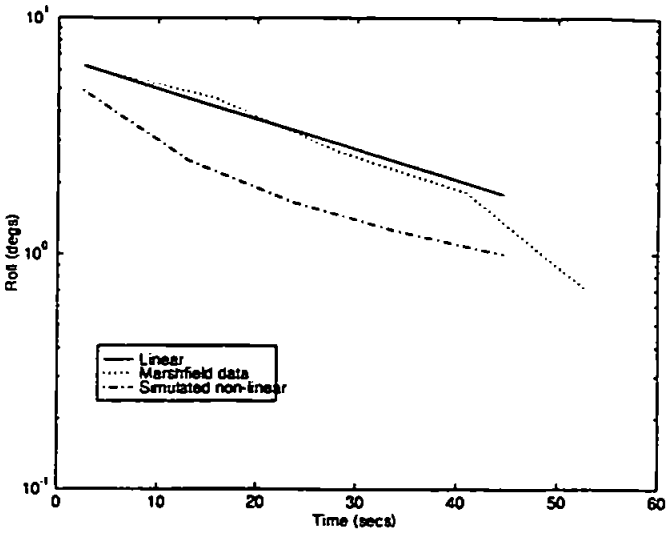

Figure 2.6 : Roll envelope response

Researchers have made concerted efforts to quantify this non-linear roll damping, Schmitke, (1978), giving the nascent impetus in his theoretical development of ship motion. Initial efforts (Dalzell, 1978 and Haddara and Nassar, 1986) concentrated on solving the associated Fokker-Plank equation and obtaining expressions for the mean-square value. The averaging technique of Fyloff-Bogoliuboff (Flower and Aljaff, 1981) was compared with the perturbation method by Bass and Haddara, (1988), in simulations studies. Subsequently the validity of these techniques were confirmed by scale-model trials by Haddara and Bennet, (1989). Using a stochastic modelling approach gave less convincing results as shown by Kwon and McGregor, (1991). The established recursive least-squares algorithm was employed by Gawthrop *et al* (1988) whose results converged with experimental values. Finally, Roberts, Dunne and Debenos (1983), and Roberts, (1984), pursues the modelling by the energy content of the roll decay envelope. Unfortunately, further examination of this work is outwith the scope of this study. Since it is desired to only establish an estimate of the extent of the variations of this parameter for robustness analysis, Chapter 5, it will suffice to adopt a rudimentary and empirical approach here.

This was achieved by analysis of extensive PAT91 simulations RMS roll data furnished by DRA Haslar. The damping ratio was ascertained by simulations and altering a gain term and adjusting the damping ratio such that the RMS values co-incides. The results of this are shown in Figure 2.7. It is apparent that the damping ratio lies within the range 0.1 and 0.3 and increases or decreases with speed depending on whether the relative ship and sea heading is at quartering or bow seas. This peculiar phenomena may be explained by hull planing effects, (Saunder, 1965, and Himeno, 1981).

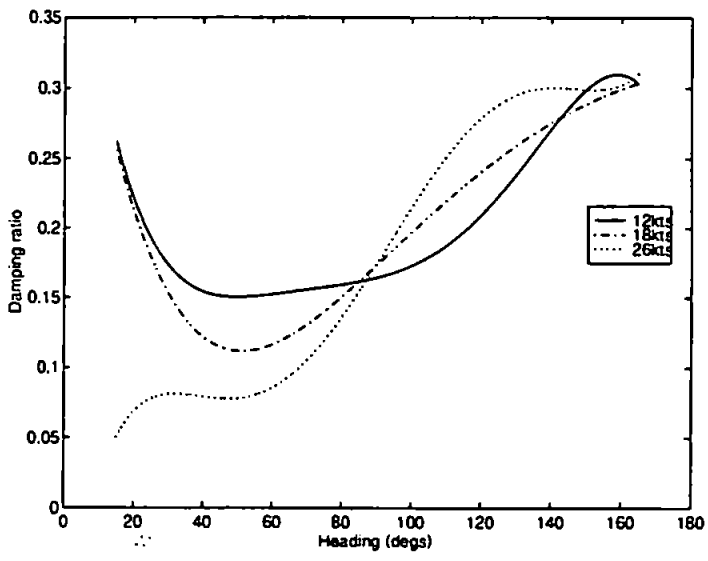

Figure 2.7 : Variation of ζ_{ss} with ship speed and heading

Roll Stabiliser Fins

In the previous section the roll excitation to the ship was wave disturbance, equation (2.25). The aim of this study is to eliminate this detrimental effect by utilising the fin stabilisers. These deliver, given an adequate controller, an opposing moment to the wave-induced roll resulting in the amelioration of rolling in ships. This is achieved by replacing $K_w\xi$ in (2.25) by the equivalent fin induced moment. Their hydrodynamic performance is compendiously considered here.

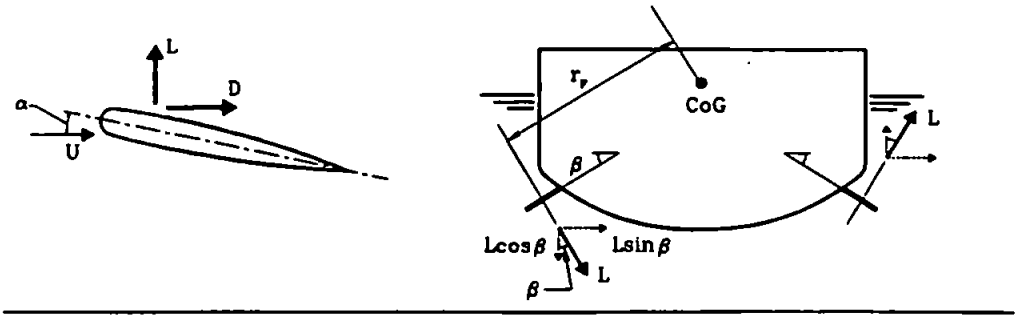

Figure 2.8 : Fin hydrodynamics

Figure 2.8 shows the components of the fin induced motions. The total roll moment exerted by the fins is given by,

$$K_\phi = \frac{\partial C_L}{\partial \alpha} \rho U^2 A_F r_F \alpha \quad Nm \tag{2.30}$$

where

$\frac{\partial C_L}{\partial \alpha}$	is the lift curve slope per degree fin deflection, ms^{-1} per deg
ρ	sea-water density, kgm^{-3}
A_F	planform area, m^2
r_F	moment arm, m
α	the fin angle which has maximum excursion of $\pm 30^0$
D	drag, (non-dimensional with respect to ship speed)
L	total lift, (non-dimensional with respect to ship speed)
β	dihedral angle, radians

Therefore, the roll equation (2.26) can be recast to reflect fin deflection induced roll angle,

$$\frac{\phi(s)}{\alpha(s)} = g11(s) = \frac{\left(\frac{\rho U^2 A_F r_F}{mg\overline{GM}} \frac{\partial C_L}{\partial \alpha}\right)\omega_n^2}{s^2 + 2\zeta_S \omega_n s + \omega_n^2} = \frac{k_{11}\omega_n^2}{s^2 + 2\zeta_S \omega_n s + \omega_n^2} \tag{2.31}$$

The term k_{11}, ($kgms^{-1}$), is the fin moment generating capacity and has been determined by (Whalley and Westcott, 1981 and Roberts, 1989) from extensive full-scale sea trials at various ship speeds and at damped roll frequency. From equation (2.31) it is possible to compute the theoretical values of k_{11}, this procedure is described in Appendix A and the results presented in Table 2.2.

Table 2.2 : Evaluation of k_{11}

			With performance degradation		
			Frequency ($rads^{-1}$)		
Speed (kts)	k_{11} -Sea trials	k_{11}- theory	0	ω_n	$2\omega_n$
12	0.11	0.64	0.18	0.29	0.33
18	0.18	1.45	0.41	0.67	0.75
26	0.17	3.03	0.86	1.41	1.57

From these results it is apparent that there is significant divergence between the theoretical and experimental results. This lack of correlation is influenced by several factors according to Cox and Lloyd, (1977) and Lloyd, (1972); as the ship is in motion a boundary layer is created on the hull surface, whose thickness is proportional to the ship speed, within this boundary the performance of the fins is severely curtailed, which may explain the paradoxically degradation of k_{11} from 0.18 to 0.17 as the ship increases speed, see (2.30). If there is an aft mounted bilge keel it will interfere with the downwash from the fins reducing their effectiveness. As seen from Figure 2.8 the lift L, has two components which reduce the net moment generating effect about the x-axis. These effects have been taken into consideration in Appendix A and the new values of k_{11} calculated at various frequencies as shown in Table 2.2.

The results although diverge from the experimental they now are closer when performance degradation is taken into account. These are then utilised in the controller synthesis and the possible variations are required to assess controller performance in the presence of this uncertainty.

Equation (2.31) demonstrates that the fin 'power' is dependent not only on ship speed but also aspect ratio as illustrated by Figure 2.8. Therefore, increasing the outreach or the decreasing the tip and root chords will in turn increase this term hence accrue larger moments about the x-axis. However, the maximum permitted fin excursion will be reduced

lest stalling occurs. This aspect of enhanced operation will be considered in the controller design.

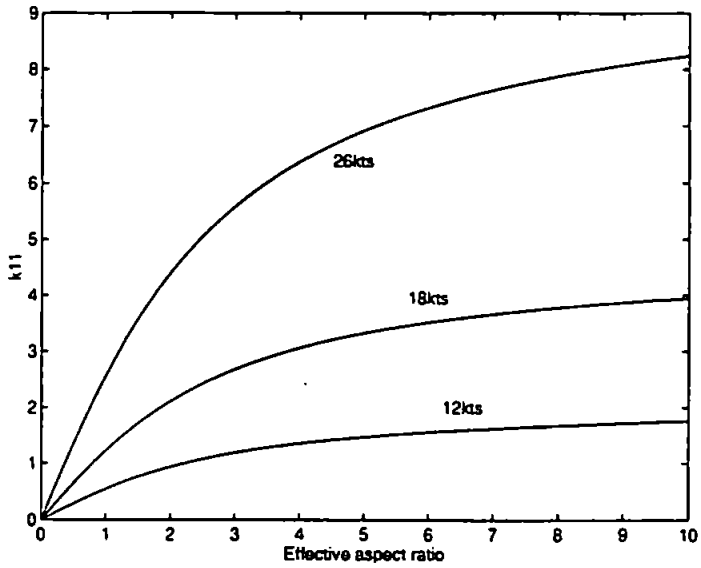

Figure 2.9 : k_{11} as a function of aspect ratio

The primary role of the stabilising fins is to develop roll moments about the CoG, however, they also engender secondary motions which are now considered.

If the fins are located in a plane close to the CoG, as in the type of ships considered in this thesis, it may be assumed that fin-induced yaw moment excitation is negligible.

As previously mentioned the fin action generates a lift force, L, which imparts the roll motion about the CoG. This can be decomposed into a horizontal and vertical component, see Figure 2.8. The latter cancel so that there is no resultant heave or pitch motion induced. However, given that the fins have been installed at a dihedral angle, the former combine to produce a sway force,

$$Y = 2L\sin(\beta) = \frac{\partial C_L}{\partial \alpha}\alpha U^2 A_F \sin(\beta) \quad Nm \tag{2.32}$$

This sway force shall be further considered in the Lateral Force Estimator problem in section 2.2.3 and Chapter 4. In steady-state conditions this force will be opposed by a hydrodynamic force acting on the hull in turn creating a roll angle. If it is assumed that this force acts at a depth equal to one third of the draught, T, the rolling moment (Lloyd, 1972) due to the sway velocity, v is

$$Y\left(\overline{KG} - \frac{T}{2}\right) = mg\overline{GM}\phi_v \tag{2.33}$$

and $$\phi_v = \left(\overline{KG} - \frac{T}{2}\right)\frac{\partial C_L}{\partial \alpha}\alpha\rho\frac{U^2 A_F \sin(\beta)}{mg\overline{GM}} \tag{2.34}$$

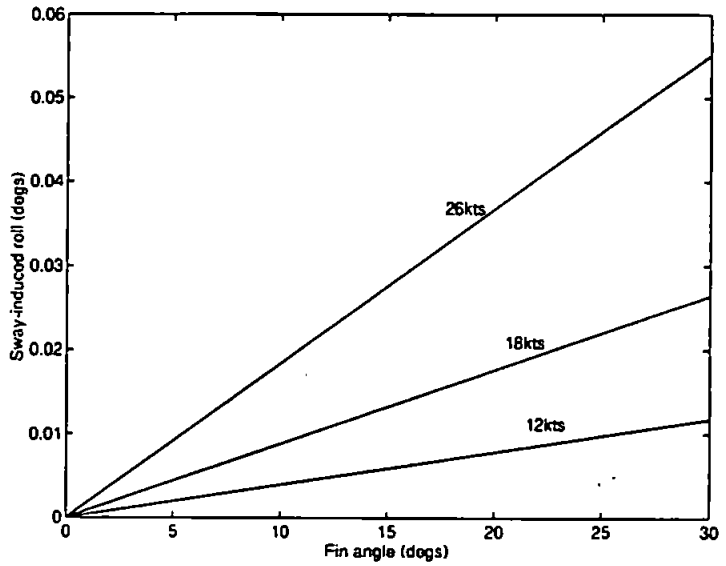

Figure 2.10 : Sway induced roll

As manifest by Figure 2.10, the sway induced roll is minimal, and may be neglected, which would concur with the experimental results presented by Marshfield, (1981b).

Rudder Roll Stabilisation (RRS)

The rudder is designed primarily as a means to change course, however, inevitably other motions are induced. Of particular interest are the lateral plane motions, in particular the roll. Consider the situation in the first phase of a starboard turn as described in Section

2.1.1, with reference to Figure 2.11 and equation (2.35), derived from (2.8) and (2.13) where all the relevant terms are gathered on one side.

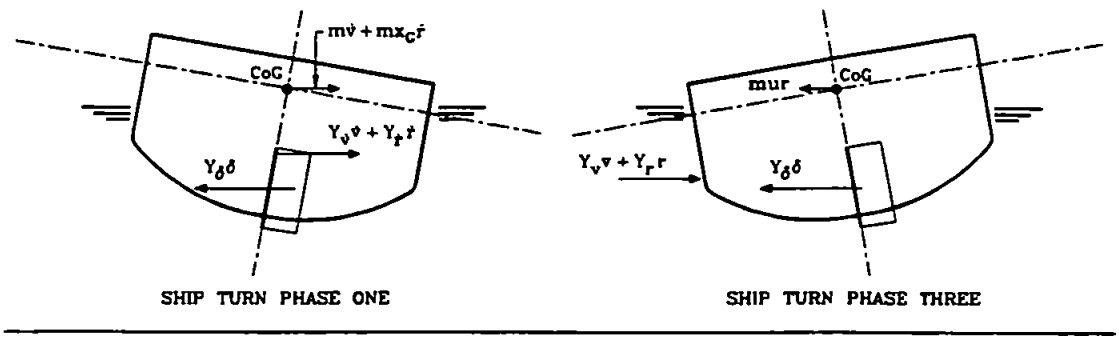

Figure 2.11 : Transverse forces acting on hull and rudder

$$Y_\delta\,\delta + Y_{\dot v}\dot v + (Y_{\dot r} + mx_G)\dot r - m\dot v = 0 \qquad (2.35)$$

By convention Y_δ, remains positive and δ is negative for a starboard turn, then the force, $Y_\delta\,\delta$, is negative or to port as shown in Figure 2.11 in the first phase. During this phase, $\dot v$, is negative, then $Y_{\dot v}\dot v$, will be directed to starboard, since $Y_{\dot v}$ is always negative. The sign of $(Y_{\dot r} - mx_G)$ is indeterminate from (2.35), but will be negligible compared with the sway force. The last term, $(-m\dot v)$, will be to starboard since $\dot v$ is negative. The water forces impinging upon the hull, $Y_{\dot v} + Y_{\dot r}$, act at half draft, $Y_\delta\,\delta$, at the vertical centre of rudder and $m\dot v$ and $mx_G\dot r$, at the CoG. From Figure 2.11, during the first phase, if the moments are taken from half-draft, then it is obvious that the ship heel, ϕ, will be to starboard. The salient characteristic is that no yaw motion has yet occurred. Figure 2.11 also illustrates the forces acting in the final steady-state phase and it is seen that the ship will roll to the expected port side.

Typical roll and yaw time responses of the ship during the three phases are shown in Figure 2.12. The positive ephemeral roll is to starboard, during this period insignificant yaw motion occurs. Utilising this initial heel in the 'wrong sense' is the foundation of RRS.

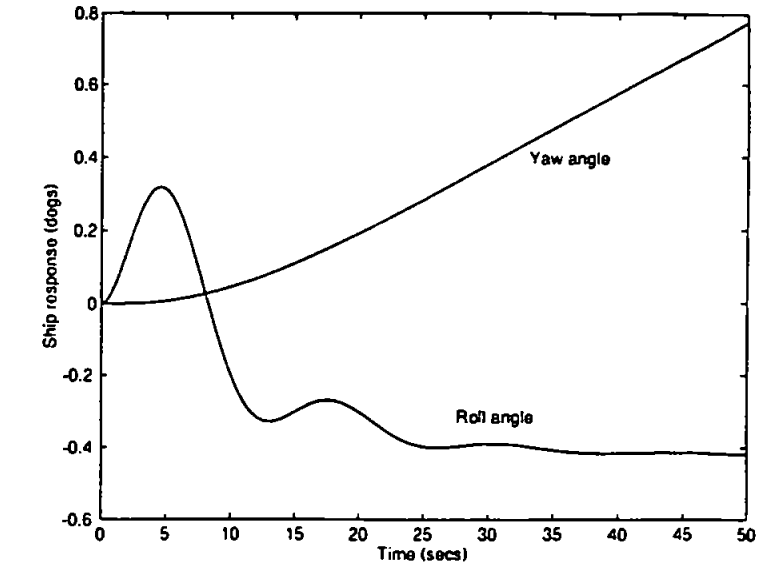

Figure 2.12 : Yaw and roll response during turn

The background of this concept and state of research has been outlined in Chapter 1. Only the mathematical modelling is considered here.

Whalley and Westcott (1981)

The transfer function model was derived through extensive sea-trials on a frigate size warship and fitting a transfer function to the subsequent rudder induced roll motion time response. (Roberts, 1989) further refined this model, again from sea trials and is given in equation (2.36). The non-minimum phase zero ensures that the roll is in the initial wrong sense as described above.

$$\frac{\phi(s)}{\delta\ (s)} = g12(s) = \frac{\omega_n^2 k_{12}(1 - 8.57s)}{(1 + 8.2s)(s^2 + 2\zeta_S \omega_n s + \omega_n^2)} \tag{2.36}$$

where k_{12}, is proportional to speed gain term to account for increased hydrodynamic forces and moments which will be generated by the rudder, g12(s) will be placed in context with the multivariable configuration.

It is of significance that the RRS models developed by Amerongen (1982 and 1984) and later in conjunction with Klugt (1987, 1990a), do not contain this characteristic of the ship transient heel in the 'wrong sense'. However, this work was the basis of redesign of the Dutch M-Class frigates (Klugt, 1990b) which incorporates RRS only and renders the fin stabilisers obsolete.

By consideration of the hydrodynamics forces alone it is apparent that the initial roll characteristic does not interfere with the ship yaw dynamics. This can be further demonstrated in the frequency domain. Figure 2.13 shows a typical roll and yaw spectrum, from which it is apparent that there is significant frequency separation between these two motion channels to render cross-coupling negligible. Furthermore, use of appropriate filters it can be ensured that these signals do not interact as demonstrated by Kallstrom and Ottosson, (1982), and Amerongen *et al* (1984), in a series of full-scale sea trials.

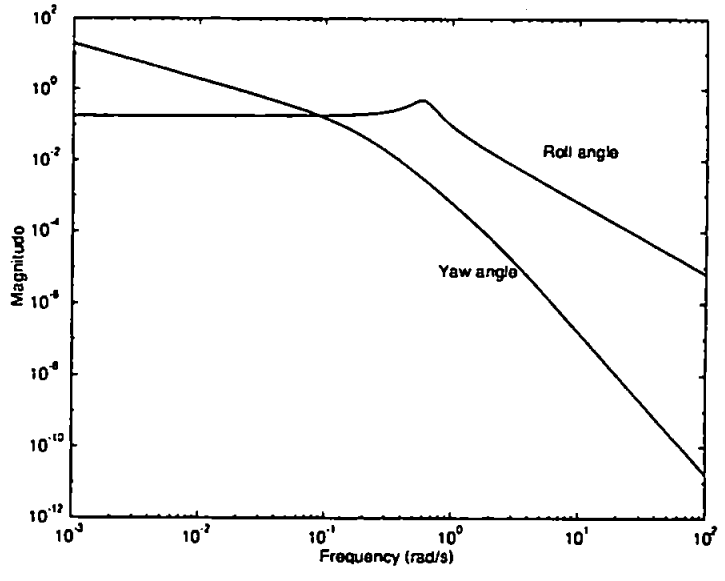

Figure 2.13 : Typical roll and yaw spectrums

The flow around the rudder is responsible for producing a lift force, if the components, parallel to the fixed x- and y-axes, of this are considered then an endeavour may be made to arrive at a theoretical evaluation of the values k_{12}, which represents the roll moment

generating capacity of the rudder, K_δ, (Lloyd, 1975). If (2.15) is recast into the form of (2.31) with the input being rudder angle then k_{12} may be determined by,

$$k_{12} = \frac{K_\delta}{I_{xx}} = \frac{K_\delta \omega_n^2}{mg\overline{GM}} \tag{2.37}$$

Specific estimation of this parameters is outlined in Appendix A, and the results tabulated in Table 2.3 at various frequencies.

Table 2.3 : Experimental and estimated theoretical values

		k_{12}, Estimated from theory		
Speed (kts)	Sea trials k_{12}	0	ω_n	$2\omega_n$
12	-0.33	-0.23	-0.21	-0.23
18	-0.42	-0.54	-0.48	-0.52
26	-0.53	-1.06	-0.94	-1.01

Given that the theoretical values are only estimates, most significantly not catering for the substantial flow effects around the rudders produced by the propellers, the comparisons correlate well at speed 12 and 18kts. The degree of variation in k_{12}, will be required in assessment of the controllers.

2.2.3 Lateral Force Estimator

The Lateral Force Estimator, LFE, is a direct measure of the lateral accelerations of a ship. These motions can be used to determine a relationship between the ability of the crew to perform routine tasks and the probability of unsecured objects sliding across the deck, and the roll motions, which shall be discussed in some detail in Chapter 4. Here consideration is given to the mathematical modelling of the LFE and it will suffice to state that, they are essentially functions of the apparent acceleration experienced by objects and people on the deck of a ship (Lloyd, 1989).

In section 2.2 the frames of reference were defined for the six degrees-of-freedom for the ship. If it is required to assess the effects of a combination of ship motions at a particular point, for example, the bridge or flight deck, then another set of axis need to be introduced. This axis, $Ox_By_Bz_B$, has the same orientation as the earth-fixed axis but with its origin at the CoG of the ship, and moves in track with it. However, unlike the Oxyz axis system (see Figure 2.1), the x, y, and z directions of the $Ox_By_Bz_B$ axis system moves with the various motions of the ship.

Although, angular motions in a ship are the same everywhere, the linear displacements depend on location. Consider a point at a position, P, (x_B,y_B,z_B) metres from the CoG. The longitudinal displacement of this point includes contributions from surge as well as the lever arm products of pitch and yaw. Assuming that the angular motions are small the longitudinal displacement of P, x_d relative to the moving origin is given by (2.38),

$$x_d = x - y_B\psi + z_B\theta \tag{2.38}$$

The lateral and vertical displacements of P are similarly given by,

$$y_d = y - z_B\phi + x_B\psi \tag{2.39}$$

$$z_d = z + y_B\phi - x_B\theta \tag{2.40}$$

Or, succinctly,

$$\begin{pmatrix} x \\ y \\ z \end{pmatrix}_d = \begin{pmatrix} x \\ y \\ z \end{pmatrix} + \begin{pmatrix} \phi \\ \theta \\ \psi \end{pmatrix} \times \begin{pmatrix} x \\ y \\ z \end{pmatrix}_B \tag{2.41}$$

where

$\times$ vector cross product

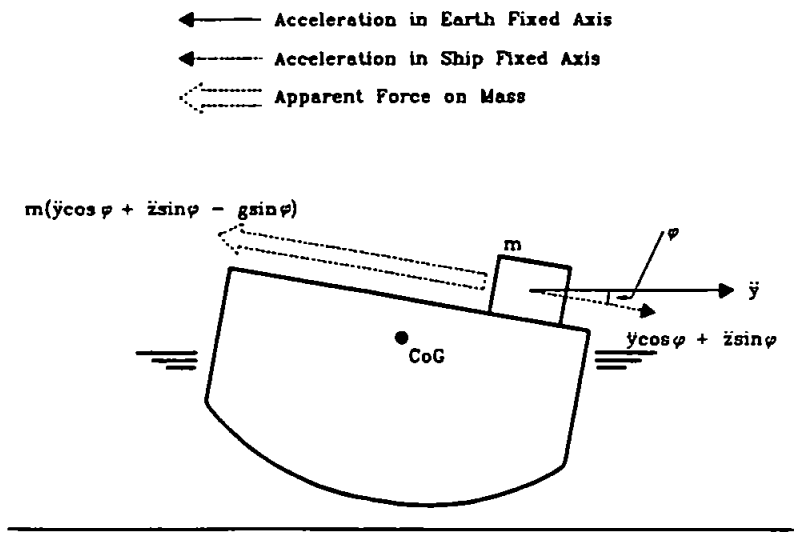

Figure 2.14 : Apparent accelerations and forces experienced by a mass

Having established these necessary preliminaries, consider Figure 2.14, which shows a mass, m, on the deck of a moving ship. If the vertical acceleration of the CoG of the mass is $\ddot{y}\,ms^{-2}$ in the fixed frame of axis with respect to the earth, then the acceleration in the plane of the deck is given by,

$$\ddot{y}\cos(\phi) + \ddot{z}\sin(\phi) \qquad ms^{-2} \quad \text{positive to starboard}$$

This acceleration will tend to slide the mass to port. Its effect may, therefore, be represented by an apparent force,

$$m(\ddot{y}\cos(\phi) + \ddot{z}\sin(\phi)) \qquad kN \quad \text{in the plane of the deck to port}$$

In addition, the ship's roll angle induces a gravitational component contribution which is given by, in the plane of the deck

$$mg\sin(\phi) \qquad kN \qquad \text{to starboard}$$

The total apparent force on the object in plane of the deck is,

$$m(\ddot{y}\cos(\phi) + \ddot{z}\sin(\phi) - g\sin(\phi))$$

Hence, the apparent acceleration perceived by the object is given by,

$$\ddot{y}_a = \ddot{y}\cos(\phi) + \ddot{z}\sin(\phi) - g\sin(\phi) \qquad ms^{-2} \tag{2.42}$$

For relatively small roll motions this simplifies to the LFE definition,

$$\text{LFE} = \ddot{y}_a = \ddot{y} - g\phi \tag{2.43}$$

From the lateral displacement motion, equation (2.39), (2.43) may be restated as,

$$\text{LFE} = \ddot{y} - z_B\ddot{\phi} + x_B\ddot{\Psi} - g\phi = \dot{v} - z_B\dot{p} + x_B\dot{r} - g\phi \tag{2.44}$$

The LFE is not only dependent upon the exact dimensional position of the point of measurement, but also the sign of each component changes depending on the relative position form the CoG. It has contributions from the sway and yaw accelerations. The former is a function of the vertical distance from the CoG, and the latter component will depend on the longitudinal distance from the CoG. These facets of the LFE shall be elaborated in Chapter 4.

Here, only the lateral plane motion has been considered. A parallel argument follows for the apparent acceleration of the mass vertical to the plane of the deck. The lateral accelerations will be shown, in Chapter 4, to contribute most profoundly to the hindrance of effective personnel operations and the LFE model (2.44) shall be utilised in an attempt to stabilise for this motion.

Sufficiently complete and reliable mathematical models of the ship dynamics for the purposes of the control design have been developed. The next stage will be the consideration of the perturbing environmental factors which impinge upon the ship system.

2.3 THE ENVIRONMENT

Thus far only the influence of the control surfaces has been considered on the ship. The very requirement for these appendages, is due to the disturbances from the environment, predominantly wind, current and waves. These phenomena are random in nature, however, their characteristics may be encapsulated by power spectral densities and categorised in terms of low frequency (<0.2 $rads^{-1}$) and high frequency (0.2-1.2 $rads^{-1}$) disturbances.

The wind may be regarded as contributing to low frequency disturbances, where the magnitude is dependent on the geometrical profile of the ship, this results in the ship developing a list angle. Although, it is possible to alter the roll angle gyroscope reference measurement from the true vertical to the "apparent" vertical, and use this signal to activate the fin stabilisers in order to correct for list, this option is not further considered here. This is due to the fact that for the type of vessels considered the roll response to wind disturbances are regarded as being insignificant.

Sea currents are also classed as a relatively low frequency perturbing force, and have detrimental ramifications on the course-keeping qualities of the ships. The usual practice is to eliminate this with the addition of integral feedback. The most significant disturbance are the waves, which have the greatest magnitude contribution to undesirable ship motions. This is the subject of investigation in the next section.

2.3.1 The Waves

At a cursory glance the sea waves would appear to be devoid of any rational coherence. However, many researchers have attempted to impose some form of meaningful mathematical description on this apparently random nature. It is concluded, (Bhattacharya, 1978), that the waves, for a particular sea, are essentially composed of an infinite sum of

sinusoids at various frequencies, magnitudes, determined from a uniform probability distribution, and random phase. In combination with this idea and the trochoidal wave concept, it is possible to predict the effects of a sea wave on the ship hull. The procedure is extremely complex and in a state of continual development. For the present purpose a simplified model will be sufficient.

The 10th International Tank Towing Conference, 1964, have considered the most favourable power spectral density that best describes the sea state, otherwise known as the Bretschneider sea spectrum, and is assumed to be unidirectional. Their recommendation takes the form of (2.45)

$$S_W(w) = \frac{172.8H_W^2}{T_W^4\omega^5}\exp\left(-\frac{691}{T_W^4\omega^4}\right) \quad \text{m}^2/\text{rad/s} \qquad (2.45)$$

where

T_w is the observed period of the waves, s

H_w is the average of the largest one third of the total observed waves known as the significant wave height, (Rawson and Tupper, 1984), m

Table 2.4 summarises the three sea states considered and the typical values associated with them and Figure 2.15, graph a, illustrates the power spectral density (PSD) as being single-peaked. Sea state 8 has been omitted since its magnitude obscures the other two.

Table 2.4 : Sea state parameter

Sea state	3	5	8
Characteristic Period (s)	5.79	9.7	18
Significant wave height (m)	0.88	3.25	11.5

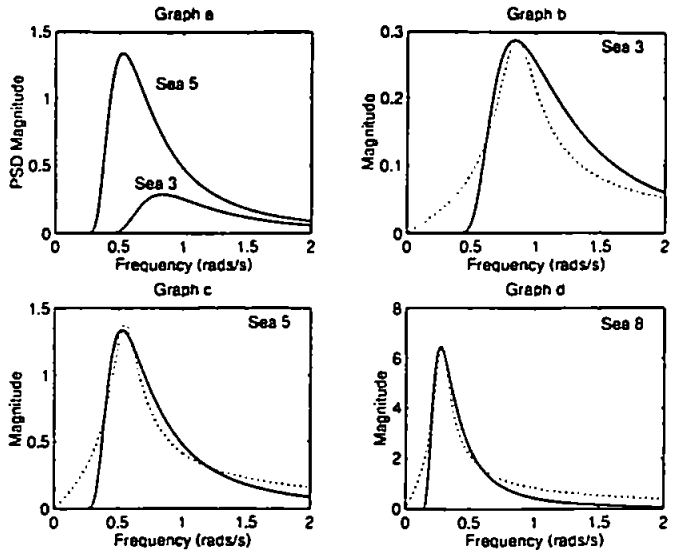

Figure 2.15 : Brestschneider sea spectrum and estimations

Although the Bretschneider sea spectrum gives an indication of the relative amplitudes and frequency components of a particular sea state, it cannot be used in isolation to other considerations when calculating the forces and moments acting on the ship. The influence of the waves are dependent, in a non-linear fashion, on the ship speed and the relative heading with respect to the wave direction as shown in Figure 2.16. These factors precipitate an alteration in the manner in which the ship 'observes' the wave, known as encounter frequency, ω_e, (2.46).

$$\omega_e = \omega_0 - \frac{\omega_0^2 U}{g}\cos(\chi) \tag{2.46}$$

where

ω_0 is the wave frequency, $rads^{-1}$

U ship speed, ms^{-1}

g gravitational acceleration, ms^{-2}

χ the encounter angle as shown in Figure 2.16, radians

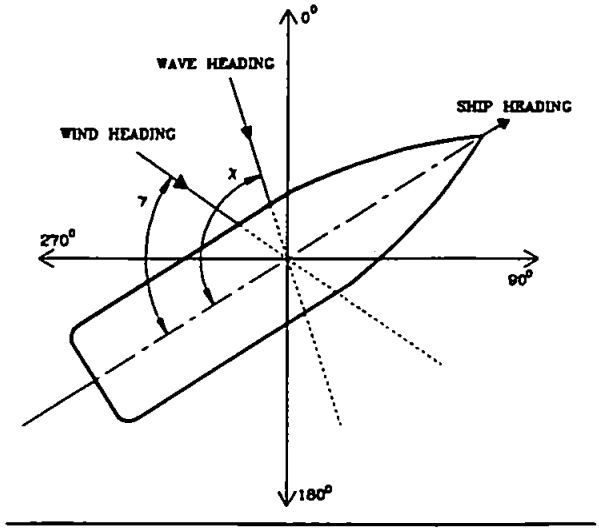

Figure 2.16 : Ship heading definition

The forces and moments, and the subsequent motion of the ship, can be approximated by integrating the hydrostatic pressure along the longitudinal axis of the vessel at each station. This is the basis of strip theory and utilised by many software routines to calculate ship motions such as the PAT-91 suite of sea-keeping programs in DRA Haslar, (Crossland, 1991). If the ship is simplified as a rectangular block, L, length, B, Breadth, and draught, D, the roll and yaw moments due to waves, of amplitude a_w and phase, can be simplified to,

$$N_W = N_1 a_W \cos(\omega_e t + \psi_W) + N_2 a_W \sin(\omega_e t + \psi_W) \tag{2.47}$$

$$K_W = K_1 a_W \cos(\omega_e t + \phi_W) + N_2 a_W \sin(\omega_e t + \phi_W) \tag{2.48}$$

where

$$N_1 = 2\rho g \exp\left(\frac{-kD}{2}\right) DL\left(\sin(KB\sin\left(\frac{\chi}{2}\right)\right)\cos(kL\cos(\chi))$$

$$N_2 = 2\rho g \exp\left(\frac{-kD}{2}\right) DL\left(\sin(KB\sin\left(\frac{\chi}{2}\right)\right)\sin(kL\cos(\chi))$$

$$K_1 = -2\rho g \exp\left(\frac{kD}{2}\right) DL\left(z_R + \frac{D}{2}\right)\sin\left(kB\sin\left(\frac{\chi}{2}\right)\right)\cos(kL\cos(\chi))$$

$$K_2 = -2\rho g \exp\left(\frac{kD}{2}\right) DL\left(z_R + \frac{D}{2}\right)\sin\left(kB\sin\left(\frac{\chi}{2}\right)\right)\sin(kL\cos(\chi))$$

and

k is the wave number = ω_e/g, $radsm^{-1}$

z_R roll lever arm, m

The equations for moments, and forces, are dependent upon encounter angle, wave heights and period, and geometry of the ship hull. Values for N_1, N_2, K_1, and K_2 may be computed in a non-dimensional manner with respect to L, D, and heading angle. The approximate spectrum can be ascertained by taking the Fourier transform of the time sequence.

2.3.2 Shaping Filters

The sea disturbance in (2.45) is not amenable to simple time series simulations which will be undertaken to assess the controllers. A linear shaping filter is required which will yield a time series wave disturbance. Considering any linear system, G(ω), which is driven by white noise, η(t), the output, y(t), has its power density spectrum given by, (2.49),

$$S_{yy}(w) = |G(j\omega)|^2 S_{\eta\eta}(\omega) \tag{2.49}$$

If the variance of the white noise, $S_{\eta\eta}(\omega)$, is unity then the output is simply the impulse response of the system.

For the Bretschneider sea spectrum a suitable emulating time process, B(t), with a single peak spectrum can be generated by,

$$B(t) = h[a(t)\cos(\omega_p t) - b(t)\sin(\omega_p t)] \tag{2.50}$$

where

ω_p corresponds to the sea disturbance frequency

h is a scaling factor

a(t) & b(t) are first order processes of the form $\dot{a}(t) + \beta a(t) = \beta\eta(t)$

β is a bandwidth factor

Therefore, the power spectral density for (2.50) will be, (2.51)

$$S_{BB}(\omega) = \frac{h^2\beta^2}{4\pi}\left[\frac{1}{\beta^2 + (\omega - \omega_p)^2} + \frac{1}{\beta^2 + (\omega + \omega_p)^2}\right] \tag{2.51}$$

Equivalently, this can then be approximated by a differential equation,

$$h\omega_p\dot{d}(t) = \ddot{\eta}(t) + \beta\dot{\eta}(t) + \omega_p\eta(t) \tag{2.52}$$

Taking the Laplace transform of this, and adjusting the parameters β and h, it can approximate the Bretschneider sea spectrum as shown in Figure 2.15, graphs b, c, and d, where the dashed lines are the spectrums of (2.52) and the solid line the actual wave disturbance (2.45), for sea states 3, 5 and 8 respectively. A close correlation is achieved. Therefore, the sea disturbance is simulated by feeding white noise to the differential equation (2.52) which is used to perturb the ship from its equilibrium.

2.4 COMPLETE SYSTEM

The individual subsystems of the ship dynamics have been investigated and modelled to be accessible to control design. This section deals with the overall control and simulation scheme.

2.4.1 Complete Lateral Motions

If the ship is viewed as a 'black-box' system, the lateral motion dynamics may be represented as shown in Figure 2.17.

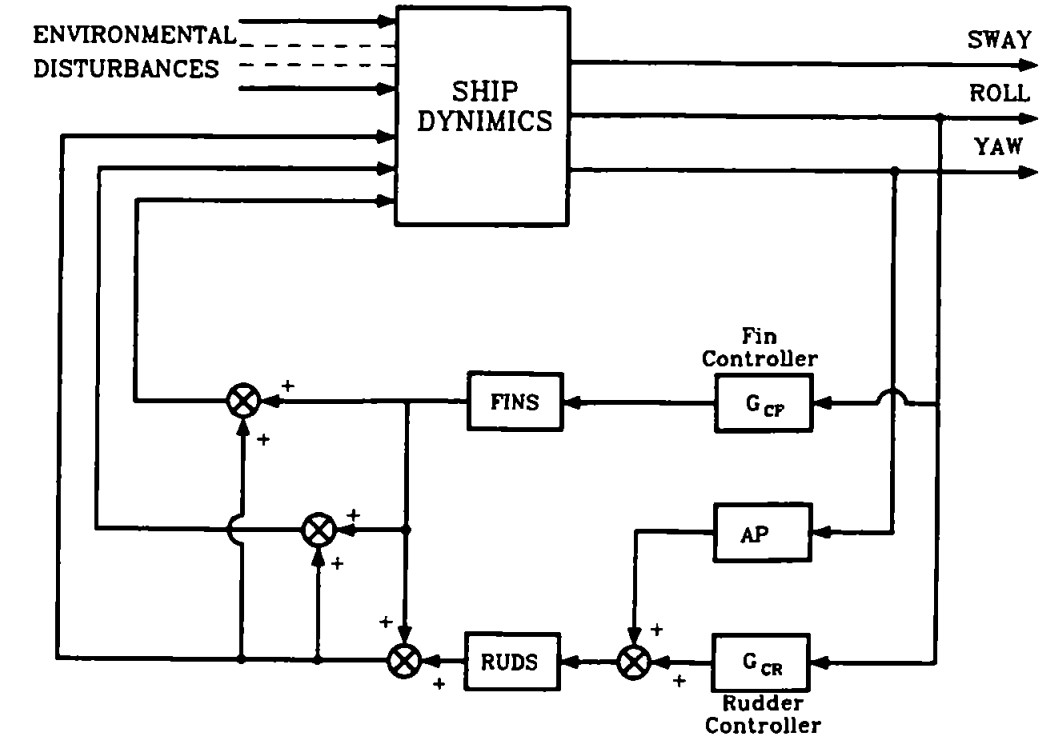

Figure 2.17 : Ship lateral motions as a 'black-box' system

The fins and rudders are activated by hydraulic servomechanisms which have been omitted for simplicity, however, their relative position has been shown in Figure 2.18. Their mathematical modelling, physical limitations and the viabilty of the existing servomechanisms will be investigated in Chapter 3.

The control surfaces, namely the fins, are dedicated to the stabilisation of roll, and the rudders are dual purpose. They have the primary function of steering the ship, course-changing, and in the autopilot (AP) mode, they are responsible for course-keeping. As discussed in the preceding sections, due to the rudder inducing an ephemeral heel angle, in the nascent stages of a manoeuvre, and without any detriment to the heading, it may be utilised in concert with the fins to enhance levels of stabilisation. Thus the aim is to achieve 'something-for-nothing'. It will be applicable to existing frigates, requiring no upgrade of rudder assembly and hydraulic motors to cope with the added loads. The mechanical implications will be discussed in the Chapter 3. Hence, this procedure is most suited to retro-fitting.

The control surfaces not only perform their desired task, but also generate other motions when excited by the controllers G_{CR} and G_{CF}, as seen in Figure 2.17. Considering the fins, if there is a dihedral angle then sway motions will also result. For the typical vessel under investigation this was shown to be negligible (section 2.2.2.1). It is known that the longitudinal distance between the CoG and the fin-moment axis will not engender any significant yaw motions. The rudder, similarly produces other motions, in particular sway. This may be useful in reducing LFE and will be considered further in Chapter 4. It has been established that the rudder's dual purpose can be considered independent in the frequency domain, and hence in the time domain (section 2.2.2), therefore, the controller design procedure may also mirror this independence. Furthermore, in order to ensure that no interference occurs, suitable filters may be placed in the feedback loops. These motions produced by the control surfaces are then reintroduced into the ship dynamics block which in turn effect the new outputs. Taking these justifiable simplifications into account the ship system, Figure 2.17, may be altered.

2.4.2 Control and Simulation Configuration

Figure 2.18 shows the modified layout of the control scheme in relation to the lateral motions. The roll disturbance spectrum, B(t), generates an effective moment. This is then modified by the roll/sea transfer function to allow the roll stabilisation loop to have an additive output disturbance configuration.

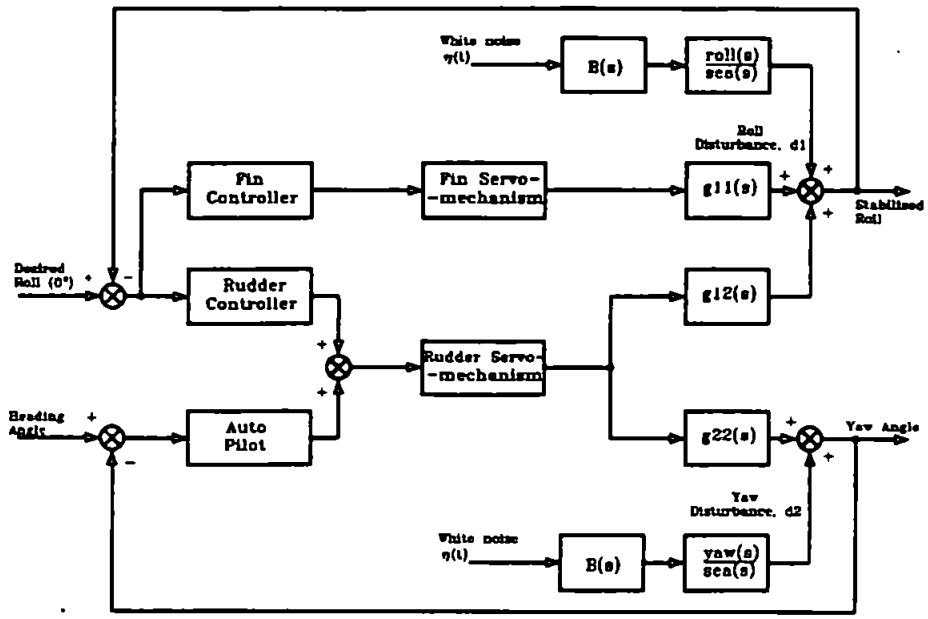

Figure 2.18 : Modified control synthesis structure

The independent nature of the rudder and fin loops are apparent. This suggests a natural control synthesis approach; design of the fin and rudder roll stabilisation loops separately Surprisingly, there are few instances in literature where the integrated fin and existing rudder approach has been adopted for roll stabilisation. The usual course of analysis being to pursue RRS/Autopilot design with a view to upgrade the rudder assembly and associated peripherals. (Grimble *et al*, 1993) conducts a paper study with an unrealistically fast moving rudder for the existing frigates. There may be some advantage in designing a multivariable controller, for the system (2.53) derived from Figure 2.18, and using the state space description of the ship (2.17), as suggested by (Broome, 1979). This option will be examined in Chapter 5.

$$\begin{pmatrix} \text{roll} \\ \text{yaw} \end{pmatrix} = \begin{bmatrix} g11(s) & g12(s) \\ g21(s) & g22(s) \end{bmatrix} \begin{pmatrix} \alpha \\ \delta \end{pmatrix} \tag{2.53}$$

The model of Figure 2.18 will be used in pc based simulations running on Matlab® software to afford a simple comparison of controller behaviour.

2.5 DISCUSSION AND CONCLUSIONS

Complex mathematical models of ship dynamics were introduced in terms of non-linear and linear parts. From these, it was shown, that it is possible to extract simplified models by retaining the dominant dynamics which are subsequently amenable to controller design. By the exclusion of other dynamics, and the simplifications made, it was shown that the accuracy of the transfer function models was not sacrificed.

An examination of the ship dynamics has demonstrated that the various parameters which encapsulate the motions are dependent upon several factors; sea wave frequency and heading, encounter frequency, ship speed, geometric construction of the appendages, loading conditions, all these factors act in conglomeration to engender a non-linear system. However, by considering the prominent motions in the lateral plane and making some assumptions, the pertinent model of the ship subsystems have been developed which will adequately predict its motion.

An identification and evaluation was also construed which would quantify the likely relative changes in the various parameters with a view to further controller analysis in the presence of this uncertainty.

Utilising filtering theory, a sea wave disturbance model was also introduced which closely emulates the Bretschneider sea spectrum. Finally, by contemplation of the complete system, in terms of stabilisation loops, some proposals were construed whereby a methodology may be envisaged for the control design.

CHAPTER 3

LIMITATIONS of the FIN and RUDDER SERVOMECHANISMS

3.1 INTRODUCTION

Many control loops have servomechanisms as actuators whether in the mode of regulation or for set-point changes. The fin/rudder roll stabilisation loops are tracking problems and require servomechanism to move the control surfaces which offset the environmental disturbances. It is crucial that they are able to respond adequately to the controller demand signals with minimal of transients. Since the objective of this project is to utilise the existing servomechanisms, it would be judicious to ensure that they, in particular the rudders, are capable of performing the desired task.

The repercussions of not meeting these criteria are multifarious which are examined in terms of maximum slew rates. A novel scheme is presented, the Anti-Saturation Algorithm (ASA), which will preserve the servomechanism within its envelope of operational capabilities. The ASA will operate as a function of the demand signal's on-line RMS value. This solution can be considered as a form of non-linear precompensation and its application is generic.

3.2 THE REQUIREMENTS

The successful application of any servomechanism depends on its mechanical abilities to respond to controller demands. Amongst the restraining factors are maximum angles of excursion and, more significantly, the maximum slew rate. This quantity is related to hydraulic valve and motor capacities of the device which essentially represent the power output of the servomechanism power.

The maximum permitted angles of travel are $\pm 30^0$ and $\pm 35^0$ for the fins and rudders respectively. Representative slew rates, for the typical fins and rudder systems fitted to Royal Naval frigates, are $27^0 s^{-1}$ and $6^0 s^{-1}$, respectively.

The fins are specifically designed for stabilisation of the ship which is reflected in their large slew rate. However, given that the rudders move approximately four times slower, an aim of this project is to assess the feasibility of utilising the existing rudders in congress with the fins to accrue enhanced levels of roll reduction.

Consider Figure 3.1, which shows a typical roll spectrum for the class of ship under investigation, and the estimated spectrums of the fin and rudder servomechanisms when operating within their linear regions (Marshfield, 1979). For satisfactory operation of a servomechanism it must be able to move as fast as the application to which it is applied. This rate of response is a direct function of bandwidth

Although the rudder servomechanism bandwidth encompasses the dynamic region of the roll spectrum, indicative of its viability in roll stabilisation, its bandwidth is rather close to the roll spectrum. This suggests that should the rudder servomechanism enter slew rate saturation, on account of its inablity to reciprocate to controller demand signals, then it may

have a degenerative effect on the bandwidth rendering it unacceptable in roll stabilisation. The faster fin slew rate translates, naturally, into a greater bandwidth, and is deemed to be more than adequate for roll stabilisation and will not be considered further.

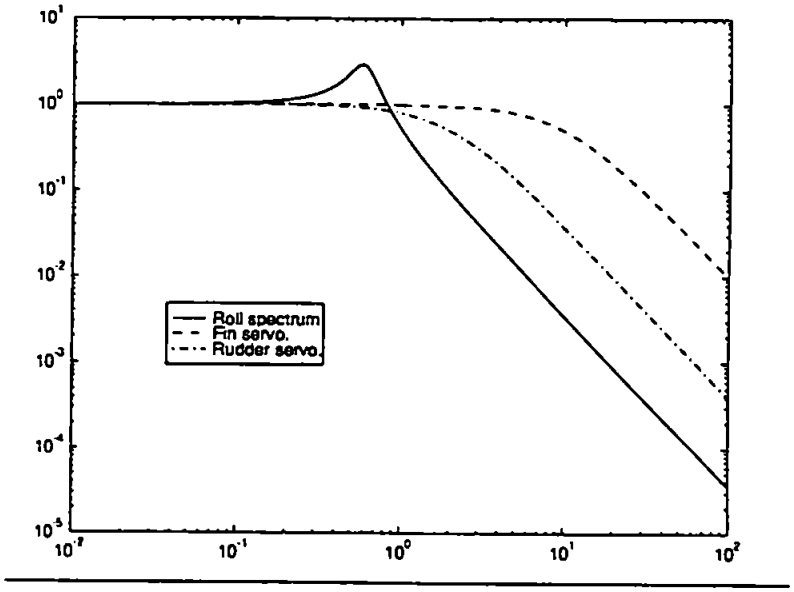

Figure 3.1 : Roll and servomechanism frequency spectra

As a tracking servomechanism, a situation may transpire such that a sea disturbance induces a correspondingly large control signal which cannot be reciprocated by the rudder servomechanism. The inevitable consequence of these demands is to force it into non-linear operation with physical saturation ensuing. These periods of saturation have pernicious repercussions on all aspects of the system; producing excessive wear and stress on the machinery thereby reducing the Mean-Time Between Failure, (MTBF) and compromising reliability. It will create intolerable phase lags precipitating system instability, or at best, amplify the effects of the disturbance. Due to the non-linear signals generated, the resulting spurious frequency components will cause operational interference. The frequency response will exhibit 'jump-resonance' and finally its bandwidth will be depleted. Irrespective of the quality of the governing control law, the non-linear operation of the servomechanism will invalidate its fundamental linear mode of functioning.

Providing that the rudder operates in its linear region it behaves as a viable stabiliser. This is now further considered through modelling and analysis of the time and frequency responses. A novel contingency will be proposed to prevent the occurrence of rate slew saturation.

3.3 SERVOMECHANISM MODELLING

The linear theory of servomechanisms is well promulgated in many elementary textbooks of control engineering for example Raven, (1978). Using linear transfer functions it can be modelled as shown in Figure 3.2.

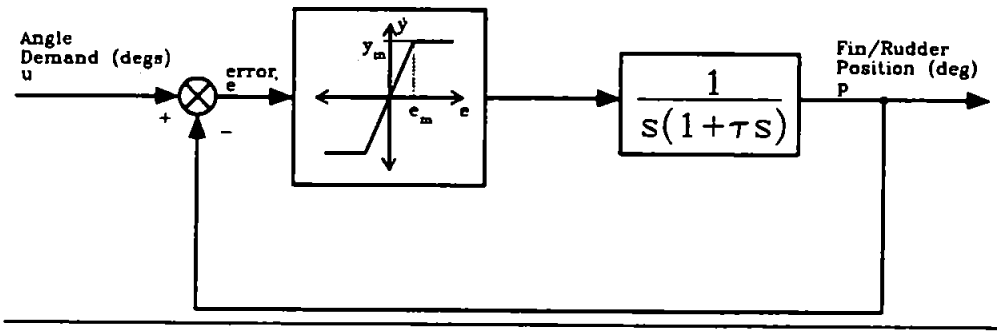

Figure 3.2 : Servomechanism non-linear model

Here the maximum excursion non-linearity has been omitted for simplicity. The transfer function part contains pure integral action to model friction and inertia. A first order lag represents the amalgamation of electrical, mechanical and field-winding delays in the time constant τ.

3.3.1 Time Response

The servomechanism faithfully replicates the demand signal, however, when the error, e, exceeds e_m, 3^0 for the rudder servomechanism which itself is a function of the physical attributes of the machinery, the non-linearity is invoked and the output of the saturation block is a constant dc signal of magnitude y_m, which is the maximum slew rate. This is

illustrated in Figure 3.3, where the rudder servomechanism is being saturated by a mono-sinusoid.

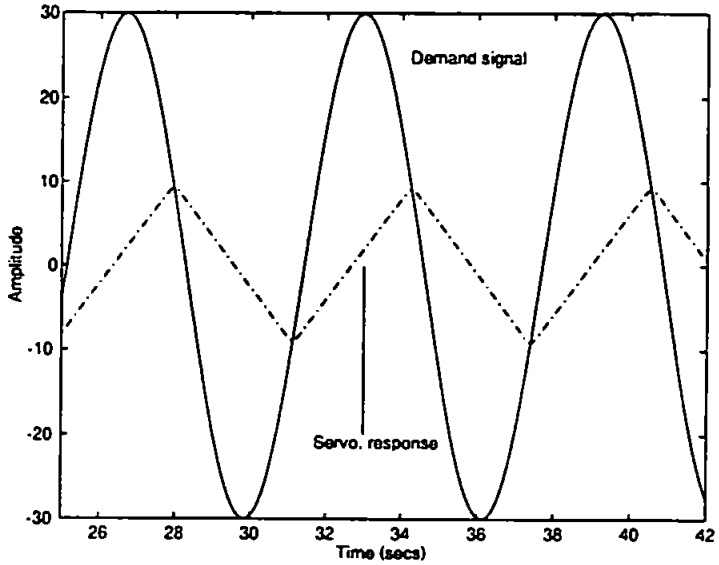

Figure 3.3 : Saturation response of servomechanism

The gradient of the servomechanism response is 6^0s^{-1} indicative of operation in the saturation region. Considerable phase lag is apparent which will exacerbate the disturbances or induce system instability. The shape of the servomechanism's output does not resemble a sinusoid as would be expected from linear theory, however, the triangular shape's frequency spectrum may be given by equation (3.1)

$$y(t) = \frac{8A}{\pi} \sum_{n=0}^{\infty} \frac{1}{(2n+1)^2} \cos((2n+1)\omega t) \qquad (3.1)$$

This shows that only frequency harmonics higher than the fundamental are generated. These spurious harmonics will interfere with other aspect of the control system and will invalidate the control law.

It may be envisaged that the rate of change of the exciting signal will invoke slew rate saturation, however, analysis of the input signal and corresponding servomechanism

operation reveals a more complex relationship. If the exciting function is of the form (3.2) its derivative is given by (3.3),

$$u(t) = A\sin(\omega t) \tag{3.2}$$

$$\dot{u}(t) = A\omega\cos(\omega t) \tag{3.3}$$

Irrespective of the amplitude Aω of (3.3), if the magnitude, A, of (3.2) does not exceed e_m, as defined in Figure 3.2, the response will never encroach into non-linear section of the saturation element, and the output will have gradient Aω. However, when A is greater than e_m, then slew rate saturation is possible and is dependent on the values of A and ω or a combination of both. Therefore, the saturation non-linearity can be seen to be a function of error, e, and frequency, ω, and can be represented by N(e,ω) as shown by (3.4),

$$N(e,\omega) = \frac{|e|y_m}{\sqrt{e_m + |e|^2}} \tag{3.4}$$

where

e_m minimum error for slew rate saturation

e error signal

y_m maximum slew rate

The response of (3.4) is shown in Figure 3.3 with the idealised version utilised in simulations.

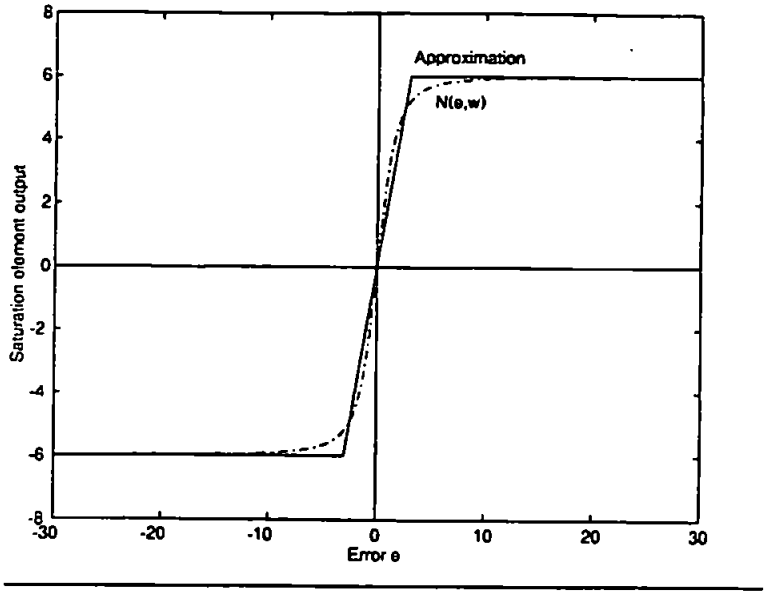

Figure 3.4 : Non-linear saturation element

The analysis of the servomechanism now proceeds in the frequency domain with a view to synthesis of the ASA.

3.3.2 Frequency Response and Bandwidth

Since, there is a non-linearity present the frequency response cannot be arrived at in a simple manner. Instead the input describing function method will be utilised (Gelb and Velde, 1968) to construct it. It is further assumed that the servomechanism dynamics sufficiently filter the signal, such that in the feedback loop, at the summing junction, the signal is close to a sinusoid.

In practice low pass filters are employed to suppress high frequency components of the demand signal to the servomechanism in order to avoid slew rate saturation. Therefore, it can be assumed that the amplitude is solely responsible for inducing saturation. It is then conjectured that this will have an influence on the frequency spectrum.

The transfer function between the error, e, and the input, u, see Figure 3.2, is given by (3.5),

$$\frac{e(s)}{u(s)} = \frac{(1+\tau s)s}{(1+\tau s)s + N(e,\omega)} \tag{3.5}$$

Replacing s by jω and taking the magnitudes in the usual way yields,

$$|e| = \frac{\omega\sqrt{1+\omega^2\tau^2}\,|u|}{\sqrt{(N(e,\omega)-\omega^2\tau)^2+\omega^2}} \tag{3.6}$$

Squaring (3.6) and transposing results in

$$N(e,\omega)|e| = \omega^2\tau|e| \pm \omega\sqrt{(1+\omega^2\tau^2)|u|^2 - |e|^2} \tag{3.7}$$

The right-hand side of (3.7) represent a series of ellipsoids intersecting with N(e,ω) which is given by (3.4). These are generated by either keeping the demsnd magnitude u constant and varying the frequency ω, or vice-versa. The first graph in Figure 3.5 is an example where the frequency, ω, is held constant and the magnitude, u, allowed to vary whilst in the second graph the input magnitude is at a constant value and the frequency, ω, is altered (Levinson, 1953).

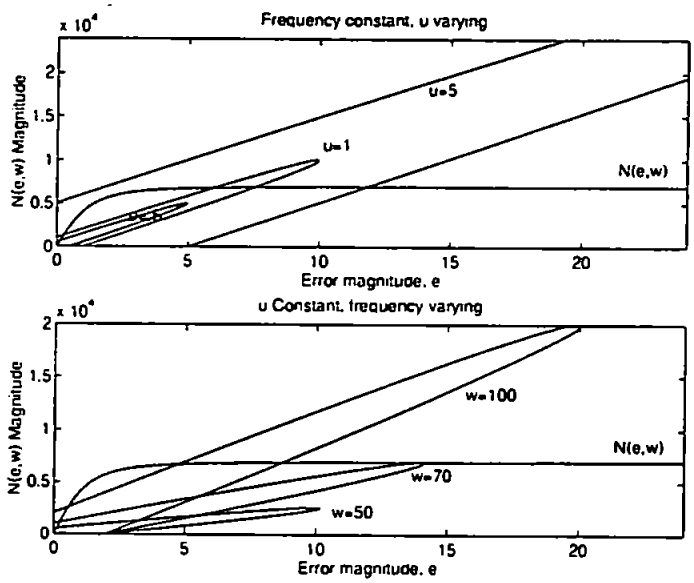

Figure 3.5 : Saturation curves and ellipses

The intersections of e at a particular frequency and input magnitude, u, can now be calculated by simultaneously solving equaions (3.4) and (3.7), or derived by inspection. Then the spectrum of the non-linear servomechanism, p(s)/u(s), as defined in Figure 3.2, may be constructed as shown in Figure 3.6, where u was a constant and the frequency varied. If u is also altered a series of similar shaped graphs will result but with the characteristics of the spectrum shifted in frequency.The idiosyncratic jump-resonance is due to multiple intersections of the relevant ellipsoid with N(e,ω).

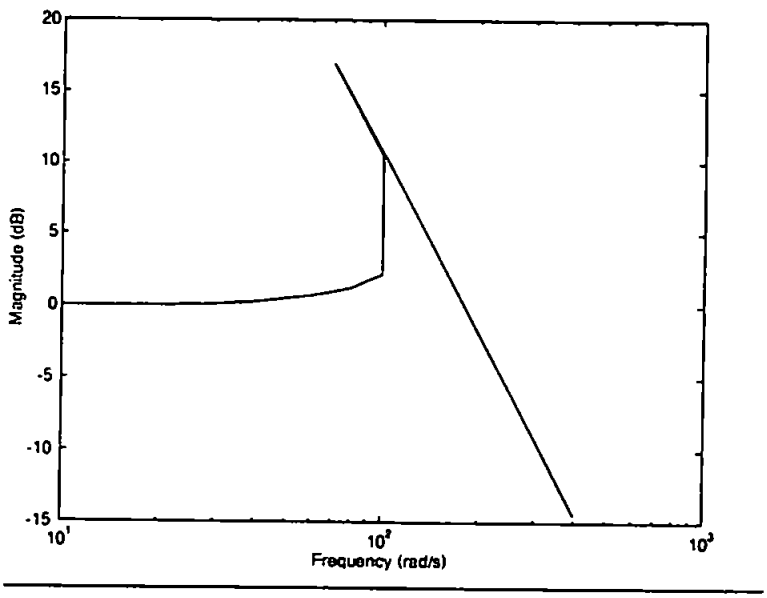

Figure 3.6 : Jump-resonance of servomechanism

It is possible to simplify the servomechanism to a pure inertial load since only the bandwidth is of concern in development of the ASA. Therefore, the expression for the complete frequency response of the rudder servomechanism (3.7) reduces to equation (3.8) and the jump resonance is eliminated. This implies that the family of ellipses reduce to straight lines with single intersections.

$$N(e,\omega) = \pm\omega\sqrt{u^2 + |e|^2} \tag{3.8}$$

A series of frequency response graphs may now be generated by employing the input describing function method with the input magnitude selected at three different RMS values of 5^0, 10^0 and 20^0. The slew rate is a variable parameter set at 3, 6, 9, 12, 15 and 18^0s^{-1}. Figure 3.7 shows the three graphs produced.

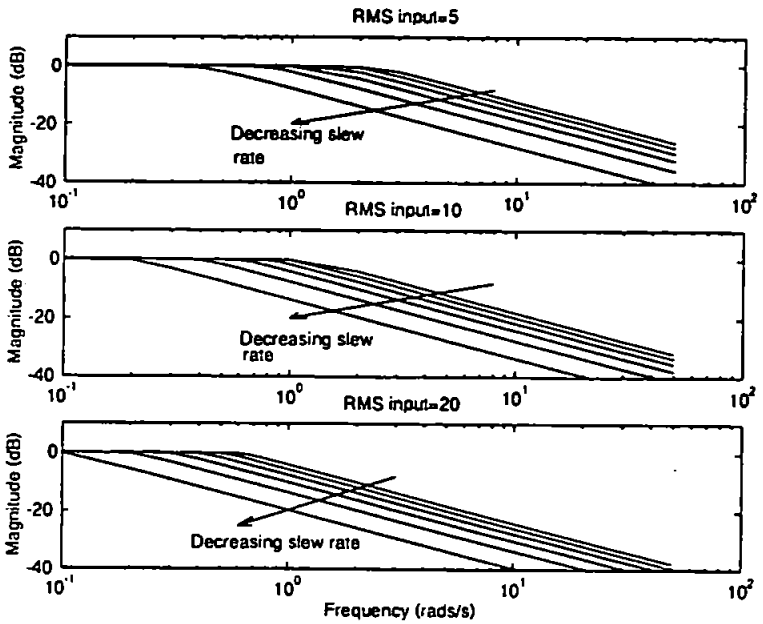

Figure 3.7 : Bandwidth at various RMS values with slew rate as parameter

It is apparent from these spectra that the bandwidth diminishes not only with increasing RMS demand input but also with decreasing slew rate. To illustrates this more vividly the -3dB points are read from the frequency spectrum and plotted on graph with bandwidth against slew rate at the prescribed RMS values, as shown in Figure 3.8.

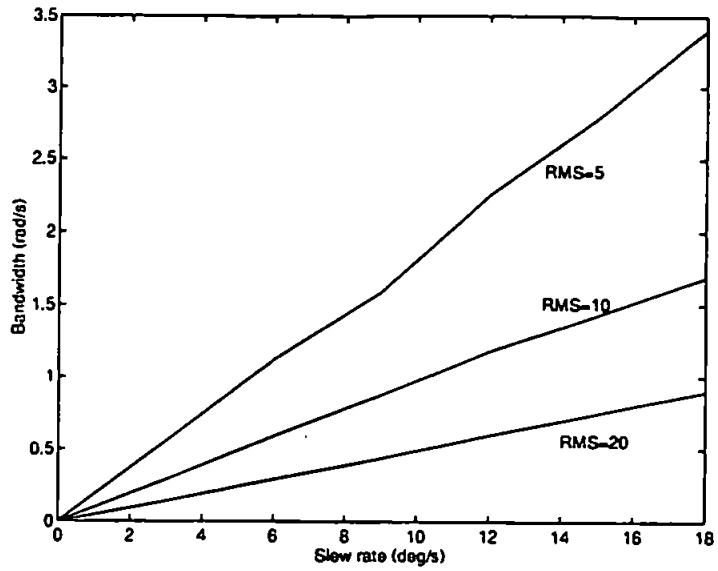

Figure 3.8 : Bandwidth variation as a function of RMS demand

The information exhibited in Figure 3.8 may be utilised in a scheme to prevent saturation occurring and thus circumvent its detrimental consequences as discussed in section 3.2. If the bandwidth of the system that is to be controlled is known, for example the ship roll bandwidth is approximately 1.5 $rads^{-1}$, then given the slew rate of the accompanying servomechanism and extrapolating from the preceding graphs, it is possible to determine the maximum permitted RMS demand to drive the servomechanism. Should this threshold value be exceeded, then the bandwidth will diminish to unacceptably low levels with ensuing saturation, thus rendering the effect of the controller redundant. For the rudder servomechanism case the maximum RMS value lies between $5\text{-}7^0$ in order to maintain an acceptable bandwidth. This information now forms the basis of the ASA.

3.4 PREVENTION OF SATURATION

Saturation avoidance of servomechanisms has rarely been reported in literature, one of the few examples being by Klugt, (1987). He achieves this by monitoring the gradient of the demand signal, u, and instantaneously attenuating it should it exceed the maximum permissible slew rate. A memory element is incorporated to sustain the gain for some time

in order to compensate for phase lags introduced, and to allow the new signal to propagate through the system. The algorithm monitors the gradient of the demand signal and not the actual signal entering the servomechanism. Since, he gives no guidance to the selection of the delay time of the memory element and having run several simulations at various values, without success, there will be no method of comparison for the ASA results.

A new arrangement is proposed here which functions on RMS values as described in section 3.3.2, for the prevention of saturation as shown in Figure 3.9. It consists of three elements; the on-line RMS calculator, an ASA block to evaluate a new gain accordingly, and a variable gain, k. The algorithm monitors the actual signal entering the servomechanism and by virtue of a 'moving-average' type procedure to calculate the RMS, requires no memory retention. Essentially the system in the dashed lines is a RMS dependent gain.

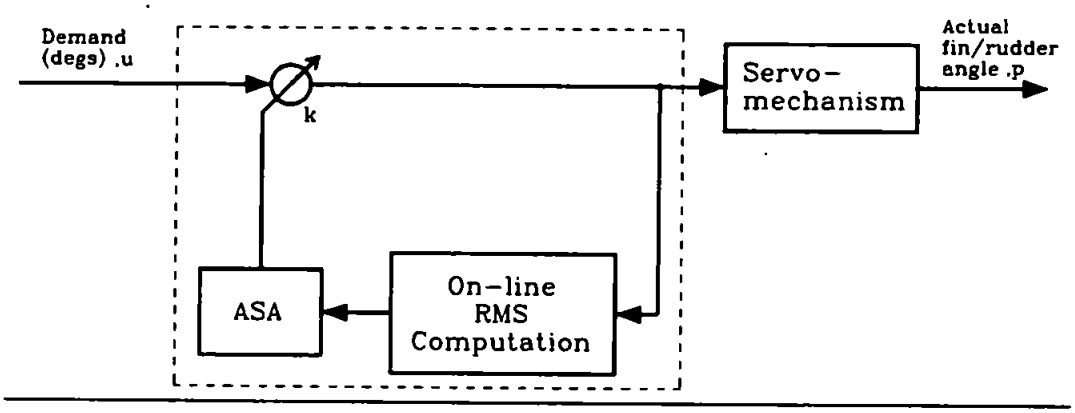

Figure 3.9 : The ASA scheme in relation to the servomechanism

The ASA algorithm is presented in the form of a flow chart shown in Figure 3.10. At each sample period, 0.1 seconds in this case, the controller generated demand value is ascertained and stored in the next slot of an array. The length of the array must be such that it can accommodate at least one complete cycle of the lowest envisaged frequency component, this was selected to be 400. This forms a moving window on the data and the

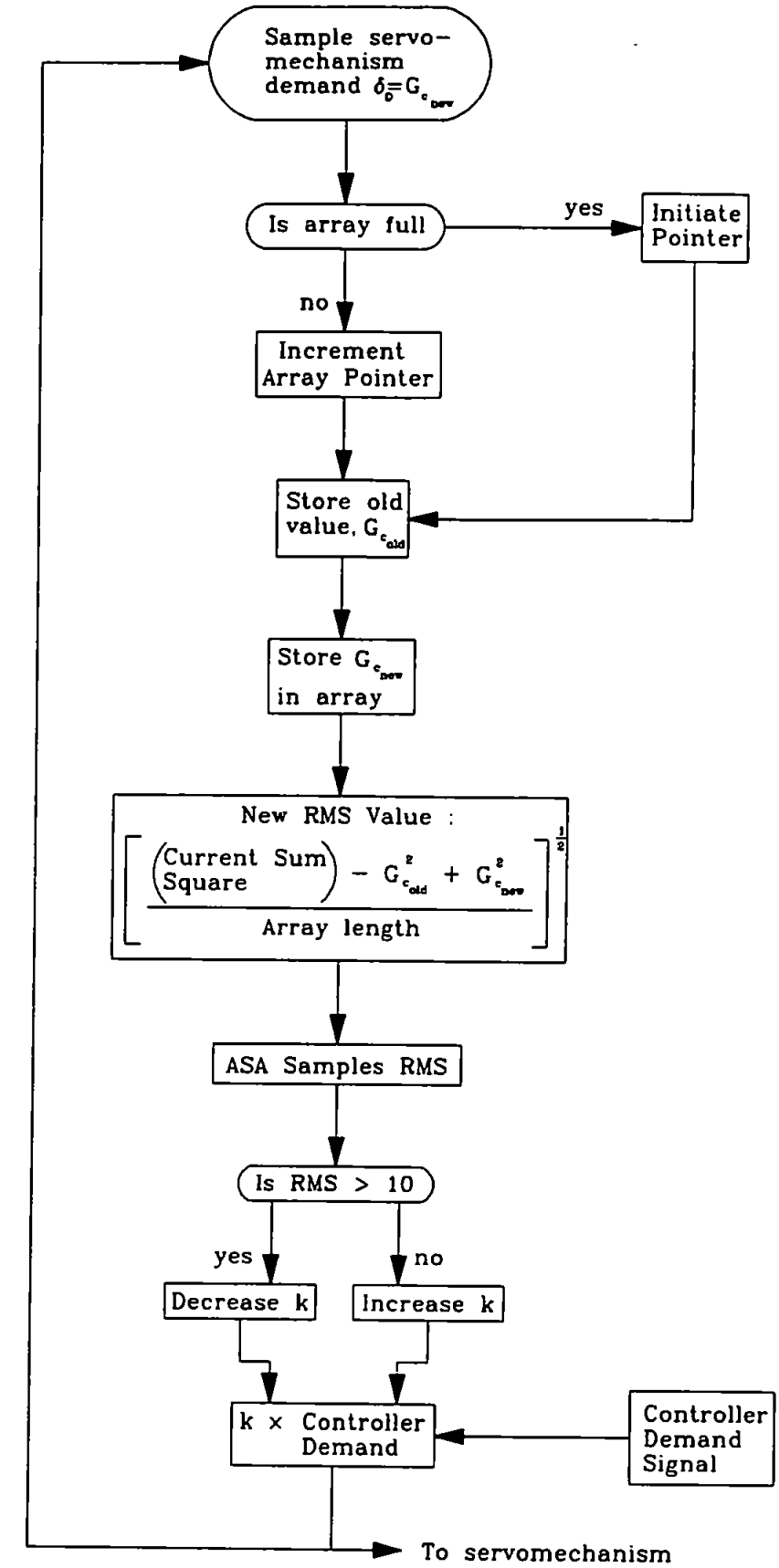

Figure 3.10 : Flow chart of the ASA

RMS value computed at each sample period. The ASA block samples the new RMS value, if it exceeds the desired level the gain is decreased by steps, 10% in this case, otherwise it is increased by default in the same step sizes. The ASA block samples the RMS at a different frequency than the on-line RMS calculator to allow for transients in the calculation this parameter was selected at 10 seconds.

3.5 SIMULATIONS STUDY

A simulation study was conducted using the control scheme shown in Figure 2.17, with only the rudder stabilisation loop engaged. The RRS controller, G_{CR} designed was a simple PID, proportional-integral-derivative, type as will be discussed in the succeeding Chapters. Using a large amplitude disturbance analogous to a high sea state it was ensured that the servomechanism would saturate. The ship was simulated at various heading with respect to the sea as defined in Figure 2.15. As well as collating other data, the percentage reduction in roll was calculated.

Firstly, consider a segment of the simulation time response of the servomechanism as shown in Figure 3.11. Graph A exhibits the controller demand signal, solid line, and the corresponding rudder motion, triangular line, without the ASA scheme engaged. It is seen that the controller demand signal is severely saturating the capabilities of the rudder servomechanism. If this situation persists the consequences already discussed will ensue. With the ASA active the results are shown in graph B, where the solid line is the modified controller demand and the dashed line the rudder servomechanism response. It is manifest that the servomechanism is able to adequately reciprocate the demand, without saturation and with insignificant phase lag.

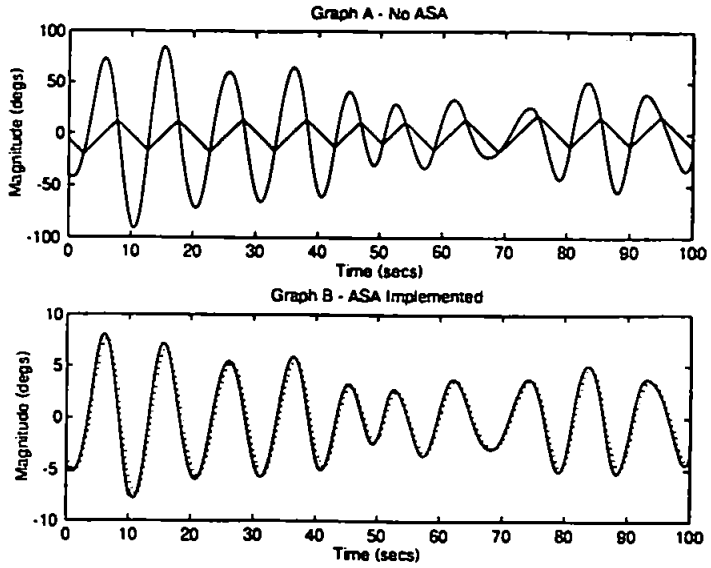

Figure 3.11 : Time response of the servomechanism

The saturation of the servomechanism responses, from Figure 3.11, can be easily appreciated if its output is differentiated as illustrated by Figure 3.12. The pulse like response is that of the saturating scenario; from the pulse amplitude of 6^0 it is lucid that saturation is in progress. The other graph is the non-saturating response and remains within the 6^0s^{-1} limitation.

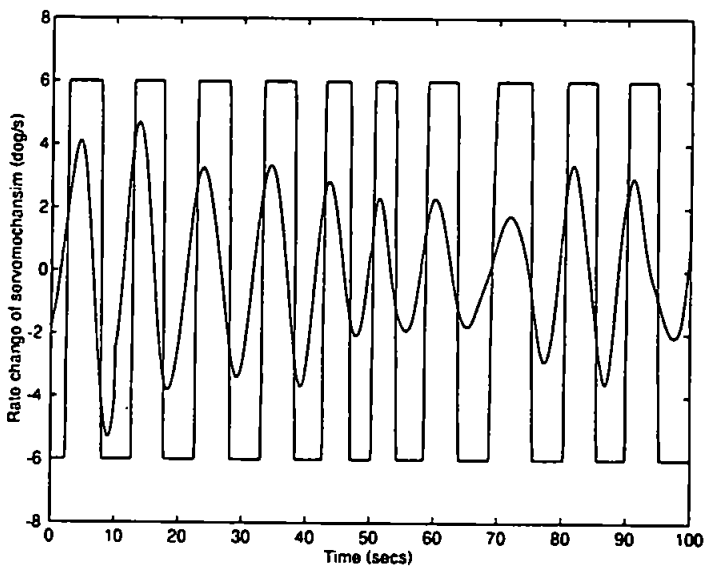

Figure 3.12 : Rate change of the servomechanism responses

The ASA functions by attenuating the demand signal by a variable gain, k, as seen by Figure 3.9. The change in gain at each ASA evaluation period is shown in Figure 3.13. After an

initial period of seeking the correct level, the gain value k settles to ensure that the RMS demand does not exceed 5-7^0 with some slow variation as the sea waves excite the roll of the ship which correspondingly increase and diminishes.

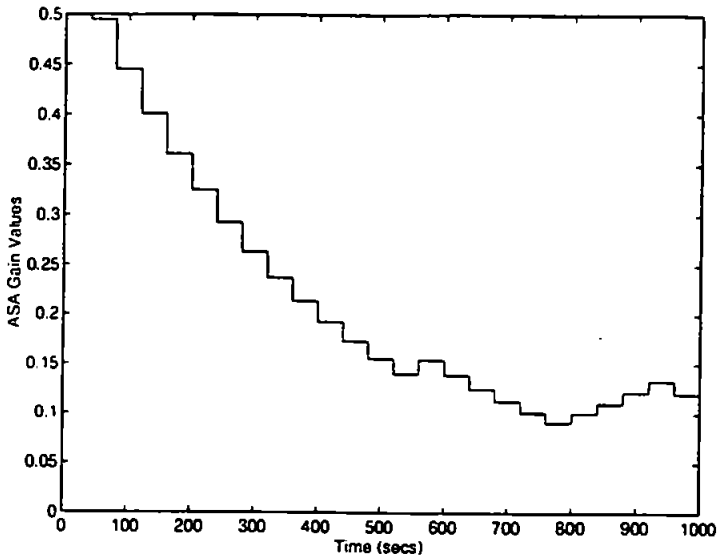

Figure 3.13 : Variation of ASA gain k

A simulation was initiated for headings of 15^0 to 165^0, with and without the ASA operating. Evaluating the roll reduction as a percentage yields the plots in Figure 3.14. With the ASA engaged the reduction levels are considerably higher. Although, the magnitude of the saturating servomechanism response is much larger, as shown by Figure 3.11, the greater roll reduction is attributed to the ASA-modified signals possessing comparatively insignificant phase lag. Indeed as predicted roll magnification occurs at higher encounter frequencies, indicative of instability, whereas the ASA maintains positive reduction, albeit at a reduced level.

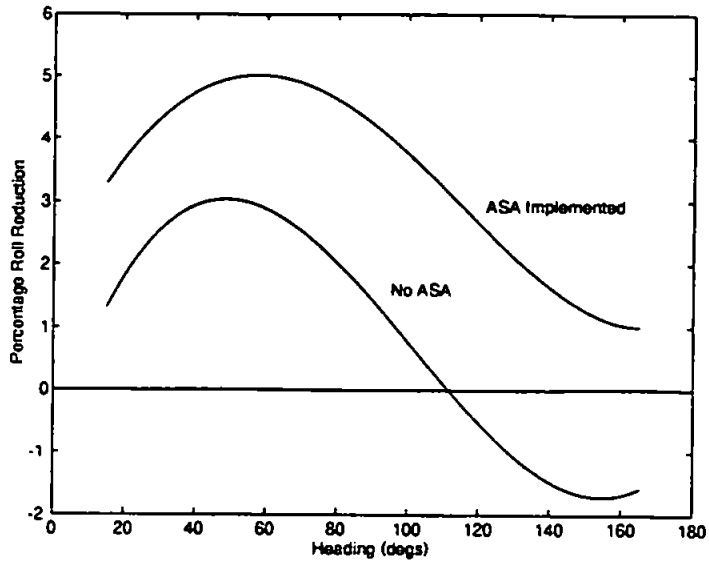

Figure 3.14 : Percentage roll reductions for ASA

Considering the RMS values of the controller generated demands, as shown by Figure 3.15, the action of the ASA is confirmed. It restrains this value between approximately 5-7^0 RMS.

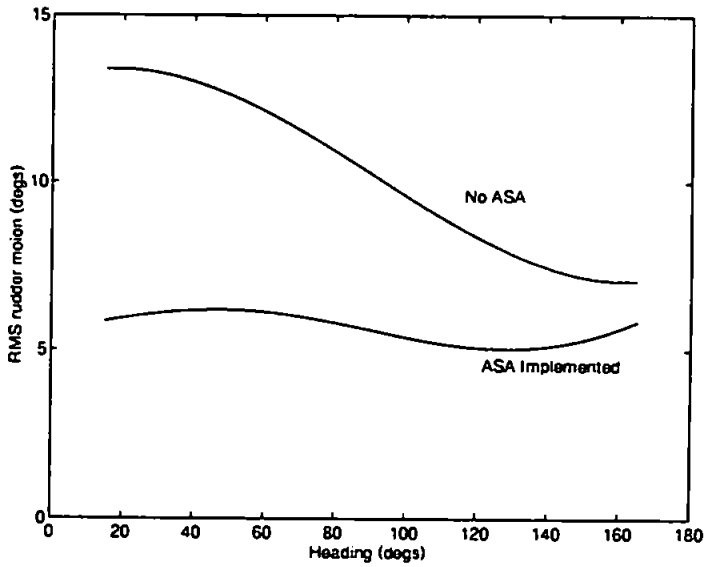

Figure 3.15 : RMS values of the controller demands

3.6 DISCUSSION AND CONCLUSIONS

The pernicious consequences of the rudder saturation have been outlined, not only in terms of the mechanical implications but also the controller behaviour. This was further investigated in time response. Utilising the input sinusoid describing function method

allowed frequency spectra to be developed, thus permitting a theoretically sound relationship between bandwidth degradation with respect to controller generated demands in terms of RMS values. By extrapolating from this data, tolerable values of RMS were derived in order to maintain the desired bandwidths of the servomechanisms.

This approach was adopted in implementing the ASA scheme to inhibit the servomechanism from encroaching into its non-linear region. The RMS values were ascertained by on-line monitoring and a gain altered according to the ASA strategy.

The simulation results demonstrated the efficacy of this scheme in its objectives, assuaging any apprehensions that the servomechanism may saturate. As anticipated the system accrues enhanced levels of stabilisation. Realising the advantages of this type of non-linear precompensation, it was decided that the ASA will be incorporated into further simulations, and sea trials software, as a matter of routine.

CHAPTER 4

LATERAL FORCE ESTIMATOR STABILISATION

4.1 INTRODUCTION

In some ships which have been stabilised for roll, experienced crew members often report the 'roughness' of the motion. This is taken as an indication of the severity of the lateral accelerations, as discussed in Chapter 2.2.3 in consideration of the Lateral Force Estimator (LFE) development, of the ship. This motion is similar to the 'apparent vertical' as demonstrated by Bell (1965) which may be described as the non-inertial apparent vertical if the ship were to be considered as a weight at the end of a swinging pendulum. Therefore, paradoxically, roll motions require to be generated in order to alleviate apparent vertical motions: analogous to a highway being inclined at an angle in order to permit automobiles to travel fast around wide bends. This is the fundamental divergence between LFE and apparent vertical motions: in LFE stabilisation roll and sway motions must be controlled.

It is acknowledged that one of the more meaningful criterion which may be utilised to assess impediments to crew effectiveness is the LFE rather than the roll motions alone. The effect of the LFE results in the crew member stumbling whilst performing a task, sliding along the deck, or under sufficiently extreme conditions, the only alternative may be to cease

operations and grasp onto an object secured to the deck in order to maintain balance. However, the roll motions criterion may be perceived as an overall assessment of the vessel as a weapons platform in terms of, for example, manning and reloading of weapons systems, helicopter launching and recovery, replenishment at sea, sensor operations and general functioning of the machinery, as well as a gauging the impact on human operators.

In this Chapter, which is essentially a diversion from the main objectives of fin/rudder roll stabilisation of the thesis, a rational framework is presented from literature to assess the impact of LFE on personnel operations. Utilising the LFE mathematical representation of Chapter 2.2.3 the performance of specifically designed RRS controllers for LFE reduction are examined. The study then proceeds with an attempt to design LFE controllers which utilise the rudders. There have been only three reports (Tang and Wilson, 1992a and 1992b, and Tang *et al*, 1994) in literature of any endeavour made to stabilise for the LFE motions in a ship. These will be considered, developed, refined and suggestions made to improve the strategy.

4.2 HUMAN FACTORS

Comparison assessments of the efficacy of roll stabiliser controllers are normally conducted and presented in terms of the percentage reductions achieved in a particular sea state. The units of this are RMS in degrees. As an absolute technical criterion this is sufficient. However, no correlation is attempted between the stabilised RMS roll motions of a ship and the performance of its crew. Intuitively one may suspect that the greater the roll stability so correspondingly should crew effectiveness increase. The percentage RMS roll reduction criterion does not, however, consider that a member of the crew encounters greater impedance in a task if grip cannot be maintained on the surface of the vessel. It is conjectured that it would be easier, for an experienced crew member, to adopt a

pre-emptive stance against the oscillatory nature of roll, rather than against the unpredictable motions of lateral acceleration. Therefore, the assertion that roll reduction equates with increased human performance, may be, a tenuous reflection of reality.

Loss of grip is induced by lateral accelerations of the ship in parallel with the deck, in essence the LFE, which is analogous to having a rug pulled from under one's feet. Thus compelling the crew member to seek a deck-secured object in order to re-establish balance. It then becomes extremely difficult to accomplish manual tasks, as outlined in section 4.1, when subject to the LFE motions. The assumed definition of the LFE will be slightly modified in section 4.3.1.

If the stabilised roll RMS is adopted as a criteria for crew performance then, initially by concluding from extensive human performance sea trials on board USS Glover, Warhurst and Cerasani (1969) and subsequently Baitis and Schmidt (1989) suggest the following quantitative measures shown in Table 4.1.

Table 4.1 : Effect on human operations with RMS roll as criterion

Level	Effect on Personnel Operations	RMS Roll (degs.)
1	No effect	0-2
2	Slight, beginning to interfere with ship operations	2-3.7
3	Moderate, could be severe due to occasional roll being $>10^0$	3.7-5.4
4	Severe, ship motion had a serious impact on human operations	5.4-6.6

The LFE induced degradation in crew performance would suggest a more meaningful criterion to assess the impact of ship motions on human operators. Baitis and others, (1983 and 1984) examined the ability of ship personnel to recover, secure and retrieve a Light Airborne Multipurpose System (LAMPS) helicopter into the ship hanger from the flight

deck, under various conditions of sea state, ship speed and heading, see Figure 2.16 for definition. The crew assessment was conducted in terms of Motion Induced Interruptions (MII). Although, other measures exist to quantify human responses to ship motions, such as Motion Sickness Incidence (MSI) and Motion Induced Fatigue (MIF), the MII directly relates the likelihood of an interruption due to LFE type accelerations. The data gathered was compiled in the form of polar charts, which resulted in the Operations Guidance Manual (OGM), indicating the optimal ship orientation to facilitate recovery of the LAMPS in any prevailing environment.

Baitis and Schmidt (1989) further develop and refine the OGM with data from sea trial of RRS on aboard various classes of US Naval ships. A rigorous and detailed mathematical approach to the LFE in terms of MII is pursued by Graham (1990). He develops a frequency domain based method to evaluate the LFE by consideration of the crew member's centre of gravity, shoe-to-deck-friction coefficients, and ship motions. These researchers however, do not propose any control design strategy to reduce these LFE motions.

Their results may be summarised as shown in Table 4.2, which details the response of the crew to LFE accelerations with respect to MII per recovery whilst engaged in retrieval of the LAMPS, and the general effects expected in routine crew functions. Here 'g' is gravitational acceleration.

Table 4.2 : MII in recovery of LAMPS

RMS LFE (g)	MII Occurrence	General Effects
0.08	0.05	Slight
0.1	0.08	Acceptable
0.12	1.44	Serious
0.14	2.61	Severe Limitations
0.16	4	Extremely Hazardous

Assessment of the human operators' percentage effectiveness are compared in Figure 4.1 in terms of RMS LFE and RMS roll criteria. If the LFE is assumed to be the limiting factor then, at a seemingly innocuous RMS LFE of, for example, 0.12g, equivalently 7^0 RMS roll, it is apparent that operations would be seriously impaired with MII being 1.44 per recovery. However, a spurious interpretation will result if the same information is to be derived from the RMS roll information of Figure 4.1, which suggests that the human operators remain 50% effective at an RMS roll of 7^0. The graph of Figure 4.1 illustrates the rapidly diminishing percentage effectiveness with relatively small changes in RMS lateral accelerations as compared with the RMS roll motions.

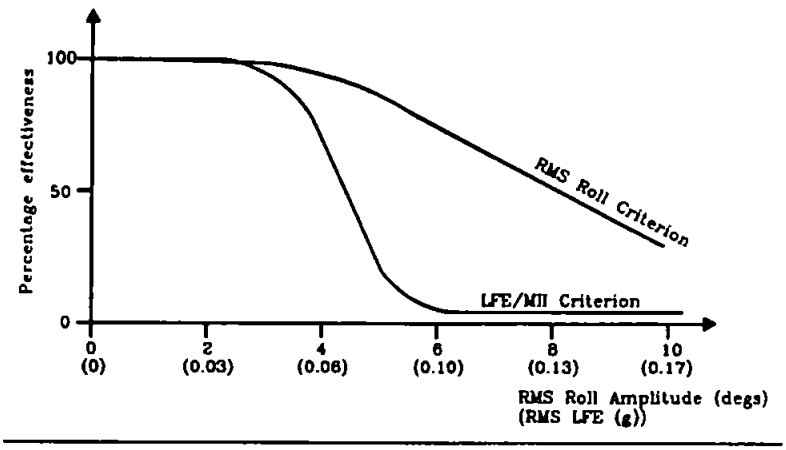

Figure 4.1 : Comparison of RMS LFE and roll in percentage effectiveness

Therefore, it is suggested that an alternative assessment of human operator efficiency with roll stabilising controllers would be achieved if it were based upon RMS LFE. Whereas the RMS roll angle affords an overall criterion for evaluation of the vessel as an integrated man-machine weapons platform in its physical environment.

In the succeeding sections an investigation is made into whether there exists a converse relationship between LFE and roll, and the RRS controllers' ability to reduce these motions is examined.

4.3 THE LFE CONTROL SYSTEM

The constituents of the LFE are now examined and a controller design methodology proposed.

4.3.1 Further Modelling Considerations

The equations to describe the LFE were developed in section 2.2.3, and the final expression (2.44) which was derived to represent the LFE is reproduced here for convenience.

$$\text{LFE} = \ddot{y} - z_B\ddot{\phi} + x_B\ddot{\psi} - g\phi \tag{4.1}$$

where

y	earth-fixed axis lateral motion
ϕ	roll angle, radian
ψ	yaw angle, radian
z_B	vertical height, m
x_B	longitudinal distance from the CoG , m

From Figure 2.14, equation (4.1) and by consideration of the axis of reference, Figure 2.1, of each part of the LFE, it is recognised that the LFE, i.e. the apparent lateral acceleration, is a vector summation of the earth referenced lateral acceleration and ship referenced lateral acceleration due to the roll angle.

The apparent vertical acceleration has been neglected in this derivation, since it is considered that the lateral motions represent the greatest disruption to personnel activities. Mcleod *et al* (1981) investigates the vertical accelerations impact on simple tasks using a physical simulator. It is known that neither the fins nor the rudders, under normal operations, can generate corrective action to compensate for vertical accelerations, sections 2.2.1 and 2.2.2. Even if the fins moved simultaneously upwards, see Figure 2.8, they would still be incapable of generating the vertical forces required, and would make the fins

redundant against roll stabilisation. Therefore, its inclusion is deemed superfluous and stabilisation of only the lateral acceleration is attempted.

However, the MII data presented in Table 4.2 and Figure 4.1 corresponds to lateral as well as vertical accelerations. Utilising this data in the assessment of the MII ramifications of the rudder stabilised LFE's, which are subsequently developed here, will, therefore, be unnecessarily pessimistic and must be interpreted with caution.

The yaw acceleration induced LFE, in general, can be regarded as being insignificant near the CoG. However, on account of the lever arm, x_B, its contribution may increase moving towards the bow, in which case x_B is positive, or towards the stern, where it becomes increasingly negative, e.g. the flight deck. Despite this, it will remain relatively small on account of the magnitudes of the inertia involved, and is, therefore, neglected.

A further simplification can be made: close to the centre of gravity the roll acceleration term will diminish to zero when the z_B component of the point of measurement is coincident with the CoG. As z_B approaches the keel it becomes increasingly positive. If this simplification is adopted equation (4.1) will reduce to a gravitational roll and sway acceleration term. A further complication is inherent in the selection of z_B: if its magnitude is 9.81 metres, which is the value of gravitational acceleration, then, since it is a coefficient of the roll acceleration, which in turn is anti-phase to the roll angle, the terms $(-z_B\ddot{\phi} - g\phi)$ will cancel and hence vanish. The residual LFE will consist of only a sway acceleration term. However, it was decided to select the point of measurement realistically, being exactly above the CoG and on the weather-deck where physically demanding work is conducted, which implies that z_B is 5.85 metres. The LFE can now be rewritten as:

$$\text{LFE} = \ddot{y} - z_B\ddot{\phi} - g\phi \qquad (4.2)$$

Each constituent of the modified LFE (4.2) is now examined in turn.

Obtaining the roll angle, ϕ, and its second derivative is a simple matter.

The rudder and fin induced roll motions, g11(s) and g12(s) respectively, can be combined with the sea induced roll angle disturbance, as shown in Figure 2.18, in order to produce the resulting stabilised roll motion. In time simulation studies this can be differentiated twice to give the roll acceleration term. Hence, $z_B\ddot{\phi}$ and $g\phi$, can be accommodated rather simply.

However, the sway acceleration term, $\ddot{y}$, requires further examination.

Consider the multivariable transfer function derived from Figure 2.18.

$$\begin{pmatrix} \text{roll} \\ \text{yaw} \\ \text{sway} \end{pmatrix} = \begin{pmatrix} \phi \\ \psi \\ y \end{pmatrix} = \begin{bmatrix} g11(s) & g12(s) \\ g21(s) & g22(s) \\ g31(s) & g32(s) \end{bmatrix} \begin{pmatrix} \alpha \\ \delta \end{pmatrix} \tag{4.3}$$

There is very little sea trials data available which measures the fin and rudder to sway motions, g31(s) and g32(s), respectively . Therefore, using simulations data furnished by DRA Haslar an attempt was made to derive these transfer functions by fitting approximations to the frequency spectrums.

Owing to significant interaction between the sway and roll frequency spectrums of the forced fin roll responses it was not possible to ascertain any reliable transfer function for g31(s). It is envisaged that given their dihedral angle, Figure 2.8, the fins would not be able to generate sufficient sway forces in order to oppose that of the LFE. Therefore, the fins are inappropriate in LFE stabilisation. The rudder to sway transfer function, g32(s), was

derived for a ship speed of 18kts by standard Bode approximations and is shown in equation (4.4)

$$g32(s) = \frac{y(s)}{\delta\ (s)} = \frac{9.596}{236.69s^2 + 30.77s + 1} \tag{4.4}$$

One the few instances of the rudder to sway dynamics being reported in literature is by Klugt (1987) for a similar type of vessel from model-scale towing tank trials, which is given in (4.5): a modified version of g32(s),

$$kg32(s) = \frac{y(s)}{\delta\ (s)} = \frac{0.176}{s(8.2s + 1)} \tag{4.5}$$

A comparison of the sway accelerations is made in Figure 4.2 for these transfer functions.

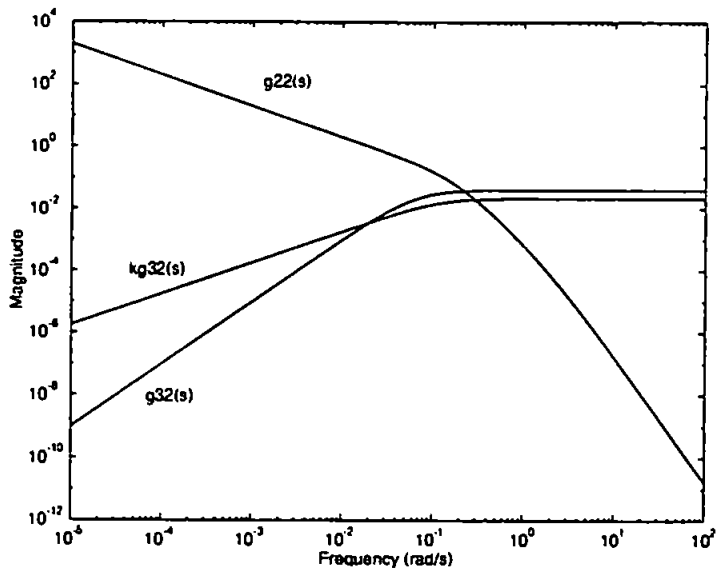

Figure 4.2 : Comparison of sway accelerations and rudder-to-yaw dynamics

The sway accelerations derived from the DRA Haslar data and that given by Klugt (1987) show some degree of correlation affording confidence in the prediction software, PAT91, and the identification technique employed.

The rudder-to-sway acceleration transfer function, $s^2g32(s)$, will be utilised in the removal of the corresponding sway disturbance in the LFE. This can be achieved only at relatively high frequency region as shown by the response in Figure 4.2. It is also seen that such a strategy will have minimal impact of the rudder-to-yaw dynamics, g22(s), which respond to low frequency rudder motions.

Thus far the components of the LFE as presented have been induced by the hydrodynamic action of the rudder. The unstabilised LFE motion can be represented if the roll and sway components of equation (4.2) are excited by the sea disturbances.

Considering the unstabilised LFE motions which are a vector summation of various components, as previously stipulated, when these are combined it is imperative to maintain their relative phases. Schmitke (1978) demonstrates that "...sway leads wave phase by 90^0 and as ω tends to zero, sway amplitude tends to wave amplitude.", similarly Bell (1965) states that "...addition is subject [roll plus sway acceleration] to a phase correction of 90^{0n}". The phase characteristics will be satisfied by a high-pass filter such as the sway acceleration produced by $s^2g32(s)$. However, the magnitude requirements will not be met by such a filter. Nevertheless, for the given range of sea disturbances it is assumed that the encounter frequency will not diminish to such low values. Adhering to these promulgations the constituent blocks of the LFE, for the purposes of time domain simulations, are shown in Figure 4.3.

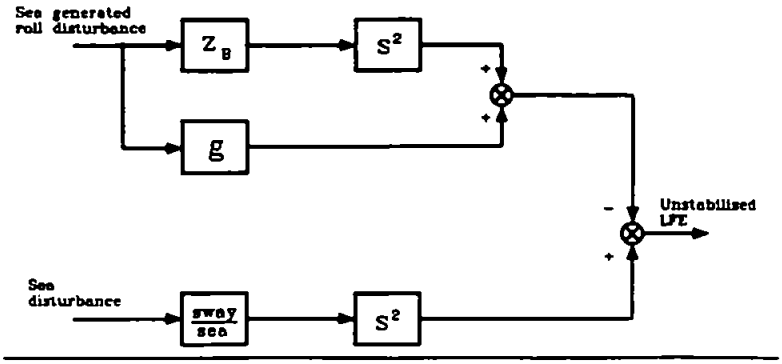

Figure 4.3 : LFE simulation block

The stabilised LFE motions are simply generated by feeding the appropriate blocks of Figure 4.3 with the stabilised roll angle and replacing the 'sway/sea' model with g32(s) which will be excited by the rudder motion. This will form the basis of the controller design and simulation models in succeeding sections.

Utilising this model, Figure 4.3, the sea induced RMS LFE at various headings were calculated for a sea state 5 disturbance and compared with the DRA Haslar data as shown in Figure 4.4. This was achieved by varying gain parameters which were introduced within the LFE dynamics model. The very close correlation vindicates the approach adopted and shall be pursued in the simulations studies.

The LFE in Figure 4.4 has a maximum value of $0.8ms^{-2}$ which equals 0.08g in terms of gravitational accelerations. Comparing this with the general operations data presented in Figure 4.1, it suggests a possible 50% decrease in crew efficiency. However, in terms of MII in the recovery of the LAMPS, Table 4.2, it appears that the level of LFE motions would not induce an intolerable effect on operations.

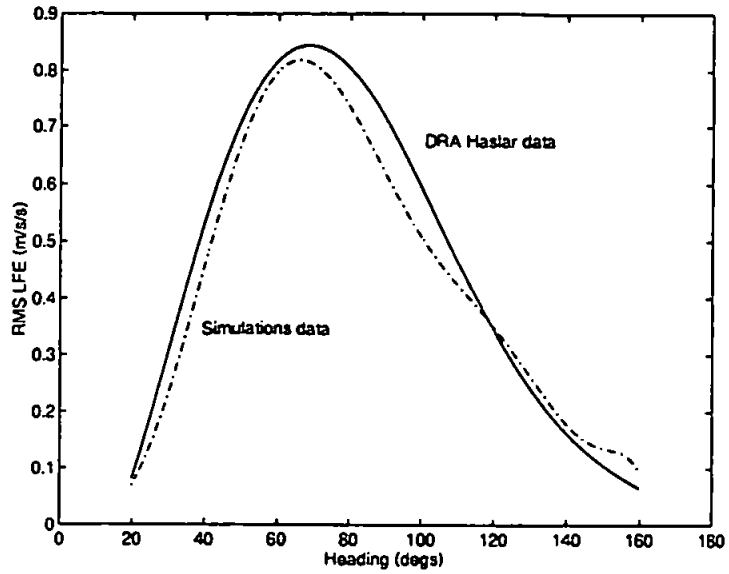

Figure 4.4 : Comparison of RMS LFE values with DRA Haslar data

The modelling of the LFE is now complete and the subsequent section deal with the controller configurations and synthesis.

4.3.2 Controller Configurations

Initially it is intended to examine the effects of the specifically designed and dedicated RRS controller on the LFE motions. The simulations configuration adopted for this investigation is shown in Figure 4.5.

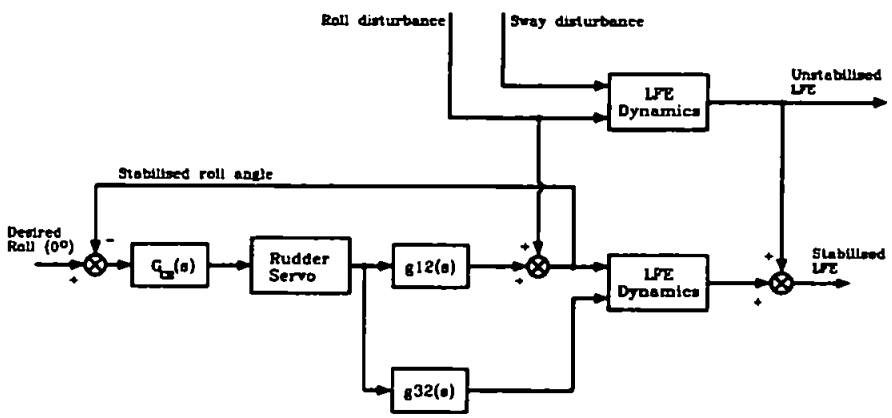

Figure 4.5 : The RRS scheme in relation to LFE stabilisation

The 'LFE Dynamics' blocks essentially contain the LFE as constructed in Figure 4.3 and as such have sway and roll motions as their input signals: one for the unstabilised generation

and the other to assess the impact of the RRS controller. The summation of these two blocks will yield the combined net LFE of the ship.

It is also envisaged that with a similar approach as in Figure 4.5 the LFE signal will be directly utilised to drive a controller which will generate rudder demand signals. In this way the LFE, as well as the roll motions, may be compensated for in an explicit fashion. This is shown in the schematic of Figure 4.6.

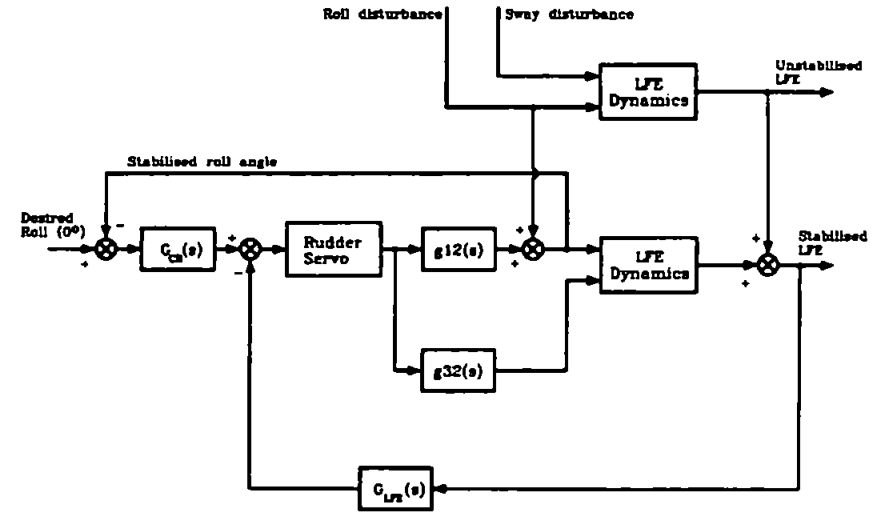

Figure 4.6 : The RRS and LFE controllers acting in unison

The only variation here as compared with Figure 4.5 is the inclusion of the LFE controller $G_{LFE}(s)$ which is exclusively engaged in reducing LFE motions. The RRS controller is retained since LFE also has roll components.

4.4 CONTROLLER SYNTHESIS

Classical phase advance and Linear Quadratic Guassian (LQG) type controllers were investigated in LFE stabilisation. Each method has inherent desirable design features which are outlined in the following sections.

4.4.1 Classical Controllers

Lloyd (1989) postulates a method of synthesising a type of classical controller which introduces phase advance into the RRS loop of Figure 2.18. This is arranged to equal the inherent phase lag of the combined rudder-to-roll, g12(s), transfer function, the servomechanism and the controller itself. If the frequency, at which phase lead is to be injected, is selected to coincide with the ship's resonance frequency, then the net phase between the disturbance, d_1, and stabilised roll will be zero hence, given the servomechanism limitations, complete roll reduction will result. At other perturbing sea frequencies stabilisation will be achieved to a lesser degree.

Adopting this approach yields controllers of the form;

$$G_{CR}(s) = \frac{(k_A s^2 + k_R s + k)k_s}{k_1 s^2 + k_2 s + k_3} \tag{4.6}$$

The specific procedure in the selection of the k_A, k_R and k, and their implications, is deferred to Chapter 5; suffice for the moment that the controller, $G_{CR}(s)$, represents a phase lead about the frequency dictated by these coefficients. The gain k_s accounts for gain- and phase-margins, and regulates the servomechanism action hence level of ship motion reduction achieved. The coefficients of denominator of controller (4.6) are selected such that they yield minimum phase lag at the regions where the controller action is applied which are selected to be k_1=0.05, k_2=0.5 and k_3=1.

The LFE controller, $G_{LFE}(s)$, of Figure 4.6 has exactly the same form as RRS controller, $G_{CR}(s)$. However, the strategy for the selection of the coefficients, in order to deliver phase lead around a particular frequency location, is not obvious due to the nature of the LFE. Their relative effects on ship motions will be assessed in Section 4.5 in an intuitive manner.

Therefore, it is seen that this type of controller can be 'tuned' to optimise the system at the desired frequency range of interest.

The coefficients, which are interchangeable, for the RRS and LFE controller in their respective loops, were selected and are summarised in Table 4.3

Table 4.3 : Controller coefficients

Controller	k_A	k_R	k	k_3
A	6.2	5	1	1
B	22	30	1	0.5
C	100	1	10.8	0.1
D	600	1	55.8	0.03

The frequency response of each controller is shown in Figure 4.7.

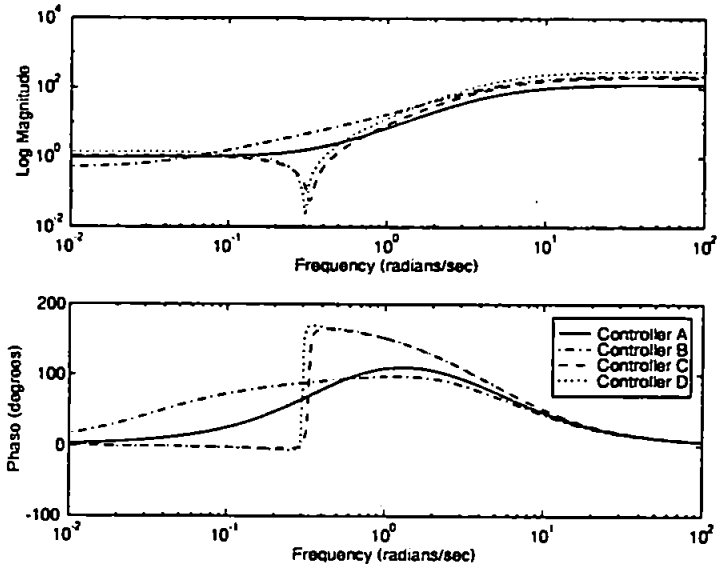

Figure 4.7 : Frequency response of controllers

Controller A is an example of a typical RRS controller where the phase advance is centred around the roll resonance of the ship and matches the total phase lag of the open loop system. Since LFE is an acceleration signal, then altering this controller to reflect a relatively higher degree of roll acceleration feedback, k_A, yields controller B. Tang and

Wilson (1992a and 1992b) suggest a strategy of having an RRS controller tuned to a low frequency will achieve acceptable LFE and roll stabilisation. This is implemented in controller C which is seen to be tuned to a lower frequency than controller A, on account of its phase information.

Considering the LFE controller as shown in Figure 4.6, since, the LFE is predominantly an acceleration signal, it is envisaged that by emphasising this coefficient of $G_{LFE}(s)$, as shown in controller D, it will accrue LFE stabilisation.

From the magnitude response of all the controllers it is apparent that the yaw dynamics will not be excited.

4.4.2 LQG Control

The alternative control methodology employed is LQG, a compendious description of which can be found at Appendix B. Essentially, the synthesis of this type of controller involves the optimisation of an energy cost function of the form;

$$J = \int_0^\infty (uQu^T + yRy^T);dt \tag{4.7}$$

The design objectives are embedded in the weights Q and R. Where the former regulates the actuator activity and the latter levels of stabilisation desired. Hence, there will be trade-offs between the competing objectives of minimising servomechanism action and motion reduction. The advantage afforded by LQG control is that by explicitly setting the relative magnitudes of matrix R, emphasis can be directed towards roll or LFE, or stabilisation of both motions.

LQG requires that the system be presented in its state space description. Appendix C details the state space description of the controller arrangement in Figure 4.5.

Table 4.4 details the strategies adopted with respect to the weighting R in order to achieve the objectives of roll and LFE amelioration.

Table 4.4 : LQG weights selection strategy

Strategy	Controller	LFE Weight	Roll Weight
Roll Only	A	0	1
	B	0	30
	C	0	60
LFE Only	A	1	0
	B	30	0
	C	60	0
Roll and LFE	A	1	25
	B	25	1
	C	25	25

These classical and LQG controllers are assessed in a simulation study.

4.5 SIMULATIONS STUDY

The simulations study is intended as an elementary investigation into the applicability of the current RRS controller design strategy in LFE stabilisation. Some modifications are proposed and their implications on LFE and roll stabilisation assessed.

Monk (1987) conducted a comprehensive examination of the LFE magnitude in various environmental permutations, such as wave encounter frequency, ship speed and sea state. The conclusion derived is that the conditions which appear to induce the most pronounced LFE are at sea state 5 and ship speed of 18kts. This, conveniently, reflects the severest

conditions in which operational efficiency must be maintained as required by the Royal Navy. Therefore, the study is restricted to disturbances which emulate these conditions.

The resulting roll and LFE motions are presented in terms of RMS statistics at a range of headings in Figures 4.8 to 4.10, 4.12, 4.15, 4.17 and 4.19, where the solid lines represent uncontrolled motions and the broken lines when the control surfaces are engaged. Since, the rudder employed has physical limitation its activity must be monitored in order to circumvent the consequences discussed in Chapter 3. It is presented in terms of RMS for the corresponding simulations in Figure 4.11, 4.13, 4.16, 4.18 and 4.20.

Initially, the effects of the RRS controller, $G_{CR}(s)$, on the LFE motions are to be examined with the simulation structure as shown in Figure 4.5. Implementing this with a set of typical RRS coefficients given by controller A, Table 4.3, the results obtained are shown in Figure 4.8. At beam sea the encounter frequency, equation (2.46), for sea state 5, Table 2.5, coincides with ship resonance. Hence, greatest roll reduction occurs, approximately 60%, on account of the controller being optimised at the ship roll resonance frequency. At quartering and following (see section 2.3 for definitions of relative headings) seas the reduction levels decrease to 20%. This controller marginally amplifies the LFE motions at headings of greater than 80^0. However, at beam sea approximately 25% reduction is achieved, due mainly to the roll component of the LFE being attenuated.

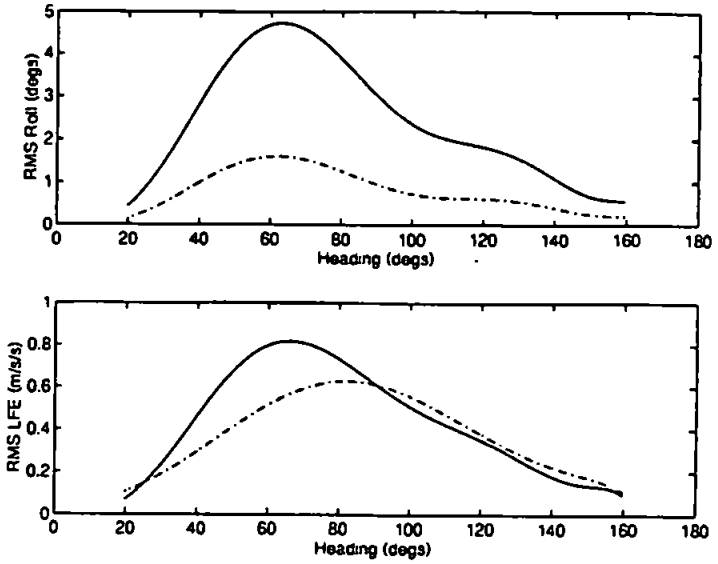

Figure 4.8 : Roll and LFE RMS with typical RRS controller, A

If the roll acceleration component of the controller is increased, as given by controller B, Table 4.3, the RMS motions are achieved as shown in Figure 4.9. Roll reduction has deteriorated to 30% around beam sea and correspondingly worse at other headings. The LFE has improved to the extent that there is now negligible amplification. Unfortunately, the increase in roll motions has correspondingly increased the LFE at around beam seas.

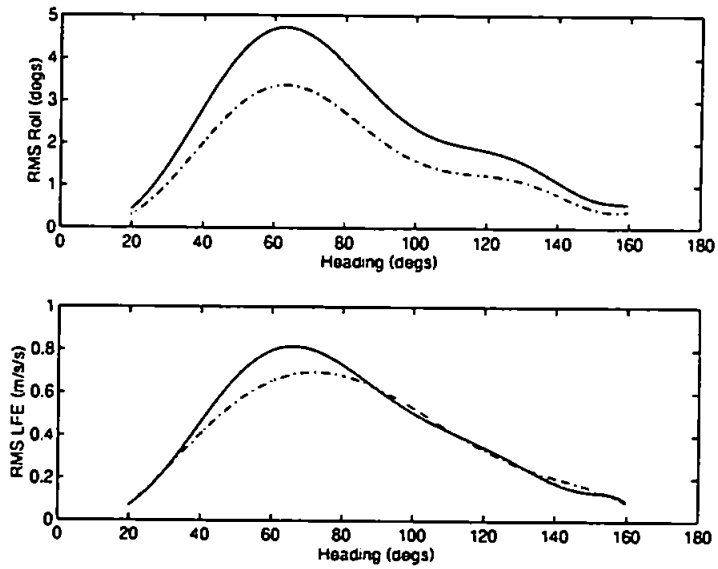

Figure 4.9 : Roll and LFE RMS with high acceleration RRS controller, B

Adhering to the recommendations of Tang and Wilson (1992a and 1992b) yields the controller C, Table 4.3, which produce the results as illustrated in Figure 4.10. Roll levels have decreased to similar magnitudes as in Figure 4.8. However, the LFE has worsened therefore, no lucid advantage is apparent in tuning the RRS controller to a lower frequency.

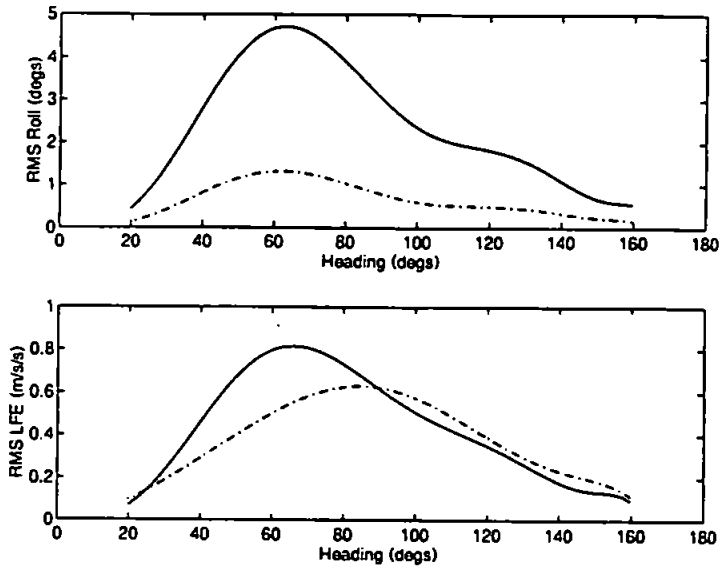

Figure 4.10 : Roll and LFE RMS with RRS controller tuned to low frequency, C

Figure 4.11 exhibits the rudder activity for the preceding simulations. In general, the controllers' demands will not saturate the rudder servomechanism. It is apparent that the only advantage offered by controller C is reduced actuator excursions.

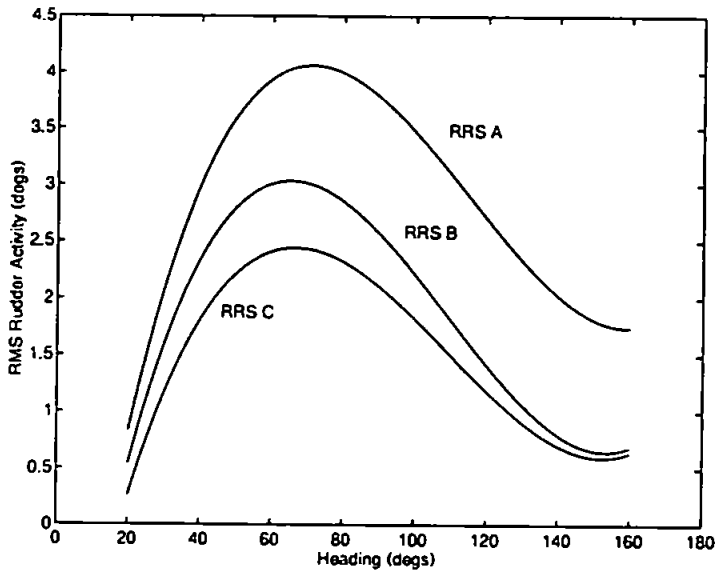

Figure 4.11 : RMS rudder activity for RRS classical controllers

From the data presented, it is evident that satisfactory LFE stabilisation cannot be achieved by using the RRS controller in isolation. Therefore, the schematic of Figure 4.6 is invoked which includes an explicit LFE controller, $G_{LFE}(s)$. Initially, with the RRS controller disengaged, in this configuration, and utilising the high acceleration feedback LFE controller D from Table 4.3, yields the following results as given by Figure 4.12. Limited roll and LFE stabilisation is achieved and negligible amplification of LFE at headings of greater than 135^0.

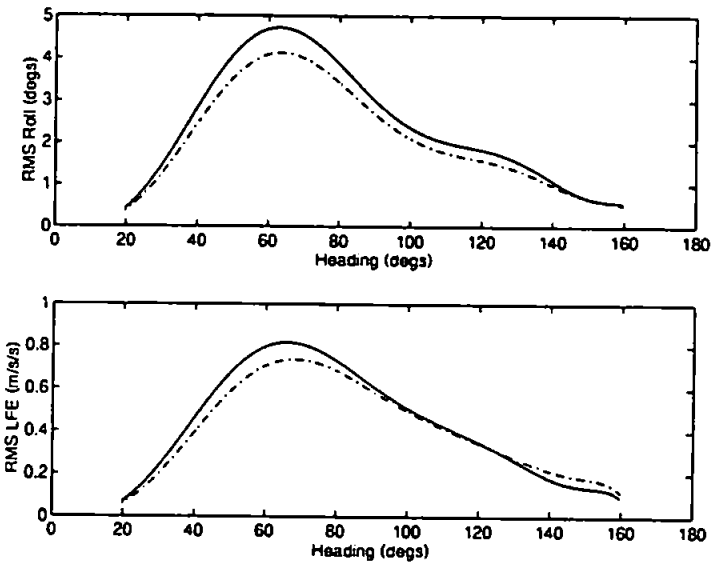

Figure 4.12 : Roll and LFE RMS with classical LFE controller only

The RRS controller is now functioning with coefficients of A, Table 4.3 together with the LFE controller which is tuned to a low frequency as suggested by Tang and Wilson (1992a and 1992b). The results obtained are illustrated in Figure 4.13. Satisfactory roll amelioration is achieved, of approximately 60% around beam seas and up to 30% off-beam. Furthermore, the principle objective of reducing LFE has been realised.

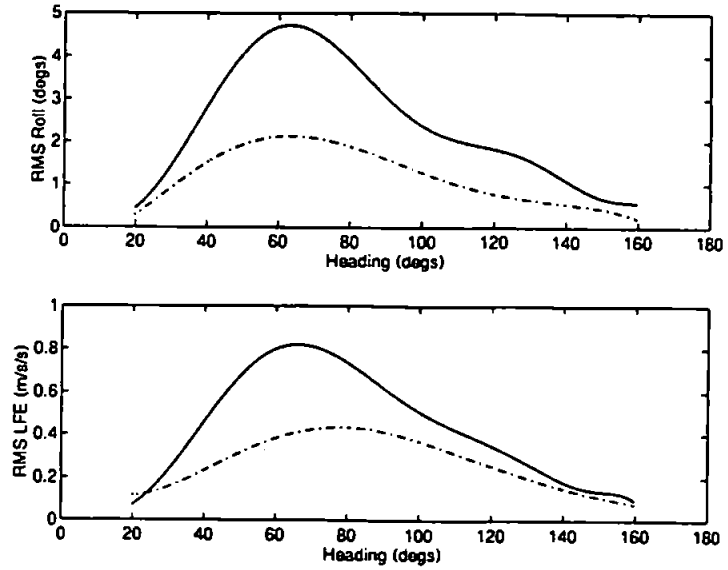

Figure 4.13 : Roll and LFE RMS with classical LFE and RRS controllers

The rudder activity implication of this strategy is given by Figure 4.14. It is seen that the servomechanism will remain within its linear region of operation, on account of the RMS level not exceeding 7^0. Curiously, the RMS level decreases somewhat, when both LFE and RRS controllers are operative.

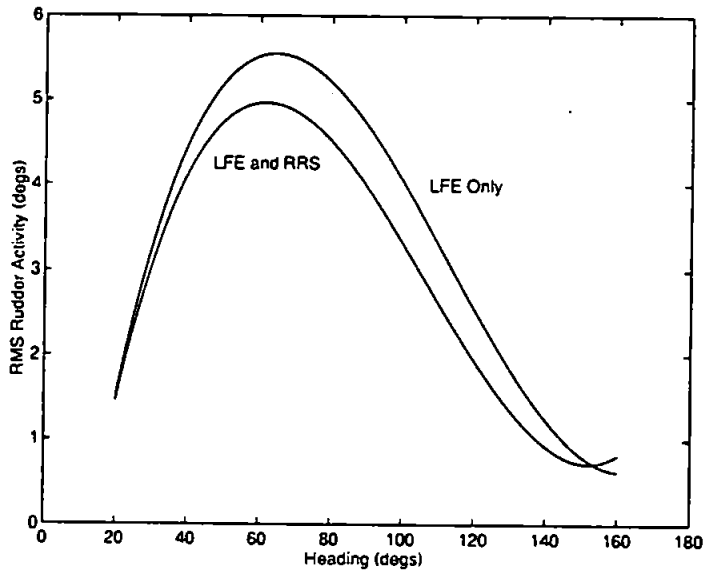

Figure 4.14 : RMS rudder activity for classical LFE controller

The LQG controller performance is now assessed with the weightings as detailed in Table 4.4.

Figure 4.15 displays the results when the weight is exclusively placed on achieving roll stabilisation. It demonstrates, as expected, that as the weight is increased roll motion diminishes. The limiting factor is the rudder servomechanism saturation considerations as illustrated in Figure 4.16. Controller C yields the greatest roll stabilisation and correspondingly largest rudder motion. The LFE amelioration for the same LQG strategy is also shown by Figure 4.15. It diminishes as the roll component of its dynamics decrease.

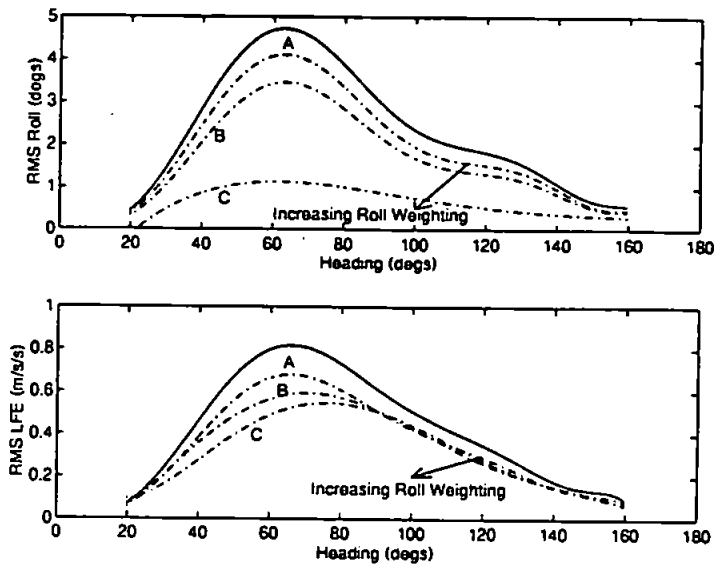

Figure 4.15 : Roll and LFE RMS with LQG controller, roll weighting only

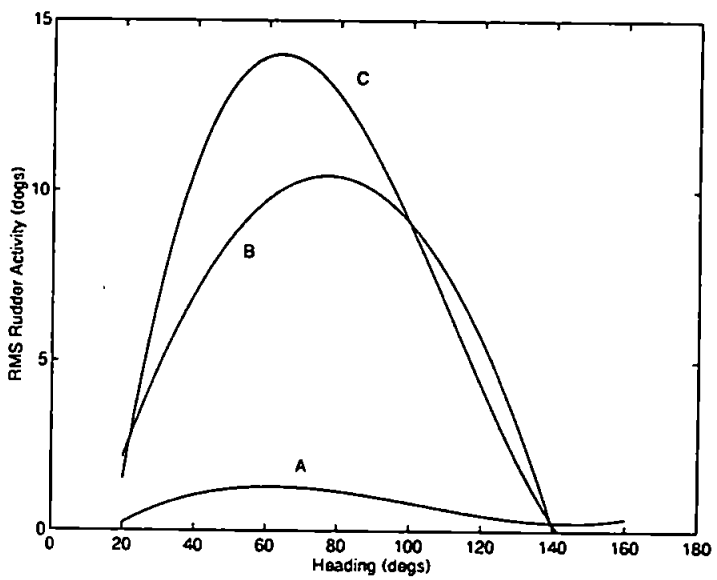

Figure 4.16 : RMS rudder activity for LQG, roll weighting only

If the weighting is now altered to exclusively reflect the objective of reducing LFE motions as shown in Table 4.4, the results obtained are shown in Figure 4.17. As the weight is increased the LFE motion diminishes with reductions of 60% being achieved. However, the corresponding roll stabilisation is less pronounced as compared with Figure 4.15, being at most 30%. For these simulations the rudder activity is within permitted range.

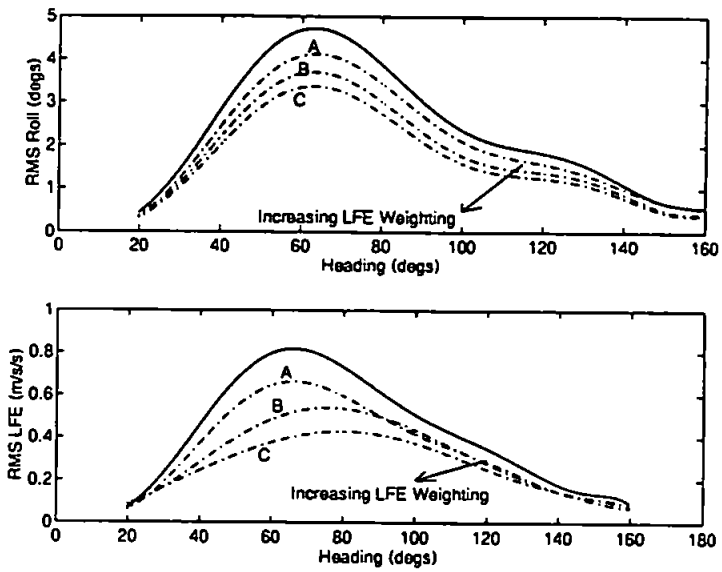

Figure 4.17 : Roll and LFE RMS with LQG controller, LFE weighting only

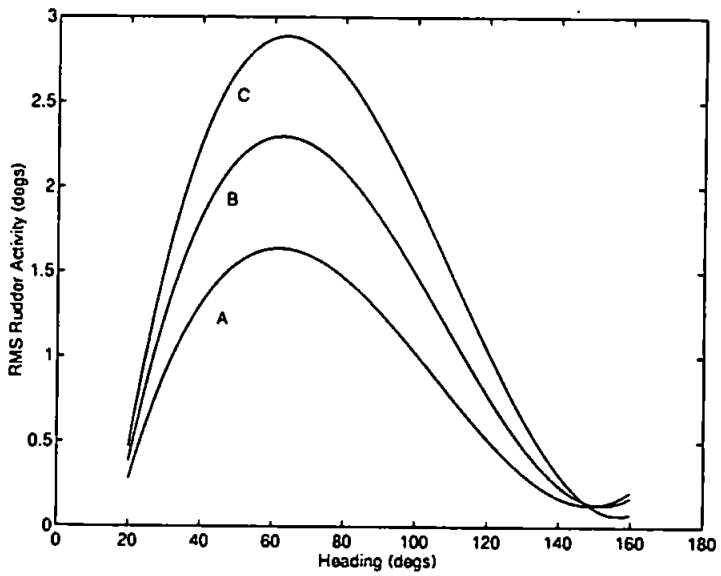

Figure 4.18 : RMS rudder activity for LQG, LFE weight only

Altering the LQG optimisation criteria to be multi-objective as shown in Table 4.4 yields the results shown in Figure 4.19. With the emphasis directed on roll, graphs A, demonstrate that considerable roll reduction is accrued but minimal LFE reduction. Conversely, if the emphasis is now on LFE stabilisation, graphs B, show that minimal roll reduction occurs but greatest LFE amelioration. A compromise is achieved if the weights are similar as illustrated by graphs C where acceptable roll and LFE reduction are achieved. Figure 4.20 illustrates that rudder activity lies within a tolerable range.

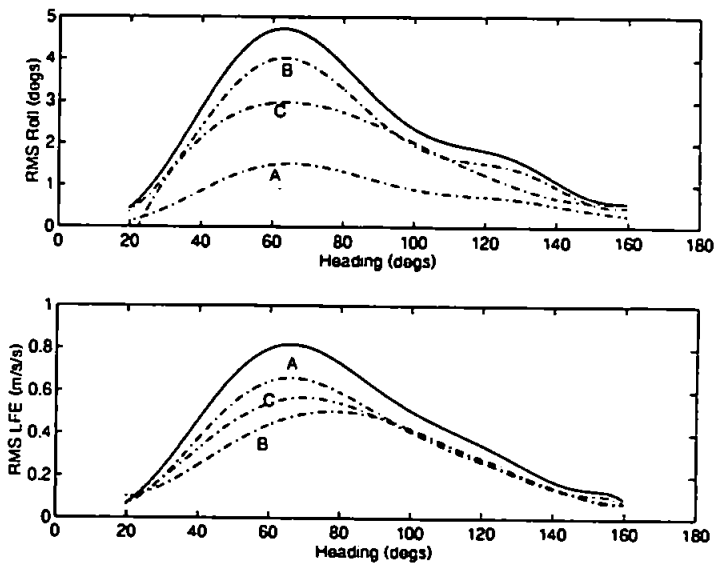

Figure 4.19 : Roll and LFE RMS with LQG controller, LFE and roll weighting

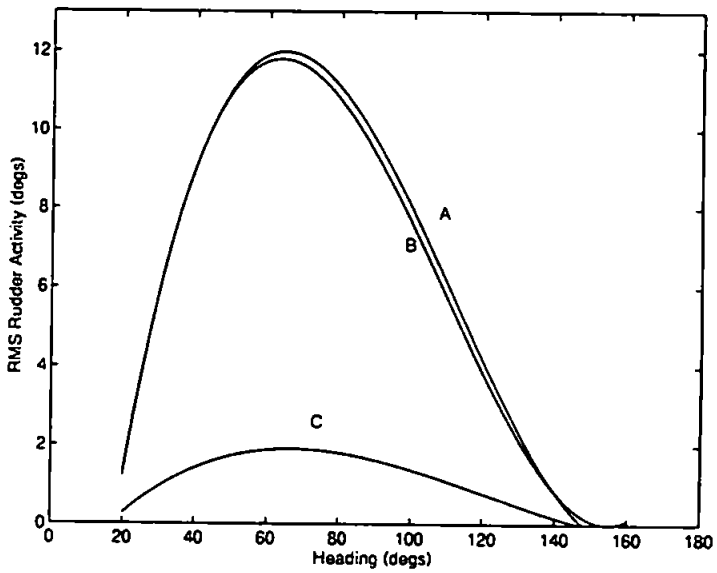

Figure 4.20 : RMS rudder activity for LQG, LFE and roll weighting

4.6 DISCUSSION AND CONCLUSIONS

The study successfully constructed a time domain simulation model of the LFE, which is a unique contribution, and synthesised controllers from an intuitive and theoretical basis by examination of the constituent parts of the LFE motions.

Utilising the classical control design various frequency regimes were applied. It appears from Figure 4.5 and the results of Figure 4.10 that the recommendations of Tang and Wilson (1992a and 1992b) require to be modified if adequate LFE and roll reduction is to be achieved. The exclusive RRS controller must be augmented with an explicit LFE controller. Their demand signals are summed and fed to the rudder servomechanism. When the LQG controller was arranged to have weights on both the motions, analogous to the classical case having dedicated RRS and LFE controllers, similar results were obtained as seen in Figure 4.19. Reinforcing the assertion for the requirement for independent motion controllers.

Normally the RRS controllers operate around the ship's resonance frequency, 0.6 $rads^{-1}$. On an intuitive basis Tang and Wilson (1992a and 1992b) suggests that this be modified by tuning it to a lower frequency, 0.1-0.3 $rads^{-1}$. Considering the rudder-to-sway acceleration characteristics as exhibited by Figure 4.2, the theoretical rational is apparent. If the normal RRS controller induced rudder operation excites the high frequency dynamics of the ship, then the sway acceleration component of the LFE will be become large. Hence, the requirement for appropriate tuning as demonstrated by the poor results of Figure 4.13. The roll component can be reduced by retaining an independent RRS controller as mentioned, resulting in an overall reduction in the LFE.

From these considerations and those detailed in section 4.3.1 the very complex nature of the LFE is manifest. The results presented here relate only to the LFE stabilisation at one position in the ship: on the weather-deck directly above the CoG. If the location changes then the appearance of the LFE dynamics change dramatically, not only in magnitude but also polarity. For control purposes an accelerometer, or, ideally, some devices to independently measure the individual constituents of the LFE, would be required at every location in the ship where LFE reduction is desired. It is obvious that this cannot be achieved simultaneously throughout the entire ship: indeed LFE stabilisation at one position may render intolerable increases at other locations.

It is envisaged that since the LFE is critical at the flight deck then a single dedicated controller may be assigned to reducing it at that location. To the author's knowledge this is being pursued in a general study of the MII by the co-researchers of Tang, in association with DRA Haslar, with the recommendations for the controller design presented here and in Sharif *et al* (1993). Some preliminary results from this investigation were presented by Crossland *et al* (1994)

The LFE stabilisation will not be further pursued for a number of reasons: there is evidence in this diversionary study, Figures 4.8 and 4.15, to suggest that LFE reduction is accrued as a direct consequence of roll stabilisation without employing dedicated LFE controllers; there is no significant difference in MII when the controllers are engaged in LFE or roll stabilisation modes (Crossland *et al*, 1994); the LFE is a complex signal and changes at different locations which necessitates an array of sensors around the ship to measure it, and would represent a considerable installation investment; finally, the results of the extensive research program at DRA Haslar will exhaustively assess the viability of the MII in ship

motion criteria. Therefore, the thesis will proceed with its primary objective of designing controllers to stabilise exclusively for roll motions.

CHAPTER 5

ROLL STABILISER CONTROLLER DESIGN

5.1 INTRODUCTION

The linear ship roll models developed in Chapter 2 will be extensively utilised in the subsequent endeavour to design controllers. These will be based exclusively on linear synthesis procedures. Initially, the efficacy of those controllers which, in practice, are most commonly implemented to govern a ship's rudders and fins, namely classical and LQG techniques, are investigated.

Classical controller generation involves shaping the open-loop frequency spectrum such that, by the appropriate introduction of poles and zeros, the closed loop system exhibits the desired characteristics and possesses sufficient safety margins. The essence of LQG synthesis is that the subsequent controller is optimal to a specific energy cost function which embodies the roll stabilisation characteristics. This technique requires that all of the states in a plant be available. When a stochastic cost function is defined and subject to the same procedure, a Kalman optimal observer results which provides a reconstruction of the state variables from the outputs of the plant.

The Chapter now proceeds with an examination of the design features and proposals for the roll stabilisation problem.

5.2 PERFORMANCE OBJECTIVES AND RESTRICTIONS

Ship roll stabilisation occurs if the fin and rudder controllers are able to induce ship rolling motion in order to counter the sea generated disturbances. Consider the control system shown of the RRS loop as shown in Figure 5.1.

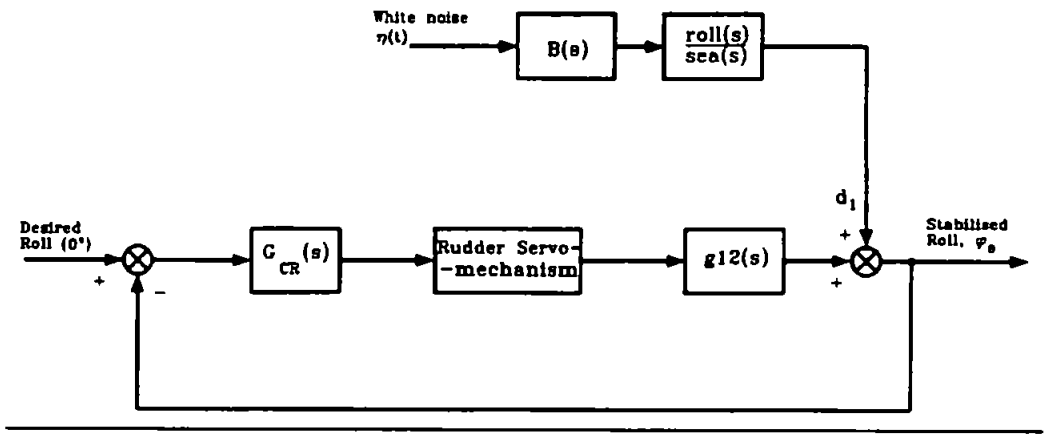

Figure 5.1 : Rudder roll stabilisation loop

The transfer function from the sea disturbance, d_1, to the stabilised roll, ϕ_s, for any such configuration is known as the Sensitivity Function, S(s).

$$S(s) = \frac{\phi_s}{d_1} = \frac{1}{1 + g12(s)G_{CR}(s)} \tag{5.1}$$

It is a measure of the combined controller and system's ability to r eject the extraneous disturbances. Ideally, it is required to ensure that $|S(j\omega)| < 1$, $\forall\omega$, then roll stabilisation occurs over the entire frequency range. However, since sea induced roll disturbances are concentrated in a specific frequency band, $\omega_L<\omega<\omega_H$, then the objective of restraining $S(j\omega)$ below unity in this region is sufficient to ensure that adequate roll stabilisation is achieved.

A controller can be constructed such that the ensuing sensitivity function is arbitrarily small over any given frequency range (Francis and Zames, 1984). If the resulting gain and phase margins are satisfactory then such an approach could be utilised for minimum phase systems such as the fin roll stabilisation loop. The only restriction would be deciding judicious levels of servomechanism activity.

However, non-minimum phase systems can cause difficulty in the design of a controller (Bode, 1950). The rudder roll transfer function, g12(s), equation (2.36), is such a system. Its performance limitations and constraints are briefly discussed in Appendix E.

Appendix E demonstrates that requiring the sensitivity function to be less than unity in a particular frequency range, where the non-minimum phase zero contributes phase lag, implies that there will exist large peaks at higher and lower frequency regions. If the zero is located outside the range of where sensitivity is to be minimised then it may marginally impede the performance obtained.

Considering the RRS loop, g12(s), it introduces a non-minimum phase zero at $\omega = 0.117$ rads^{-1}. Fortunately, the envisaged frequency spectrum where sea disturbance predominates is in the range $0.2<\omega<2$ rads^{-1}. Hence, the non-minimum phase zero of g12(s) may, to some extent, limit the sensitivity reduction achieved at the lower encounter frequencies. This will be manifest in large peaks in the sensitivity function at these locations as shall be demonstrated in consideration of the controller sensitivity functions.

5.3 CLASSICAL CONTROLLERS

Almost invariably the geneses of stabiliser controllers and autopilots fitted in Royal Navy vessels is in the classical control theory. The foundation of this was by Bode (1950). It

manipulates the shape of the frequency response of a system in order to achieve the desired time domain properties. They have proven to be reliable and deliver adequate levels of stabilisation (Marshfield, 1981a and 1981b). Therefore, they will form a basis for comparison with other controller design methodologies investigated.

5.3.1 Objectives

Consider the RRS loop of Figure 5.1 and the sensitivity function as given in equation (5.1), assuming that the servomechanism is ideal, then for a typical controller, $G_{CR}(s)$, the Nyquist plot of the open loop system will resemble that of Figure 5.2.

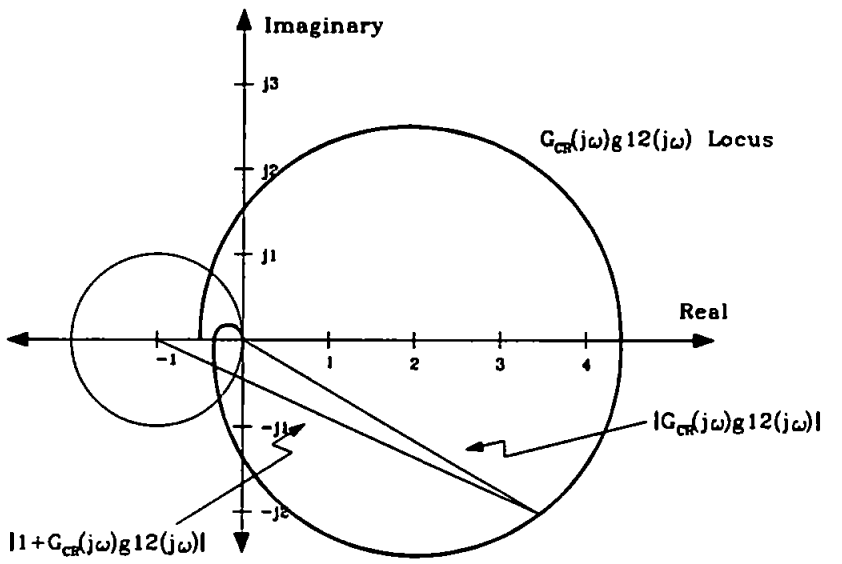

Figure 5.2 : Nyquist plot of RRS

The vector from the point (-1,0) to the locus represents the magnitude of the denominator of the sensitivity function. At those locations where the locus resides outside the unit-radius circle centred at (-1,0) the magnitude of the sensitivity function will be less than unity hence sea disturbances will be attenuated. However, inside the unit circle roll amplification will occur on account of the vector being of magnitude less than unity. Therefore, the objective is to maximise the length of locus lying outside the unit circle.

The actual magnitude of the vector from (-1,0) will dictate the degree of stabilisation achieved which is usually controlled by a simple gain term. A constraining factor being servomechanism slew rate considerations. The other limitation is the requirement to ensure that adequate gain and phase margins are provided by the controller in closed loop operation. The fins and rudders exhibit non-linear hydrodynamic moment generating capability as a function of ship speed, as shown in Chapter 2. Therefore, it will necessitate some form of gain-scheduling in the controllers to account for this fluctuation. A parallel argument follows for the fin stabiliser loop by the Nyquist plot.

Two methods to design the controllers utilising classical frequency domain techniques to meet these objectives are now presented.

5.3.2 Method One - Phase Compensator

The ship exhibits a natural roll frequency at ω_n, which produces a resonance peak in the frequency spectrum, as seen in Figure 2.13, engendered by the complex poles of the transfer function (2.26). Since, roll amplification will occur around this frequency region it suggests the strategy of applying corrective action specifically in this vicinity.

If a controller injects phase advance equal to the inherent phase lag of the combined rudder (fin) to roll transfer function and the servomechanism, then the net phase change from d_1 to the output of g12(s) will be zero. Hence, the stabilisers will be able to generate roll opposing moments instantaneously in response to sea disturbances at ω_n. If the sea's dominant wave period coincides with the ship's damped natural roll frequency then maximum stabilisation is envisaged. Disturbances which occur outside this region may also be attenuated depending upon the controller providing sufficient gain.

The general form of the rudder, $G_{CR}(s)$, and fin, $G_{CF}(s)$ controller is :

$$G_{CR}(s) = \frac{(k_{aR}s^2 + k_{rR}s + k_R)k_{sR}}{A_{3R}s^2 + A_{2R}s + A_{1R}} \qquad G_{CF}(s) = \frac{(k_{aF}s^2 + k_{rF}s + k_F)k_{sF}}{A_{3F}s^2 + A_{2F}s + A_{1F}} \tag{5.2}$$

where

k_{aR}, k_{aF} roll acceleration feedback sensitivity

k_{rR}, k_{rF} roll rate feedback sensitivity

k_R, k_F roll angle feedback sensitivity

k_{sR}, k_{sF} speed dependent gain

The denominator coefficients were selected in order to minimise the phase lag introduced by the controller itself at ω_n: A_{3R}, A_{2R}, and A_{1R} are 0.05, 0.5 and 1.0 for $G_{CR}(s)$ respectively and for $G_{CF}(s)$, A_{3F}, A_{2F}, and A_{1F} are 0.05, 0.5 and 1.0 respectively. The fins and rudders are a non-linear function of ship speed which is accounted for by the speed dependent coefficients, k_{sR} and k_{sF}. These gains can also be deployed to regulate the servomechanism activity and to ensure satisfactory safety margins.

Consider the RRS controller, the procedure is identical for the fin controller, it must provide phase advance of

$$\varepsilon_c = -(\varepsilon_R + \varepsilon_{12}) \tag{5.3}$$

where

ε_R phase lag of rudder servomechanism evaluated at ω_n

ε_{12} phase lag of g12(s) evaluated at ω_n

The phase lag of the servomechanism, ε_R, may be evaluated from the data presented in Figure 3.7 or by approximating a linear transfer function for the servomechanism at the appropriate slew rates. The phase change of the $G_{CR}(s)$ at ω_n, is given by:

$$\varepsilon_c = \arctan\left(\frac{k_{rR}\omega_n}{k_R - k_{aR}\omega_n^2}\right) - \arctan\left(\frac{A_{2R}\omega_n}{A_{1R} - A_{3R}\omega_n^2}\right) \tag{5.4}$$

Hence, the controller must satisfy the relationship:

$$\tan\varepsilon = \frac{k_{rR}\omega_n}{k_R - k_{aR}\omega_n^2} \tag{5.5}$$

where the required phase advance, ε, is a combination of the three elements :

$$\varepsilon = -\left(\varepsilon_R + \varepsilon_{12} + \arctan\left(\frac{A_{2R}\omega_n}{A_{1R} - A_{3R}\omega_n^2}\right)\right) \tag{5.6}$$

Equation (5.5) may be rewritten as :

$$\frac{k_{rR}}{k_{aR}} = \frac{\tan\varepsilon}{\omega_n}\left[\frac{k_R}{k_{aR}} - \omega_n^2\right] \tag{5.7}$$

The required phase advance is, therefore, selected by the sensitivities to meet specific operational objectives which are considered presently.

Selection of Controller Sensitivities and Yaw Interference

A phase compensating controller of the form (5.2) introduces a pair of zeros on the s-plane. The location of these is selected by the relative magnitudes of the coefficients such that their effect in conglomeration produces maximum stabilisation whilst not degrading any other aspect of the system. In particular, the effect on the yaw response of the ship must not be compromised by the RRS controller. The following considerations are taken at a ship speed of 18 kts for the RRS loop and assuming an ideal servomechanism. A parallel argument is obvious for the fin loop.

Examining the consequences of roll angle feedback, k_R, if this magnitude is varied, the acceleration term, k_{aR} kept constant, the roll rate, k_{rR}, altered in order to maintain the phase

relationship (5.7) and the gain k_{sR}, modified to achieve comparable levels of stabilisation then the zeros of the controllers (5.2) will move increasingly to the left of ω_n, i.e. towards a lower frequency location. Hence, the 40dB/dec slope associated with the pair of zeros will act over a longer frequency region before encountering the poles of g12(s). This will be reflected in the sensitivity function as increased disturbance attenuation in the same frequency region. These characteristics are demonstrated in the frequency spectrums of the controllers in the graphs of Figure 5.3, where the direction of the arrows indicate increasing roll angle feedback. The corresponding effects on the sensitivity functions are demonstrated, together with the associated Nyquist plots in Figure 5.3.

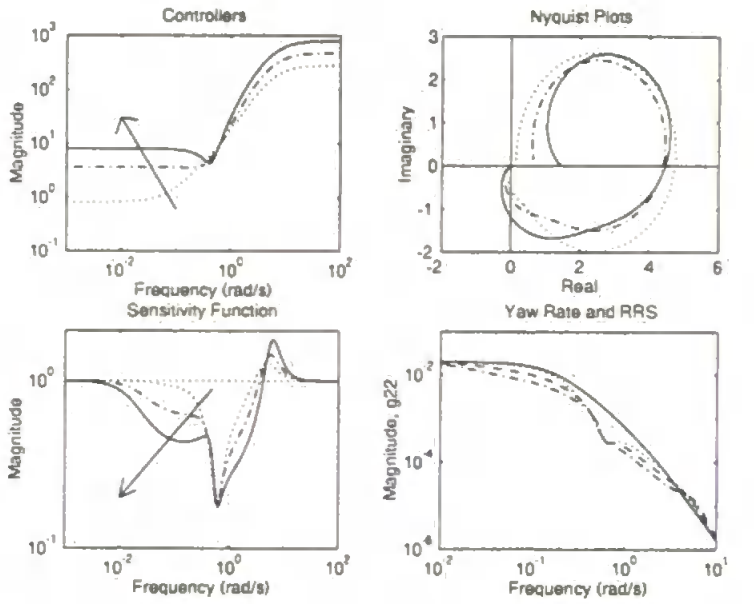

Figure 5.3 : Effects of increasing roll angle feedback

Since the yaw dynamics of a ship are a low frequency phenomena and it is apparent that the controller exhibits some alacrity in this region, further examination is required to ascertain the degree of interference expected. Figure 5.4 illustrates a schematic of the interaction of the RRS controller and roll dynamics with the ship's yaw response.

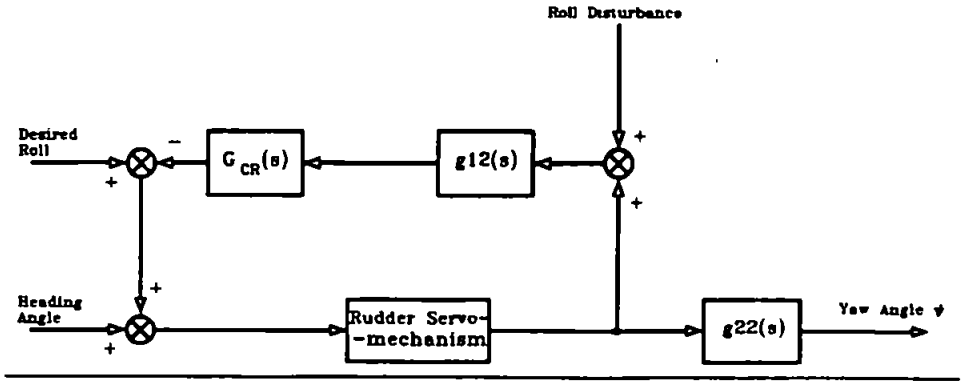

Figure 5.4 : Yaw and RRS loop

Assuming the servomechanism to be ideal then the transfer function, with the RRS controller active, from the heading angle to yaw rate, r, is:

$$\frac{r}{\text{Heading}} = \frac{g22(s)s}{1 + G_{CR}(s)g12(s)} \tag{5.8}$$

Utilising this relationship, the effects on the open loop yaw response, and by implication the closed loop, induced by the RRS controllers can be determined as depicted in the final graph of Figure 5.3, where the solid line represents the unperturbed yaw response of g22(s). Increasing the roll angle feedback of $G_{CR}(s)$, has a corresponding detrimental repercussion on the rudder's yaw generating capability which will increase the difficulty of steering and likelihood of broaching. This may be minimised by judicious selection of k_R if it is introduced into the controller with the other components.

Considering the impact of roll rate feedback, k_{rR}. This coefficient is varied in combination with k_{aR} thus adhering to the phase relationship (5.7), and keeping k_{aR} and k_R constant. Roll rate feedback increases the damping of a dominant second-order system hence decreasing the peak resonance amplitude. This characteristic is portrayed with lucidity in the graphs of Figure 5.5, where the direction of the arrows indicate increasing magnitude of k_{rR}. The sensitivity peak produces increasing levels of stabilisation around the resonance frequency, confirmed by the resulting Nyquist and controller spectrums as shown. The attendant yaw

interference graphs are also shown, where the solid line is the yaw rate, which indicates minimal yaw interference at the critical low frequency.

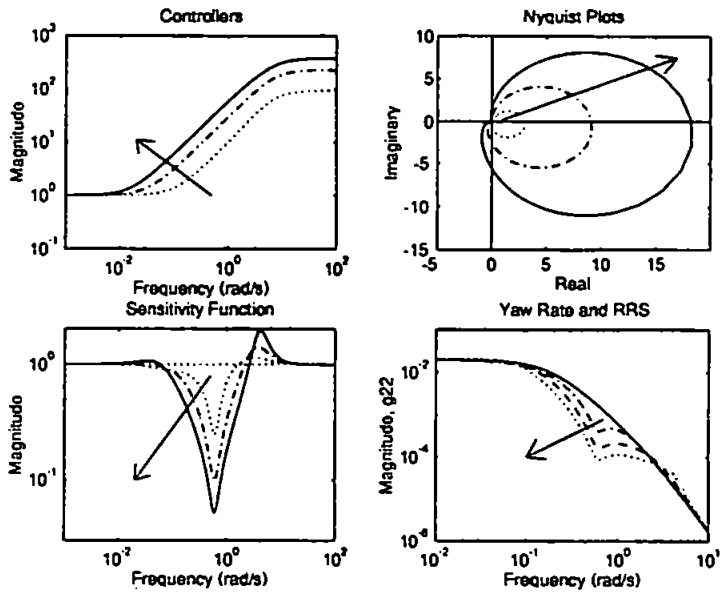

Figure 5.5 : Effects of increasing roll rate feedback

If the roll acceleration coefficient, k_{aR}, is increased the zeros of the controller will move to the right of ω_n. Thus it provides an access to achieve stabilisation at higher encounter frequencies whilst limiting servomechanism slew rate saturation.

The following coefficients were selected, Table 5.1, having considered the preceding limitations and advantages. Simulations studies were also conducted, the results of which will be presented in Chapter 7, in order to establish these values.

Table 5.1 : Table of controller coefficients

	Fin Loop			RRS Loop		
Speed (kts)	12	18	26	12	18	26
Roll acceleration, k_{aF}, k_{aR}	6.77	6.77	6.77	8.2	8.2	8.2
Roll rate, k_F, k_R	5	5	5	10	10	10
Roll angle, k_F, k_R	1	1	1	1	1	1
Speed gain, k_{SF}, k_{SR}	7	5	5	1.4	1	1.3
Gain margin (dB)	17	18	18	5	6	7
Phase margin (degs)	46	38	42	85	84	75

Table 5.1 also records the relevant gain and phase margins which appear to be adequate. However, the gain margin of the RRS loop is perhaps rather limited.

Filtering Requirements

A characteristic of phase compensators such as (5.2) is that they usually possess constant gains at zero and infinite frequencies as demonstrated by Figures 5.3 and 5.5. This may have undesired ramifications on the operation of the stabiliser control systems. At zero frequency the controllers will generate commands to the fins and rudders which in effect attempt to correct constant list angles developed by the ship. However, a lack of static heeling power renders the fins, section 2.2.2, ineffective in this mode. Furthermore, such low frequency action generated by the RRS loop may have debilitating repercussions on the yaw dynamics of the ship. Despite these low frequency restrictions the controller must, nevertheless, retain the faculty, by adequate gains, to stabilise the ship when perturbed by following (low frequency) sea disturbances. Sensor noise usually predominates at the high frequencies which will propagate through the controllers multiplied by their gains, consequently generating spurious motions in the servomechanism which will cause unnecessary wear and saturation.

This scenario can be avoided by an appropriate filtering contingency. A low-pass, $W_{LP}(s)$, and high-pass, $W_{HP}(s)$, filter will ensure that the controllers' gains are zero at zero and infinite frequencies. These filters have the form:

$$W_{LP}(s) = \frac{1}{\frac{0.1}{\omega_n}s + 1} \qquad W_{HP}(s) = \frac{\frac{15}{\omega_n}s}{\frac{15}{\omega_n}s + 1} \tag{5.9}$$

5.3.3 Method Two - PID Controller

Conolly (1969) proposed that the zeros of a PID controller be used to cancel the second order under-damped poles of the ship roll. The controller, acting on the roll rate, for the fin stabilisers is represented by:

$$\alpha = k_1\phi + k_2 p + k_3\dot{p} \tag{5.10}$$

where

$$\frac{k_1}{k_3} = \omega_n^2 \quad \text{and} \quad \frac{k_2}{k_3} = 2\zeta_s\omega_n$$

The terms $k_1\phi$ and $k_3\dot{p}$ cancel at ship natural roll frequency such that the fin angle demand consists entirely of the roll rate term. The k_2 term is then a function of the required roll reduction at ω_n.

This approach has inherent limitations. The method would be satisfactory if the roll of the ship in response to environmental conditions was limited to a narrow band around the resonance frequency. However, cancellation of the poles by the controller's zeros implies that the sensitivity function is a constant for all frequencies. At very low frequencies the controllers would demand correction of constant list angles and at high frequency be susceptible to sensor noise. Although, this can be rectified by appropriate filtering, an alternative PID controller which at the design stage restricts the frequency range where stabilisation is to occur is proposed.

The PID controller is essentially a system with two zeros and a pole at the origin. If the zeros are placed on the negative real axis at either side of the natural roll frequency the resulting controller will be an extended-'V' shape. If correctly aligned, the integral and derivative terms will cancel each other at ω_n leaving the residual proportional term to dictate the level of stabilisation achieved. The resulting open loop transfer function will have

two 0-dB cross-over points which subsequently ensure that the sensitivity function provides disturbance attenuation around roll resonance only.

The controller has the form:

$$G_{PID}(s) = k_P + \frac{1}{k_I s} + k_D s \tag{5.11}$$

The coefficients were selected heuristically. The integral term ensures that at low sea encounter frequencies some stabilisation is provided. Noise propagation and high frequency slew rate saturation of the servomechanisms is prevented by suitable selection of k_D. Appropriate selection of k_P not only restricts the control effort but also regulates the width of the frequency region where it is applied.

As in Method One, the fin and rudder hydrodynamic performance is a function of ship speed and is accounted for by gain scheduling through the proportional term, k_P. The controller also requires filtering of the form in equations (5.9) in order to prevent the high and low frequency limitations as previously discussed. Table 5.2 collates the values of the coefficients and the resulting gain and phase margins. Simulations studies suggest these to be appropriate values such that saturation is avoided. These results will be deferred to Chapter 7.

Table 5.2 : PID controller coefficients

	Fin Loop			RRS Loop		
Speed kts	12	18	26	12	18	26
k_P	35	30	30	10	8	8
k_I	5	5	5	5	5	5
k_D	0.3	0.3	0.3	0.3	0.3	0.3
Gain Margin (dB)	17	20	19	5	4	6
Phase Margin (degs)	85	80	81	66	66	52

The controller at 12 kts only, for clarity, in the RRS loop, is shown in Figure 5.6 without any filtering modifications, where the extended-'V' shape is apparent. The sensitivity function indicates that roll stabilisation occurs predominantly at the natural roll frequency with an amplification of 5dB centred at approximately 1.3 rads^{-1}. This is irrelevant since there is insignificant sea disturbance at these frequencies. Around the lower encounter frequencies 5dB attenuation is achieved which is envisaged will be within the rudder's moment generating capabilities. Considering yaw interference, Figure 5.6, where the solid line is the undisturbed yaw response spectrum, it indicates that this low frequency activity has negligible effect on the yaw dynamics. The controllers at 18 and 26 kts also achieve adequate roll stabilisation with minimal impact on yaw dynamics. Their sensitivity functions are illustrated in the final graph of Figure 5.6.

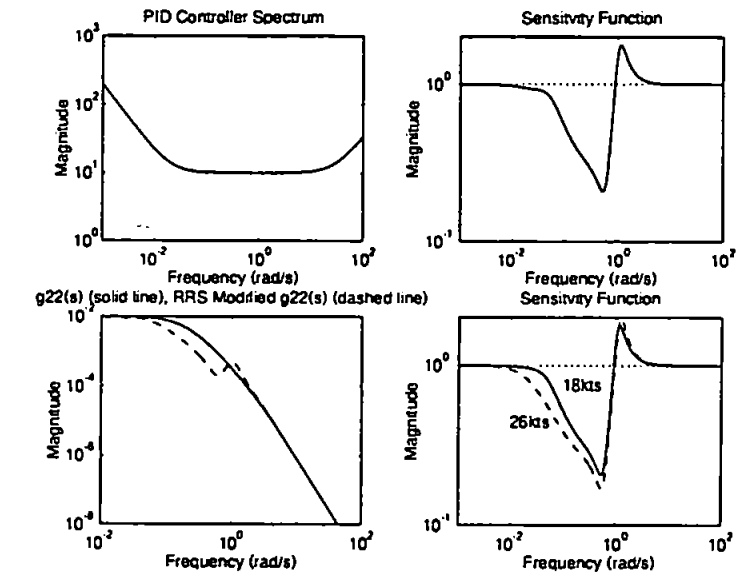

Figure 5.6 : PID controller in the RRS loop

Figure 5.7 shows the fin loop characteristics. The controller has greater amplitude around the natural frequency which is extended over a longer frequency region than the RRS controller: reflecting the fin stabiliser's superior moment generating capability. The sensitivity function provides adequate disturbance rejection around the natural and low

encounter frequencies with negligible amplification at 0.08 and 4 rads^{-1}, it is envisaged that since there will be insignificant sea disturbances at these frequencies then roll amplification will not occur.

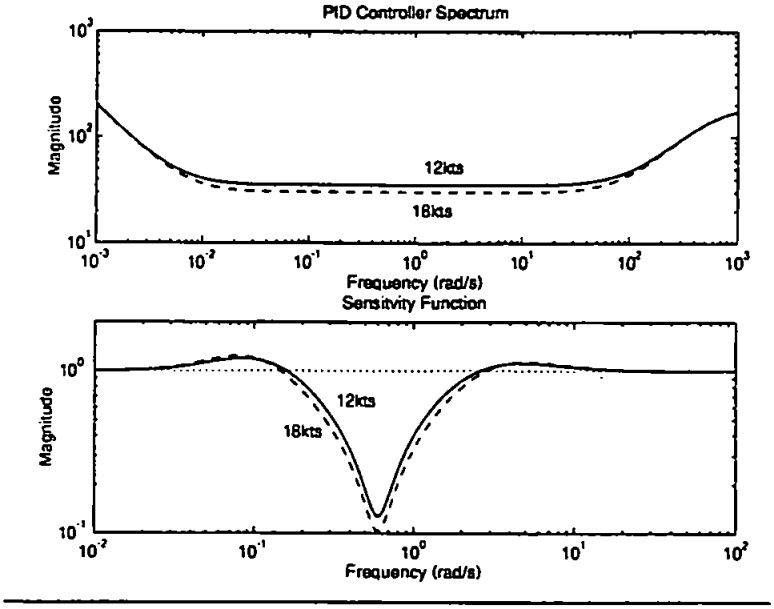

Figure 5.7 : PID controller and fin stabilisation loop

5.3.4 Combination of Fin/Rudder Stabilisation Loops

Controllers for the fin and rudder loops have been developed independently. Their roll stabilisation ability in conglomeration is now examined with respect to the sensitivity function. Consider both the RRS and fins stabilisation loops engaged as illustrated in Figure 2.18 then the sensitivity function from the roll disturbance to the stabilised roll, ϕ_s, is

$$\frac{\phi_s}{d_1} = \frac{1}{1 + G_{CR}(s)g12(s) + G_{CF}(s)g11(s)} \tag{5.12}$$

Figure 5.8 shows this together with the sensitivity functions achieved for the fins and rudders acting independently utilising controllers derived from Methods One and Two. With the fins active alone the controller of Method One attenuates disturbances at lower encounter frequencies as compared to the maximum 5dB amplification induced by the controller generated from Method Two, whilst at high encounter frequencies the reverse is

apparent. A similar scenario exists with the RRS controllers from both methods. The sensitivity functions of (5.12) for both design methods are similar although there is an amplification of 6dB with the controller of Method One as compared with 1dB for Method Two at 4 rads^{-1}.

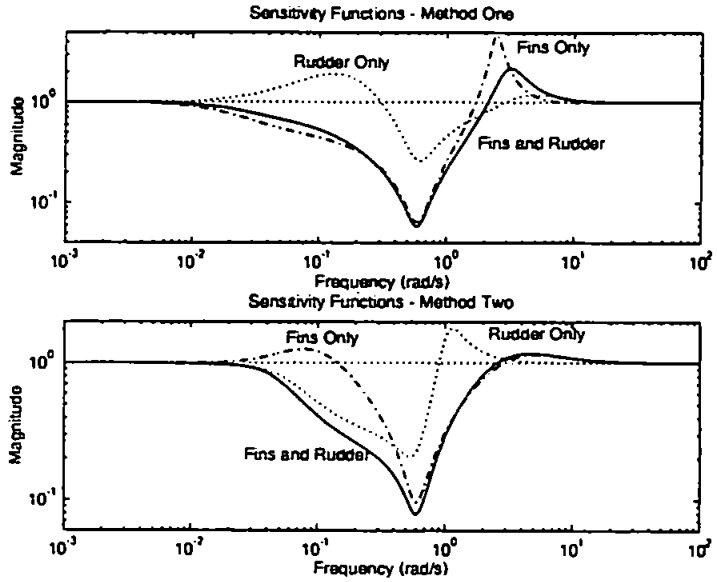

Figure 5.8 : Sensitivity functions of combined fin/rudder loops

Two controllers for each of the RRS and fin loops have been generated, utilising classical techniques, which appear to provide adequate levels of stabilisation and possesses sufficient safety margins. Results from the time domain simulations of the controllers will be presented in Chapter 7 in combination with the LQG and robust controllers. The LQG design in now considered.

5.4 LQG CONTROLLERS

The preceding classical and PID controllers require rules for the selection of the coefficients based on experience. A vast body of literature, with a myriad of applications, is evidence of the fecundity of such a generally heuristic procedure. Since these types of controllers are essentially a SISO process, the problem becomes critical in MIMO systems.

Optimal controllers attempt to embody the heuristic design specifications in a cost function. Once the parameters have been assigned, based on engineering constraints, a standard algorithm provides the optimal feedback gains. The algorithm is a procedure which optimises the cost function.

The general LQG theory is briefly outlined here. There are many excellent textbooks on the subject: Kwakernaak and Sivan (1972), Friedland (1986), and Grimble and Johnson (1988) amongst others.

5.4.1 Optimal Controller and Stochastic Filtering

Optimal Feedback

LQG controller synthesis requires that the plant be described by the state space format such as shown in equation (5.13). In order that there are no hidden unstable modes, the system's unobservable and uncontrollable modes must be asymptotically stable (Friedland, 1986).

$$\begin{aligned} \dot{x} &= Ax + Bu \\ y &= Cx + Du \end{aligned} \tag{5.13}$$

where

$$x \in \mathbb{R}^{n\times 1} \quad u \in \mathbb{R}^{1\times m} \quad y \in \mathbb{R}^{r\times 1}$$
$$A \in \mathbb{R}^{n\times n} \quad B \in \mathbb{R}^{n\times m}$$
$$C \in \mathbb{R}^{r\times n} \quad D \in \mathbb{R}^{r\times m}$$

and the transfer function may be arrived at by:

$$G(s) = C(sI - A)^{-1}B \tag{5.14}$$

A state space representation of the ship roll dynamics, Figure 2.18, is placed in Appendix D.

The objective of LQG is to minimise the energy of the cost function:

$$J = \int_0^\infty (y^T Q_c y + u^T R_c u)\,dt \tag{5.15}$$

where

$$Q_c \in \mathbb{R}^{r \times r} \quad R_c \in \mathbb{R}^{m \times m}$$

and the conditions must be adhered:

$$(i) \quad Q_c = Q_c^T \geq 0$$
$$(ii) \quad R_c = R_c^T > 0$$

The design objectives are embodied in the selection of the output, Q_c, and control, R_c, weights. Condition *(i)* implies that not all the outputs are of relevance in the optimisation process. The control weight must remain positive definite as postulated by condition *(ii)*. It would be impossible to control the output, y, defined in Q_c, if control action were not permissible (i.e. R_c=0). Therefore, R_c affords a variable to restrict the level of control energy utilised. By its judicious selection the rudder servomechanism can be prevented from encroaching into non-linear regions of operation such as slew rate saturation.

The optimal full-state feedback controller is generated by solving a matrix generalised quadratic equation: the Algebraic Ricatti Equation (ARE), equation (5.16).

$$A^T P + PA - PBR_c^{-1}B^T P + C^T Q_c C = 0 \quad \in \mathbb{R}^{n \times n} \tag{5.16}$$

where

$$P^T = P \geq 0$$

The optimal controller is then given by:

$$K_c = R^{-1}B^T P \tag{5.17}$$

which is inserted in the feedback loop as shown in Figure 5.9 such that the control signal, u, for the regulator problem is:

$$u = -K_c x \tag{5.18}$$

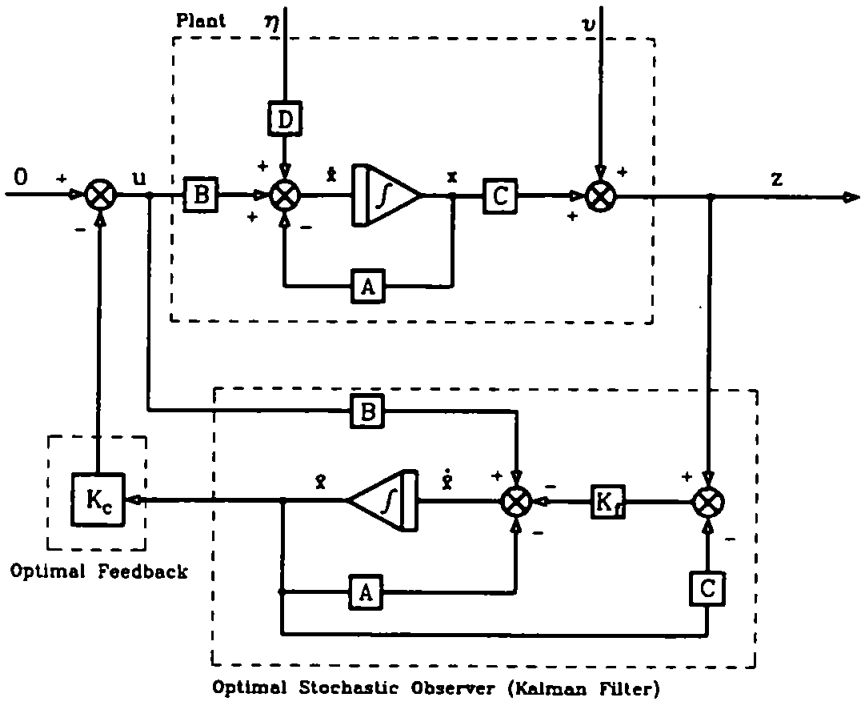

Figure 5.9 : Optimal controller and observer strategy

Stochastic Filtering (Kalman Filter)

The implementation of (5.18) is only feasible if the full states of the plant are directly available. In general, only a few states can be interpreted as physical phenomena hence subject to measurement. An observer is required in order to reconstruct an estimate of the states based on these measurements. In reality the measured variables will be corrupted by noise, $\upsilon(t)$ and the plant will have its own internally generated noise process, $\eta(t)$, thus exacerbating the integrity of the states produced by the estimator. The state space description, (5.13), can be rewritten to reflect these external processes.

$$\begin{aligned} \dot{x} &= Ax + Bu + D\eta \\ z &= Cx + \upsilon \end{aligned} \tag{5.19}$$

A stochastic observer (Kalman filter) is an optimal estimator, with respect to white noise disturbances, of the states of a plant. It is generated by minimisation of the cost function:

$$J = \mathrm{E}\left[\sum_{i=1}^{n} (x_i - \hat{x}_i)^2\right] \tag{5.20}$$

where

E Expectation

$\hat{x}$ Estimation of state variable

The white noise statistics which impinge on the plant have means and variances given by:

$$\begin{aligned} \mathrm{E}[\eta] &= 0 \quad \mathrm{E}[\eta\eta^T] = Q_f\delta\ (t-\tau) \\ \mathrm{E}[\upsilon] &= 0 \quad \mathrm{E}[\upsilon\upsilon^T] = R_f\delta\ (t-\tau) \end{aligned} \tag{5.21}$$

where

δ (t) The Kronekar delta

The resulting optimal filter gain, K_f, can be derived by solving the ARE for S such that:

$$K_f = SC^T R_f^{-1} \tag{5.22}$$

The full implementation is depicted in Figure 5.9.

The ship roll model suggests that it is not perturbed by unadulterated white noise but this is modified by filters (Figure 2.18) which represent the appropriate sea states and heading conditions. Since, these filter are driven by white noise, they are incorporated into the Kalman structure hence, the conditions for the optimality of the cost function (5.20) and ARE are not violated. Thus the performance of the resulting controllers will be optimised in the presence of the chosen sea state.

Subsequent optimisation of (5.20) will be performed with the sea state acting at state 5 and ship orientation at beam sea (Figure 2.16). This affords sufficiently severe unstabilised rolling motion representing the expected operational limits for Royal Navy frigate size warships and indeed most other classes of ship. A variance of 0.1 for Q_ρ in conjunction with internal filter gains, generates the approximate RMS magnitude sea disturbance roll moments representing sea state 5 as furnished by DRA Haslar. It will be shown in Chapter 8, that the sensor environment permits a reliable measurement of the roll angle by the gyroscope.

The Kalman filter cannot be updated for changing sea conditions, although this was addressed by adaptive filtering by Klugt (1987) and Amerongen *et al* (1987). The controllers will be gain scheduled in order to reflect the variable hydrodynamic performance of the fins and rudders with ship speed.

The separability principle of a optimal controller observer structures implies that the poles of the controller and Kalman filter may be placed arbitrarily on the complex plane by selecting the gain matrices.

LQG controllers and observers are now generated for the fin and RRS loops.

5.4.2 Independent Loop LQG Control Design

Design of the LQG controllers is initially pursued for the individual RRS and fin stabilisation loops of Figure 2.18. Section 5.4.3 will approach the design as a single input-two-output problem. The last section, 5.4.4, compares the stabilisation performance of both approaches by utilising the sensitivity function.

The ARE's associated with the cost functions (5.15) and (5.20) are solved by a standard numerical package operating in the Matlab® environment hosted on a personal computer.

RRS Controller

If the control weight, R_c, is reduced the implication is that an increasing degree of control action is permissible hence accruing greater roll stabilisation. Conversely, by decreasing the output weight, Q_c, the connotation is that a relatively small degree of stabilisation is acceptable.

The control weight, R_c, in the optimal cost function (5.15) is varied, whilst maintaining the output weight, Q_c, constant at unity, in order to ascertain the achievable characteristics. The resulting frequency spectrum of the controllers, Nyquist plots and sensitivity functions are illustrated in Figure 5.10, where the direction of the arrow indicates increasing R_c.

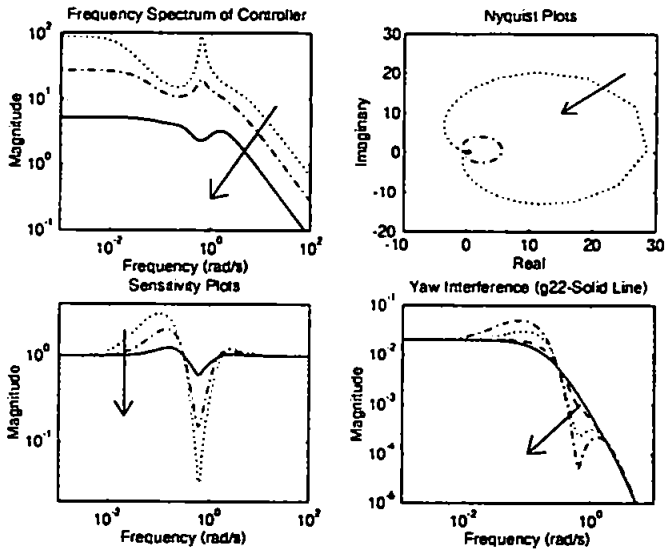

Figure 5.10: Variation of control weighting on RRS loop

As the control weight, R_c, is increased the corresponding magnitude of the frequency spectrum of the resulting controllers diminishes. In particular, the 'trough' centred around $\omega = 0.1$ rads^{-1}, the location of the non-minimum phase zero, becomes less pronounced

indicating possible amplification in the sensitivity function at relatively low R_c. Also the peak centred around ω_n reduces implying that in the closed loop the controller will exhibit less alacrity in reducing sea disturbances. Considering the sensitivity function, the prediction of disturbance amplification on account of the non-minimum phase zero, as stipulated in section 5.2, is vindicated by the 10 dB amplification at $\omega = 0.1$ rads^{-1}. As R_c increases, in general, the controller tends to impede the roll disturbance attenuation potential of the RRS loop thereby dictating servomechanism activity.

The final series of graphs in Figure 5.10 determine the degree of interaction with the yaw loop according to relationship (5.8). Again it is demonstrated that at the low frequencies, where the yaw action is concentrated which coincides with the proximity of the non-minimum phase zero, introduction of the RRS controller will cause the ship to turn quicker than expected if R_c is permitted to be small.

The values of R_c were determined as 0.04, 0.01 and 0.01 for ship speeds of 12, 18 and 26 kts respectively having conducted iterative simulations, to be presented for comparison with other controller design techniques in Chapter 7. It was ensured that slew rate saturation is avoided and minimal yaw interference occurs. The closed loop system possess sufficient safety margins, which is 60^0 of phase margin and 40dB gain margin as determined from the resulting Nyquist plot.

Fin Stabilisers Controller

A similar procedure to the RRS controller design above was pursued. The results are shown in Figure 5.11.

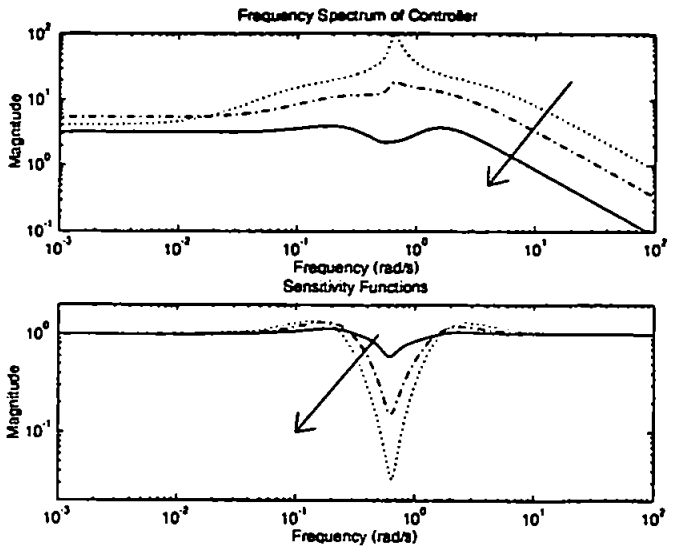

Figure 5.11: Variation of control weighting on fin stabiliser loop

As the control weighting is increased, naturally, the controller restricts the amount of roll attenuation achieved as demonstrated by the attendant sensitivity functions of Figure 5.11. The controller delivers the control action around the roll resonance peak of the ship. Simulation results, to be presented in Chapter 7, suggests that an optimal value for R_c is 0.001 at all three speeds. The resulting phase and gain margins were 30-50^0 and 20-40dB which are adequate.

The frequency spectrums of the controllers in Figures 5.10 and 5.11 suggest that a filtering contingency is required lest the problems as discussed in section 5.3.2 ensue. These filters take the form of equations (5.9).

Controllers generated in this section are for the independent operation of the fin and stabiliser loops. The next section determines whether a more efficacious controller results by treating the ship roll model as a mutlivariable system.

5.4.3 Multivariable LQG Control Design

The controller for the combined RRS and fin stabiliser loop is now constructed based on the values of R_c and Q_c determined in the preceding section.

Figure 5.12 illustrates the sensitivity function, at 18 kts, of the multivariable system and the combined effects of the controllers which were generated for the stabilisation loops independently as derived from equation (5.12). The consequences of the latter controllers acting in conglomeration appear to amplify the sea disturbances marginally greater than the multivarible controller at 0.1 rads^{-1}. In general the performance is almost identical. Hence, the methodology pursued of independently designing controller for the two stabilisation loops is vindicated.

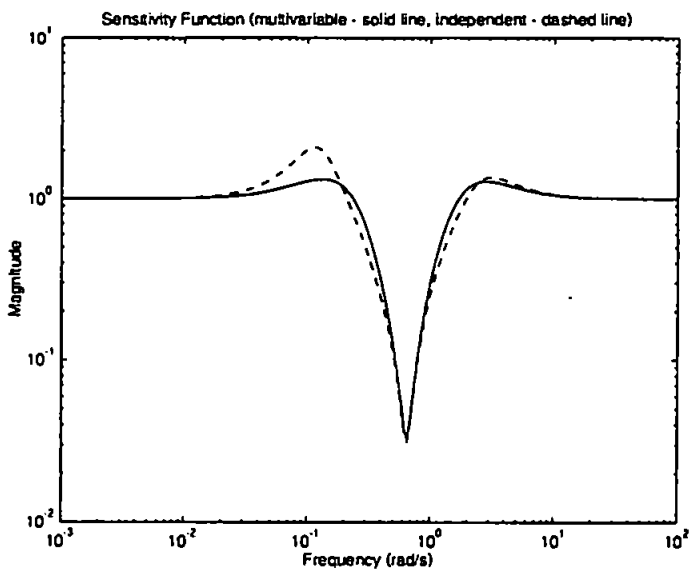

Figure 5.12: Multivariable and independent controllers' sensitivity functions

5.5 DISCUSSION AND CONCLUSIONS

At the outset it was known that the rudder roll dynamics contain a non-minimum phase zero. Therefore, at the incipiency of this Chapter it was decided to evaluate the limitations that may be imposed by this phenomenon. It was concluded that, irrespective of the RRS

controller, it will of necessity amplify roll disturbances at the frequency region where the zeros are located. Hence, the subsequent sensitivity functions were correctly interpreted, and not regarded as inherent shortcomings of the controller design procedures. The controller design proceeded with the objective that it does not inadvertently impart pernicious consequences to the roll stabilisation ability of the closed-loop system.

The traditional classical techniques appeared to offer an attractive and intuitive synthesis procedure to arrive at the controllers. The objectives are established with lucidity and the subsequent controller's poles and zeros can be related to the desired closed-loop time domain characteristics. The other control strategy investigated was LQG. Although, the objectives are transparent and encapsulated in a cost function, the controller synthesis is usually concealed from the designer in software routines. The apparent impediment in this method was the inflexible requirement to incorporate the sea dynamics within the controller structure. Therefore, the performance inevitably deteriorates should the sea state alter in it predominant wave height and period as shall be demonstrated by simulation studies in Chapter 7.

CHAPTER 6

OPTIMAL LINEAR ROBUST CONTROLLERS

6.1 INTRODUCTION

The controllers of the previous sections perform adequately provided that the ship roll models, g12(s) and g11(s) do not diverge from their nominal behaviour. However, the linear transfer functions remain a crude approximation to the ship's complex dynamics, for example: the hydrodynamic coefficients, equation (2.14), are frequency dependent and generally subject to non-linear distortion, the loading conditions of the ship change, the speed of a multirole warship and its orientation to the waves is rarely constant thus inducing varying responses. The ubiquitous waves of the oceans are constantly changing the energy of their constituent harmonic frequencies thus invoking different sea states and dominant wave periods. All these uncertainties not only contribute to the degradation of a controller's performance but also compromise its safety limits. The objective of optimal robust control (H_∞) techniques is to minimise the largest possible excursion from this set of defined perturbations.

In classical frequency methods the approach usually adopted to contend with such a scenario is to ensure that the controller possesses sufficient robust margins which relate to the uncertainties in a somewhat nebulous fashion. The controller may now be stable against

uncertainties which are not possible, resulting in a conservative system. Since, the sensitivity function is inextricably linked with robustness, the roll disturbance rejection abilities will be compromised.

The LQG is a state space optimisation approach to feedback design (Athans and Falb, 1966, Anderson and Moore, 1978) which assumes that white noise processes exclusively impinge on the system. This is a severe restriction for most applications. The time domain LQG, by Parseval's theorem is equivalent to H_2 optimisation as shown by Youla *et al* (1976) in the frequency domain context of the Wiener-Hopf filter.

LQG's advantage is that it can readily be adapted for multivariable systems which have Guassian white noise disturbances. However, since it cannot directly encapsulate uncertainties, the subsequent controllers may not be robust. Although, the optimal state feedback controller has guaranteed phase margins (60^0) and infinite gain margins in each control channel (Safonov and Athans, 1977), these evaporate for the full stochastic LQG controllers as demonstrated by Doyle (1978) in an ostensibly simple application. Robustness recovery techniques (Loop Transfer Recovery, LTR) have been proposed by Stein and Athans (1987). However, the results are asymptotic and limited to minimum phase systems which restricts their practical applications and were not pursued in section 5.4. Perhaps LQG's severest limitation, as previously mentioned, is the assumption that the disturbance processes can be completely encapsulated by white noise which is not appropriate in many applications. In section 5.4 the sea disturbance filters represent the perturbations which were absorbed into the state space description. Therefore, the controller is optimised for roll stabilisation in the presence of sea state 5. Its performance will significantly deteriorate when the sea state changes.

H_∞ optimisation, originated by Zames (1981) amongst others, in contrast with LQG, assumes that the disturbances belong to a pre-specified set of signals. The gain of the closed loop transfer function matrix is minimised for the worst possible combination of disturbances in this set. The controller is synthesised by the minimisation of the H_∞ norm over the set of all stabilising controllers. Although, the H_∞ and LQG appear unconnected, the latter can be shown as a particular case of the generalised former (Doyle *et al*, 1988).

The robust controller theory will be shown to encapsulate this information in a pseudo-explicit manner in terms of weight functions. Thus the optimisation process will produce controllers which have desired characteristics despite these uncertainties. Further analysis by the Structured Singular Value (SSV) permits explicit uncertainty in parameter variations to be incorporated. The uncertainties presented in Chapter 2 will be utilised in order to evaluate the coefficient variations. Thus the application of the technique is novel in this respect. Initially, a digression is made to state some preliminary results. A brief outline is presented of the motivation and results of the technique. The later sections deal with weight selection. A more detailed account of the optimisation methods may be found in the various references cited.

6.2 SYSTEM REPRESENTATIONS

6.2.1 Closed Loop Systems Relationships

Consider the feedback control configuration of Figure 6.1, where r is the reference or command signal, u, is the actuator signal, y, the output signal, n the measurement noise, and d represents extraneous disturbances. The transfer function G(s) embodies the known plant and actuator behaviour as a linear transfer function and K(s) is the controller.

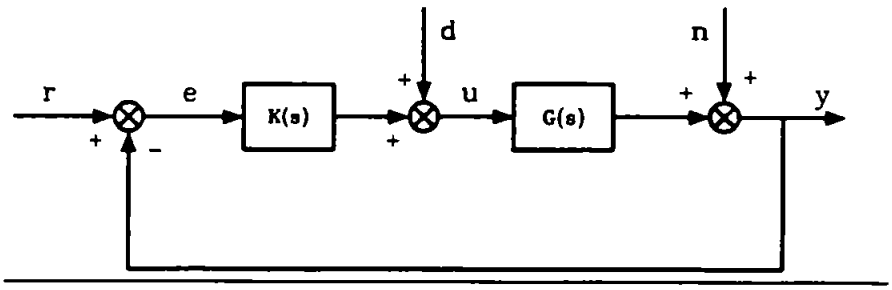

Figure 6.1 : Closed loop control system

The closed loop system may be concisely represented by the following equations where the Laplace operator, s, is assumed, and therefore, omitted for clarity.

$$y = Tr + S(Gd + n) \tag{6.1a}$$

$$u = Sd + C(r - n) \tag{6.1b}$$

$$e = S(r - n - Gd) \tag{6.1c}$$

The transfer function matrices, S, C and T are termed the sensitivity function, control sensitivity and the complimentary sensitivity respectively which are given as:

$$S = (1 + GK)^{-1} \tag{6.2a}$$

$$C = K(1 + KG)^{-1} \tag{6.2b}$$

$$T = GK(1 + GK)^{-1} \tag{6.2c}$$

It can be shown that a complementary relationship exists between S and T:

$$S + T = 1 \quad \forall s \in \mathbb{C} \tag{6.3}$$

6.2.2 Linear Fractional Transformations

A system, when presented as a linear fractional, lends itself to be more amenable to the general algorithms of optimal control theory (Redheffer, 1960, Francis, 1988, and Hung, 1989). Although, other transformations are possible, viz. the upper and double fractional representations, by convention in literature the controller is embedded in the lower

transformation, whilst the perturbations structure is contained within the upper loop. The transformation with both loops engaged may be considered as double as is demonstrated presently.

If the plant, G, of Figure 6.1 is partitioned into a 2-by-2 matrix:

$$\begin{pmatrix} y \\ e \end{pmatrix} = \begin{bmatrix} G_{11} & G_{12} \\ G_{21} & G_{22} \end{bmatrix} \begin{pmatrix} r \\ u \end{pmatrix} \tag{6.4}$$

where y is the vector of signals which completely characterises the closed loop behaviour. Then by application of the feedback law,

$$u = Ke \tag{6.5}$$

a general representation of Figure 6.1 is depicted in Figure 6.2.

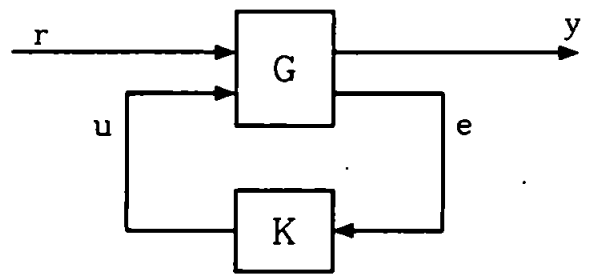

Figure 6.2 : Feedback control system for LFT

The transfer function from r to y is known as the lower linear fractional transformation (LFT) (Francis, 1988):

$$F_l(G,K) = G_{11} + G_{12}K(I - G_{22}K)^{-1}G_{21} \tag{6.6}$$

The complimentary sensitivity (6.2c) is recognised as the closed-loop transfer function of Figure 6.1 with d and n removed. Equation (6.6) may be used as an alternative representation for T(s):

$$F_l(G_T, K) = GK(1+GK)^{-1} \tag{6.7}$$

where

$$G_T = \begin{bmatrix} 0 & G \\ 1 & -G \end{bmatrix}$$

By defining appropriate partitions of G(s) the LFT may be used to embody any pair of input/output combinations of Figure 6.1. This concept will be central in formulating the definition for the optimisation procedure.

If the external disturbances are now reintroduced into the LFT configuration the resulting system appears as a generalisation shown in Figure 6.3.

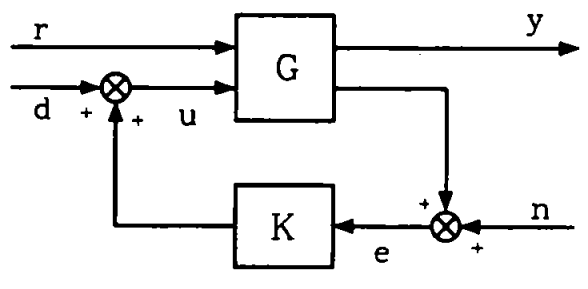

Figure 6.3 : Complete generalised representation of system

The input/output relations are defined by:

$$y = G_{11}r + G_{12}u \tag{6.8a}$$

$$u = d + Ke \tag{6.8b}$$

$$e = n + G_{21}r + G_{22}u \tag{6.8c}$$

This may be characterised by $F_l(G,K)$ from corresponding inputs and output which are derived in the matrix form as:

$$\begin{pmatrix} y \\ u \\ e \end{pmatrix} = [I - G_{22}K]^{-1} \begin{bmatrix} G_{11}(I - G_{22}K) + G_{12}KG_{21} & G_{12} & G_{12}K \\ KG_{21} & I & K \\ G_{21} & G_{22} & I \end{bmatrix} \begin{pmatrix} r \\ d \\ n \end{pmatrix} \tag{6.9}$$

Incidentally, this forms the basis of Glover and MacFarlane's (1989) approach to internal stability by co-prime factorisation. If the first term on the right side of (6.9) is analytic in the rhp (Nyquist stability theorem) then the internal signals remain bounded. It also gave the impetus for Q-parameterisation of all controllers (Youla *et al*, 1976) which is fundamental in the solution of the optimal controller.

Thus an LFT is a generalisation of the standard plant's closed loop transfer function, G_T which can be evaluated as (6.10). The terminology adopted is consistent with the definitions of S, C and T.

$$F_G\left(\begin{bmatrix} 0 & G \\ I & -G \end{bmatrix}, K\right) = \begin{bmatrix} T & -T & SG \\ C & -C & I-CG \\ S & -S & SG \end{bmatrix} \tag{6.10}$$

The upper fractional transformation (UFT) is determined when K of Figure 6.2 is connected to the r and y with the same orientation and the subsequent fractional evaluated between u and e:

$$F_U(G,K) = G_{22} + G_{21}K(I - G_{11}K)^{-1}G_{21} \tag{6.11}$$

It can be further extended to the double fractional transformation, DFT, for dual feedback loops as shown in Figure 6.4.

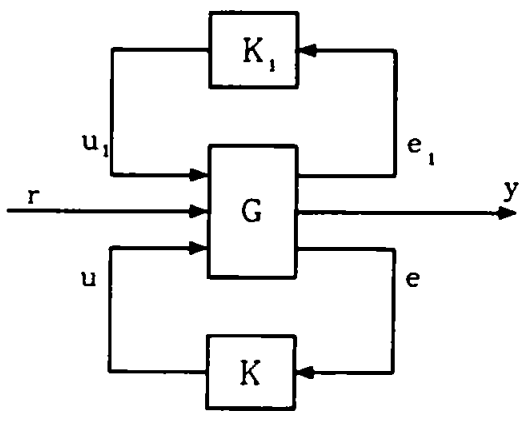

Figure 6.4 : Double fractional transformation configuration

The system is now endowed with two feedback loops. By convention, the upper loop contains a specific uncertainty structure extracted from the plant. The transformation is given by:

$$y = F_D(G, K_1, K)r \tag{6.12}$$

Glover and MacFarlane (1989) demonstrates that the DFT is an LFT nested within a UFT, or vice-versa.

6.2.3 Spaces and System Norms

The framework of H_∞ control resides within the domain of operator theory. Therefore, a brief digression may be advantageous in order to make fundamental definitions which will assist the subsequent development. Further details may be found in Young (1988), Kreyszig (1978) and Maciejowski (1990).

When any two rational functions $p(t)$ and $q(t)$ assume values in the complex plane, $\mathbb{C}^{m\times n}$, $\forall t \in \mathbb{R}$, they reside in the function space $\mathbf{L}_2(\mathbb{R}, \mathbb{C}^{m\times n})$, i.e. a mapping from the real domain to the complex by an arbitrary operator, iff $p(t)$ and $q(t)$ are square-(Lebesgue)-integrable. This property ensures that the constituents of the function space are bounded. Such signals, if they are convergent, are termed Cauchey sequences or complete. A Banach space is a linear space over $\mathbb{C}^{m\times n}$ which is complete and possesses a norm: this is elaborated presently.

The signal space $\mathbf{L}_2(\mathbb{R}, \mathbb{C}^{m\times n})$ is a Hilbert space with the inner product defined as:

$$\langle p, q \rangle = \int_{-\infty}^{\infty} \text{trace}[p^*(t)q(t)]\,dt \tag{6.13}$$

where

$$p^*(t) = [p(t)]^T$$

Associated with these signals there exists the concept of norms, specifically the 2-norm is given by:

$$\|p\|_2^2 = \langle p,p\rangle = \int_{-\infty}^{\infty} trace[p^*(t)p(t)]dt \qquad (6.14)$$

Since it was assumed that the signal is square-(Lebesgue)-integrable, then the 2-norm must remain finite. Conversely, if the norm (6.14) remains bounded it is a sufficient condition to ensure it belongs in $\mathbf{L}_2(\mathcal{R}, \mathcal{C}^{m\times n})$. The 2-norm can be interpreted as the energy of the LQG cost function. Thus the ARE is a minimisation of the 2-norm.

The sub-space $\mathcal{R}\mathbf{L}_2(\mathcal{R}, \mathcal{C}^{m\times n}) \subset \mathbf{L}_2(\mathcal{R}, \mathcal{C}^{m\times n})$ consists of rational functions with real coefficients which represent the physical systems under investigation here. The adjoint, $p^*(t)$, is now equivalent to its transpose.

Frequency Domain Functions

If a function space $\mathbf{L}_2(j\mathcal{R}, \mathcal{C}^{m\times n})$ is defined which contains rational functions, e.g. F(s), with no poles on the imaginary axis such that $F(j\omega) \in \mathcal{C}^{m\times n}$, $\forall\omega \in \mathcal{R}$ and which are also square-(Lebesgue)-integrable, it is apparent that the inferences are analogous to the signal spaces discussed previously. Similarly, the function space $\mathbf{L}_2(j\mathcal{R}, \mathcal{C}^{m\times n})$ is a Hilbert space with inner product defined as:

$$\langle F,G\rangle = \frac{1}{2\pi}\int_{-\infty}^{\infty} \text{trace}[F^*(j\omega)G(j\omega)]d\omega \qquad (6.15)$$

where

$$F^*(j\omega) = [F(-j\omega)]^T$$

The function space $\mathbf{L}_2(j\mathcal{R}, \mathcal{C}^{m\times n})$ also possesses a 2-norm, amongst others:

$$\|F\|_2^2 = \langle F,F\rangle = \frac{1}{2\pi}\int_{-\infty}^{\infty} \text{trace}[F^*(j\omega)F(j\omega)]d\omega \qquad (6.16)$$

By definition $\mathcal{R}\mathbf{L}_2(j\mathcal{R}, \mathcal{C}^{m\times n}) \subset \mathbf{L}_2(j\mathcal{R}, \mathcal{C}^{m\times n})$ consists of real rational functions such as

g11(s).

A connection between the function spaces $\mathbf{L}_2(\mathbb{R}, \mathbb{C}^{m\times n})$ and $\mathbf{L}_2(j\mathbb{R}, \mathbb{C}^{m\times n})$ is that they are isomorphic when certain operators function on their constituents. For example, the Fourier transform (6.17) of a time domain function $f \subset \mathbf{L}_2(\mathbb{R}, \mathbb{C}^{m\times n})$ lies in the function space $\mathbf{L}_2(j\mathbb{R}, \mathbb{C}^{m\times n})$.

$$F(j\omega) = \int_{-\infty}^{\infty} f(t)e^{-j\omega t}\,dt \tag{6.17}$$

Transfer Function Spaces

A transfer function matrix, $G(s) \in \mathbb{C}^{m\times n}$, is analytic in the rhp if it contains no rhp poles, hence bounded (finite) in Re(s)>0. This is the definition of the Hardy space of functions, $\mathbf{H}_\infty(\mathbb{R}, \mathbb{C}^{m\times n})$ such that:

$$\bar{\sigma}(G(s)) < \infty, \quad \forall s \in \mathbb{C}^{m\times n} \tag{6.18}$$

where

$\bar{\sigma}$ maximum singular value

If the transfer function matrix, $G(s)$, is evaluated at a discrete frequency, ω, then a matrix of complex values will result. The maximum singular value is the largest of the square root of the eigenvalues, λ, of the corresponding Hermitian (6.19). In this manner the singular values may be plotted as a function of frequency.

$$\sigma_i(A) = \sqrt{\lambda_i(A^*A)}, \quad A \in \mathbb{C}^{m\times n} \tag{6.19}$$

Hilbert spaces, $\mathbf{L}_2(\mathbb{R}, \mathbb{C}^{m\times n})$ and $\mathbf{L}_2(j\mathbb{R}, \mathbb{C}^{m\times n})$, by definition are normed spaces with inner products. However, the Hardy space is a Banach space with an ∞–norm defined of the transfer function matrix $G \in \mathbf{H}_\infty(\mathbb{R}, \mathbb{C}^{m\times n})$ as shown below:

$$\|G\|_\infty = \sup_{\omega>0\in\mathbb{R}} \sigma(G(j\omega)) \tag{6.20}$$

A frequency response, in the space $\mathbf{L}_2(j\mathbb{R}, \mathbb{C}^{m\times n})$, when subject to an arbitrary operator from

the Hardy space, $\mathbf{H}_\infty(\mathbb{C}, \mathbb{C}^{m\times n})$, results in a frequency spectrum in the same space, namely $\mathbf{L}_2(j\mathbb{R}, \mathbb{C}^{m\times n})$. A similar analogy exists on signals from space $\mathbf{L}_2(\mathbb{R}, \mathbb{C}^{m\times n})$:

$$\forall f \in \mathbf{L}_2(\mathbb{R}, \mathbb{C}^{m\times n}) \text{ and } \forall G \in \mathbf{H}_\infty(\mathbb{C}, \mathbb{C}^{m\times n}): \quad fG \in \mathbf{L}_2(j\mathbb{R}, \mathbb{C}^{m\times n}) \tag{6.21}$$

Essentially any operator in the Hardy space acting on a bounded frequency response results in a bounded frequency spectrum. By equation (6.16) a relationship between the 2-norm and the ∞–norm of the Hardy space is apparent:

$$\forall f \in \mathbf{L}_2(\mathbb{R}, \mathbb{C}^{m\times n}) \text{ and } \forall G \in \mathbf{H}_\infty(\mathbb{C}, \mathbb{C}^{m\times n}): \quad \|fG\|_\infty \le \|G\|_\infty \|f\|_2 \tag{6.22}$$

The ∞–norm for an arbitrary transfer function matrix may be evaluated from the supremum of $\|G\|_\infty$ and $\|f\|_2$ over the signal space $\mathbf{L}_2(\mathbb{R}, \mathbb{C}^{m\times n})$ for the non-trivial case when $\|F\|_2 \neq 0$:

$$\|G\|_\infty = \sup_{F \in \mathbf{L}_2(\mathbb{R}, \mathbb{C}^{m\times n})} \frac{\|fG\|_2}{\|f\|_2} \tag{6.23}$$

The ∞–norm is induced by the signal $\|f\|_2$ and is essentially the maximum gain of the transfer function matrix $G(s)$. For real-rational transfer function matrices their space is defined as $\mathbb{R}\mathbf{H}_\infty(\mathbb{R}, \mathbb{C}^{m\times n}) \subset \mathbf{H}_\infty(\mathbb{C}, \mathbb{C}^{m\times n})$. Its ramifications are profound in that the $\mathbf{H}_\infty$ optimisation attempts to minimise this norm in the presence of uncertainties which is now considered. The range and domain of the space is suppressed, the context in which they are employed determines them.

6.3 OBJECTIVES

A linear optimal controller is sought which is imbued with the following properties:

(*i*) Remain stable when perturbed by a pre-specified class of disturbances
(*ii*) Minimisation of sea induced roll motions
(*iii*) Minimisation of the servomechanism activity

Each of these objectives are characterised by the appropriate input/output pairs of Figure 6.1. The interpretation of objective (*i*) is that the closed loop transfer function, T(s), from r to y, remains stable even if the system countenances unmodelled, albeit specified, dynamics. Sea induced roll disturbance minimisation, objective (*ii*), implies that the sensitivity function, S(s), from n to y, must be restrained below unity as postulated in section 5.1. Objective (*iii*) requires that roll stabilisation is achieved at minimal cost in terms of fuel consumed by the actuators and, more critically, the servomechanisms must not be permitted to operate outside their design limitations. This criterion is encapsulated in the transfer function from n to u, the control sensitivity, C(s).

The importance of the LFT is now apparent. Its constituents are all the transfer functions from r, d and n to y, u and z as seen in equation (6.10). By selection of the appropriate pairs and setting the others to zero, the LFT succinctly captures the characteristics which adhere to the designer's objectives for a particular application. The LFT is then amenable to the minimisation (optimisation) procedures which synthesis the robust controllers. This is in complete accordance with the objectives listed above, which require minimisation, and H_∞ theory which seeks to limit the maximum gains of the LFT input/outputs.

These objectives are now further elaborated in the succeeding sections.

6.4 ROBUST STABILITY

A robustly stable plant is one in which the controller ensures that the structure's stability between internal signals is maintained irrespective of the prespecified uncertainty which impinges on the system. The procedure is to formulate the conditions for internal stability and define the nature of the uncertainty in order that the controller may be synthesised. This is now pursued in the remainder of this section.

6.4.1 Internal Stability

There are several avenues of investigation for the definitions of internal stability. For example Lyapunov, coprime factorisation of (6.9) and singular values in the context of Nyquist stability criteria (Doyle and Stein, 1981). Here it is examined in the developed framework of operator theory and LFT's of section 6.2.3. It is noted that all these methods focus on the expression $(I - G_{22}K)^{-1}$ from equation (6.9).

Consider the open loop plant of Figure 6.1 with only the signal u and y. If the output signal is finite, i.e. $y \in \mathbf{L}_2$, when excited by the signal $u \in \mathbf{L}_2$ the system will remain stable with the condition that the plant $G(s) \in \mathcal{R}\mathbf{H}_\infty$.

However, when the plant is in closed-loop mode then it is not sufficient simply to confirm the stability between u and y. The system now contains internal control and error signals. For the modified definition of internal stability now requires that if the signals $r, d, n \in \mathbf{L}_2$ the signals $y, u, e \in \mathbf{L}_2$. Despite the system being ostensibly stable between r and y, if these conditions are not simultaneously achieved then internal damage may result on components on account of unbounded signals. The LFT may be utilised for the very purpose it was generated: as a representation of all the internal transfer functions in order that internal stability results may be determined.

To these ends, K(s) is known as a stabilising controller of the plant when represented by the LFT of G(s) and K(s). This is verified by the modified small gain theory (Zames, 1966), which implies that (6.9) will be analytic in the rhp.

Theorem 6.1 : Assume that $G(s)$ and $K(s) \in \mathcal{R}\mathbf{H}_\infty$, then the system represented by the LFT is internally stable if:

$$\|G_{22}\|_\infty < 1 \tag{6.24}$$

Proof : Substituting (6.8b) into (6.8c) yields:

$$(I - G_{22}K)e = G_{12}r + G_{22}d + n \tag{6.25}$$

where

$$(I - G_{22}K)e \in \mathcal{R}\mathbf{L}_2, \quad \forall\{r, d, n\} \in \mathcal{R}\mathbf{L}_2$$

since

$$G_{12},\ G_{22} \text{ and } I \in \mathcal{R}\mathbf{H}_\infty$$

Therefore:

$$\begin{aligned} &\|(I - G_{22}K)\|_2 \le \|G_{12}r\|_2 + \|G_{22}d\| + \|n\|_2 < \infty \\ &\Rightarrow \exists\{r, d, n\} \in \mathcal{R}\mathbf{L}_2 : (I - G_{22}k)e \neq 0 \end{aligned} \tag{6.26}$$

since

$(I - G_{22}K)^{-1}$ is analytic in the rhp (i.e. Hardy space)
$\Rightarrow e \in \mathcal{R}\mathbf{L}_2$ □

Thus for internal stability it is sufficient to ensure that the ∞–norm G_{22} entry of the LFT is less than unity. Theorem 6.1 details the demanded qualities of K(s) however, it does not yield a solution. Fortunately, K(s) can be generated within the framework of operator theory by solving the Nehari extension problem (O'Young and Francis, 1986, Chu *et al*, 1986, and Hung, 1989).

6.4.2 Internal Stability of Uncertain Systems

Theorem 6.1 has assumed that the transfer function matrix G(s) is a complete representation of the plant for which a stabilising controller may be generated. If the plant reflects reality by containing some of the pervasive unmodelled dynamics and other uncertainties the internal stability conditions are required to be ascertained.

The plant $\tilde{G}(s)$ is the matrix transfer function of the intrinsic uncertainties and a defined nominal plant. It was decided that an input multiplicative uncertainty is the most appropriate uncertainty structures for the roll stabilisation models having contemplated other representations (Doyle, 1982 and 1985), this is given below:

$$\tilde{G}(s) = G(s)(1 + \Delta(s)) \tag{6.27}$$

where

$\Delta(s) \in \mathcal{R}\mathbf{H}_\infty$ and $\|\Delta(s)\|_\infty \leq 1$

Generally, it is not possible for a controller to be robustly stable for all envisaged uncertainties over the Hardy space. Therefore, Δ it is restricted to an admissible set:

$$D = \left\{\Delta(s), \Delta \in \mathcal{R}\mathbf{H}_\infty : \left\|\Delta W_d^{-1}\right\|_\infty \leq \|\Delta\|_\infty \left\|W_d^{-1}\right\|_\infty \leq 1\right\} \tag{6.28}$$

where

$W_d \in \mathcal{R}\mathbf{H}_\infty$ weighting function.

The weighting function characterises the location in the frequency spectrum where the uncertainty regarding the plant is predominant.

The multiplicative input uncertainty as defined in (6.27) may be determined for the fin and rudder to roll transfer functions, g11(s) and g12(s) respectively. It is demonstrated for the g11(s) transfer function. The nominal plant is defined by (2.31) and the perturbed plant is given as:

$$g11(s) = \frac{\tilde{k}_{11}\tilde{\omega}_n^2}{s^2 + 2\tilde{\zeta}_s\tilde{\omega}_n s + \tilde{\omega}_n^2} \tag{6.29}$$

Variations in the coefficients may be explicitly derived as proportional changes as detailed in Chapter 2. They arise on account of parameteric variations in hydrodynamic forces on the ship and non-linear distortion. Therefore, the uncertainty may be encapsulated by $\Delta(s)$ which is evaluated to be:

$$\Delta(s) = \frac{\left(\tilde{k}_{11}\tilde{\omega}_n^2 - k_{11}\omega_n^2\right)s^2 + \left(2\zeta_s\omega_n\tilde{k}_{11}\tilde{\omega}_n^2 - 2\tilde{\zeta}_s\tilde{\omega}_n k_{11}\omega_n^2\right)s + \left(\tilde{k}_{11}\tilde{\omega}_n^2\omega_n^2 - k_{11}\omega_n^2\tilde{\omega}_n^2\right)}{k_{11}\omega_n^2 s^2 + 2\tilde{\zeta}_s\tilde{\omega}_n k_{11}\omega_n^2 s + \tilde{k}_{11}\tilde{\omega}_n^2\omega_n^2} \tag{6.30}$$

A similar, albeit more elaborate counterpart may be established for g12(s). This expression gives an indication of the form of $W_d(s)$, which will be subsequently simplified.

Consider the closed loop control system of Figure 6.5 with the multiplicative uncertainty inserted. The controller has two objectives. Not only is it required to stabilise the nominal plant but also maintain internal stability when the system countenances admissible uncertainties.

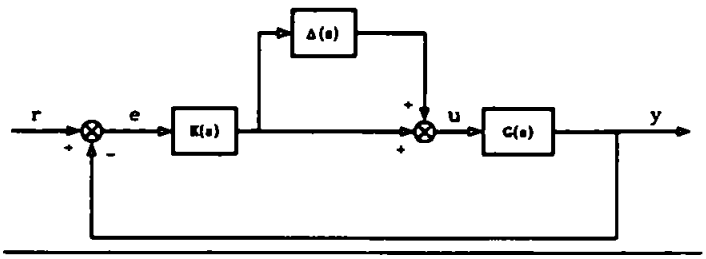

Figure 6.5 : Closed loop control with input multiplicative uncertainty

If the Figure 6.5 is altered to resemble the standard LFT configuration of Figure 6.6 the following schematic results:

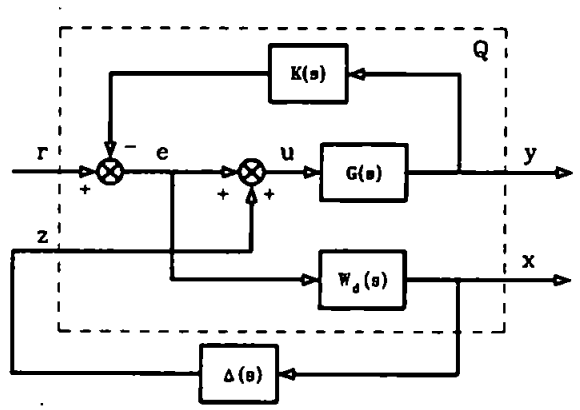

Figure 6.6 : Multiplicative uncertainty as LFT configuration

Partitioning Q results in the following transfer function matrix:

$$\begin{pmatrix} y \\ x \end{pmatrix} = Q\begin{pmatrix} r \\ z \end{pmatrix} = \begin{bmatrix} (I+GK)^{-1} & G(I+GK)^{-1} \\ W_dK(I+GK)^{-1} & W_dKG(I+KG)^{-1} \end{bmatrix}\begin{pmatrix} r \\ z \end{pmatrix} \qquad (6.31)$$

The (2,2) entry in the partitioned Q matrix is not the same as T(s) as defined in (6.2c). In general there are a number of possible variations of the structure selected to represent the uncertainties. Subsequently, the entries in the Q matrix will changes to reflect the new relationships. This suggests a completely analogous result as the development culminating in Theorem 6.1 where K(s) internally stabilises the feedback control system.

Theorem 6.2 : Assume K(s) internally stabilises the nominal plant, G(s), then a sufficient condition to ensure the same stability characteristics for admissible uncertainty, Δ(s):

$$\|W_d KG(I+KG)\|_\infty = \|F_l(Q,\Delta)\|_\infty < 1 \qquad (6.32)$$

where

$$Q = \begin{bmatrix} 0 & W_d G \\ I & -G \end{bmatrix}$$

□

Proof : Follows Theorem 6.1. □

6.5 PERFORMANCE OPTIMISATION

6.5.1 Sensitivity Minimisation

The specifications of the envisaged controller have been stipulated in terms of robustness to uncertainty. It is also desired that the controller be able to reject sea disturbances as described in section 6.1. More specifically it is required to ensure that the sensitivity function between n and y of Figure 6.1 lies below unity over the frequency region where sea disturbances exist. Since the roll stabilisation problem is one of regulation about a set point then tracking considerations are neglected.

Consider Figure 6.1 the output is given by:

$$y(s) = S(s)G(s)d(s) + T(s)r(s) + S(s)n(s) \qquad (6.33)$$

It has been established that the spectra of r(s), d(s) and n(s) lie in the $\mathcal{RL}_2$ function space and S(s), and T(s) are members of $\mathcal{RH}_\infty$. Application of the triangle inequality, (Kreyszig, 1978) yields:

$$\|y\|_2 \leq \|S\|_\infty \|G\|_\infty \|d\|_2 + \|T\|_\infty \|r\|_2 + \|S\|_\infty \|n\|_2 \tag{6.34}$$

The inequality together with Theorem 6.2, implies that for internal stability and roll stabilisation the ∞–norms of S(s) and T(s) be simultaneously minimised. The optimisation algorithm will attempt to minimise S(s) over the entire frequency region. Since, S(s) and T(s) are complementary (6.3) a conflict arises between these objectives. It is reconciled by introducing a weighting function, $W_p(s)$, on S(s) in parallel with $W_d(s)$ on T(s). This permits roll stabilisation over the frequency range outside that of where uncertainties exist as described by $W_d(s)$. Therefore, the roll stabilisation via S(s) is modified:

$$\min_K \|W_p(s)S(s)\|_\infty : \bar{\sigma}(W_p(s)S(s)) \leq 1 \tag{6.35}$$

where

$$W_p(s) \in \mathcal{RH}_\infty$$

If the inequality (6.35) is satisfied then the controller endows the 'nominal' disturbance performance on the closed-loop stabilisation system.

The sensitivity function may be recapitulated in terms of the LFT:

$$F_l(G_S, K) = (I + GK)^{-1} \tag{6.36}$$

where

$$G_S = \begin{bmatrix} W_p & -W_pG \\ I & -G \end{bmatrix}$$

6.5.2 Control Activity Minimisation

The controller generates demand signals which actuate the servomechanisms. There are two incentives for the requirement of constraining servomechanism activity. Firstly, fuel is a finite and precious resource. At a cursory contemplation it may be considered that the fuel consumption incurs a marginal expense. However, the power required to oppose the ship's inertia in generating a roll moment in a relatively limited time period is substantial. More crucial, the control action is limited in order to restrict the operation of the servomechanisms in their linear regions and prevent the consequences discussed in Chapter 3.

Since, the roll stabilisation is one of regulation it only requires that the transfer function between roll disturbance, n, and controller, u, output be minimised. This relationship is given by C(s) (6.2b). The nature of the sea frequency spectrum naturally suggests that efficacious stabilisation will result if servomechanism action is minimised at those frequencies where sea disturbances are not present. The restriction on the servomechanism is relaxed at roll resonance. This objective may be realised by a weighting function $W_c(s)$. The aim is now represented by a minimisation of:

$$\min_K \|W_c(s)C(s)\|_\infty \tag{6.37}$$

It is a simple procedure to designate a LFT for C(s):

$$F_l(G_C, K) = K(I + KG)^{-1} \tag{6.38}$$

where

$$G_C = \begin{bmatrix} 0 & W_c K \\ I & -G \end{bmatrix}$$

The requirements of the controller as detailed in section 6.3 have been expressed within the realms of operator spaces. However, before the definitions are formulated for the H_∞

procedure the structure of the uncertainty is re-examined in context of the Structured Singular Values.

6.6 STRUCTURED SINGULAR VALUE

The uncertainty as defined in section 6.4 is assumed to possess a cognate, nebulous structure imposed on all the input/output pairs. Robust stability and performances objectives in the presence of these perturbations have been embodied in the weighting functions between the signals which represent desirable characteristics of the closed-loop system. However, the controller may be unnecessarily conservative if any combination of the perturbations are physically impossible.

An alternative 'measure' of robustness is required which operates only on the perturbations which are possible. Doyle (1982) conceived the Structured Singular Value (SSV) or μ, from various sources, as a means of taking into account perturbation structure not only in the robust stability but also robust performance analysis. This may include weighting functions, and coefficient variations in the transfer functions which can be real or complex to reflect gains and phase perturbations.

6.6.1 Structured Robust Stability

Utilising the small gain theory (Theorem 6.2) conditions for guaranteed stability were derived in terms of the ∞–norm. This may be recast as maximum singular value test of equation (6.20) for the particular case of input multiplicative perturbations:

$$\bar{\sigma}(\Delta(s))\bar{\sigma}\Big((1+K(s)G(s))^{-1}K(s)G(s)\Big) < 1 \qquad (6.39)$$

Safonov (1981) demonstrated that the maximum singular value tests were often conservative in their ability to predict near instability. If the gain, phase and parameter

perturbations, Δ_i, are extracted from each loop and placed in a diagonal uncertainty matrix as defined in (6.40) the general feedback system of Figure 6.7 results (Safonov and Athans, 1977).

$$\Delta = \text{diag}(\Delta_1, ..., \Delta_n) \tag{6.40}$$

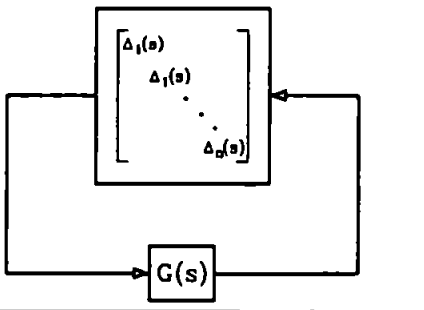

Figure 6.7 : Structured perturbations feedback

It can be demonstrated (Doyle, 1982 and 1985) that any combination of structured, unstructured weighting functions and real parameter variations, can be expressed in a format amenable to LFT decomposition as in Figure 6.8. The $\Delta(s)$ has a block-diagonal structure whose diagonal elements are scalars, weighting functions or blocks matrices. Absorbing these into the plant G(s) results in M(s). The $\Delta(s)$ is norm-bounded:

$$\underline{\Delta} = \text{diag}(\Delta_1, ..., \Delta_n), \quad \underline{B\Delta} = (\Delta \in \underline{\Delta}, \bar{\sigma}(\Delta(s)) \leq 1) \tag{6.41}$$

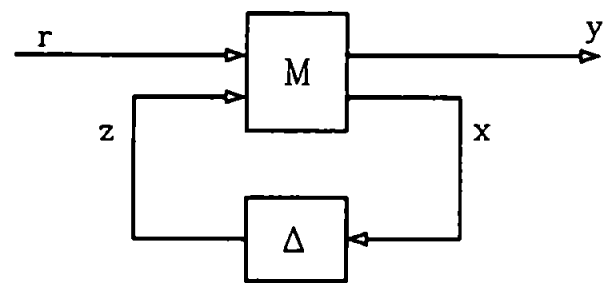

Figure 6.8 : Standard perturbation structure

Then the LFT is obtained as:

$$F_l(N, \Delta) = M_{11} + M_{12}\Delta(I - M_{22}\Delta)^{-1}M_{21} \tag{6.42}$$

It is apparent from (6.42) and for the general case (6.9), where K=Δ, that a permissible perturbation destabilises the system if:

$$\det(I - M_{22}(j\omega)\Delta(j\omega)) = 0, \quad \forall \Delta \in \underline{B\Delta} \tag{6.43}$$

Therefore, the SSV obtains any permissible uncertainty which engenders the equality (6.43) and is given as:

$$\mu_{\Delta}(M) = \left\{ \begin{array}{l} 0 \text{ if } \det(I - M_{22}(j\omega)\Delta(j\omega)) \neq 0, \Delta \in \underline{B\Delta} \\ \left[\min_{\Delta \in \underline{B\Delta}} (\bar{\sigma}(j\omega) : \det(I - M_{22}(j\omega)\Delta(j\omega)) = 0) \right]^{-1} \end{array} \right\} \tag{6.44}$$

which may be succinctly defined:

$$\|M(j\omega)\|_{\mu} = \max_{\omega} \mu(M(j\omega)) \tag{6.45}$$

where

$\|\cdot\|_{\mu}$ is not a norm.

Although, this establishes a sufficient test for robustness in the presence of structured perturbations, there is yet no algorithm available to evaluate is directly. Fortunately, its upper and lower bounds may be defined as (Maciejowski, 1990):

$$\rho(M) \leq \mu_{\Delta}(M) \leq \bar{\sigma}(M) \tag{6.46}$$

where

ρ spectral radius

Unfortunately the upper bound is again the conservative maximum singular value and the distance between the bounds can be arbitrarily large. By rescaling, which does not alter μ, but changes the magnitudes, not direction, of ρ and σ, an estimate of μ can be ascertained. Let

$$\underline{U} = \text{diag}(U_1, ..., U_n), U_i^* U_i = I$$
$$\underline{D} = \text{diag}(D_1, D_2, .., D_s, d_1 I, ..., d_n I), D_i \in \mathbb{C}^{r_i \times r_i}, d_i \in \mathbb{R} \quad (6.47)$$

The bounds of (6.46) are now obtained as:

$$\rho(MU) \leq \mu_\Delta(M) \leq \bar{\sigma}(DMD^{-1}) \quad (6.48)$$

which leads directly to Theorem 6.3 (Doyle, 1982).

Theorem 6.3 : The system of Figure 6.8 remains stable for all $\Delta \in \underline{B\Delta}$ iff,

$$\|M_{22}\|_\mu < 1$$ □

Proof : Since $\bar{\sigma}(\Delta) \leq 1$

$$\begin{aligned} \sup_\omega \rho(M\Delta) &\leq \sup_\omega \mu(M\Delta) \\ &\leq \sup_\omega (\mu(M)\bar{\sigma}(\Delta)) \\ &\leq \|M\|_\mu \end{aligned}$$

Thus in order to avoid the destabilising condition (6.43) $\|M\|_\mu \leq 1$ □

Further details for the evaluation of μ can be found in Gaston and Safonov (1988). In subsequent sections an analysis will be conducted on the roll stabilisation control configuration of Figure 2.19. The parameter variations will be (k_{12}, k_{11}, ω_n and ζ_s) furnished by Chapter 2 which is considered a novel application of the SSV.

6.6.2 Performance Robustness via μ

Although, as will be demonstrated in the next section, the H_∞ optimisation provides nominal performance (6.35) in terms of disturbance rejection when no perturbations impinge on the system. It will not adhere to this criterion when norm-bounded perturbations require to be accommodated.

In the structure of Figure 6.1 where r represents the sea disturbance and y the stabilised roll of the ship. The requisite for robust performance from the LFT between r and y may be sufficiently stated as:

$$\bar{\sigma}(F_l(M(j\omega), \Delta(j\omega))) < 1 \tag{6.49}$$

An alternative approach is to introduce a pseudo-uncertainty block, Δ_S, which encapsulates the performance requirements between r and y. The perturbation structure (6.41) is augmented with this new 'perturbation':

$$\Delta_f = \text{diag}(\Delta_S, \Delta) \tag{6.50}$$

This renders the performance robustness and robust stability to be amalgamated into one measurement (Maciejowski, 1990):

$$\mu_{\Delta_f}(M) < 1 \tag{6.51}$$

Structured singular values thus afford an analytic procedure to ascertain not only, the robust stability, but also performance qualities of a particular controller in the feedback configuration when the disturbance are norm-bounded perturbations. Three tests may be applied to the system in terms of the weights of S(s), T(s) and C(s) in order confirm the same characteristics.

The next section proceeds with the H_∞ optimisation formulation in order to generate the controllers.

6.7 H_∞ OPTIMAL CONTROLLER

Although the H_∞ optimal control has only recently evolved as a practical methodology to controller design, it is well promulgated in literature, (Francis and Zames, 1984, Chu *et al*, 1984, O'Young and Francis, 1986, Francis 1988, and Hung 1989). Therefore, a

comprehensive account is beyond the scope of this thesis. This section concentrates on the novel application of the theory to roll stabilisation scenario.

The framework of LFT's developed to analyse the robust properties of feedback systems is not redundant in H_∞ optimisation. They are the protagonists in the foundation of linear robust theory and subsequent algorithms. The standard problem is formulated as an LFT in order to obtain a stabilising controller, K(s), for the generalised plant, P(s), when expressed in the configuration of Figure 6.2:

$$\min_{K(s)\in RH_\infty} \|F_l(P,K)\| \tag{6.52}$$

The multivariable optimisation remains unsolved in an analytic fashion. However, Glover and Doyle (1988) have proposed an algorithm which functions on state space representations and subsequently resolves for a sub-optimal controller, $K_\gamma(s)$, by γ–iteration. Appropriately, this is an iterative procedure where the value of γ remains positive and increased such that the inequality given below is not violated. This is the algorithm employed by the Matlab® software which was used to generate the controllers (Balas *et al*, 1991).

$$\inf_{K\in RH_\infty} \|F_l(P,K)\|_\infty \le \|F_l(P,K_\gamma)\|_\infty < \frac{1}{\gamma} \tag{6.53}$$

The objectives of roll stabilisation are to obtain a controller which minimises the weighted sensitivity and control sensitivity functions. In addition a constraint is imposed on the controller that it must stabilise the nominal plant and also remain internally stable for the class of perturbation, **D**, equation (6.28). If these are formulated as a standard H_∞ optimisation (6.52) then the γ-iteration procedure may be utilised to give an appropriate controller.

In pursuit of this aspiration the closed loop system of Figure 6.1 is reconfigured in Figure 6.9. The roll disturbance influences the output of G(s), therefore, the outputs e_i, i={1,2,3}, when evaluated from n(s), transpire, in conjunction with the weights, to be the functions which were stipulated as requiring minimisation in the previous sections. These evolve into transfer functions given in equation (6.54).

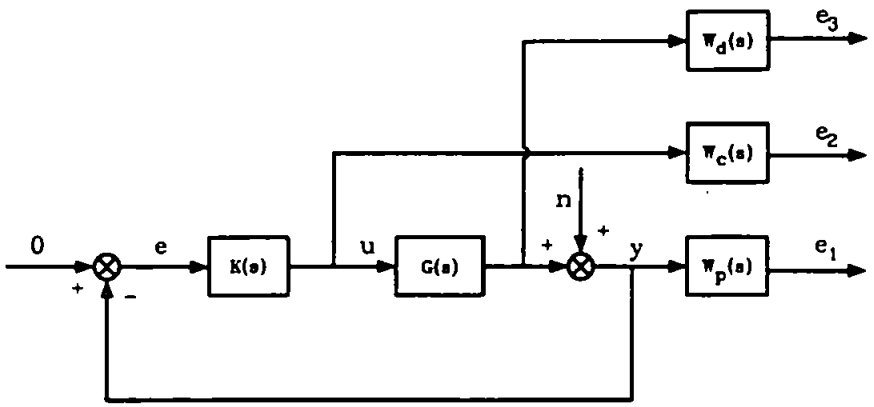

Figure 6.9 : The roll stabilisation scenario as a standard infinity norm optimisation problem

$$\begin{pmatrix} e_1(s) \\ e_2(s) \\ e_3(s) \end{pmatrix} = \begin{bmatrix} W_p(s)S(s) \\ W_c(s)C(s) \\ W_d(s)T(s) \end{bmatrix} n(s) \tag{6.54}$$

where

$$\{W_p(s), W_c(s), W_d(s)\} \in \mathcal{R}\mathbf{H}_\infty$$

The augmented system with the weighting functions is termed a mixed sensitivity minimisation with the LFT obtained as, omitting the Laplace operator:

$$F_l(G_a, K) = \begin{bmatrix} W_pS \\ W_cC \\ W_dT \end{bmatrix} \tag{6.55}$$

where

$$G_a = \begin{bmatrix} \begin{pmatrix} W_p \\ 0 \\ 0 \end{pmatrix} & \begin{pmatrix} -W_pG \\ W_c \\ W_dG \end{pmatrix} \\ (I) & (-G) \end{bmatrix}$$

The mixed sensitivity problem is amenable to the γ–iteration. Its application endeavours to minimise the ∞–norm of the LFT defined above with the constraint that the controller $K_\gamma(s)$ stabilises the system of Figure 6.9:

$$\gamma \| F_l(G_a, K) \|_\infty < 1 \tag{6.56}$$

which is achieved, in terms of singular values, if the inequalities are satisfied simultaneously:

$$\gamma \bar{\sigma}(W_p(j\omega)S(j\omega)) < 1, \quad \gamma \bar{\sigma}(W_c(j\omega)C(j\omega)) < 1, \quad \gamma \bar{\sigma}(W_d(j\omega)T(j\omega)) < 1, \quad \forall \omega \in \mathbb{R} \tag{6.57}$$

6.7.1 μ-Synthesis

Combining the procedure to generate robust controllers, elucidated above, with the SSV analysis, μ, (section 6.6) results in an iterative process called μ-synthesis. Controllers are resynthesised by modifying the weighting functions, or relaxing the severity of the perturbations, such that robust performance and stability are attained as determined by the structured singular value theorem. Consider the standard LFT structure, Figure 6.2, and assuming that the perturbations (6.50) are absorbed into the plant, the stages for μ-synthesis can be defined as:

- Define interconnections structure and perform H_∞ optimisation to yield controller K(s).
- Absorb controller into the interconnections structure and perform μ-analysis to obtain optimum D-scales, equation (6.47).
- Absorb D-scale matrices into interconnections structure and re-synthesise controller.

It now remains to construct the weighting functions based on the requirements and limitations of the roll stabilisers. This is the most crucial aspect of linear robust control

design, where the designer has the opportunity to influence the optimisation process. The designer can bring to bear his experience and human intuition in order to achieve the desired objectives: without which the controller synthesis procedure would be futile. This is considered a new application of this theory.

6.8 SELECTION OF WEIGHTING FUNCTIONS

The weighting functions embody the desired characteristics of the closed loop system. Therefore, when the roll stabilisers are operating in this mode the controller will ensure that it exhibits the qualities determined by the weights. In general the construction of the weights is a heuristic and iterative procedure. It requires that they are formulated correctly in order to minimise conflicts (e.g. between S(s) and T(s)) when subject to the optimisation algorithms. The three weights which distinguish the objectives of servomechanism activity, roll stabilisation performance and stability are considered for the fins and rudder loops.

6.8.1 Performance Weighting, $W_p(s)$

The performance required of the system is to reject sea disturbances whilst it must not attempt to correct list angles induced by loading conditions, wind and constant currents. It was shown that the sea spectrum can be modelled by a two parameter Bretschneider representation as depicted in Figure 2.16. Therefore, the stabilisers need only be deployed in this well defined frequency region. Furthermore, the ship amplifies sea induced roll motions at its resonance peak. Therefore, in parallel with classical techniques, it may be judicious to concentrate control action in this frequency region. A performance weighting function which demands controller activity in this vicinity will resemble a band-pass filter (Grimble *et al*, 1993). The weighting is given by (6.58) a modified form of the second order transfer function.

$$W_p(s) = \frac{\omega_n^{-2}\left(\frac{2B}{1-A}\right)s}{s^2\omega_n^{-2} + 2B\omega_n^{-1}s + 1} \qquad (6.58)$$

Here A represents the desired level of roll disturbance attenuation expressed as a fraction. B is a bandwidth parameter in order to regulate the stabilisation about a particular frequency regime and ω_n is selected to coincide with the resonance peak. Thus stabilisation is concentrated at this vicinity reminiscent of classical design techniques.

The controller achieves nominal performance if the condition (6.35) is achieved, restated as:

$$\bar{\sigma}(S(j\omega)) \leq [\bar{\sigma}(W_p(j\omega))]^{-1} \qquad (6.59)$$

Thus the inverse of the weighting function will have the same shape as the sensitivity function around the crucial resonance peak. Its shape will also be similar to the spectrum of the sea disturbances.

With this established, consider Figure 6.10, where the solid line represents the weighting function for typical values of A and B which may be selected for the fin stabilisers. It illustrates the relationship between the weighting function and sea spectra at various speed and sea states (Table 2.4). The other three lines in each graph represent the Bretschneider encounter sea spectra reflecting the ship's orientation and speed with respect to the waves (equation (2.46)).

It is apparent from the magnitude of $W_p(s)$ in comparison with sea state 3, first row of graphs, that the stabilisers will render the ship practically devoid of rolling motions. Row two depicts the sea increasing to state 5 which represents the maximum expected operational limits of the ship. At beam seas the wave period coincides with the natural roll

frequency. Hence, the stabilisation achieved will be maximised. At sea state 8, third row, although limited stabilisation will be accrued it will be much reduced. The overwhelming concern here will be to limit servomechanism activity. This state is regarded as an occasional severe disturbance. The shift in the peaks from 15^0 to 150^0 headings are displayed with lucidity where the double peaks visible in row three are a combination of ship's roll resonance and the sea spectra.

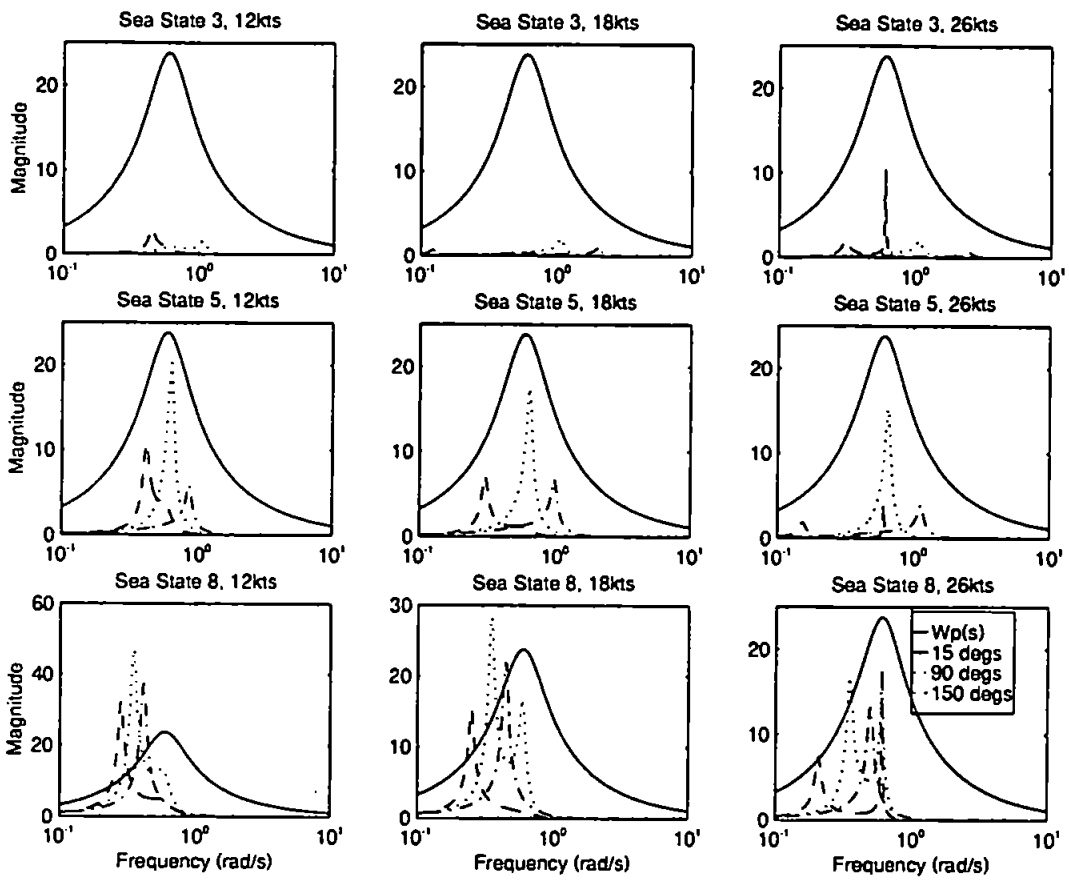

Figure 6.10 : Weighting function, $W_p(s)$, and sea spectra

Selection of appropriate values for A and B for the RRS and fin stabilisers are now examined in the context of sensitivity functions (S(s)) which will be obtained from the closed loop system with the H_∞ controller.

Consider Figure 6.11 which exhibits S(s) as a function of the parameters A and B for the RRS loop, where the direction of the arrows indicate increasing values for A and B. The

first set of graphs, entries (1,1) and (2,1), demonstrate the effects of variation in the gain parameter A. As it increases $W_p(s)$ retains its shape but shifts the spectrum upwards thus demanding greater stabilisation performance. The sensitivity function reciprocates by marginally decreasing in magnitude at the resonance area. However, there is an accompanying severe amplification at 0.03 and 10 rads^{-1} on account of the non-minimum phase zero as predicted by Appendix E. Although negligible roll disturbances exist at these frequencies, the amplification at the low frequency will degrade the course-keeping ability of the ship. As anticipated an increment in B, entries (2,1) and (2,2), results in the bandwidth expanding. The corresponding sensitivity function adheres to the relationship of Theorem E1 resulting in the attendant amplification with increasing stabilisation performance.

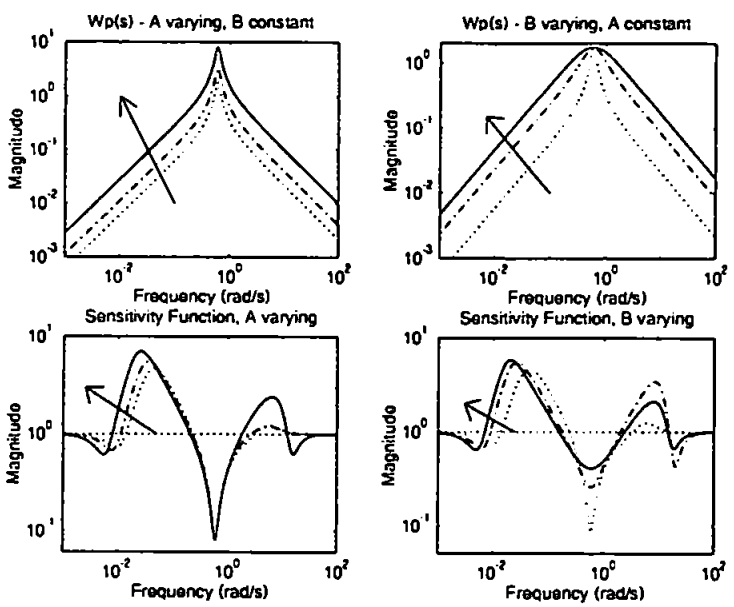

Figure 6.11 : RRS loop and variations in $W_p(s)$

An examination of the responses for the fin stabilisers reveals a more satisfactory situation as illustrated in Figure 6.12. Increasing either, or a combination of, A or B exacts greater levels of roll stabilisation. The fin stabilisers oblige in a well behaved manner. The only complication is the physical constraints on the servomechanism.

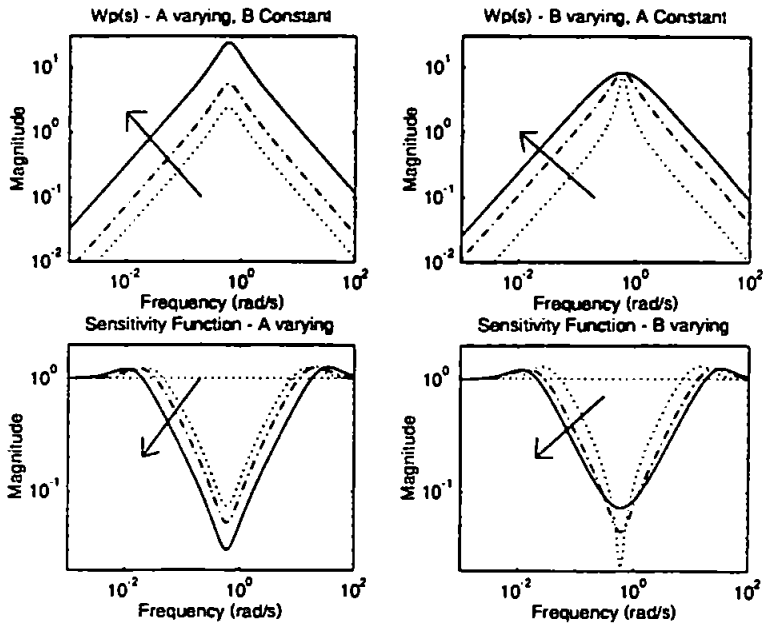

Figure 6.12 : Fin stabilisers and variation in $W_p(s)$

Although, it is possible to select a single set of values for A and B for all three speeds, 12kts, 18kts and 26kts, the controller will be required to maintain robust performance and stability at all speeds. Regardless of ship speed it will demand the same level of servomechanism activity in order to meet these performance requirements. The fin's and rudder's roll moment generating capabilities are proportionally dependent on ship speed, therefore, at low speeds, the consequences will be saturation of the servomechanisms. Conversely, if the controller is optimised at low speed it requires large movements of the fins and rudders to generate roll moments of adequate magnitude. Here the controller's objective is to restrict actuator activity, thus preventing saturation, whilst maintaining limited levels of roll stabilisation. Now, if the ship speed increases the controller will not be able to realise their full potency. Since, it is a simple matter to update the coefficients in software routines it is decided that in order to optimise performance at all speeds the controller will be gain scheduled. Simulation studies, the results of which are to be presented in Chapter 7, advocate that the values for A and B are as collated in Table 6.1.

Table 6.1 : Parameter values for $W_p(s)$

Ship Speed (kts)	12		18		26	
Control Loop	A	B	A	B	A	B
RRS	0.08	0.2	0.1	0.2	0.1	0.2
Fins	0.9	0.4	0.93	0.4	0.93	0.4

6.8.2 Control Weighting, $W_c(s)$

The purpose of the control weight is to minimise servomechanism activity thereby maintaining its operation in a linear envelope. It may be envisaged that the performance weight, $W_p(s)$, parameters may be appropriately selected such that the subsequent sensitivity function will not saturate the servomechanism. This must be achieved for the worst combination of ship speed, heading and, in particular, sea states. For example, say at sea state 8, S(s) dictates a stabilisation of 10% at ω_n, which compels the servomechanism to the limits of its operation. If the sea state now diminishes to 5 it is manifest that, since the controller's coefficients do not change, the resulting stabilisation will be marginal on account of the servomechanism being shackled by the gain of the controller, which is designed for the worst case. Hence, the requirement for explicit regulation of the servomechanism activity.

Utilising the control weight explicitly to embody the limitations of the servomechanism as a frequency spectrum permits the performance weight to exclusively concentrate on achieving stabilisation. The power spectral density (PSD) can be derived from an estimation of the frequency spectrum of the servomechanism (Chapter 3) which affords a measure of the energy content of the device. If the plant, g11(s) and g12(s), can deliver the level of performance, irrespective of sea state, whilst ensuring that the servomechanism does not exceed its PSD, the H_∞ optimisation will yield a controller to achieve this. However, if the plant cannot countenance these requirements then the performance demanded by $W_p(s)$ must be relaxed, or the PSD of the servomechanism must be increased. Since, an increase in

the PSD will lead to saturation it is judicious to modify $W_p(s)$ and repeat the optimisation.

The shape of $W_c(s)$ will be an approximate inverse of $W_p(s)$: a notch filter. The notch accentuates control activity by virtue of its relatively smaller magnitude. The peak of the notch is at roll resonance lest $W_c(s)$ conflict with the requirements of $W_p(s)$. At low frequency $W_c(s)$ has a roll-off of -20dB/dec whilst at high frequency it is 20dB/dec. This ensures that the servomechanism operation is restricted exclusively at the roll resonance area. An appropriate weight which exhibits these qualities is given in (6.60). It consists of two zeros contained on either side by poles on the Bode plot.

$$W_c(s) = \left(\frac{\omega_L^{-1}s + g}{\omega_L^{-1}gs + 1}\right)\left(\frac{\omega_H^{-1}gs + 1}{\omega_H^{-1}s + g}\right) \tag{6.60}$$

The coefficients ω_H and ω_L dictate the positions of the zeros, hence, width of the notch. These values are selected to prevent high-frequency controller action which saturates the servomechanism. More crucially, for the RRS loop, low frequency action must be curtailed lest interference with the yaw dynamics ensue. The coefficient g is a general gain of $W_c(s)$. Figure 6.13 demonstrated the effects on sensitivity when the controllers is generated by the optimisation process. The direction of the arrow indicates increasing g.

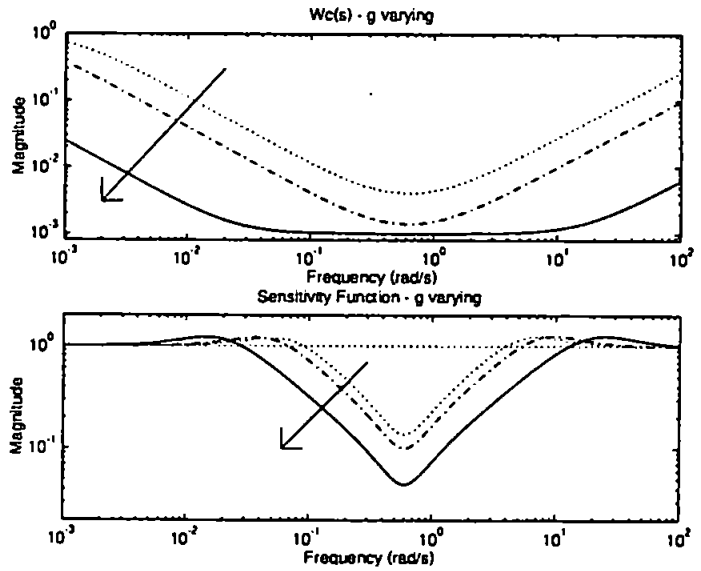

Figure 6.13 : Fin stabilisation loop sensitivity function and variation of $W_c(s)$

As g is incremented the control weight around roll resonance diminishes, thus increased levels of servomechanism activity are permissible. The sensitivity function takes advantage of the increased ability of the device reflecting it in enhanced stabilisation levels. A similar scenario exists for the RRS loop but burdened by the limitations imposed by the non-minimum phase zero.

Simulation results, deferred to the next Chapter, suggest appropriate values for ω_H, ω_L and g for the RRS and fins stabiliser as in Table 6.2.

Table 6.2 : Coefficients for control weight, $W_c(s)$

Ship Speed (kts)	12			18			26		
Control Loop	ω_L	ω_H	g	ω_L	ω_H	g	ω_L	ω_H	g
RRS	0.5	10	5	0.5	10	18	0.5	10	18
Fins	0.02	20	500	0.02	20	800	0.02	20	800

6.8.3 Uncertainty Weight, $W_d(s)$

The transfer function between the multiplicative input uncertainty has a profound impact on the stability of the system. Its magnitude must be minimal over the frequency region where uncertainty exists in order to guarantee internal stability. The condition to achieve this is recapitulated from (6.57c):

$$\bar{\sigma}(I + K(s)G(s)) < [\bar{\sigma}(W_d(s))]^{-1} \tag{6.61}$$

The dynamics of the ship roll can be stated with confidence at the roll resonance area (Marshfield, 1981b). This knowledge becomes imperceptible and nebulous at the high and low frequencies. A weighting function, $W_d(s)$, is required to encapsulate this information.

This spectrum of knowledge suggests that the general form of the $W_d(s)$ should resemble a notch filter. The low magnitude at the notch representing confidence regarding the

dynamics. At other frequencies the greater magnitude reflects the uncertainty. The weight is given by (6.62) which has a pair of coincident zeros with poles on either side on the Bode plot.

$$W_d(s) = \frac{\beta(\omega_n^{-1}s+1)^2}{(\beta\omega_n^{-1}s+0.01)(0.01\omega_n^{-1}s+\beta)} \tag{6.62}$$

The parameter β regulates the desired levels of confidence imbued in the dynamics of g11(s) and g12(s). ω_n ensures that the notch is centred around the roll resonance peak.

Figure 6.14 demonstrates the effects of changing β where the direction of the arrows indicate increasing values. As it increases, so the confidence in the system is reinforced. This is reflected as a larger magnitude in the closed loop transfer function. A corresponding increase in roll stabilisation is indicated by the sensitivity functions.

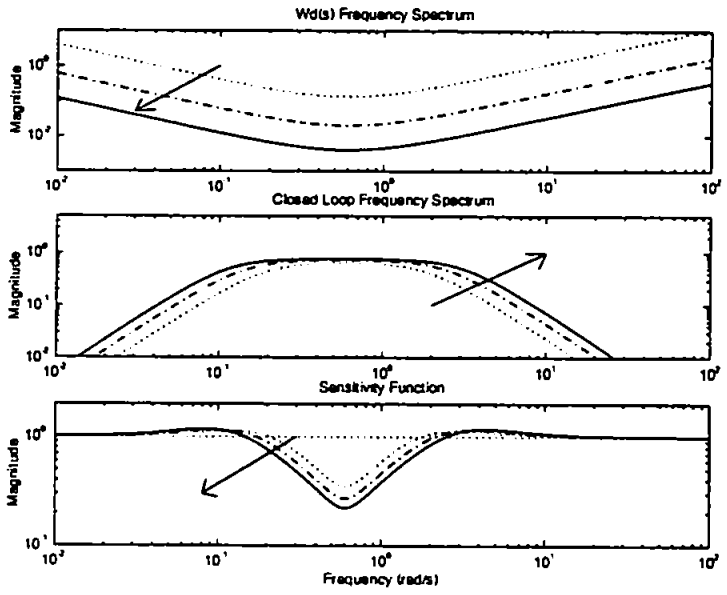

Figure 6.14 : Effects on closed loop transfer function and S(s) as $W_d(s)$ varies

Appropriate values for β are given in Table 6.3. The relatively smaller values for the RRS loop represents a greater weight, reflecting the increased uncertainty regarding the g12(s) dynamics.

Table 6.3 : Coefficients for uncertainty weight, $W_d(s)$

Ship Speed (kts)	12	18	26
RRS Loop	10	30	10
Fin Loop	30	50	30

With the weights as defined in these sections the controllers are now generated for the RRS and fin roll stabilisation loops and their properties examined with respect to them.

6.9 THE CONTROLLERS

6.9.1 Independent Loop Design

The controllers are generated by the optimisation procedure with the weighting functions as evaluated. In order for robust stability and performance to be achieved the sensitivities must adhere to the conditions of (6.51), or equivalently (6.57). The μ value must be less than unity and the maximum singular values must lie below their corresponding inverse weights. Since, it is a SISO case the singular value of the transfer functions are the same as their magnitude when evaluated on the jω-axis.

Figure 6.15 depicts this information for the fin stabilisation loop with ship speed at 18kts. The solid lines represent the weights and the dashed lines the relevant sensitivities. They all lie below their respective weights indicative of robust stability and performance being achieved which is confirmed by the structured singular values. Utilising the same controller at different speeds suggests that robust stability and performance are achieved, although at 12kts μ is closer to unity.

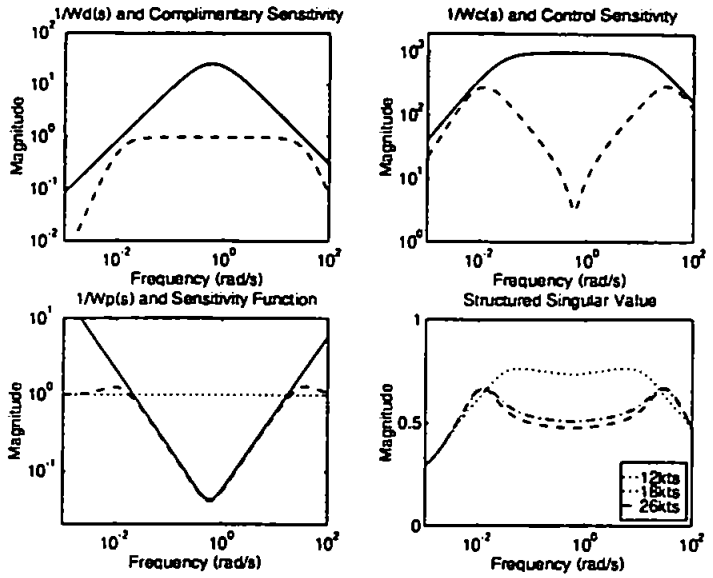

Figure 6.15 : Fin stabilisation loop weights and sensitivities

The results of the RRS controller are shown in Figure 6.16. Similar conclusions are drawn as in the fin stabilisation loop. Although at 26 kts the SSV indicates that robust performance is not achieved by the same controller on account of it being greater than unity. The peak at 0.07 $rads^{-1}$ of the sensitivity function is attributed to the non-minimum phase zero as predicted by the integral of the log sensitivity function relationship (Appendix E).

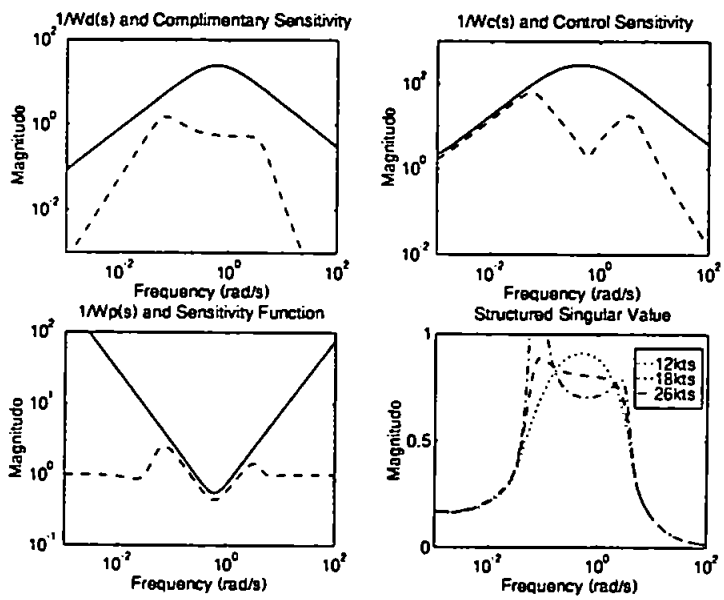

Figure 6.16 : RRS stabilisation loop weights and sensitivities

The controller spectra for each loop and all three speeds are shown in Figure 6.17. Their transfer functions can be found in Appendix F. It is observed that the fin loop controllers have correspondingly greater magnitudes than the RRS case, reflecting their superior moment generating faculty. The controller frequency responses roll-off at high and low frequency, thus the necessity for filtering is redundant as discussed in section 5.3.2. This is a natural consequence of the shape of the derived weights. This dip at 0.6 rads^{-1} in the fin controller spectra is expected, since, reduced control action is required at roll resonance to produce the same stabilisation levels.

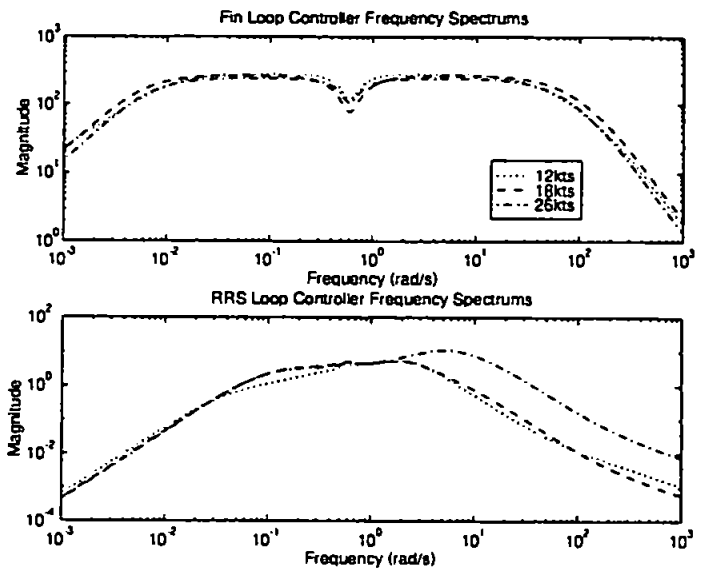

Figure 6.17 : Controller frequency responses

6.9.2 Multivariable Controller

The previous controllers were designed independently for each stabilisation loop. If the fins and rudders are now combined into a multivariable system, the resulting controllers, having been submitted to the optimisation process, are shown in Figure 6.18. The response of the multivariable controller is identical to the RRS controller. There is apparent marginal divergence between the two controllers for the fin stabilisation loop. Thus the decision to pursue controllers for the loops independently has been vindicated.

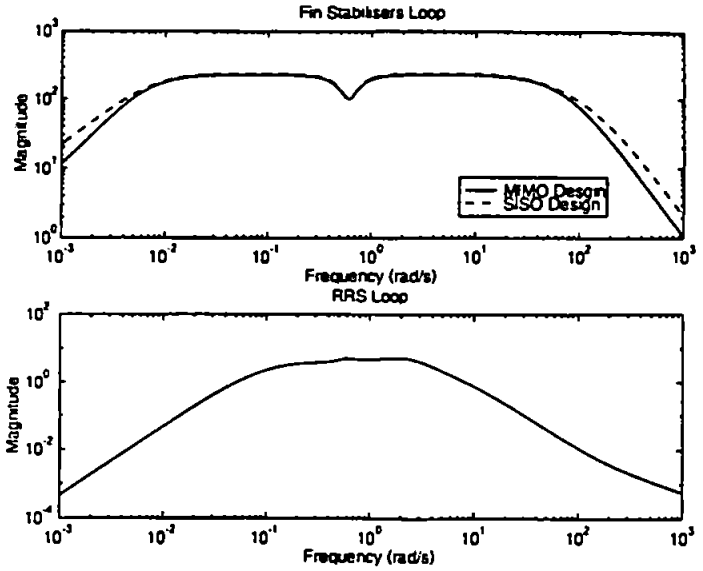

Figure 6.18 : Multivariable and independent controller comparisons

6.10 COMPARISON OF CONTROLLER METHODOLOGIES

It has been shown that the H_∞ controllers guarantee robust stability and performance. In order to conduct a valid comparison of this controller with the classical controllers of Methods One and Two, section 5.3.2 and 5.3.3, and their LQG counterparts, section 5.4, the sensitivity functions and μ values are calculated as shown in Figure 6.19. The solid lines represent the inverse weights.

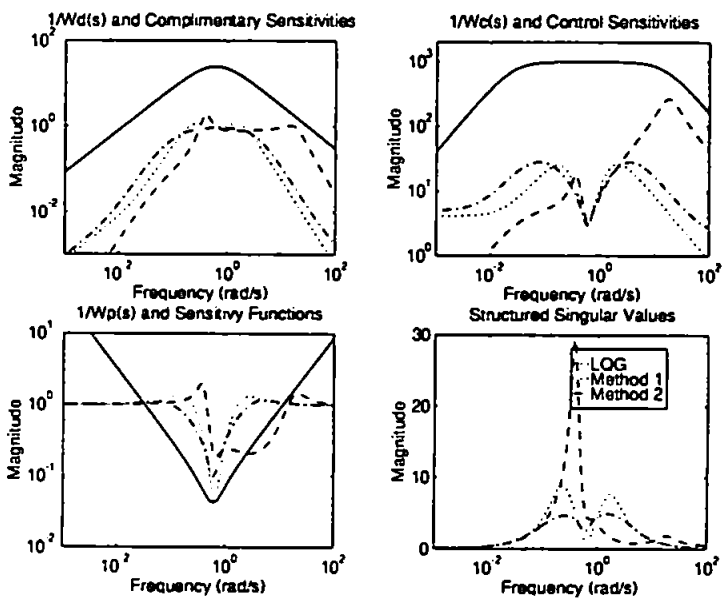

Figure 6.19 : Fin stabilisation loop and sensitivity functions

The complementary sensitivity magnitudes for all controllers are less than the inverse uncertainty weight. Similarly the control sensitivities magnitudes are smaller than their corresponding inverse control weight. This is indicative of the system being able to yield greater servomechanism activity than is being demanded by the controllers. Despite this reserve potential the sensitivity functions violate the inverse performance weight criterion for all controllers, principally, on account of all the stabilisation effort being concentrated in extremely narrow peaks. The prediction that robust stability and performance will not be achieved simultaneously, for any of these controllers, is confirmed on account of the μ value being significantly greater than unity as displayed in the final graphs.

Figure 6.20 exhibits the same range of information regarding the RRS loop. The complimentary sensitivity function's magnitudes with each controller engaged adhere to the criteria with respect to the inverse uncertainty weight. Only the classical controller of Method One and the LQG controllers achieve the performance requisites as demonstrated by the sensitivity functions. However, their sensitivities violate the control weight. The inference being that the roll stabilisation proposed by the controllers will saturate the servomechanism. These factors are succinctly portrayed by the μ values which are all considerably greater than unity.

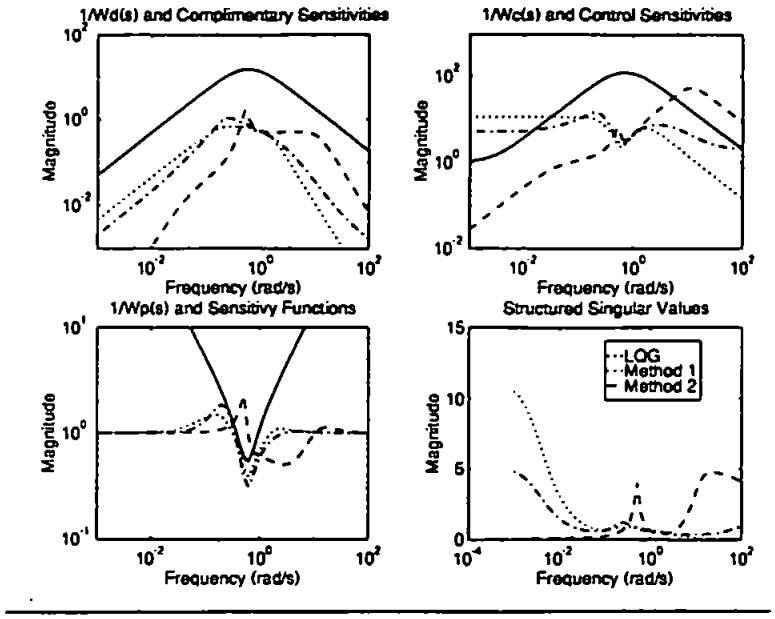

Figure 6.20 : RRS loop and sensitivity functions

It has been shown that only the H_∞ controllers can contemplate robust performance and stability in the presence of uncertainty when defined as a weighting. The controllers derived from the other methodologies have μ values significantly greater than unity. Thus it would be injudicious to attempt to alter these in order achieve the requirements for robustness without repercussions on the roll stabilisation performance. The analysis now proceeds to ascertain whether the controllers, particularly the H_∞ controller, can achieve and retain these qualities in the presence of specific parameter variations within the ship roll model.

6.11 ROBUSTNESS TO PARAMETER VARIATIONS

μ-Analysis can accommodate uncertainty in specific parameters, coefficients and state space matrices of the closed loop configuration. It is possible to ascertain the robustness characteristics of the system in this mode not only in presence of this type of highly structured perturbations but also for unstructured uncertainty represented by weight functions.

In context of the roll stabilisation system the weights represent frequency dependent hydrodynamic coefficients, servomechanism activity and performance. Whilst the explicit

coefficient variations could denote changes in fin and rudder hydrodynamic efficiency. These types of uncertainties are illustrated in Figure 6.21. The parameter variations have been extracted into the Δ matrix reminiscent of Figure 6.7. This is the closed loop schematic which is subsequently employed in the μ-analysis.

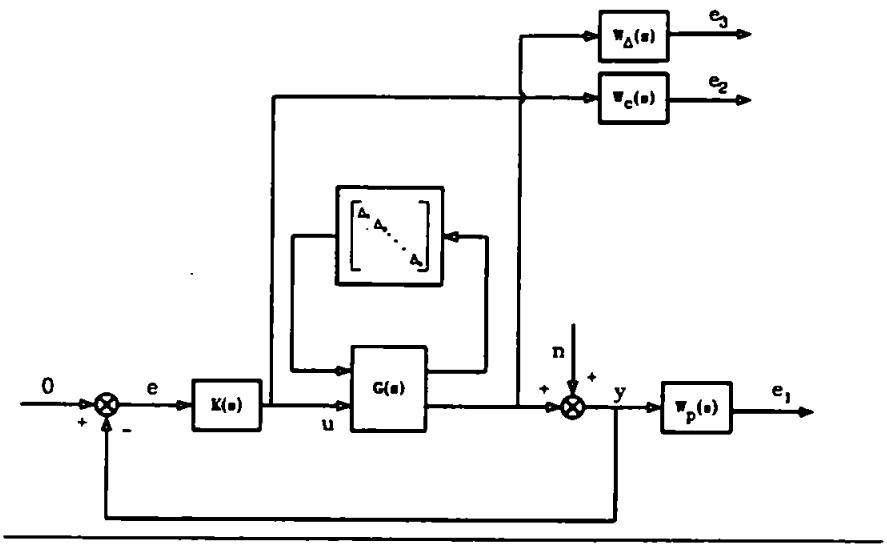

Figure 6.21 : Structured and unstructured perturbations

The variables in the fin stabilisation loop are k_{11}, ζ_s and ω_n. Utilising the data calculated in Table 2.2 it is expected that the k_{11} will alter by 50%. The damping ratio fluctuations as derived from data furnished by DRA Haslar is 50%. The natural frequency of oscillation for a large vessel, such as a frigate, is, generally, well defined and is not susceptible to uncertainty . However, it is assumed to lie within 5% of its nominal value. These fractional variations necessitate that the block Δ in Figure 6.21 is output multiplicative uncertainty. In order to ensure the relationship (6.41) the parameter variations are absorbed into G(s). The μ-analysis solution to these type of uncertainties was derived by Gaston and Safonov (1988).

Figure 6.22 displays the μ-values for the fin stabilisation loop. From Figure 6.15 the maximum μ for the H_∞ controller is approximately 0.6. With the additional burden of uncertainty in the parameters it still remains below unity albeit the maximum is now 0.97.

Therefore, although this controller will yield robust stability and performance, it cannot tolerate more than another 3% variation in the relevant coefficients. The other controllers were shown to lack these qualities (Figure 6.19) which is also borne out by this analysis.

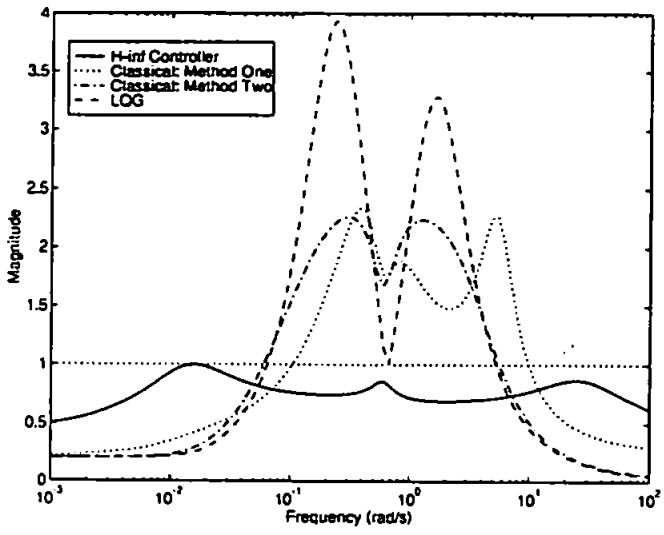

Figure 6.22 : μ-Analysis for controllers of fin stabilisation loop

The same tolerances were imposed on the RRS loop with k_{12} also varying by 50%. An additional uncertainty is introduced by the location of the non-minimum phase zero which is assumed to be 30%. This is a indication of the roll moment generating capacity of the rudder. Figure 6.23 shows the results obtained. It demonstrates that H_∞ controller can be contend with these variations which do not distract it from its achievement of robustness qualities. However, it is extremely close to unity and will be not be able to accommodate any further uncertainties. All the other controllers as expected founder on this criterion.

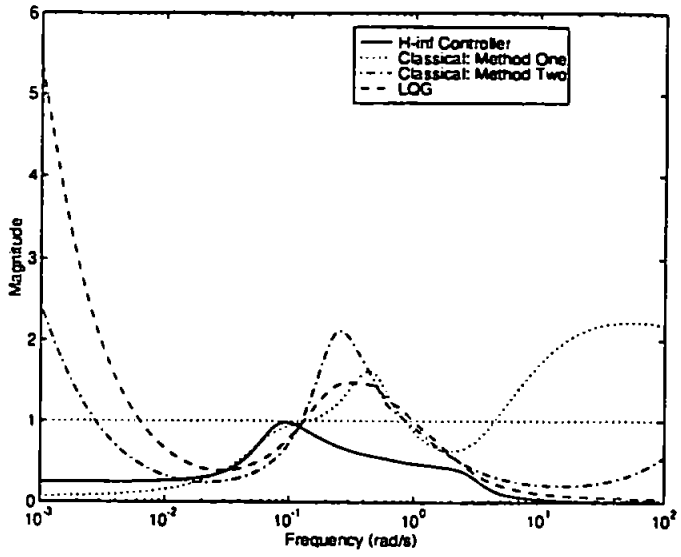

Figure 6.23 : μ-Analysis for controllers of RRS stabilisation loop

6.12 DISCUSSION AND CONCLUSIONS

The concept of uncertainty perturbations were introduced with respect to the closed loop system. Without exception every system's mathematical model has dynamics which cannot be modelled by a linear representation. These sources of uncertainty are multifarious and a few prominent factors were detailed. Control systems also have perturbations which impinge upon them from diverse sources such as environmental sea disturbances. In the closed loop mode the controller generates signals for an actuator such as a servomechanism. These devices have physically finite capabilities and in order to ensure integrity of operation must not be exceeded. Despite the limitations of knowledge, it is also desirable that the system in synergy be able to deliver performance in terms of roll stabilisation. It is concluded that these uncertainty features and desired objectives can be evaluated as transfer functions between appropriate input/output signals of the system.

Central to the development of robust linear controllers was the derivation of frequency dependent weighting functions which embody the uncertainty and performance requirements. A considerable amount of effort was dissipated in their correct representation.

It was crucial to construct the weights with experience, insight and intuition, in order that the resulting objectives were harmonious. For example, the performance weight stipulated that the disturbance rejection be most pronounced at roll resonance. The control weight reciprocated by relaxing the penalty at this frequency regime whilst ensuring that saturation will not occur. In general, the desired characteristics of a system can usually be apprehended in context of frequency domain functions between various internal signals as demonstrated in the preceding development. Hence, the design procedure for a robust controller will be amenable to intuition and the objectives will be portrayed with lucidity in the frequency domain. It is concluded that decisive essence of robust controller design resides in the construction of the weights.

Utilising this information and the concept of function spaces, whose constituents are transfer functions, an ∞-norm optimisation procedure generates the controller. These controllers are shown to guarantee robust internal stability and also robust performance with respect to the weighting functions.

A less conservative method than traditional gain and phase margins is the μ analysis technique. The uncertainties can be represented as unstructured weighting functions, depicting for example frequency dependent hydrodynamic coefficients. Highly structured uncertainty can also be incorporated which relate explicitly to specific coefficients within the model. If minimum performance requirements are also desired these can be defined as an augmentation of the uncertainty specification. The μ procedure then seeks any destabilising perturbation which violates these conditions. The H_∞ controller was shown to be robustly stable and yield a minimum performance level in the presence of all these uncertainties acting in conglomeration.

The efficacy of other controller design methods, as detailed in the previous Chapter, were also investigated for roll stabilisation. When subject to the scrutiny of μ analysis procedures these control techniques were revealed to be devoid of the criteria of robust stability and performance. It is concluded that if appropriate objectives can be identified and adequate weight functions constructed the linear optimal controller will be superior in all respects. The development of this Chapter represents a novel application of these advanced control techniques.

CHAPTER 7

SIMULATIONS AND FULL-SCALE SEA TRIALS RESULTS

7.1 INTRODUCTION

The previous two Chapters were concerned with the design and synthesis of the controllers in context of their frequency domain properties. In particular, Chapter 6, described the novel application of linear robust controller theory. Proposals were made for construction of the weighting functions which would achieve the desired robustness characteristics. The attendant simulations studies have been deferred to this Chapter in order to afford a comparison of the various design strategies.

It is also required to ascertain the performance of the controllers when they are subject to the inclemency of the environment and the complex behaviour of the ship dynamics. Two sets of sea trials were allocated within the schedule of a frigate size warship. The preparations for these trials are detailed and the results presented for analysis.

7.2 SIMULATION STUDIES

The simulation studies was conducted utilising the software made available by DRA Haslar. This is a suite of ship motion prediction programs called PAT91 (Crossland, 1991). It has

been under continual development since the beginning of the last decade. During this time it has exploited advances in computer technology to permit the computationally intensive calculations associated with fluid dynamics to be performed ever faster. Significant developments in the theory of ship motion prediction have been incorporated into the algorithms. It is in a state of evolution, for example recently the program has been modified to include the lift forces created by the brackets which hold the propeller shafts in place.

PAT91 calculates the motions by operating on a strip theory model of the ship (Ogilvie, 1969). This method divides the ship into sections. The forces acting on each section are calculated given the geometry of the hull. A resultant ship motion is produced when the sections congregate in the appropriate orientation. The forces are recalculated given their direction and magnitudes for the complete ship. Thus the program is able to accommodate non-linearities in the hydrodynamic coefficients. Essentially, the method functions in the frequency domain, yielding ship motion statistics as RMS values.

The results of the software have been extensively compared with full-scale and model-scale sea trials (Lloyd and Crossland, 1989). Predictions of the ship rolling at beam sea were reported as extremely reliable. However, at quartering and following seas the predictions deteriorate with a divergence of 20% to 40% between simulations and sea trials results. Despite these limitation, PAT91 is generally regarded as state-of-the-art technology. It is certainly far superior than the simple time domain based simulations packages commercially available for personal computers.

Although, the software incorporates fin stabiliser and RRS faculties, it was necessary to alter it in order that higher order controller transfer functions could be accommodated. This entailed reprogramming the module which calculates forces from these appendages.

An extensive programme of simulations was conducted of the ship stabilisation performance. Each controller was simulated at ship speed of 12kts, 18kts and 26kts with sea states at 3, 5 and 8 (Table 2.4) and from 15^0 to 165^0 in 15^0 increments encounter angle. The procedure was reiterated for the three modes of stabilisation viz. RRS only, fins only and the fins and rudders operating in congress. Statistics collated were percentage reduction, RMS rudder and fin controller demand and where appropriate the yaw error RMS. The data is presented in graphical form in Appendix G.

7.2.1 RRS Simulations Results

Initially simulations were conducted in order to assess the efficacy of the RRS controllers when operating independently.

Figures G1 to G3 illustrate the stabilisation achieved at sea states 3 to 8 respectively and with the ship moving at 12kts. The corresponding rudder activity is displayed in Figure G4 to G6. At sea state 3 and in quartering seas the classical controllers yield up to 20% greater roll reduction than the H_∞ or LQG controllers. Whilst in bow encounter seas the situation is reversed with the H_∞ controller's performance exceeding all other controllers. If the sea state increases to 5, it also delivers consistent levels of roll amelioration whilst the other controllers' efficiency is variable over the entire heading ranges. The rudder activity for these conditions remain with permissible levels, hence slew rate saturation is not induced.

At the worst sea state, Figure G3, the response of the H_∞ controller yields almost a constant 25% roll reduction irrespective of the encounter frequency. All other controllers which were tested exacerbated the roll motions at quartering seas. Only the classical-1 controller marginally accrues greater roll stabilisation at following seas.

It may be expected that the superior performance of the H_∞ controller, in particular at sea state 8, incurs proportionally greater demand on the rudder servomechanism. However,

Figure G6, indicates that its RMS magnitudes are considerably reduced as compared with the classical controllers and similar to the LQG controller. It was postulated that slew rate saturation, and the attendant pernicious consequences, are inevitable if the RMS demand to the rudder servomechanism exceeds 5-7^0 (section 3.4). The classical controllers will saturate the servomechanism on account of the RMS demands being up to 25^0, Figure G6. Considering the H_∞ controller, at the same sea state, the graph indicates that the marginal saturation will occur, which will be eliminated by the ASA scheme proposed in Chapter 3.

Examining the roll reduction capabilities at a cruising speed of 18kts (Figure G7 to G9), it is manifest that a very similar scenario to ship speed of 12kts exists. The overall performance of the H_∞ controller exceeds the other controllers. In particular at sea state 8, the stabilisation achieved is a constant 35% over 80% of the encounter frequencies. This does not provoke servomechanism saturation, since Figure G12 indicates that the controller induces the least activity as compared with the other controller designs. In contrast, the classical and LQG controllers consistently excite roll motions, in addition to the sea disturbances which impinge on the ship as manifest by the negative percentage reductions at quartering seas.

If the ship is moving at high speeds of 26kts the performance of the controller is exhibited by Figures G13 to G15. The corresponding rudder activity is displayed in the graphs G16 to G19. At sea state 3 and 45^0 heading an inexplicable dip occurs. This was assumed to be an idiosyncrasy of the software since, the ship's orientation and sea state engender a negative encounter frequency as calculated from equation (2.46).

In the ship's maximum operational environment of sea state 5 and headings of less than 45^0 the classical and LQG controller amplify the roll of the ship. Whereas, the H_∞ controller produces stabilisation of 20% at the encounter extremities which rises to 45% at beam sea.

Its performance deteriorates in waves of higher encounter frequencies when compared with the classical and LQG types.

The H_∞ controller performance is revealed to be constant for sea state 8, achieving 35% roll reduction at headings greater than 30^0. Again, it is seen that the other controllers will amplify roll at low encounter frequencies.

Investigating the rudder activity of all these sea states indicates it to be favourable for the H_∞ controller given its demonstrably superior roll stabilisation capabilities.

As stated earlier, a major reason for the reluctance of the Royal Navy to adopt RRS on existing steering systems was the propensity of the system to become unstable, particularly at low encounter frequencies as observed by Cowley and Lambert (1975) and Lloyd (1975). The test vessels which exhibited this behaviour were also equipped with classical type RRS controllers This deficiency of RRS, the hydrodynamic reasons for which are as yet not fully understood, has been vividly illustrated in the stabilisation results of the classical and LQG controllers. These controllers exacerbate the roll motions of the ship at quartering seas. However, significantly, this characteristic is absent in the stabilisation results of the H_∞ controller. This type of controller may be a solution to the reported destabilising idiosyncrasy of RRS.

Chapter 2, in consideration of the dual purpose of the rudder, accentuated that the yaw and roll controller can be designed independently on account of the frequency separation between these dynamics. It was judicious to examine the possible effects on the course keeping ability of the ship when the autopilot is augmented with RRS. Typical yaw errors are shown in Figures G19 to G21 for a ship speed of 18kts. The values lie below 0.3^0 which

represents negligible yaw interference. Thus vindicating the dual channel approach to controller design. Therefore, this aspect will not be further considered as an impediment.

7.2.2 Fin Stabilisers Simulation Results

The graphs of Figures G22 to G24 portray the roll stabilisation achieved when the fin stabilisers are active in isolation. The most conspicuous feature of these graphs is the unprecedented roll stabilisation provided by the fin stabilisers. Unlike the RRS, the fin/roll dynamics are not encumbered by non-minimum phase zero limitations, and are able to deploy disturbance correcting roll moments in a broader encounter spectrum. At all three sea states the H_∞ controller delivers between 70% and 80% roll stabilisation irrespective of encounter frequency. The classical and LQG controllers are maximised at around the roll resonance of the ship with diminishing performance at other frequency excitation ranges. The LQG controller at headings of greater than 150^0 and less than 45^0 and at sea states 3 and 8 respectively appear to amplify the roll.

The corresponding fin demands in terms of RMS values are depicted in the graphs of Figure G25 to G26. Despite the H_∞ controller possessing unrivalled roll stabilisation qualities the RMS demand signals are not only comparable with the other techniques but is often of reduced magnitude, for example in Figure G27 for sea state 8. In Chapter 3 (section 3.4) an interpolation of the data presented, suggested that the maximum permissible RMS values for the fin servomechanism is 15^0 to 18^0. If this is exceeded the controllers will compel the device into non-linear operation and inevitable saturation. For sea state 8 which represents an occasional severe disturbance, Figure G27 illustrates that the servomechanism will not be able to reciprocate the controller demand signals. However, the ASA is an eminently suitable contingency and will prevent saturation in such isolated environmental conditions.

It is evident from the results at ship speed 18kts and sea states 3 , 5 and 8 that the selection of the robust controller weights were justified. Again, the H_∞ controller provides between 70% and 80% roll stabilisation in all ship orientations and sea states. At sea state 3 and in quartering seas there is some deterioration of performance, nevertheless it remains above 60%. The performance optimisation of the LQG and classical controllers at beam seas is pronounced with approximately 50% roll reduction here, degrading to 30% in higher and lower encounter frequencies. The corresponding fin demand activity, Figures G31 to G33, indicates comparable servomechanism utilisation for all controllers. This is achieved despite the H_∞ controller yielding between 15% and 20% greater roll stabilisation at beam seas and sea states 3 , 5 and 8 respectively.

The conspicuous characteristic observed at ship speed of 26kts is the continual formidable levels of roll amelioration achieved by the H_∞ controller, being again between 70% and 80%. There is evidence of diminishing performance at sea state 5. Although the roll stabilisation accrued by the classical and LQG controllers are comparable with each other, they do not approach the levels of the H_∞ controller. For example at sea state 8 there is a difference of 15% over the entire frequency range.

Figures G37 to G39 show that the controller output will not saturate the servomechanisms. Given its superior roll stabilisation faculty, the H_∞ controller's RMS demand does not exceed the LQG or classical cases.

7.2.3 Fin and RRS Simulations Results

The principle objective of this study is to ascertain whether enhanced levels of roll stabilisation result when both the fins and rudder are engaged simultaneously. Figures G40 to G42 illustrate the results for this mode of operation at a speed of 12kts. The hypothesis is confirmed by the 85% to 95% roll stabilisation achieved at all sea states and irrespective of encounter angle for the H_∞ controller. The LQG and classical controllers, although, exhibit increased roll amelioration, their performance is not only inferior to the robust controller,

but also deteriorates at quartering and bow seas. Approximately 20% additional roll stabilisation can be expected at all ship speeds when compared with the case of the fins functioning alone, Figures G49 to G51 and G58 to G60.

Considering the fin activity, it was envisaged that this would decrease on account of a portion of the stabilisation being delivered by the rudders. Examining a typical example at 18kts and sea state 5, Figure G53, at beam seas the RMS level demanded is 6^0. However, when the fins are functioning in isolation 9^0 of RMS demand is generated in the same environmental conditions (Figure G32). From all the graphs of fin activity it is seen that, despite stabilising the roll motions with greatest alacrity, the H_∞ controller does proportionally not penalise the fins servomechanism: the values being comparable with the LQG and classical controllers, e.g. Figures G54 and G62.

Conversely, with the fins and rudders functioning in congress the RMS demand to the rudders also decreases. This is demonstrated in Figure G56, where it is apparent that, at beam sea, the RMS rudder demand is 1.5^0. Whilst for the same conditions and with the RRS engaged alone the demand is 4.5^0. These characteristics are extracted from data in Appendix G in order to afford a vivid comparison in Figures 7.1 and 7.2, which depicts the stabilisation achieved in three modes of operation for the H_∞ controller with sea state 5 and 18kts ship speed. The ensuing rudder and fin demands are displayed in Figure 7.2.

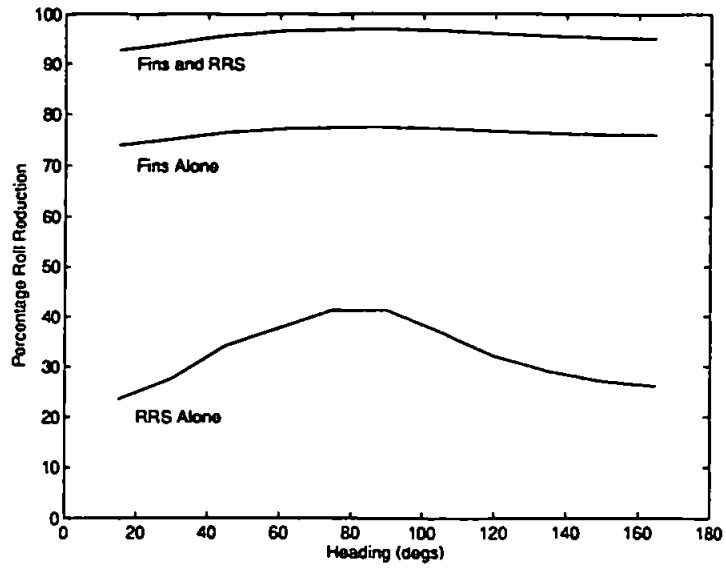

Figure 7.1 : Roll stabilisation with three modes of operation

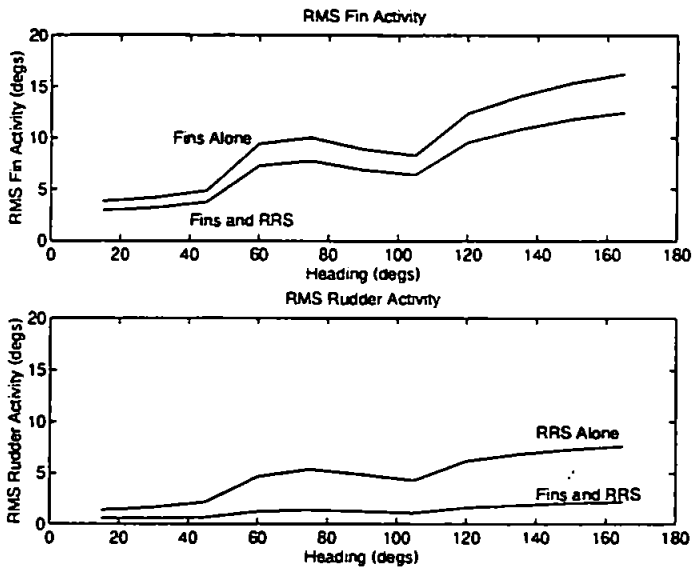

Figure 7.2 : Fin and rudder activity for three modes of operation

7.2.4 Actuator Excursion Limits

The RMS values generated by the controllers were related to the slew rate saturation requirements as stipulated in Chapter 3 in order to restrain the servomechanism from encroaching into non-linear operation. Unfortunately, this is not the only source of non-linearity.

Since, the fin's and rudder's angle of excursion are limited by their physical dimensions, it is imperative that the controllers do not force them to continually bang against the mechanical stoppers, lest damage to the devices and the ship occurs. In practice, there is a stringent requirement to ensure that this does not occur by an explicit conditional loop in the control algorithm. However, this will introduce further non-linear motion and is reserved as a contingency. It would be 'good' practice if this desired objective can be imparted to the controller at the design stage and to avoid invocation of the software induced non-linearity.

It is not theoretically possible to directly relate an RMS value of a stochastic signal to the magnitude of its peaks. A criterion is proposed in order to compare this characteristic of the controllers through the use of significant heights. The peaks of the controller demand are recorded and the average taken of the largest third, the other two-thirds of the data are disregarded. This is an established technical method to determine prevalent sea states from sea wave height measurements.

Figure 7.3 illustrates a typical RMS demand with the corresponding significant heights. It indicates that with an RMS demand of 15^0 the fins will begin to reach their physically permissible range. Incidentally, the maximum RMS value, interpolated from the data of Chapter 3, in order to avoid saturation for the fin stabilisers is 15^0-18^0 which correlates well with the requirements for fin travel. From the simulation studies data of Appendix G, it is apparent that at sea state 8 the controllers' demands will often exceed the maximum permitted magnitudes. If the controllers' gains are restrained to avoid this then roll amelioration at the, more frequent, lower sea states will be compromised. In general, sea state 8 is an occasional severe disturbance, at other sea states the RMS values indicative of this scenario being avoided.

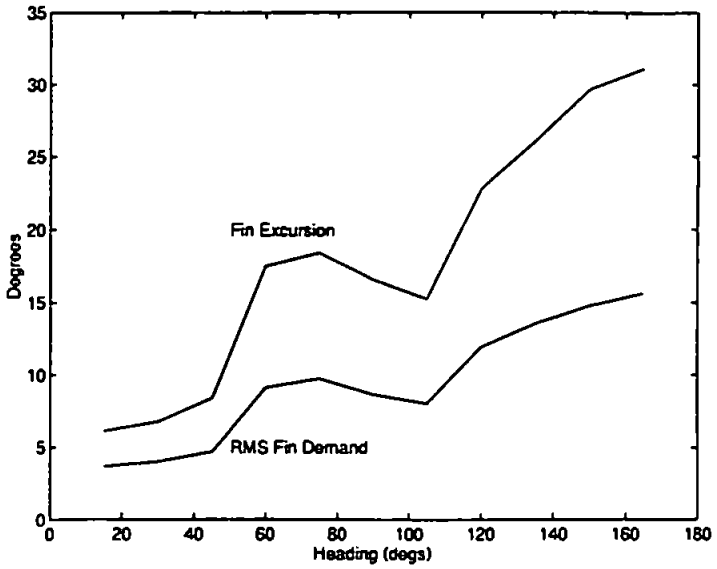

Figure 7.3 : RMS and significant height values for typical fin demand

In summary it may be said that the controllers have now been exhaustively tested in simulations and frequency domain studies. They appear to perform adequately within the realms of the software. Simulation software which attempts to encapsulate the complete behaviour of any physical system will intrinsically have limitations on account of unmodelled dynamics. In the case of a large vessel, many of its dynamics are nebulous rendering them beyond analytic comprehension. Therefore, at best, its mathematical representations remains an approximation to reality, albeit embued with considerable accuracy. Although, these simulations afford an indication of the envisaged roll reduction, the controllers require to be subject to the harsh inclemency of a real operational environment.

Thus as will be seen in the following sections, the preparations required for the sea trials are briefly outlined and subsequently the procedures and results from the trials are presented.

7.2.5 Faster Rudder

The Royal Navy, as previously mentioned, has stipulated that the integrated ship roll stabilisation strategy must not necessitate any mechanical modifications of the rudder system. However, Brown Brothers confirms that the reserve capacity can be realised by

adjustment of the valves of the rudder servomechanisms currently installed on the ship. This would result in an increase of slew rate from 6^0s^{-1} to 9^0s^{-1}. This procedure could be performed at minimal cost. Therefore, a cursory study is made to assess the impact of the faster rudder on roll stabilisation performance.

A pc based non-linear simulation package was utilised to represent the servomechanism action. Employing the robust type controllers in a ship speed of 18kts and sea state 5 the roll stabilisation as shown in Figure 7.4 resulted with the attendant rudder activity depicted in Figure 7.5.

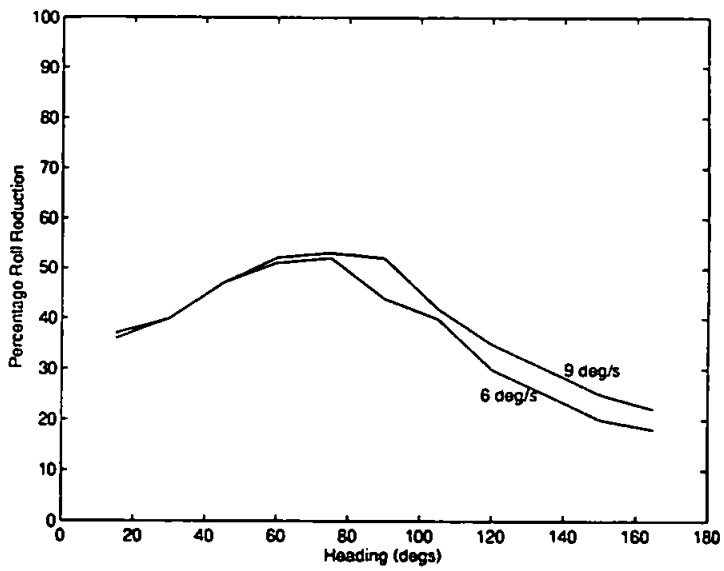

Figure 7.4 : Roll stabilisation achieved with faster rudder

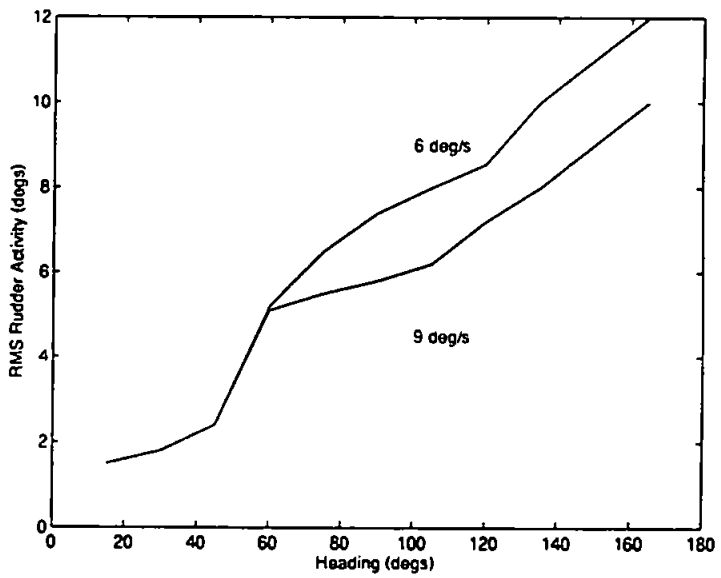

Figure 7.5 : Rudder activity with faster rudder

At higher excitation frequencies the controller's demands reflect these increased frequency demands. The faster rudder exhibits a maximum of 5% to 8% greater roll stabilisation capacity than the slower rudder. However, at lower encounter frequencies there appears to be no advantage accrued with the faster rudder.

The controller demand will tend to saturate both the servomechanism at these higher encounter angles. However, the faster servomechanism will naturally be effected to a comparatively less degree. It appears from these results that there may be some advantage in incurring the expense to modestly upgrade the speed of the servomechanisms.

7.3 PREPARATIONS FOR THE SEA TRIALS

In order to record the data and control the actuators, a considerable amount of preparation was required, in terms of not only the software and controller design, but also of the hardware implications necessary to interface with the fin and rudders, given the nature of the environment on board a warship.

7.3.1 Software Development

The controllers were implemented digitally in a personal computer. This necessitated the Laplace domain transfer functions to be converted into their corresponding discrete representations. Utilising the bilinear transformation technique (Oppenheim *et al*, 1983) the appropriate digital depiction's were generated. This is essentially a mapping of the jω-axis in the s-plane from zero to infinity onto a unit semicircle in the z-plane. From these, difference equations were derived for the controllers and subsequently encoded into software routines in C++. As an example consider the controller:

$$G(s) = \frac{\alpha(s)}{\phi(s)} = \frac{6.2s^2 + 5s + 1}{0.05s^2 + 0.5s + 1} \qquad (7.1)$$

It has a digital counterpart via the bilinear transformation

$$G(z) = \frac{(34.8 + T^2) + (2T^2 - 49.6)z^{-1} + (14.8 + T^2)z^{-2}}{(T + T^2 + 0.2) + (2T^2 - 0.4)z^{-1} + (T^2 + T + 0.2)z^{-2}} \tag{7.2}$$

hence, the difference equation can be derived as:

$$\begin{aligned}\alpha(n) = (T^2 + T + 0.2)^{-1}[&(34.8 + T^2)\phi(n) + (2T^2 - 49.6)\phi(n-1) + (14.8 + T^2)\phi(n-2) \\ &-(2T^2 - 0.4)\alpha(n-1) + (T^2 + T + 0.2)\alpha(n-2)]\end{aligned} \tag{7.3}$$

where

n	time index
T	sampling period (seconds)
z	discrete operator
s	Laplace operator
α	fin demand
ϕ	roll angle

A prerequisite for this method is the selection of a sampling time which must adhere to the Nyquist sampling criteria. The natural roll period of the ship is approximately 10.5 seconds. Accuracy in reconstruction of a signal is proportionally dependent upon the sampling time. Therefore, it was decided to realise the computer's optimal capabilities. Examination of the clock speed of the personal computer in terms of calculating the next demand value, storage of signal, update of graphical display and excitation of the appropriate voltage revealed the maximum possible sampling frequency as 10Hz. This affording approximately 100 data values per cycle of ship oscillation.

The software written to perform this function is listed in Appendix H and Figure 7.6 illustrates a simplified flow chart of its operation. The software has a routine which allows the user to define the desired permutations and timings of when fin and RRS are to be operational. The initial step is to read the controller coefficients after which the trial begins.

Various data, such as fin angles, roll angle, yaw error, and the control signals produced by the ship are read via a ADC and stored in an array. Upon calculating the next controller demands, they are immediately output via the DAC card and amplifier circuits to the fins and rudders. Whilst waiting for the next sample period the computer updates the graphical display and records the data on disk.

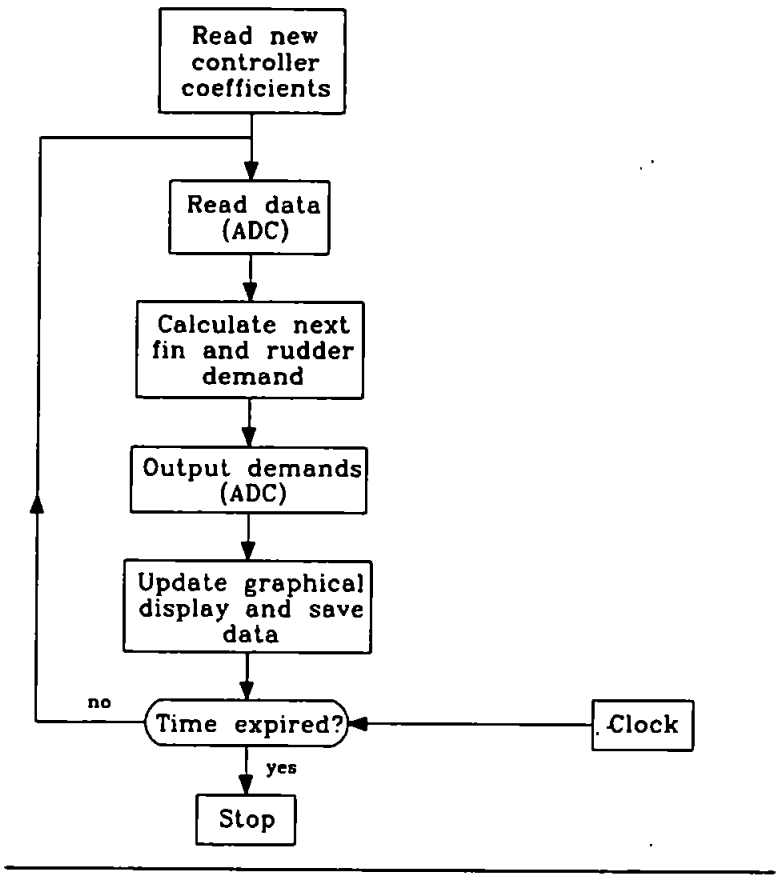

Figure 7.6 : Flow diagram of trial software

7.3.2 Hardware and Filtering Requirements

The ship sensors and conditioning circuitry provides uncorrupted signals of the parameters requiring to be monitored. However, in order to ensure the compatible voltage levels with the ADC card and for calibration purposes, regulation circuits were constructed. The voltages generated by the DAC card were subject to correction by equivalent circuits.

As elaborated in section 5.3.2 the fins and rudders are not capable of correcting for constant list angles. A high-pass filter, with a cut-off at two decades below roll resonance, incorporated into the software will suffice to circumvent this problem. High frequency noise may compromise the numerical integrity of the control algorithms and create spurious actuator motions. The implementation of a low-pass filter, with a cut-off two decades above roll resonance will ensure that high frequency noise does not penetrate the system. These filters by virtue of their cut-off locations will not interfere in the frequency regime where control action is applied.

7.3.3 Interface to Ship

It was imperative to interface with the ship's fin/rudders with the minimal of disruption to ship operations and machinery. A schematic of the wiring configuration is given in Figure 7.7.

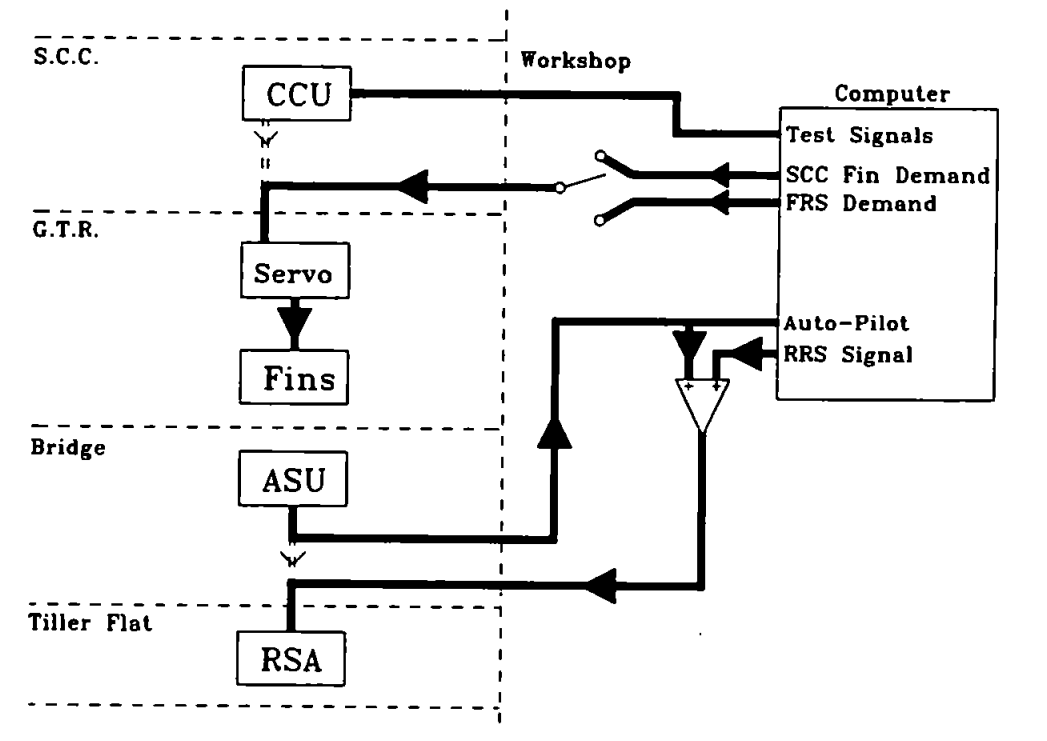

Figure 7.7 : Ship wiring schematic

The computer was installed in the workshop. Normally the fins are controlled by the ship's Central Control Unit (CCU) located in the Ship Control Centre (SCC) (BR6510). The CCU provides demand signals to the servomechanisms situated in the Gas Turbine Room (GTR, BR6510) and appropriate signals outputs for test purposes. It was possible to disconnect this route and replace it with the computer-generated fin demand signals. The configuration incorporates a safety feature, in that it is physically possible to revert to CCU control of the fins should a malfunction occur in the computer or in the event of power failure by means of a simple bipole switch.

The signals required to be associated with the rudder loop are heading error and autopilot demand. The Auto Steering Unit (ASU), which is located at the bridge, furnishes both these signals (BR6509). The connections between the bridge (ASU) and the rudder servomechanism, located in the tiller flat, were broken and re-routed via the workshop and computer. This necessitated the signals travelling approximately 50 metres one way to the computer without the aid of boosters. Fortunately, it did not prove to be a serious impediment to effective signal reception.

External circuitry provides the facility to superimpose the RRS generated demand onto the autopilot (ASU) signal by means of a summing amplifier. This augmented signal is subsequently calibrated and fed to the rudder servomechanisms. If RRS is not required then the autopilot signal is permitted to travel to the tiller flat unaltered. Again a simple switch allows control of the rudders to revert to the ASU in the event of an emergency. Therefore, when the RRS is not engaged, the autopilot is the default signal to the rudders.

The controllers were designed assuming that the rudder's slew rate is 6^0s^{-1}. This is achieved if both the Hydraulic Power Units (HPU) are active which was ensured for the duration of the trials.

7.4 SEA TRIALS RESULTS

As mentioned in Chapter 1 the study was permitted to conduct two sets of sea trials. The first session was during 7-8th March 1994 in the Plymouth exercise area in the English channel and the second from 31st October to 3rd November 1995 on the ship's passage between Gibraltar and Plymouth. The results are presented in chronological order.

7.4.1 First Sea Trials

A large number of individual trials were conducted with various classical controllers and fin/RRS modes of operation. The fins and rudders were engaged with three different sequences, and repeated several times with an assortment of controllers. Each sequence had a duration of 400 seconds. The data was subsequently analysed and presented in terms of RMS values.

For the entire duration of the trials the sea remained at around state two. Unfortunately, such calm weather is not expedient for roll stabilisation trials. Typical roll motions which were experienced are shown in Figure 7.8 for ship speeds of between 12kts and 15kts and have a corresponding RMS of 1.5^0.

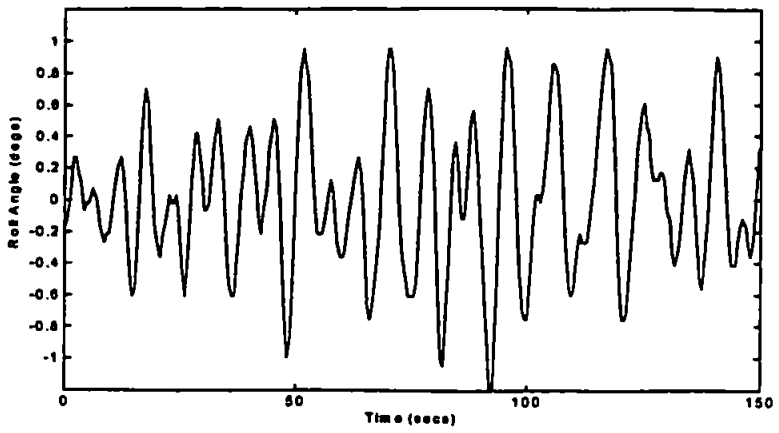

Figure 7.8 : Typical roll motions experienced

However, significant fin motion was observed indicative of stabilisation occurring, therefore, it was decided to proceed with the trials. The conduction of the trials were arranged in three sequences are detailed in Table 7.1.

Table 7.1 : Summary of modes of operation for trials.

	Time (secs)	<100	100-400
Sequence 1	Fins	✓	-
	RRS	-	✓
Sequence 2	Fins	✓	✓
	RRS	-	✓
Sequence 3	Fins	✓(CCU)	✓(p.c.)
	RRS	-	✓

Sequence 1 involved having the ship stabilised by the fins for the first 100 seconds using the CCU generated signal. After 100 seconds the RRS was engaged and the fins switched off and locked in their neutral position. This would afford direct comparison of stabilisation achieved between the fins and RRS when functioning in isolation.

In accordance with the primary objectives of this study the sequence 2 will establish whether employing the rudders in a supplementary role will result in enhanced levels of roll

reduction. This trial entailed employing the CCU fin stabilisers during the entire 400 seconds test period. After 100s the RRS was engaged in congress with the fins.

Finally, sequence 3 involves controlling both the rudders and fins from the computer. Therefore, the CCU signal was replaced by the computer signals after 100s. At the same time the rudders were engaged in the stabilisation mode.

RRS Alone

Two sets of runs are shown with sequence 1 in Table 7.2 for two classical controllers. RMS statistics are collated for various relevant signals, before and after 100 seconds. It is seen that when the fins are switched off the roll value does not change significantly for either controller during RRS operation. This is not indicative that RRS is as potent as the fins, but rather the sea induced roll motions were insignificant. Also, the fins and rudder activity remain within acceptable bounds.

Table 7.2 : Typical results of sequence 1

RMS (degs.)	Roll		Fin Activity		Rudder Motion		Heading Error	
Time (s)	<100	>100	<100	>100	<100	>100	<100	>100
Run 1	0.19	0.19	0.94	0	0	2.39	8.21	10.4
Run 2	0.42	0.49	1.46	0	0	5.83	9.81	10.9

Fins and RRS in Congress

Typical results for sequence 2 are illustrated in Table 7.3. Both runs show that, when the rudders are engaged, greater levels of roll stabilisation are achieved, of approximately 25%. Note also that fin activity correspondingly diminishes as the rudders assist in generating the roll-correcting moments.

Table 7.3 : Typical results of sequence 2

RMS (degs.)	Roll		Fin Activity		Rudder Motion		Heading Error	
Time	<100	>100	<100	>100	<100	>100	<100	>100
Run 1	0.63	0.46	4.48	1.08	0	3.46	10.1	11.3
Run 2	0.61	0.45	4.17	1.01	0	3.13	10.3	10.8

Computer Generated Control

The purpose of this sequence, number 3 (Table 7.1), was to afford a comparison of roll stabilisation achieved between the controller synthesised and the one currently installed on the warship. The results are collated in Table 7.4. When the computer controls both the fins and rudders the roll RMS exhibits a marginal improvement as expected from previous results. The fin activity decreases due to RRS being operational.

Table 7.4 : Typical results of sequence 3

RMS (degs.)	Roll		Fin Activity		Rudder Motion		Heading Error	
Time	<100	>100	<100	>100	<100	>100	<100	>100
Run 1	0.57	0.47	1.28	0.85	0	3.41	9.94	11
Run 2	0.58	0.44	1.3	0.77	0	2.99	10.8	11.1

From the Tables of trials data it is seen that the heading error irrespective of RRS being engaged would be considered as being unacceptably high. At the time of the trials this was brought to the attention of the Marine Engineer Officer (MEO). Apparently the reason for this was indeterminable and attributed to either a malfunctioning or simply an inadequate autopilot. The manufacturers were aware of the problem which was to be rectified at the ship's next convient visit to port.

7.4.2 Second Sea Trials

The controllers tested in the first sea trials were exclusively the classical type of Chapter 5. Since, the primary objective was to ensure that the equipment and software algorithms

functioned correctly and that the rudders and the fins could be invoked from the computer to yield roll stabilisation, it was expedient to employ only the classical controllers. The second set of trials exhaustively tested and compared the performance of all the controllers synthesised.

These trials were conducted on board the same warship during her passage from Gibraltar, departing at 08:30 on 31st October, to the Plymouth Naval Base, arriving at 10:00 on 3rd November 1994. This included travelling through the Bay of Biscay. The Royal Navy and meteorologists report an extremely high probability of encountering rough weather, which would be ideally to the beam of the ship, in this vicinity and time of year. However, during the trials period the sea did not achieve more than sea state 2. Unfortunately, as in the first sea trials, these conditions are patently not a conducive environment in which to investigate the properties of roll stabilisation systems. However, some trials were conducted principally to confirm the simulations studies and, by implication, to validate the mathematical ship models utilised in the controller design.

Typical roll motions which were experienced are shown in Figure 7.9. Since, the sea state remained low it was not necessary to request that the ship speed be increased, thus it remained at 12kts to 15kts throughout the trials period. The trials data was subsequently analysed and is presented in terms of RMS values and significant heights.

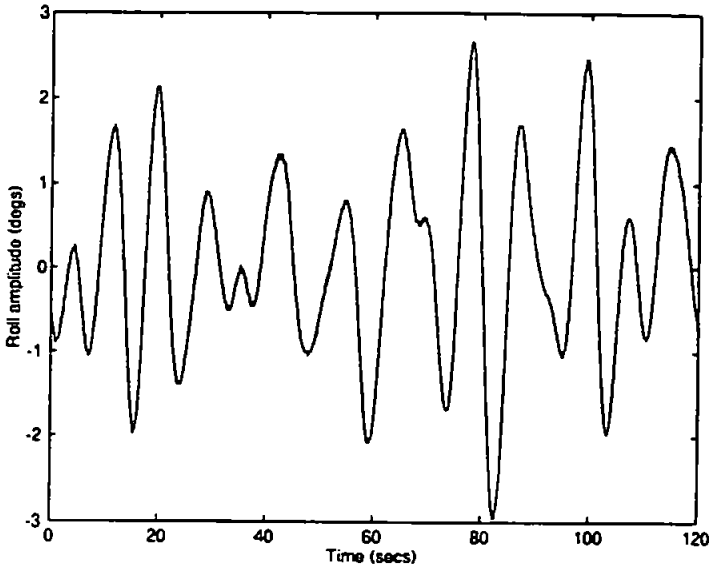

Figure 7.9 : Typical roll motions experienced

Utilising simulation results in predicting controller performance affords the significant advantage that sea trials need not be conducted. This avenue of investigation is dependent upon the integrity and accuracy of the mathematical models and integration methods used in the simulations. Since, the models are not subject to the many variable factors in the environment, which cannot be quantified, these simulations data remain, at best, inconclusive. The trials engendered an invaluable opportunity to assess the repeatability and accuracy of these simulations with the real data acquired. Therefore, validation of the software affords an opportunity to emulate the real environment without incurring the cost of actual sea trials.

A large number of individual trials were conducted with various controllers and modes of fin/rudder operation. The fins and rudders were engaged with two different sequences; namely rudders alone and fins with rudder stabilisation. Each sequence was for a duration of 420 seconds. Table 7.5 summarises the sequence of the trials performed.

Table 7.5 : Summary of trials configuration

	Time (secs)	<120	120-420
RRS Only	Fins	✓	-
	RRS	-	✓
Fins and RRS in congress	Fins	✓(CCU)	✓(p.c.)
	RRS	-	✓

Rudder Roll Stabilisation

In this sequence of trials the ship was stabilised normally by the fins for the first 120 seconds utilising the controller currently installed on the vessel. The fins were then switched off and the rudder stabilisation activated. Hence, affording a direct comparison between RRS and fin stabilisation. Table 7.6 shows the typical RMS roll and controller demand values achieved for the three types of controllers. Before the RRS is implemented the RMS of the rudder is that of the autopilot demand signal and thereafter of the two signals summed. The last column depicts the corresponding data produced by the PAT91 prediction software which is for RRS engaged permanently.

Table 7.6 : Results for RRS

Model	Sea Trials								PAT91	
RMS (°)	Roll RMS		Fin Demand		Rudder		Heading Error		Roll	Rudder
Time (s)	<120	>120	<120	>120	<120	>120	<120	>120	n/a	n/a
Classical	0.7	0.6	8	0	2.9	2.71	0.26	0.18	0.75	2.8
LQG	1.12	1.61	4	0	3.78	4.24	0.28	0.26	0.96	1.5
H-inf	0.41	0.41	10.5	0	4.09	5.11	0.27	0.28	0.55	3.1

The roll stabilisation with the RRS engaged alone marginally diverges when compared with the fin stabilisation case. Confirming the results of the first sea trials (Table 7.2), these do not infer that the rudders are as potent as the fin stabilisers but rather that the insignificant roll motions experienced can be eliminated as effectively with the rudders. The activity increases by approximately 1^0 in all cases. The problem experienced with the autopilot in the

first sea trials seems to have been rectified as suggested by the greater reduced yaw error values.

The stabilised roll values from the PAT91 simulations data with the corresponding ship and environmental conditions and the attendant RRS demand are shown in the final two columns. These values diverge by up to approximately 30%. However, given the relatively small numbers involved this is not a cause for concern.

Fin Stabilisation and RRS Active

The primary aim of this project was to ascertain the efficacy of the rudders as secondary stabilisers. To these ends the next sequence of trials were performed with the fins permanently engaged and controlled by the CCU and subsequently by the pc signals. The rudders were activated for stabilisation after 120 seconds (Table 7.5).

The results are shown at Table 7.7 again with the PAT91 predicted RMS values. As expected, since a portion of the stabilisation is performed by the rudders, roll and fin activity both diminish, with the H_∞ controller consistently yielding better results. After 120 seconds the fins are controlled by the pc generated demand.

Table 7.7 : Results for RRS and fins active simultaneously

Model	Sea Trials								PAT91	
RRS (°)	Roll RMS		Fin Demand		Rudder		Heading Error		Roll	Rudder
Time (s)	<120	>120	<120	>120	<120	>120	<120	>120	n/a	n/a
Classical	0.59	0.52	7.4	6.3	1.88	2.5	0.44	0.42	0.17	2.59
LQG	0.75	0.45	7.58	5.8	3.3	4.8	0.39	0.35	0.6	4.1
H-inf	1.78	0.48	9.92	5.21	1.47	4.69	0.35	0.35	0.8	4.5

Comparing the trials data with the PAT91 simulations, Table 7.7 shows the predictions are being overestimated. However, they may be considered to be reasonably accurate given the relatively small magnitudes of motion.

Forced Roll Trials

Due to the calm nature of the sea it was decided to force roll the ship and endeavour to damp the oscillations using various types of controllers. The procedure invoked the fins with a 20^0 sinusoidal signal, upon establishing sufficient rolling motions, the fins were neutralised, usually after 250 seconds, and then by employing various permutations of RRS and fins, an attempt was initiated to stabilise the motions.

It was frustrating that due to a technical malfunction in the radar which was exacerbated by the relatively large roll motions created compelled the abandonment of these trials. Only two runs were completed and their results are shown in Figure 7.10 for information only.

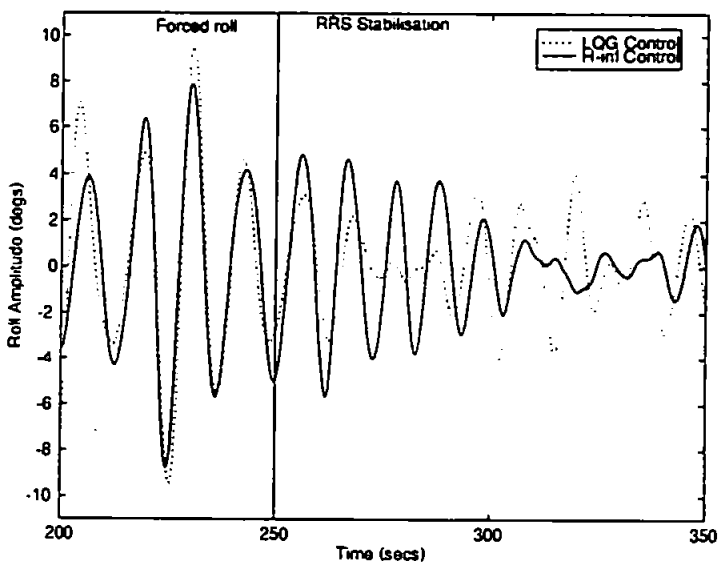

Figure 7.10 : Forced roll motions

7.5 DISCUSSION AND CONCLUSIONS

The previous two chapters were concerned with deriving linear controllers utilising the appropriate mathematical models. Their frequency domain and robustness properties were analysed which revealed that the H_∞ controllers remain not only internally stable but accrue the same levels of performance in the presence of structured and explicit uncertainty.

The roll stabilisation performance aspect of the controllers was in abeyance until the current Chapter in order to complete their development and afford a comparison amongst them. An advanced strip theory model of the complete ship dynamics was employed in software simulations. This model is a mutivariable system which incorporates the interactions of the various ship motions and accommodates many of the non-linear distortions associated with the ship's equations of motion.

A series of exhaustive simulations were conducted to ascertain the roll stabilisation characteristics of each controller. As indicated by the analysis of Chapter 6, the robust controllers' roll stabilisation capabilities were confirmed to exceeded that of the LQG and classical controllers. This was particularly pronounced in the case of the fin stabilisers which realised stabilisation levels of 70% to 80% irrespective of encounter frequency. As expected the rudders could not countenance the same levels of performance. However, again the RRS robust controller's performance, when considering all aspects, was unsurpassed. It is concluded that the selection of the performance weighting (section 6.8.1) to encompass those regions of the frequency spectrum where sea disturbances occur, particularly sea state 5, is justified. Furthermore, it is asserted that, since the fins, when operating in congress with the RRS, yields greater levels of roll stabilisation without modification to the rudder system, the primary objective of the study was attained.

The RMS demand signals generated were also examined. A salient feature observed is that, although, the robust controllers achieve considerably greater levels of roll stabilisation, they do not proportionally penalise the capability of the servomechanisms. On the contrary, the robust controllers often extract significantly greater roll stabilisation from reduced actuator activity. Therefore, it is concluded that the selection of the control weight (section 6.8.2) was judicious in its application of the control energy in the frequency regime of disturbances.

A cursory investigation into the consequences of modestly increasing the slew rate was mode. The results (Figures 7.4 and 7.5), conclude that considering the minimal cost, there is some limited advantage gained in increasing the slew rate particularly at higher encounter frequencies.

The developments and preparation pertaining to the sea trials were elaborated upon and the actual data presented. In general, the full-scale sea trials experience tested the reliability and versatility of all aspects of the software and hardware which was developed.

As mentioned earlier the sea state remained very low through-out the trials. Such comparatively small amplitudes of motion did not greatly exert the controllers and therefore, their full effectiveness cannot be appreciated. Furthermore, due to ship operations the speed remained at 12kts to 15kts, limiting the moment generating capabilities of the actuators.

Despite these unsuitable environmental conditions valuable conclusions can be derived from the trials data acquired. The results of sections 7.4.1 and 7.4.2 manifests the similar effectiveness of the rudders with the fins in roll stabilisation at low sea states. The trials

vindicated the most important objective, that of employing the rudders in a supplementary role with the fins enhances roll stabilisation, as can be demonstrated by the results from Tables 7.3 and 7.6.

Although not conclusive from the sea trials, the simulations data implies that the performance, in terms of roll reduction, can be increased by implementing the robust type controller in both the fin and rudder loops, particularly over a very wide environmental envelope.

A programme of forced roll trials was envisaged. However, it was curtailed on account of technical difficulties. Since, the predominant roll period would have been the same as the excitation frequency of the fin stabilisers, the environment would be somewhat contrived. The controller would not have been subject to the full spectrum of genuine sea disturbances but a mono-sinusoid. Therefore, although, advantageous, these type of trials would not have illustrated conclusively the roll stabilisation abilities of the controllers.

The trials results at the low sea states compare favourably with the PAT91 simulation data generated at the design stage. This software is a reasonably reliable evaluation tool for controller performance purposes which can be utilised at the initial stages of the design process, without incurring the expense of conducting sea trials. Therefore, it is inferred that the linear roll models employed in the controller synthesis are imbued with considerable confidence for future control design. By implication, the predictions of the simulation software for stabilisation performance generated by the controllers at other sea states must be regarded as a reasonably accurate reflection of reality.

Comparing the simulations with the real data there is ample evidence to show that the robust type controllers yield greater roll amelioration.

The PAT91 ship motions prediction software verified, in conjunction with the sea trials results, that the potential for using the rudders in concert with the fins as stabilisers is a practicable reality. Crucially, since this does not require the rudder system or its peripherals to be modified, such that expenses incurred will be minimal.

CHAPTER 8

CONCLUDING REMARKS

8.1 DISCUSSION AND CONCLUSIONS

Successful linear controller design requires that the dynamics of the plant are accurately embedded in mathematical representations. To these ends the ship dynamics were investigated in terms of their non-linear and linear constituents. From the resulting complex models it was possible to define the dominant behaviour of the ship. By extracting these dynamics, simplification ensued which did not compromise the accuracy of the model. These were subsequently amenable to controller design. The models of ship roll motion promulgated in literature were considerably refined by comprehensively identifying the sources of uncertainty the models and evaluating them. This information would be required in the controller analysis.

This investigation of the plant's behaviour was concluded with an analysis and formulation of the frequency range and magnitudes of the disturbances which will impinge on it. It was deduced that the sea wave disturbances could be adequately emulated by various filters.

The complete roll stabilisation configuration was considered. It was decided that controllers for the yaw and roll motions could be constructed independently as with the fin and RRS loop. The multivariable approach was subsequently demonstrated as achieving almost identical characteristics.

A crucial objective of this study is the requirement to utilise the rudders currently installed on Royal Navy vessels. Since, these move some five time slower than the fins, it was imperative to investigate the repercussions on the closed-loop system in general and the servomechanisms in particular. It was concluded that a contingency to avoid slew rate saturation was indispensable, lest the servomechanism be compelled into non-linear operation with the attendant pernicious ramifications outlined in Chapter 3.

Initially the frequency spectrum of the servomechanism was constructed via sinusoidal input describing functions and related to the demand RMS values. A new algorithm (ASA) was proposed utilising this information. It functions by restraining the on-line RMS values of the demand signal beyond which it is known that saturation occurs. The principal of the method is generic by interpolating the data presented for specific applications.

In most literature concerning the roll stabilisation of ships, the humans' ability to perform operations effectively in this environment are vaguely mentioned in general terms. Therefore, this aspect was researched and placed in context of rolling motions and lateral accelerations (LFE). It was concluded that the human operators' ability to perform a task is specifically in inverse proportion to the magnitude of the LFE.

The nature of the LFE was examined to ascertain whether it is amenable to be regulated by the fins. It was demonstrated that they could not be utilised to ameliorate this motion.

However, the rudders were suitable to be employed for LFE stabilisation. Following from this a contribution was made by constructing a time domain simulation model of the LFE which correlates with the data produced at DRA Haslar. This knowledge permitted the development of linear LQG and classical controllers which will actuate the rudders. The tuning of the classical controllers revealed that interference with the yaw dynamics and exacerbation of roll motions cannot be avoided. The possible reasons for this were stipulated. The LQG controller on account of simply programming a cost function achieved more satisfactory results. However, the limitations of controlling for LFE were abundantly apparent.

The constituents of the algebraic equation describing LFE alter not only in magnitude but also polarity depending on the location of the transducer in the ship. Therefore, it was observed that stabilisation at one location may cause intolerable increases elsewhere. In order to control for LFE throughout the ship requires the installation of sensors at various locations. However, it was suggested that the LFE stabilisation mode could be engaged at the flight deck which would facilitate the human operators and the recovery of the helicopter, reverting to RRS on completion. It was concluded that since, roll acceleration is a significant component of LFE, then it would be judicious to exclusively stabilise for roll, which would also naturally precipitate in LFE amelioration.

Proceeding with the RRS controller design, the initial effort was dissipated in determining the limitations which might result on account of the non-minimum phase zero inherent in the rudder/roll transfer function. This was evaluated by the integral of log magnitude of the sensitivity function relationship. It was concluded that, irrespective of the RRS controller, the sensitivity function will exhibit, of necessity, amplifications in roll disturbances at the frequency region where the zeros are located. Therefore, the subsequent analysis of the

sensitivity functions were correctly interpreted, and not regarded as inherent shortcomings of the controller design procedures. The controller design proceeded with the objective that it does not inadvertently impart pernicious consequences to the roll stabilisation ability of the closed-loop system.

Chapter 5 proposed two methods for designing classical controllers. The synthesis procedure for the classical controllers appeared to be attractive in its simplicity and intuitive qualities. Essentially, the closed-loops poles and zeros of the system can be related to the desired time domain properties. Therefore, the controller attempts to produce this in conglomeration with the plant.

The other control strategy investigated, in Chapter 5, was the LQG type regulator. Although, the objectives of roll stabilisation are readily reflected in a cost function, the controller synthesis is usually concealed from the designer in software routines. Since, a prerequisite of these types of controllers is that the states of the plant be available for feedback, a full-state observer (Kalman filter) is designed to provide them. However, Kalman filters are optimal to white noise and since the ship is perturbed by filtered noise, there is an inflexible requirement to incorporate the sea dynamics within the controller structure. This presents an impediment to effective roll stabilisation qualities. The controller is now optimised in the presence of the chosen sea state. When the predominant wave height and period alters the performance inevitably deteriorates.

The concept of uncertainty perturbations were introduced with respect to the closed-loop system in Chapter 6. It was recognised in Chapter 2 that without exception any mathematical model is subject to uncertainty from multifarious sources. For example, the ship's dynamics are multivariable with motions interacting, they are non-linear and exhibit

strong parametric dependence on ship speed and excitation frequency. Other sources of uncertainty are the servomechanisms. These devices have physically finite capabilities which must not be exceeded in order to ensure integrity of operation. Despite these uncertainties, a paramount requirement of the controller is that it should remain internally stable in their presence. In order to guarantee this, specific conditions were formulated for the LFT representations of the closed-loop system between the pertinent signals. Another desirable feature of the controller is that it be able to deliver adequate levels of roll stabilisation. This requirement can also be represented between the appropriate signals and encapsulated by the LFT. The salient characteristic to observe being the versatility of the LFT's ability to succinctly characterise all the desired requirements of a plant.

The development of robust linear controllers requires the derivation of frequency dependent weighting functions which embody the uncertainty and performance characteristics. Normally, the frequency regions of a closed-loop system where uncertainty exists is known, the locations where regulation is expected and the judicious manner in which the control effort is deployed can be ascertained by experimentation or experience and insight to the application. Coupled with the LFT, this offers a natural and intuitive procedure for controller synthesis.

Utilising this information and the concept of function spaces, whose constituents are transfer functions, a procedure which minimises the infinity norm of the LFT generates the controllers. These controllers are shown to exhibit the properties which guarantee robust internal stability and also robust performance with respect to the weighting functions. The development of this Chapter represents a novel application of these advanced control techniques.

The structured singular value was introduced as an analysis tool which can determine whether the objectives of internal stability and levels of performance are maintained in the presence of a predefined set of uncertainty. The uncertainties can be represented as unstructured weighting functions. Highly structured uncertainty can also be incorporated which relate explicitly to specific coefficients within the model defined in Chapter 2. These can subsequently be extracted into a single block whose inputs and outputs are denoted by the appropriate uncertainty structure. By simply augmenting the uncertainty matrix between the signals which characterise roll stabilisation, the procedure will determine whether specified levels of performance are maintained in the presence of these uncertainties acting in concert.

The controllers of Chapter 5 and the linear robust controllers were subject to the singular value tests in order to determine their robustness properties. Unlike the H_∞ controller, the LQG and classical control techniques were revealed to be devoid of the criteria of robust stability and performance. This was confirmed by scrutiny of μ analysis procedures.

Chapter 7 investigated the roll stabilisation performance aspect of the controllers. An advanced strip theory based model of the complete ship dynamics was employed in software simulations. This model is a mutivariable system which functions in the realms of strip-theory representations of the ship.

An exhaustive series of simulations were conducted to ascertain the roll stabilisation characteristics of each controller. It was expected from the analysis of Chapter 6, that the robust controllers' roll stabilisation capabilities would exceeded that of the LQG and classical controllers. This was confirmed with the H_∞ controller achieving stabilisation levels of 70% to 80% irrespective of encounter frequency for the fin stabilisers. Although the rudder's hydrodynamic capabilities are not as potent as the fins, it was observed that the

RRS robust controller's performance, when considering all aspects, was unsurpassed. Furthermore, it is asserted that, since the fins, when operating in congress with the RRS, yields greater levels of roll stabilisation without modification to the rudder system, the primary objective of the study was attained.

The servomechanism demand signals' RMS values were also monitored. A salient feature observed is that, the robust controllers often extract significantly greater roll stabilisation from reduced actuator activity.

It is concluded that the frequency regime of the desired performance with respect to the disturbances and application of the control effort as encapsulated by the weighting functions was justified. The results presented for the robust controller are a cogent expedient for their implementation on Royal Navy frigate stabilisation systems.

The sea trials conducted represent a previously unexplored approach to roll stabilisation viz. the practical utilisation of the currently installed rudder in conjunction with the fin stabilisers. The Royal Navy permitted two sets of sea trials. The developments and preparation pertaining to these were described and the actual data presented. In general, the full-scale sea trials experience tested the reliability and versatility of all aspects of the software and hardware which was developed.

Unfortunately, the sea state remained very low throughout both trials periods. The sea induced a maximum of 2.5^0 of roll motions which will not greatly exert the controllers. Therefore, their full effectiveness cannot be appreciated. Furthermore, due to ship operations the speed remained at 12kts to 15kts, limiting the moment generating capabilities of the actuators.

Despite these unsuitable environmental conditions valuable conclusions can be derived from the trials data acquired. It was demonstrated by results of sections 7.4.1 and 7.4.2 that in low sea states the performance of the RRS did not diverge significantly from that of the fins stabilisers. Roll stabilisation levels increased when both the fins and RRS were engaged thus fulfilling the objectives of the study.

In conjunction with the advanced simulation software predictions the sea trials results implies that the performance, in terms of roll reduction, can be increased by implementing the robust type controller in both the fin and rudder loops, particularly over a very wide environmental envelope.

The fundamental conclusion which may be drawn regarding the PAT91 data and the models employed in the controller synthesis is that they are imbued with considerable confidence for future control design. This is evident since the trials results compare favourably with the PAT91 simulation data generated at the design stage. Therefore, it is concluded that the predictions of the PAT91 simulation software in terms of the roll stabilisation can be projected to higher sea states with a degree of accuracy.

The potential for using the rudders in concert with the fins as stabilisers is a practicable reality as demonstrated by the PAT91 ship motions prediction software and verified by the sea trials results. Furthermore, the novel application of linear roust controllers has been completely successful and exceed previous precedents for roll stabilisation.

8.2 RECOMMENDATIONS

Based on the conclusions regarding the sea trials and the efficacy of the various controllers some proposals were submitted to Naval Procurement (ES251) for the Future Frigate design.

The simulation studies have demonstrated unequivocally that the robust type controllers' roll stabilisation capabilities are superior in most respects. This conclusion must be further reinforced by sea trials. A strategy which may permit this at minimal cost is proposed.

A member of the ship's company be trained to operate a dedicated pc which generates fin and RRS demand signals. This would be activated in various permutations of sea conditions, ship speeds and orientations. The scheme would be operational for several months. The accumulated data would be returned to the ES251 and upon analysis of the stabilisation statistics, either reiterate the procedure with adjustments to the controllers or ensuring that the H_∞ controllers are achieving superior performance, commission the manufacturers to reconfigure the autopilot of the test ship to incorporate the RRS controllers.

Concurrently, the applicability and performance of the ASA scheme would be assessed by the pc implemented on the ship.

After, several months of further trials it is envisaged that the existing vessels be equipped with the integrated roll stabilisation scheme.

It was observed in Chapter 7 that since the ship is occasionally excited by sea wave frequencies beyond the slew rate capabilities of the rudder servomechanism to eliminate,

and considering the minimal cost that will be increased to modestly increase the slew rate, this aspect should be further pursued. The ramifications in terms of added stress on the rudder bearings should be assessed by the manufacturers.

REFERENCES

Abkowitz, M.A., (1972) "Stability and Motion Control of Ocean Vehicles", MIT Press

Allan, F.J., (1945) "The Stabilisation of Ships by Activated Fins", *Institute of Naval Architects* Vol. 87, 123-159

Amerongen, J. van (1982) "Adaptive Steering of Ships", *PhD Thesis*, Delft University of Technology

Amerongen, J. van, (1984) "Adaptive Steering of Ships - A Model Reference Approach", *Automatica*, Vol. 20, No. 1, 3-14

Amerongen, J. van and H.C. Haarman (1975) "Mathematical Modelling of Ships", *4th Ship Control Systems Symposium*, Vol. 4, 163-178

Amerongen, J.van and N. van Lemke, (1982) "Rudder Roll Stabilisation", *4th International Symposium on Ship Operation and Automation*, Genoa, 43-50

Amerongen, J.van, H.R.N. Lemke and Klugt P.G.M. van der, (1983) "Roll Stabilisation by Means of Rudder", *Proc. 3rd Yale Workshop on Applications of Adaptive Systems Theory*, 19-26

Amerongen, J.van, P.G.M. van der Klugt and J.B.M. Pieffers, (1984) "Model Test and Full-Scale Trials with a Rudder Roll Stabilisation System", *7th International Ship Control Systems Symposium*, Bethesda, Vol. 2, 95-114

Amerongen, J.van, P.G.M. van der Klugt and J.B.M. Pieffers, (1987) "Rudder Roll Stabilisation-Controller Design and Experimental Results", *8th International Ship Control Systems Symposium*, The Hague, Vol. 2, 120-142

Anderson, B.O. and J.B. Moore (1971) "Linear Optimal Control" , Prentice-Hall

Astrom, K.J. and Kallstrom, C.G., (1976) "Identification of Ship Steering Dynamics", *Automatica*, Vol. 12, 9-22

Athans, M and P.C. Falb, (1966) "Optimal Control" McGraw-Hill

Baitis, A.E., (1980) "The Development and Evaluation of a Rudder Roll Stabilisation for the WHEC Hamilton Class", *David W. Taylor Naval Ship Research and Development Centre*, Report No. NTNSRDC/SPD-0930-02

Baitis, A.E. and G.G. Cox, (1972) "The Evaluation of Vosper Active Fin Roll Stabilisers", *3rd Ship Control Systems Symposium*, Bath, Sept.

Baitis, A.E., D.A. Wollaver and T.A. Beck, (1983) "Rudder Roll Stabilisation for Coast Guard Cutters and Frigates", *Naval Engineers Journal*, May, 267-282

Baitis, A.E., T.R. Applebee and T.M. McNamara, (1984) "Human Factors Considerations Applied to Operations of the FFG-8 and LAMPS Mk II", *Naval Engineers Journal*, May, 191-199

Baitis, E.A. and L.V. Schmidt, (1989) "Ship Roll Stabilisation in the US Navy", *Naval Engineers Journal*, May, 45-53

Balas, G.J., J.C. Doyle, K. Glover, A. Packard and R. Smith, (1991) "μ–Analysis and Synthesis Toolbox: User Guide", *The Math Works*

Bass, D.W. and M.R. Haddara, (1988) "Nonlinear Models of Ship Roll Damping", *International Shipbuilding Progress*, Vol. 35, Pt. 401, 5-24

Bell, J., (1957a) "Ship Stabilisation Controls and Computation", *Institute of Naval Architects*, Vol. 99, 729-744

Bell, J., (1957b) "Ship Stabilisation : Automatic Controls Computed and Practice", *IEE, Prt B*, Vol. 104, 20-26

Bell, J., (1965) "Stabilisation to the Apparent Vertical-Measurement of Sway", *The Royal Institution of Naval Architects*, Vol. 107, 257-264

Bhattacharya, R.C., (1978) "Dynamics of Marine Vehicles", John Wiley

Bode, H.W., (1950) "Network Analysis and Feedback Amplifier Design", D. Van Nostrand

BR6509 Books of Reference, Type ** Rudder System, Ministry of Defence, Ship Department (Restricted)

BR6509 Books of Reference, Type ** Fin Stabiliser System, Ministry of Defence, Ship Department (Restricted)

Broome, D.R., (1979) "An Integrated Ship Control System for CS Manchester Challenge", *Royal Institution of Naval Architects*, 127-135

Burns, R.S., (1991) "An Optimal Control System for Pitch, Heave and Roll Stabilisation of Surface Vessels", *IEE Control '91*, Vol. 2, 833-837

Carley, J.B., and W.H. Duberley, (1972) "Design Considerations for Optimum Ship Motion Control", *3rd Ship Control Systems Symposium*, Bath

Carley, J.B., (1975) "Feasibility Study of Steering and Stabilising by Rudder", *4th Ship Control Systems Symposium*, The Hague, Vol. 2, 172-193

Chadwick, J.H., (1955) "On the Stabilisation of Roll", *The Royal Institution of Naval Architects*, 237-281

Chu, C.C., J.C. Doyle and E.B. Lee, (1986) "The General Distance Problem in H_∞ Optimal Control Theory", *Int. J. Control*, Vol. 44, 565-596

Clarke, M., (1981) "Designing a Microprocessor-Based Fin Stabiliser Control System", *6th Ship Control Systems Symposium*, Ottawa, Vol. F2, 1-15

Conolly, J.E., (1969) "Rolling and its Stabilisation by Active Fins", *The Royal Institution of Naval Architects*, Vol. 3, 21-48

Cowley, W.E. (1974) "Development of an Autopilot to Control Yaw and Roll", *The Naval Architect*, Jan, 18-19

Cowley, W.E. and T.H. Lambert, (1972) "The Use of Rudder as a Roll Stabiliser", *3rd Ship Control Systems Symposium*, Sept., Vol. C

Cowley, W.E. and T.H. Lambert, (1975) "Sea Trials on a Roll Stabiliser Using the Ship's Rudder", *4th Ship Control Systems Symposium*, The Hague, Vol. 2, 195-213

Comstock, J.P., (1967) "Principles of Naval Architecture", *Society of Naval Architects and Marine Engineers*

Conolly, J.E., (1969) "Rolling and its Stabilisation by Active Fins", *Royal Institution of Naval Architects*, Vol. 3, 21-48

Cox, G.C., and A.R.J.M. Lloyd, (1977) "Hydrodynamic Design Basis for Navy Ship Roll Motion Stabilisation", *Society of Naval Architects and Marine Engineers*, Vol. 85, 51-93

Crossland, P., (1991) "User Guide for the PAT91 Suite of Ship Motion Computer Programs", *DRA Haslar*, Report No. DRA/Mar TR91316

Crossland, P., (1992) Private Telephonic Communication, November

Crossland, P, A.J. Thomas and R. Strong, (1994) "Assessing the Effects of LFE Stabilisation on Human Performance", *International Seminar on Comfort on Board and Operability Evaluation of High Speed Marine Vehicles*, Genoa

Dallzell, J.F., (1978) "A Note on the Form of Ship Roll Damping", *Journal of Ship Research*, Vol. 22, No. 3, Sept., 178-185

Davidson, K.S.M. and L.I. Schiff, (1946) "Turning and Course Keeping Qualities", *Society of Naval Architects and Marine Engineers*, Vol. 54, 85-105

Davies, C. and R. Chase (1987) "A New Adaptive Digital Fin-stabiliser Controller", *8th Ship Control Systems Symposium*, The Hague 1987, Vol. 1, 143-159

De Heere, R.F.S. and A.R. Bakker, (1970) "Buoyancy and Stability of Ships", George G. Harrap

Doyle, J.C., (1978) "Guaranteed Margins for LQG Regulators", *IEEE Trans. on Auto. Control*, Vol. AC-23 756-757

Doyle, J.C., (1982) "Analysis of Feedback Systems with Structured Uncertainties", *IEE Proc. Prt D.*, Vol. 129 242-250

Doyle, J.C., (1985) "Structured Uncertainty in Control Systems Design", *24th IEEE Conf. on Decision and Control Prt D.*, Fort. Lauderdale, 260-265

Doyle, J.C., and G. Stein, (1981) "Multivariable Feedback Design: Concepts for a Classical/Modern Synthesis", *IEEE Trans. on Auto Control.*, Vol. AC-26, 4-16

Doyle, J.C., P. Khargonekar and B. Francis (1988) "State Space Solutions to Standard H_∞ Control Problems", *Proc. American Control Conference*, Atlanta, 1691-1696

Dunne, J.F. and A. Debonos, (1992) "Estimation of Ship Roll Parameters in Random Waves", *J. Offshore Mech. and Arctic Eng.*, Vol. 114, 114-121

Eda, H. and C.L. Crane, (1965) "Steering Characteristics in Calm Water and Waves", *Society of Naval Architects and Marine Engineers*, Vol. 173, 135-177

Flower, J.O. and W.A.K.S. Aljaff, (1981) "Fyloff-Bogoliuboff's Solution to Decaying Nonlinear Oscillations", *International Shipbuilding Progress*, Vol. 27, prt. 313, 225-230

Francis, B.A., (1988) "A Course in H_∞ Control Theory", *Lecture Notes in Information Sciences 88*, Springer-Verlag

Francis, B.A. and G. Zames, (1984) "On H_∞-Optimal Sensitivity Theory for SISO Feedback Systems", *IEEE Trans. on Auto. Control*, Vol. AC-29, 1-16

Freudenburg, J.S. and D.P. Looze, (1985) "Right Half Plane Poles and Zeros and Design Tradeoffs in Feedback Systems", *IEEE Trans. on Auto. Control*, Vol. AC-30, 555-565

Friedland, B., (1986) "Control Systems Design", McGraw-Hill

Gaston, R.R.E.De. and M.G. Safonov, (1988) "Exact Calculation of the Mulitloop Stability Margin", *IEEE Trans. on Auto. Control*, Vol. AC-33, 156-171

Gawthrop, P.J., A. Kountzeris, J.B. and Roberts, (1988) "Parametric Identification of Non-Linear Motion Forced Roll Data", *Journal of Ship Research*, Vol. 32, No. 2, 101-111

Gelb, A. and W.E.V. Velde, (1968) "Multiple-Input Describing Functions and Non-linear Systems Design", McGraw-Hill

Glover, K. and J.C. Doyle, (1988) "State-space Formulae for all Stabilising Controllers that Satisfy an H_∞ Norm Bound and Relations to Risk Sensitivity", *System and Control Letters*, Vol. 11, 167-172

Glover, K. and D. McFarlane, (1989) "Robust Stabilisation of Normalised Coprime Factor Plant Descriptions with H_∞-Bounded Uncertainty", *IEEE Trans. on Auto. Control.*, Vol. AC-34, 821-830

Graham, R., (1990) "Motion-Induced Interruptions as Ship Operability Criteria", *Naval Engineers Journal*, March, 65-71

Grimble, M.J. and M.A. Johnson, (1988) "Optimal Control and Stochastic Estimation", John Wiley

Grimble, M.J., M.R. Katebi and Y. Zhang, (1993) "H_∞ Based Ship Fin-Rudder Roll Stabilisation Design", *10th Ship Control Systems Symposium*, Ottawa, Vol. 5, 251-265

Gunsteren, F.F. van, (1974) "Analysis of Stabiliser Performance", *International Ship Building Progress*, Vol. 21, prt. 237, 125-146

Haddara, M.R. and M.A. Nassar, (1986) "A Stochastic Model for Analysis of Rolling Motion in a Realistic Seaway", *International Shipbuilding Progress*, Vol. 33, No. 384, 144-150

Haddara, M.R. and G. Bennet, (1989) "A Study of the Angle Dependence of Roll Damping Moment", *Ocean Engineering*, Vol. 16, prt. 4, 411-427

Himeno, Y., (1981) "Prediction of Ship Roll Damping", *University of Michigan, College of Naval Architecture and Marine Engineering*, Report No. Sep. '91

Hung, Y.S., (1989) "H_∞ Optimal Control: Part 1. Model Matching", *Int. J. Control, Vol.* 49, 1291-1330

Kallstrom, C.G., (1981) "Control of Yaw and Roll by a Rudder/Fin Stabilisation System", *6th Ship Control Systems Symposium*, Ottawa, Vol. F2, 1-21

Kallstrom, C.G. and Ottosson, (1982) "The Generation and Control of Roll Motions of Ship in Close Turns", *4th International Symposium on Ship Operation and Automation*, Genoa

Kallstrom, C.G. and W.L. Schultz, (1990) "An Integrated Rudder Control System for Roll Damping and Course Maintenance", *9th International Ship Control Systems Symposium*, Bethesda, Vol. 3, 278-296

Katebi, M.R. and D.K.K. Wong, (1987) "LQG Autopilot and Rudder Roll Stabilisation Control Systems Design", *8th Ship Control Systems Symposium*, The Hague, Vol. 3, 69-84

Klugt, P.G.M. van der, (1987) "Rudder Roll Stabilisation", *PhD Thesis*, Delft University of Technology, The Netherlands

Klugt, P.G.M. van der, (1990a) "Rudder Roll Stabilisation : The Dutch Solution", *Naval Engineer Journal*, May, 83-92

Klugt, P.G.M. van der, (1990b) "ASSA : The RRS Autopilot for Dutch M-Class Frigates", *9th Ship Control Systems Symposium*, Bethesda, Vol. 2, 265-275

Kreyszig, E., (1978) "Introductory Functional Analysis with Applications", John Wiley

Kwakernaak, H., and R. Sivan, (1972) "Linear Optimal Control Systems", John Wiley

Kwon, S.H. and R.C. McGregor, (1991) "A Stochastic Analysis of Rolling Motion of Ships in Irregular Waves", *1st International Offshore and Polar Eng. Conf.*, 428-433

Levinson, E, (1953) "Some Saturation Phenomena in Servomechanisms", *American Institute of Electrical Engineers*, Vol. 72, 1-9

Lloyd, A.R.J.M., (1972) "The Hydrodynamic Performance of Roll Stabiliser Fins", *3rd International Ship Control Systems Symposium*, Bath, Vol. 2, 1-18

Lloyd, A.R.J.M., (1974) "Roll Stabiliser Fins: A Design Procedure", *The Royal Intitution of Naval Architects*, 233-254

Lloyd, A.R.J.M. (1975) "Roll Stabilisation by Rudder", *4th International Ship Control Systems Symposium*, The Hague, Vol. 2, 214-241

Lloyd, A.R.J.M., (1989) "Seakeepng: Ship Behaviour in Rough Weather", Ellis Horwood

Lloyd, A.R.J.M. and P. Crossland, (1989) "Motions of Model Warship in Oblique Waves", *Royal Institution of Naval Architects*, April, 79-98

Maciejowski, J.M., (1990) "Multivariable Feedback Design", Addison-Wesley

Marshfield, W.B., (1979) "HMS ****** Rudder Servo Performance Trials", *DRA Haslar*, Report No. AMTE(H) R79042, Restricted

Marshfield, W.B., (1981a) "Auto Steering and Stabiliser Trials in HM Warships", *6th Ship Control Systems Symposium*, Ottawa, Vol. F2, 1-27

Marshfield, W.B., (1981b) "HMS ****** Roll Stabiliser Trials", *DRA Haslar*, Report No. AMTE(H) R81012, Restricted

Marshfield, W.B., (1981c) "Auto Steering and Stabiliser Trials in HM Warships", *6th International Ship Control Systems Symposium*, Ottawa, Vol. F2, 1-27

Martin, J.P., (1994) "Roll Stabilisation of Small Ships", *Marine Technology*, Vol. 31, No. 4, 286-295

McLeod, P, C. Poulton, H. du. Ross and W, Lewis, (1981) "The Influence of Ship Motion on Manual Control Skills", *Journal of Naval Science*, Vol. 7, No. 3, 202-210 (Restricted)

Monk, K., (1987) "A Warship Roll Criterion", *Royal Institution of Naval Architects*, Vol. 130, 219-240

Mort, N. (1983) "Autopilot Design For Surface Ship Steering Using Self-Tuning Controller Algorithms", *PhD Thesis*, University of Sheffield

Nomoto, K.G., K. Tagachi, T Honda and S. Hirano, (1957) "On The Steering Qualities of Ships", *International Shipbuilding Progress*, Vol. 4

Norbin, N.H., (1963) "On the Design and Analysis of the Zig-Zag Test on Base of Quasi-Linear Frequency Response", *10th International Tank Towing Conf.*, London

Ogilvie, T.F and E.O. Tuck, (1969) "A Rational Strip Theory of Ship Motions", *University of Michigan, College of Engineering*, Report No. 013

Oppenheim, A.V., A.S. Wilsky and I.T. Young (1983) "Signals and Systems", Prentice-Hall

O'Young, S.D. and B.A. Francis, (1986) "Optimal Performance and Robust Stabilisation", *Automatica*, Vol. 22, 171-183

Raven, F.H., (1978) "Automatic Control Engineering", McGraw-Hill, Singapore

Rawson, K.J. and E.C. Tupper, (1984) "Basic Ship Theory", Longman

Redheffer, M., (1960) "On A Certain Linear Fractional Transformation", *Journal of Maths and Physics*, Vol. 39, 269-286

Roberts, G.N., (1989) "Ship Motion Control Using a Multivariable Approach", *PhD Thesis*, University of Wales

Roberts, G.N. and S.W. Braham, (1990) "Warship Roll Stabilisation Using Integrated Control of Rudder and Fins", 9th *Ship Control Systems Symposium*, Bethesda, Vol. 2, 234-248

Roberts, G.N. and S.W. Braham, (1991) "A Design Study on the Control of Warship Rolling Motion Using Rudder and Stabilising Fins", *IEE Control '91*, Vol. 2, 838-843

Roberts, J.B., (1983) "Estimation of Non-linear Ship Roll Damping from Free Decay Data", *National Maritime Institute*, Report No. 164

Roberts, J.B., (1984) "Comparison Between Simulation and Theoretical Predictions for Ship Rolling in Random Beam Seas", *International Shipbuilding Progress*, July, No. 359, 168-180

Safonov, M.G., (1981) "Stability Margins of Diagonally Perturbed Multivariable Feedback Systems", *IEEE Trans. on Auto. Control*, Vol. AC-26, 93-11

Safonov, M.G. and M. Athans, (1977) "Gain and Phase Margins for Multiloop LQG Regulation", *IEEE Trans. on Auto. Control*, Vol. AC-22, 173-179

Saunders, H.E., (1965) "Hydrodynamics in Ship Design", *Society of Naval Architects and Marine Engineers*

Schmitke, R.T, (1978) "Ship Sway, Roll and Yaw Motions in Oblique Seas", *Society of Naval Architects and Marine Engineers*, Vol. 86, 26-46

Sellars, F.H. and J.P. Martin, (1992) "Selection and Evaluation of Ship Roll Stabilisation Systems", *Marine Technology*, Vol. 29, No. 2, April, 84-101

Sharif, M.T., G.N. Roberts, S. French and R. Sutton, (1993) "Lateral Force Stabilisation: A Comparison of Controller Designs", 10th *Ship Control Systems Symposium*, Ottawa, Vol. 5, 149-169

Stein, G. and M. Athans, (1987) "The LQG/LTR Procedure for Multivariable Feedback Control Design", *IEEE Trans. on Auto. Control*, Vol. AC-32, 105-115

Taggart, R., (1970) "Anomalous Behaviour of Merchant Ship Steering Systems", *Marine Technology*, Vol. 7, No. 2, 205-215

Tang, A. and P.A. Wilson, (1992a) "Lateral Force Estimator Stabilisation", *Control Applications in Marine Systems*, Genoa, 141-149

Tang, A. and P.A. Wilson, (1992b) "LFE Stabilisation Using the Rudder", *Manoeuvring and Control of Marine Craft*, Southampton, 379-392

Tang, A., P. Crossland and P.A. Wilson, (1994) "Stabilising a Frigate Using Lateral Force Estimator", *10th Ship Control Systems Symposium*, Ottawa, Vol. 3, 1-19

Tinn, S.J.O. (1970) "A Control System for Active Fin Roll Stabilisation", *Naval Engineers Journal*, Aug., 78-85

Troesch, A.W., (1981) "Sway, Roll and Yaw Motion Coefficients Based on a Forward-Speed Slender Body Theory part 1 &2", *Journal of Ship Research*, Vol. 25, No. 1, 8-20

Warhurst, F. and A.J. Cerasani, (1969) "Evaluation of the Performance of Human Operators as a Function of Ship Motion", *Naval Ship Research and Development Laboratory*, Annapolis, Report No. 21402

Whalley, R. and J.W. Westcott, (1981) "Ship Motion Control", *6th International Ship Control Systems Symposium*, Ottawa, Vol. H1, 1-16

Whalley, R. and J.W. Westcott, (1981) "Ship Motion Control", *6th Ship Control Systems Symposium*, Ottawa, Vol. H1, 1-16

Whyte, P.H., (1977) "A Note on the Application of Modern Control Theory to Ship Roll Stabilisation", *18th ATTC*, Maryland, 517-532

Wibrans, K.C.J. and P.G.M van der Klugt, (1991) "The Implementation of a Transputer Based Rudder Roll Stabilisation System", *Transputing '91*, 859-870

Yamasaki, K and F. Fasataka, (1985) "Linear Hydrodynamic Coefficients of Ship with Forward Speed During Harmonic Sway, Yaw and Roll Oscillations", *4th International Conference on Numerical Ship Hydrodynamics*, Washington, Sept., 56-70

Youla, D.C., H.A. Jabr and J.J. Bongiorno, (1976) "Modern Wiener-Hopf Design of Optimal Controllers Part II : The Multivariable Case", *IEEE Trans. on Auto. Control*, Vol. AC-21, 319-338

Young, N., (1988), "An Introduction to Hilbert Spaces", Cambridge University Press

Zames, G., (1966) "On Input-Output Stability of Time-Varying Non-linear Feedback Systems, Part 1", *IEEE Trans. on Auto. Control*, Vol. AC-11, 228-238

Zames, G., (1981) "Feedback and Optimal Sensitivity : Model Reference Transformations, Multiplicative Seminorms and Approximate Inverses", *IEEE Trans. on Auto. Control*, Vol. AC-26, 301-321

Zhou Wei-Wu, D.B. Cherchas, S. Calisal and A. Tiano, (1990) "A New Approach for Adaptive Rudder Roll Stabilisation Control", *9th Ship Control Systems Symposium*, Bethesda, Vol. 1, 115-131

APPENDIX A - ACTUATOR MOMENT CALCULATIONS

A1. Calculation for Fin Stabilisers

Lift curve slope for fins (equation 2.30)

From Comstock (1967) an empirical relationship for this quantity is derived as :

$$\frac{\partial C_L}{\partial \alpha} = \frac{1.8\pi a_e}{\cos(\Omega)\sqrt{(a_e^2 \sec^2(\Omega) + 4)} + 1.8} \qquad \text{(A1)}$$

where

a_e is the effective aspect ratio, m^2

Ω quarter chord sweep angle, (degs)

Substituting these values yields the lift curve slope as, in the free-stream

$$\left(\frac{\partial C_L}{\partial \alpha}\right)_{FS} = 0.032 \ \text{ms}^{-1} \text{ per degree of fin deflection.}$$

Fin performance degradation

The fin performance degradation can be written as :

$$\frac{\partial C_L}{\partial \alpha} = h_F(\omega_n)\left(\frac{\partial C_L}{\partial \alpha}\right)_{FS} \qquad \text{(A2)}$$

Where $h_F(\omega_\phi)$ is the degradation factor as discussed in Chapter 2 at ship's natural roll frequency.

Boundary layer loss :

$$e_{BL} = 1 - 0.5\left(\frac{\delta}{s_F}\right)\left(\frac{\partial C_L}{\partial \alpha}\right)_{FS}^{-1} \qquad \text{(A3)}$$

where

δ boundary-layer thickness = $0.377 x_{FP}(R_c)^{-0.2}$

s_F is the fin span, m

Re is local Reynolds number = $x_{FP}U\upsilon^{-1}$, (non-dimensional)

and υ kinematic viscosity for seawater at 15C = 1.191×10^{-6} ms^{-1}

x_{FP} is distance from ship forward perpendicular to fin axis, m.

the performance degradation may now be estimated with corrections for fin-induced sway and yaw motions, assuming this is negligible at ω_n and there is no bilge-fin interference,

$$h_F(\omega_n) = \frac{e_{BL}}{2} \tag{A4}$$

$$h_F(0) = h_F(\omega_n)\left[0.568 + 0.463\left(\frac{x_{F\psi}}{L}\right)\right]\left[2.279 - 0.034297\alpha_D + 0.000174\alpha_D^2\right] \tag{A5}$$

$$h_F(2\omega_n) = h_F(\omega_n)\left[1.109 - 0.080\left(\frac{x_{F\psi}}{L}\right)\right] \tag{A6}$$

where

$x_{F\psi}$ is the fin yaw moment arm about the CoG, m

α_D is the dihedral angle, rads

These values are calculated and the lift curve slope modified according to (A2). The data is presented in Table 2.1

Theoretical calculation of k_{11}

From equation (2.30) following it is apparent that the moment generating capacity is given by (A2)

$$k_{11} = \frac{\rho U^2 A_F r_F}{mg\overline{GM}}\frac{\partial C_L}{\partial \alpha} \tag{A7}$$

where

ρ seawater density, 1025 kgm^{-3}

A_F fin plane are, 5.34m^2

r_F fin moment arm, m

m tonnes, ship mass, tonnes

g gravitational acceleration, ms^{-2}

$\overline{GM}$ metacentric height, m

U is the ship speed (ms^{-1})

The moment generating value (A7) is calculated and the results are shown in Table 2.2, together with the values when fin degradation is taken into account.

A2. Calculations for Rudder Moments

Rudder lift curve slope

The rudder lift curve $\frac{\partial C_L}{\partial \delta}$, is calculated in the same manner as equation (A1). Where the aspect ratio, a_c, is 2.89, and Ω, the quarter chord sweep angle is 6.7^0. Therefore the lift curve slope is 0.0537 per degree rudder deflection.

Rudder roll generating moment and k_{12}

The hydrodynamic transverse forces are assumed to act at a depth z^* below the centre of gravity,

$$K_v = -z^* Y_v \qquad K_r = z^* Y_r \tag{A8}$$

Utilising data from lateral motions sea trials, (Lloyd, 1975) who quotes another source, shows that z^*, is frequency dependent and is assumed to be,

$$z^* = \overline{OG} + z_R T(1 + z_{R1}\omega_e^2 + z_{R2}\omega_e^3) \tag{A9}$$

where,

T is the draught, m

$\overline{OG}$ height of CoG above waterline, m

ω_e wave encounter frequency, $rads^{-1}$

$z_{R1} = 0.6$, $z_{R2} = -0.75$, $z_{R3} = 0.25$,

If it assumed that a portion of the lateral Y_δ, then

$$K_\delta = \left[(1-q)Y_\delta z^* + \frac{n_R \rho U^2 A_R r_R}{2}\frac{\partial C_L}{\partial \delta}\right] \tag{A10}$$

where

$$q = \frac{n_R \rho U^2 A_R}{2Y_\delta} \frac{\partial C_L}{\partial \delta}$$

n_R the number of rudders = 2

A_R rudder planform area, m^2

r_R roll moment arm for rudder, m

APPENDIX B - OPTIMAL CONTROL THEORY

Consider a control system described by the differential equations:

$$\dot{x} = f(x, u) \tag{B1}$$

where

$x \in \mathbb{R}^{n\times 1}$ state vector
$u \in \mathbb{R}^{m\times 1}$ control vector

It is desired to select the components of u such that the measure of the system performance, given as equation (B2) is minimised.

$$J = K[x(t_1)] + \int_{t_0}^{t_1} L[x(t), u(t)]\, dt \tag{B2}$$

where K and L are scalar functions. It assumed that t_0, t_1 and $x(t_0)$ are specified but the final state, $x(t_1)$ is unknown, which is a particular example of a wide variety of end conditions. The Pontryagin method is utilised to solve this problem. Introduce an Hamiltonian function:

$$H = L(x, u) + p^T f \tag{B3}$$

and a set of associated differential equations:

$$\begin{aligned} \dot{x}_i &= \frac{\partial H}{\partial p_i} \\ \dot{p}_i &= -\frac{\partial H}{\partial x_i} \end{aligned} \tag{B4}$$

where

$i = 1, 2, \ldots, n$
$p = [p_1, \ldots, p_n]^T$ co-state vectors

The solution to (B4) is required to satisfy the two-point boundary conditions:

$$x(t_0) = x_0, \quad p_i(t_1) = \left[\frac{\partial K}{\partial x_i}\right]_{t=t_1} \tag{B5}$$

Pontryagin's maximum principle states that equation (B2) will be minimised if u is chosen so as to maximise H.

Applying this to the linear control system:

$$\begin{aligned} \dot{x}(t) &= A(t)x(t) + B(t)u(t) \\ x(t_0) &= x_0 \end{aligned} \tag{B6}$$

with quadratic cost function:

$$J = \tfrac{1}{2}\, x^T(t_1)Mx(t_1) + \tfrac{1}{2}\int_{t_0}^{t_1} [x^T(t)Q(t)x(t) + u^T(t)R(t)u(t)]\,dt \tag{B7}$$

The Hamiltonian (B3) is:

$$H = \tfrac{1}{2}x^TQx + \tfrac{1}{2}u^TRu + p^TAx + p^TBu \tag{B8}$$

and (B4) gives:

$$\dot{p} = -Qx - A^Tp \tag{B9}$$

Setting the derivative of H in (B8) with respect to u equal to zero in order to find an extreme value, yields $Ru + B^Tp = 0$ which is:

$$u = -R^{-1}B^Tp \tag{B10}$$

Equations (B6) and (B9) then become:

$$\begin{aligned} \dot{x} &= Ax - BR^{-1}B^Tp \\ \dot{p} &= -Qx - A^Tp \end{aligned} \tag{B11}$$

with boundary conditions:

$$x(t_0) = x_0, \quad p(t_1) = Mx(t_1) \tag{B12}$$

It can be shown that the unique optimal control is obtained by setting $p(t) = P(t)x(t)$, where $P(t)$ is a symmetric matrix. Substitution into (B11) yields:

$$\dot{P}x + P(Ax - BR^{-1}B^TPx) = -Qx - A^TPx$$

which must hold for all $x(t)$, showing that $P(t)$ satisfies

$$\dot{P} = PBR^{-1}B^Tp - A^TP - PA - Q \qquad \text{(B13)}$$

with boundary conditions obtained from (B12) as $P(t_1) = M$. Thus the quadratic performance index (B7) leads to linear feedback:

$$u = -R^{-1}(t)B^T(t)P(t)x(t)$$

where $P(t)$ is the unique positive definite solution of the Ricatti equation (B13) satisfying the conditions. The minimum value of (B7) is then $\frac{1}{2}x_0^TP(t_0)x_0$. Further information may be found in Athans and Falb (1966).

References

Athans, M. and P.L. Falb, (1966) "Optimal Control", *McGraw-Hill*, New-York

APPENDIX C - STATE SPACE DESCRIPTION OF LFE MODEL

The state space description takes the form

$$\begin{aligned} \dot{x} &= Ax + Bu + b\eta \\ y &= Cx + Du \end{aligned} \tag{C1}$$

see Appendix B for nomenclature.

The various state space representations of the sub-systems of the LFE dynamics are listed and then combined to synthesise the complete model of Figure 4.5.

Sea disturbance (Bretschneider representation, equation (2.45))

$$\begin{aligned} A_{sea} &= \begin{bmatrix} 0 & 1 \\ -\omega_e^2 & -0.1\omega_e \end{bmatrix} & B_{sea} &= \begin{bmatrix} 0 \\ 1 \end{bmatrix} \\ C_{sea} &= \begin{bmatrix} 0 & \omega_e^2 \end{bmatrix} & D_{sea} &= [0] \end{aligned} \tag{C2}$$

Sea-roll transfer function

Yields roll disturbing moment.

$$\begin{aligned} A_{g11} &= \begin{bmatrix} 0 & 1 \\ -\omega_n^2 & -2\zeta_s\omega_n \end{bmatrix} & B_{g11} &= \begin{bmatrix} 0 \\ 1 \end{bmatrix} \\ C_{g11} &= \begin{bmatrix} 0 & k11\omega_n^2 k \end{bmatrix} & D_{g11} &= [0] \end{aligned} \tag{C3}$$

Sea-sway disturbance

Sea induced sway for contribution to unstabilised LFE.

$$\begin{aligned} A_{ss} &= \begin{bmatrix} 0 & 1 \\ -1.2 & -2.3 \end{bmatrix} & B_{ss} &= \begin{bmatrix} 0 \\ 1 \end{bmatrix} \\ C_{ss} &= \begin{bmatrix} 1.057k_{sw} & 0 \end{bmatrix} & D_{ss} &= [0] \end{aligned} \tag{C4}$$

where

$k_{sw} = 1.22$

Rudder-roll, g12(s)

$$\begin{aligned} A_{g12} &= \begin{bmatrix} 0 & 1 & 0 \\ 0 & 0 & 1 \\ -0.0305 & -0.28 & -0.372 \end{bmatrix} & B_{g12} &= \begin{bmatrix} 0 \\ 0 \\ 1 \end{bmatrix} \\ C_{g12} &= \begin{bmatrix} 0.0305k_{12} & -k_{12}0.1372 & 0 \end{bmatrix} & D_{g12} &= [0] \end{aligned} \tag{C5}$$

Rudder-sway, g32(s)

$$A_{g32} = \begin{bmatrix} 0 & 1 \\ -0.004225 & -0.13 \end{bmatrix} \quad B_{g32} = \begin{bmatrix} 0 \\ 1 \end{bmatrix}$$
$$C_{g32} = \begin{bmatrix} 0.004225k_{32} & 0 \end{bmatrix} \quad D_{g32} = [0] \qquad \text{(C6)}$$

where

k_{32}=9.596

Unstabilised roll acceleration

The roll acceleration is achieved by double differentiation. However, there was a requirement for poles to be introduced necessitated by simulation technicalities. These were placed at a high frequency location and affords low-pass filtering. The resulting system emulates a double differentiation at the frequency range of interest.

$$A_{g11a} = \begin{bmatrix} 0 & 1 \\ -420 & -41 \end{bmatrix} \quad B_{g11a} = \begin{bmatrix} 0 \\ 1 \end{bmatrix}$$
$$C_{g11a} = \begin{bmatrix} gz_B k_{dr} 420 - k_z k_{dr} 420^2 & -k_{dr} k_z 17200 \end{bmatrix} \quad D_{g11a} = [0] \qquad \text{(C7)}$$

where

g	gravitational acceleration, 9.81 ms^{-2}
z_B	vertical height to weather-deck directly above the CoG, 5.85 m
k_z	scaling factor, 1.846
k_{dr}	degree to radian conversion factor

Sway acceleration

Again poles placed in order to achieve low pass filtering.

$$A_{sa1} = \begin{bmatrix} 0 & 1 \\ -506 & -45 \end{bmatrix} \quad B_{sa1} = \begin{bmatrix} 0 \\ 1 \end{bmatrix}$$
$$C_{sa1} = \begin{bmatrix} -256036 & -227700 \end{bmatrix} \quad D_{sa1} = [0] \qquad \text{(C8)}$$

Stabilised roll

Output of the stabilised LFE and roll transfer functions, with high frequency poles for filtering.

$$A_{g11b} = \begin{bmatrix} 0 & 1 \\ -600 & -49 \end{bmatrix} \quad B_{g11b} = \begin{bmatrix} 0 \\ 1 \end{bmatrix}$$
$$C_{g11b} = \begin{bmatrix} gz_B k_{dr} 600 - 600^2 k_z k_{dr} & -29400 k_z k_{dr} \end{bmatrix} \quad D_{g11b} = [0] \qquad \text{(C9)}$$

Rudder sway acceleration

$$A_{a2} = \begin{bmatrix} 0 & 1 \\ -702 & -53 \end{bmatrix} \qquad B_{a2} = \begin{bmatrix} 0 \\ 1 \end{bmatrix}$$
$$C_{a2} = \begin{bmatrix} -492804 & -37206 \end{bmatrix} \quad D_{a2} = [0] \tag{C10}$$

The complete system is given by:

$$A = \begin{bmatrix}
A_{sea} & 0\ 0 & 0\ 0 & 0\ 0\ 0 & 0\ 0 & 0\ 0 & 0\ 0 & 0\ 0 & 0\ 0 \\
 & 0\ 0 & 0\ 0 & 0\ 0\ 0 & 0\ 0 & 0\ 0 & 0\ 0 & 0\ 0 & 0\ 0 \\
A_{sg11} & A_{g11} & 0\ 0 & 0\ 0\ 0 & 0\ 0 & 0\ 0 & 0\ 0 & 0\ 0 & 0\ 0 \\
 & & 0\ 0 & 0\ 0\ 0 & 0\ 0 & 0\ 0 & 0\ 0 & 0\ 0 & 0\ 0 \\
A_{sssea} & 0\ 0 & A_{ss} & 0\ 0\ 0 & 0\ 0 & 0\ 0 & 0\ 0 & 0\ 0 & 0\ 0 \\
 & 0\ 0 & & 0\ 0\ 0 & 0\ 0 & 0\ 0 & 0\ 0 & 0\ 0 & 0\ 0 \\
0\ 0 & & 0\ 0 & & 0\ 0 & 0\ 0 & 0\ 0 & 0\ 0 & 0\ 0 \\
0\ 0 & A_{dist} & 0\ 0 & A_{g12} & 0\ 0 & 0\ 0 & 0\ 0 & 0\ 0 & 0\ 0 \\
0\ 0 & & 0\ 0 & & 0\ 0 & 0\ 0 & 0\ 0 & 0\ 0 & 0\ 0 \\
0\ 0 & 0\ 0 & 0\ 0 & 0\ 0\ 0 & & 0\ 0 & 0\ 0 & 0\ 0 & 0\ 0 \\
0\ 0 & 0\ 0 & 0\ 0 & 0\ 0\ 0 & A_{g32} & 0\ 0 & 0\ 0 & 0\ 0 & 0\ 0 \\
0\ 0 & 0\ 0 & 0\ 0 & 0\ 0\ 0 & 0\ 0 & & 0\ 0 & 0\ 0 & 0\ 0 \\
0\ 0 & 0\ 0 & 0\ 0 & 0\ 0\ 0 & 0\ 0 & A_{g11a} & 0\ 0 & 0\ 0 & 0\ 0 \\
0\ 0 & 0\ 0 & A_{sa1d1} & 0\ 0\ 0 & 0\ 0 & 0\ 0 & & 0\ 0 & 0\ 0 \\
0\ 0 & 0\ 0 & & 0\ 0\ 0 & 0\ 0 & 0\ 0 & A_{sa1} & 0\ 0 & 0\ 0 \\
0\ 0 & 0\ 0 & 0\ 0 & & 0\ 0 & 0\ 0 & 0\ 0 & & 0\ 0 \\
0\ 0 & 0\ 0 & 0\ 0 & A_{g11bg12} & 0\ 0 & 0\ 0 & 0\ 0 & A_{g11b} & 0\ 0 \\
0\ 0 & 0\ 0 & A_{ssa2} & 0\ 0\ 0 & A_{g32a2} & 0\ 0 & 0\ 0 & 0\ 0 & \\
0\ 0 & 0\ 0 & & 0\ 0\ 0 & & 0\ 0 & 0\ 0 & 0\ 0 & A_{a2}
\end{bmatrix} \tag{C11}$$

$$B = \begin{bmatrix} 0 & \\ 0 & B_{sea} \\ 0 & 0 \\ 0 & 0 \\ 0 & 0 \\ 0 & 0 \\ & 0 \\ B_{g12} & 0 \\ & 0 \\ B_{g32} & 0 \\ & 0 \\ 0 & 0 \\ 0 & 0 \\ 0 & 0 \\ 0 & 0 \\ 0 & 0 \\ 0 & 0 \\ 0 & 0 \\ 0 & 0 \end{bmatrix}$$

$$C = \begin{bmatrix} C_{sea} & 0\ 0 & 0\ 0 & 0\ 0\ 0 & 0\ 0 & 0\ 0 & 0\ 0 & 0\ 0 & 0\ 0 \\ 0\ 0 & -C_{g11}k_{12} & C_{ss}k_{13} & 0\ 0\ 0 & 0\ 0 & -C_{g11a} & C_{sa1} & 0\ 0 & 0\ 0 \\ 0\ 0 & 0\ 0 & C_{ss}k_{23} & -C_{g12}k_{25} & C_{g32}k_{26} & 0\ 0 & 0\ 0 & -C_{g11b} & C_{a2} \\ 0\ 0 & C_{g11} & 0\ 0 & 0\ 0\ 0 & 0\ 0 & 0\ 0 & 0\ 0 & 0\ 0 & 0\ 0 \\ 0\ 0 & 0\ 0 & 0\ 0 & C_{g12} & 0\ 0 & 0\ 0 & 0\ 0 & 0\ 0 & 0\ 0 \\ 0\ 0 & 0\ 0 & C_{ss} & 0\ 0\ 0 & 0\ 0 & 0\ 0 & 0\ 0 & 0\ 0 & 0\ 0 \\ 0\ 0 & 0\ 0 & 0\ 0 & 0\ 0\ 0 & C_{g32} & 0\ 0 & 0\ 0 & 0\ 0 & 0\ 0 \end{bmatrix}$$

$$D = \begin{bmatrix} 0\ 0\ 0\ 0\ 0\ 0\ 0 \\ 0\ 0\ 0\ 0\ 0\ 0\ 0 \end{bmatrix}^T$$

where

$A_{sg11}=B_{g11}C_{sea}$

$A_{sssea}=B_{ss}C_{sea}$

$A_{g11ag11}=B_{g11a}C_{g11}$

$A_{sa1d1}=B_{sa1}C_{ss}$

$A_{g11bg12}=B_{g11b}C_{g12}$

$A_{g32a2}=B_{a2}C_{g32}$

$A_{ssa2}=B_{a2}C_{ss}$

$k_{12}=420*k_{dr}k_z$

$k_{13}=506$

$k_{25}=600k_z k_{dr}$

$k_{26}=702$

$k_{23}=702$

$$A_{dist} = \begin{bmatrix} 0 & 1 \\ 0 & 0 \\ 0 & 0 \end{bmatrix}$$

k_{13}, k_{25}, k_{26}, and k_{23}, arise on account of the requirement for low-pass filtering of the acceleration of the roll signal in order to normalise the magnitudes.

The output of the system may be described as :

$$Y = \begin{bmatrix} \text{Sea disturbance} \\ \text{Unstabilised LFE Motion} \\ \text{Stabilised LFE Motion} \\ \text{Unstabilised Roll} \\ \text{Stabilised Roll} \\ \text{Unstabilised Sway} \\ \text{Stabilised Sway} \end{bmatrix}$$

APPENDIX D - STATE SPACE DESCRIPTION OF RRS/FIN STABILISATION MODEL

The state space representation is of Figure 2.18.

$$A = \begin{bmatrix} 0 & 1 & 0 & 0 & 0 & 0 & 0 & 0 & 0 \\ -\omega_e^2 & -0.1\omega_e & 0 & 0 & 0 & 0 & 0 & 0 & 0 \\ 0 & 0 & 0 & 1 & 0 & 0 & 0 & 0 & 0 \\ 0 & \omega_e^2 G & \omega_n^2 & -2\zeta_s\omega_n & 0 & 0 & 0 & 0 & 0 \\ 0 & 0 & 0 & 0 & 0 & 1 & 0 & 0 & 0 \\ 0 & 0 & 0 & 0 & -\omega_n^2 & -0.334\omega_n & 0 & 0 & 0 \\ 0 & 0 & 0 & 0 & 0 & 0 & 0 & 1 & 0 \\ 0 & 0 & 0 & 0 & 0 & 0 & 0 & 0 & 1 \\ 0 & 0 & 0 & 0 & 0 & 0 & \frac{\omega_n^2}{8.2} & \frac{-\omega_n(2\zeta_s+8.2\omega_n)}{8.2} & \frac{-(1+16.4\zeta_s\omega_n)}{8.2} \end{bmatrix}$$

$$B = \begin{bmatrix} 0 & 0 & 0 & 0 & 0 & 1 & 0 & 0 & 0 \\ 0 & 0 & 0 & 0 & 0 & 0 & 0 & 0 & 1 \\ 0 & 1 & 0 & 0 & 0 & 0 & 0 & 0 & 0 \end{bmatrix}^T$$

$$C = \begin{bmatrix} 0 & 0 & \omega_n^2 k_{11} & 0 & \omega_n^2 k_{11} & 0 & \frac{\omega_n^2 k_{12}}{8.2} & \frac{-\omega_n^2 k_{12} 4.5}{8.2} & 0 \\ 0 & 0 & \omega_n^2 k_{11} & 0 & 0 & 0 & 0 & 0 & 0 \end{bmatrix}$$

$$D = \begin{bmatrix} 0 & 0 & 0 \\ 0 & 0 & 0 \end{bmatrix}$$

where

$$C = \begin{bmatrix} \phi_s \\ \phi \end{bmatrix}$$

APPENDIX E - NON-MINIMUM PHASE RESTRICTIONS

It is known that, non-minimum phase systems can cause difficulty in the design of a controller (Bode, 1950). The rudder roll transfer function, g12(s), equation (2.36), is such a system. Its performance limitations and constraints are briefly discussed.

Let L(s) denote the open loop transfer function, with the controller, K(s), and plant, P(s) connected in series, which contains all the non-minimum phase zeros, $Z=\{z_i ;i=1,..,N_z\}$. Thus observability and controllability is assured as dictated by the requirements for internal stability. Defining the Blaschke product as (Francis and Zames, 1984):

$$B(s) = \prod_{i=1}^{N_z} \frac{z_i - s}{z_i + s} \tag{E1}$$

It is possible to factor L(s),

$$L(s) = L_m(s)B(s) \tag{E2}$$

such that

$$|L(s)| = |L_m(s)| \qquad \text{and} \qquad \arg\left(\frac{z_i - j\omega}{z_i + j\omega}\right) \to -180^o;\text{as } \omega \to \infty \tag{E3}$$

and $L_m(s)$ is proper, rational and does not contain any of the rhp zeros of the plant.

An obvious theoretical constraint is imposed by the non-minimum phase zero on the sensitivity function, equation (5.1). If it is evaluated at the location of the zero, $s = z_i$, then, $S(z_i) = 1$. Therefore, the controller will permit disturbances to propagate through the system unattenuated. However, in reality the sensitivity function is evaluated along the jω-axis.

Therefore, the design trade-off imposed by the non-minimum phase zeros can be interpreted with physical significance.

The value of any function say, S(s), at any point z = x+jy in the complex plane can be recovered from the values of S(jω) via the Poisson integral formula:

$$S(s) = \frac{1}{\pi}\int_{-\infty}^{\infty} S(j\omega)\frac{x}{x^2 + (y-\omega)^2}d\omega \qquad \text{(E4)}$$

Since the sensitivity function is constrained below unity, in order to achieve disturbance rejection, then it yields an integral constraint on S(s) as demonstrated by the Poisson integral formula. If the plant has, in addition, non-minimum phase zeros and is stable then the integral constraint of Theorem 5.1 also results on the sensitivity function by utilising equation (E4)

Theorem E.1 : If the open loop transfer function, L(s), has a zero at s = x+jy, x>0. Then S(s) must satisfy (Bode, 1950, and Freudenberg and Looze, 1985)

$$\int_0^{\infty} \log(|S(j\omega)|)W(z,\omega)d\omega = 0 \qquad \text{(E5)}$$

where W(z,ω) is a weighting function. For real non-minimum phase zeros such as in g12(s)

$$W(x,\omega) = \frac{2x}{x^2 + \omega^2} \qquad \text{(E6)}$$

where x = 0.117 for g12(s). □

The integral relation (E5) implies the existence of trade-offs. Since $W(z,\omega) > 0$, $\forall\omega$, then

requiring $\log|S(j\omega)| < 0$ over the frequency range of interest (i.e. achieving sea disturbance attenuation) necessitates $\log|S(j\omega)| > 0$ in other frequency r anges. The severity of this trade-off is a function of the phase lag contributed by the zero directly at the frequencies where sensitivity attenuation is desired. The additional phase lag contributed by a real non-minimum phase zero is:

$$\Theta(x,\omega) = \arg\frac{x-j\omega}{x+j\omega} \tag{E7}$$

The weighting function, W(z,ω), may be used to evaluate the weighted length of a frequency interval. If the sensitivity function is required to be minimised over the range $\Omega=[\omega_L,\omega_H]$, $(\omega_L<\omega_H)$ which contain the sea disturbances, then the weighted length, for a real zero, may be given by a modified version from Freudenberg and Looze (1985) which is required presently:

$$W(x,\Omega) = \int_0^{\omega_H} W(x,\omega)\,d\omega - \int_0^{\omega_L} W(x,\omega)\,d\omega = -[\Theta(x,\omega_H)-\Theta(x,\omega_L)] \tag{E8}$$

The integral constraint (E5) may be employed to obtain lower bounds on the peak of the sensitivity function which necessarily accompanies the reduction achieved over the frequency interval Ω (Francis and Zames, 1984). Given that S(s) is to satisfy an upper bound on the interval:

$$|S(j\omega)| \le \varepsilon < 1,\ \omega \in \Omega \tag{E9}$$

and defining the maximum gain of the sensitivity function as:

$$\|S\|_\infty = \sup_{\omega\ge 0}|S(j\omega)| \tag{E10}$$

yields the following:

Corollary E.1 : Assuming that a controller, K(s), has satisfied the upper bound (E9) then the integral (E5) may be used to evaluate a lower bound on (E10) for the non-minimum phase zero.

$$\|S\|_\infty \geq \left(\frac{1}{\varepsilon}\right)^{\frac{W(z,\Omega)}{\pi - W(z,\Omega)}} \tag{E11}$$

where W(z,Ω) is given by (E8). □

Proof : From (E5), modified from (Francis and Zames, 1984), since $|S(j\omega)| \leq \varepsilon$ by (E9) and $|S(j\omega)| < \|S\|_\infty$, $\omega \notin \Omega$

$$\begin{aligned} 0 &= \int_0^{\omega_L} \log|S(j\omega)|W(z,\omega)\,d\omega + \int_{\omega_L}^{\omega_H} \log|S(j\omega)|W(z,\omega)\,d\omega + \int_{\omega_H}^{\infty} \log|S(j\omega)|W(z,\omega)\,d\omega \\ &\leq 2\log(\varepsilon)W(z,\Omega) + \log(\|S\|_\infty)(\pi - W(z,\Omega)) \end{aligned} \tag{E12}$$

Inequality (E12) follows by taking exponents of (E5) and rearranging. □

The weighted length of interval is simply the reverse polarity phase lag contributed by the zero at the upper endpoint of Ω. Since $\omega_H \to \infty$, $W(z,\Omega) \to \pi$ hence the exponent in (E11) becomes unbounded resulting in the sensitivity function becoming extremely large. Thus requiring the sensitivity function to be less than unity in a particular frequency range where the non-minimum phase zero contributes phase lag implies that there will exist large peaks at higher and lower frequency regions. If the zero is located outside the range of where sensitivity is to be minimised then it may marginally impede the performance obtained.

Considering the RRS loop, g12(s), introduces a non-minimum phase zero at $\omega = 0.117$ rads^{-1}. Fortunately, the envisaged frequency spectrum where sea disturbance predominates is in the range $0.2<\omega<2$ rads^{-1}. Hence, the non-minimum phase zero of g12(s) may, to some extent, limit the sensitivity reduction achieved at the lower encounter frequencies. This will

be manifest in large peaks in the sensitivity function at these locations as shall be demonstrated in consideration of the controller sensitivity functions.

APPENDIX F - TRANSFER FUNCTIONS OF H_∞ CONTROLLERS

Fin Loop

12kts

$$g_{CF}(s) = \frac{178.6s^5 + 1785900s^4 + 381538s^3 + 645577s^2 + 4631.7s + 0.18}{s^6 + 219.1s^5 + 6475.6s^4 + 3258.1s^3 + 2352.2s^2 + 44s + 0.2} \quad \text{(F1)}$$

18kts

$$g_{CF}(s) = \frac{13.4s^5 + 2165635s^4 + 450169s^3 + 780266s^2 + 1130s + 0.028}{s^6 + 191.8s^5 + 8221s^4 + 5967s^3 + 2967s^2 + 28.3s + 0.059} \quad \text{(F2)}$$

26kts

$$g_{CF}(s) = \frac{85.9s^5 + 1375298s^4 + 286060s^3 + 49555s^2 + 781s + 0.19}{s^6 + 156.6s^5 + 5746s^4 + 2842s^3 + 2072s^2 + 22.9s + 0.057} \quad \text{(F3)}$$

RRS Loop

12kts

$$g_{CR}(s) = \frac{s^6 + 54.3s^5 + 29.5s^4 + 6.7s^3 + 20.8s^2 + 4.5s + 0.25}{s^9 + 7.1s^8 + 20.1s^7 + 34.0s^6 + 23.9s^5 + 13.8s^4 + 4.3s^3 + 0.54s^2 + 0.02s + 0.0004} \quad \text{(F4)}$$

18kts

$$g_{CR}(s) = \frac{0.56s^6 + 100.1s^5 + 137.9s^4 + 14.3s^3 + 68.9s^2 + 9.88s + 0.22}{s^9 + 12.48s^8 + 37.7s^7 + 71.0s^6 + 42.6s^5 + 26.7s^4 + 6.3s^3 + 0.7s^2 + 0.03s + 0.004} \quad \text{(F5)}$$

26kts

$$g_{CR}(s) = \frac{7.5s^6 + 149.5s^5 + 90.7s^4 + 9.88s^3 + 55.8s^2 + 8.2s + 1.7}{s^9 + 23.9s^8 + 178.6s^7 + 583.6s^6 + 333.4s^5 + 242.4s^4 + 56.1s^3 + 5.9s^2 + 0.26s + 0.004} \quad \text{(F6)}$$

APPENDIX G - SIMULATION STUDIES DATA

RRS Only - Ship speed 12 kts - Percentage roll reduction graphs

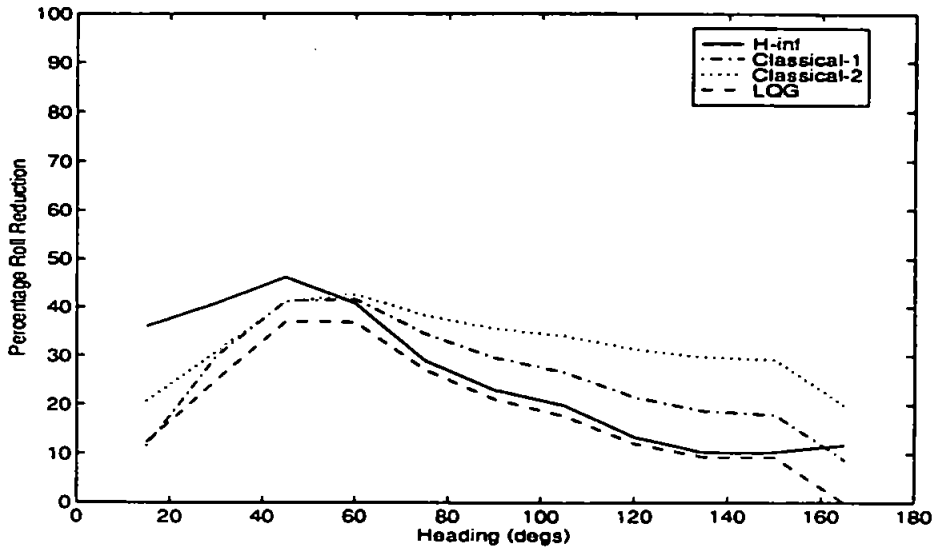

Figure G1 : Sea State 3

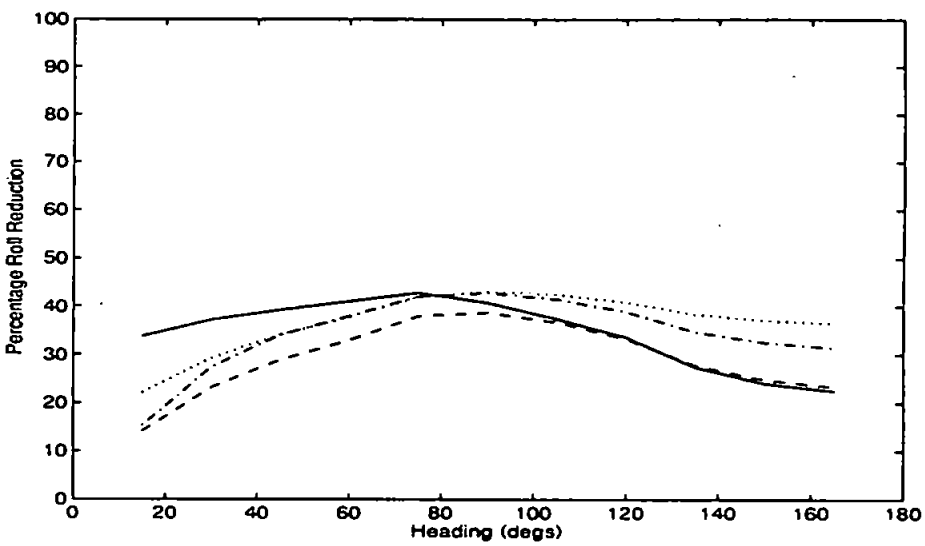

Figure G2 : Sea State 5

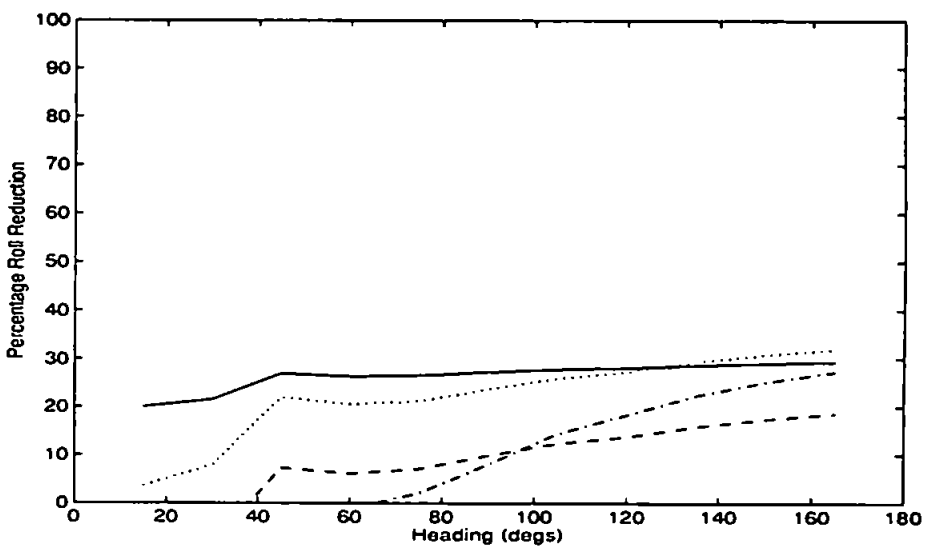

Figure G3 : Sea State 8

RRS Only - Ship speed 12 kts - RMS rudder activity

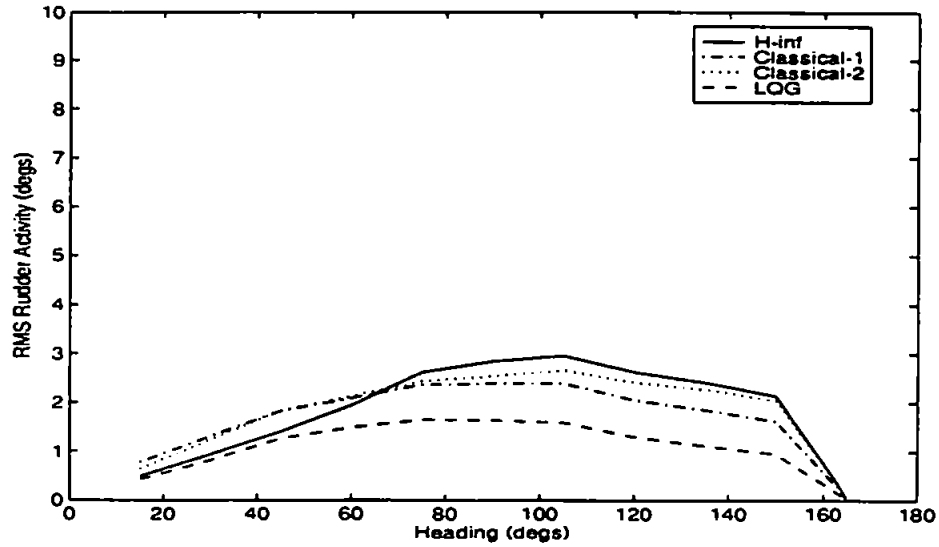

Figure G4 : Sea State 3

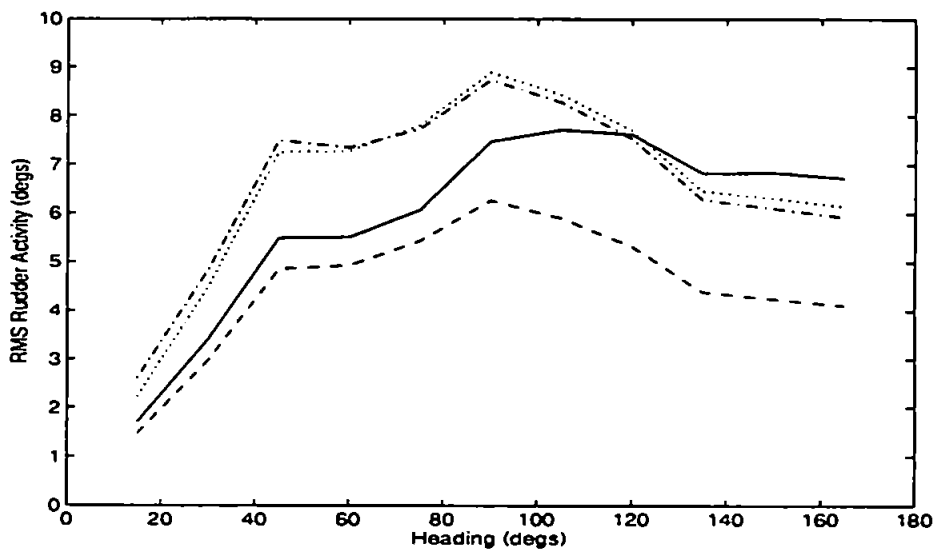

Figure G5 : Sea State 5

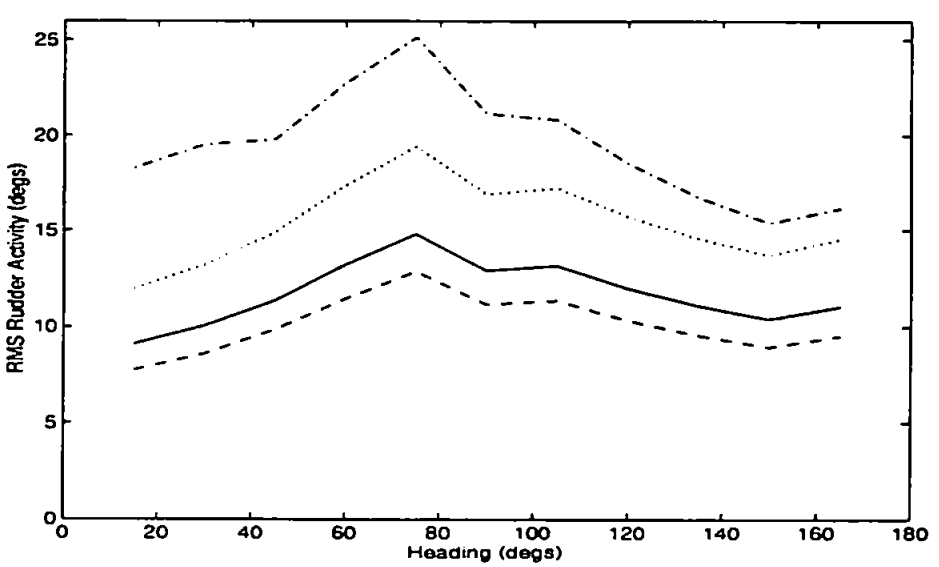

Figure G6 : Sea State 8

RRS Only - Ship speed 18 kts - Percentage roll reduction graphs

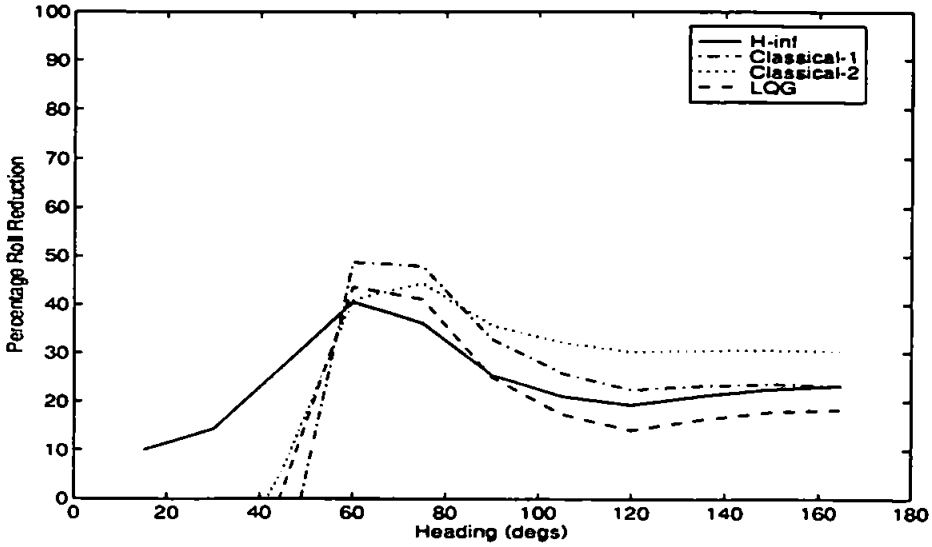

Figure G7 : Sea State 3

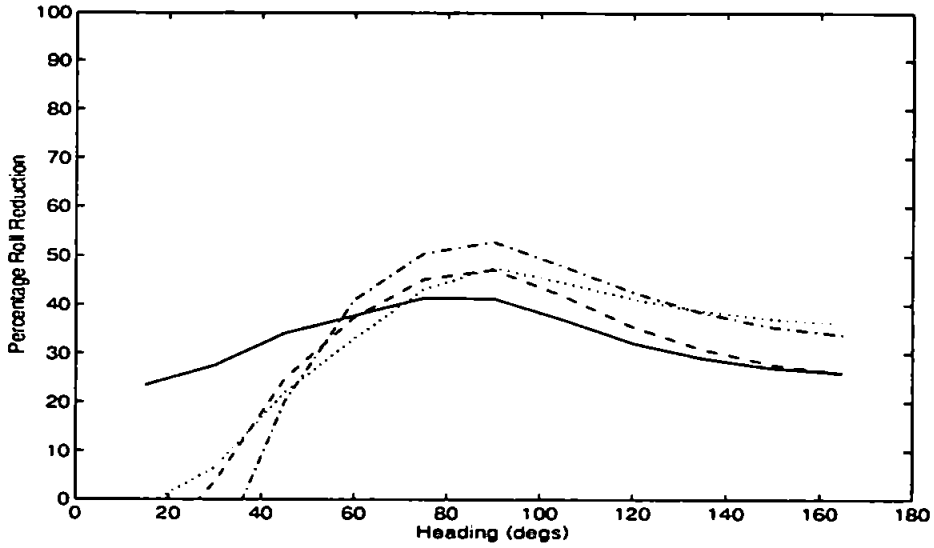

Figure G8 : Sea State 5

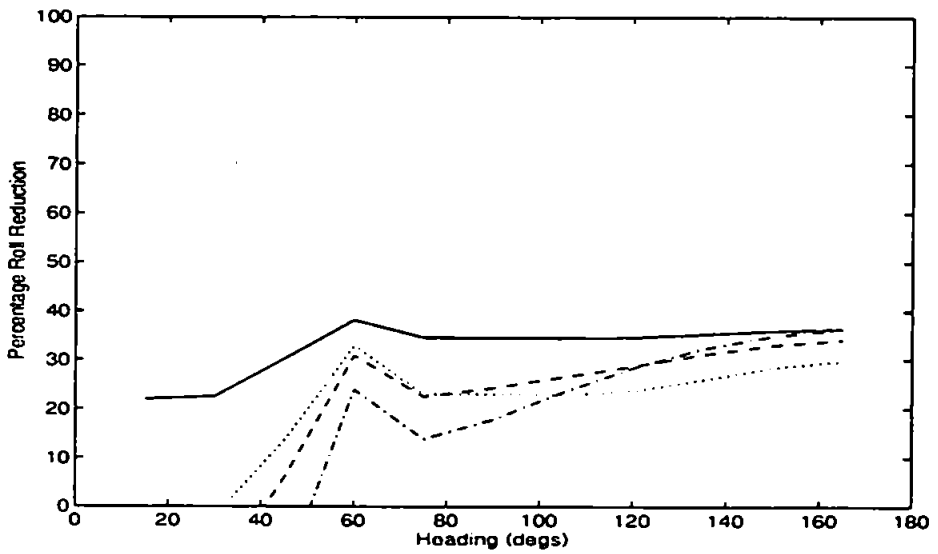

Figure G9 : Sea State 8

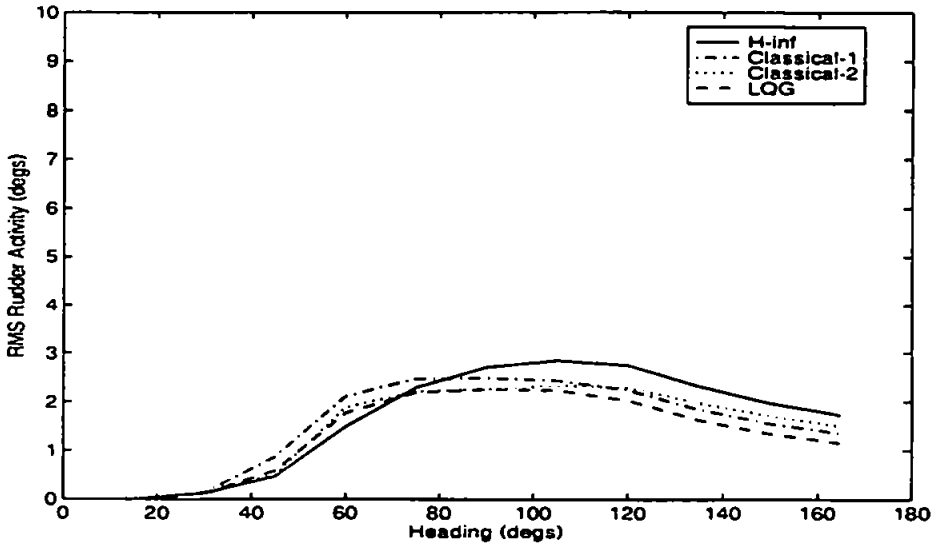

Figure G10 : Sea State 3

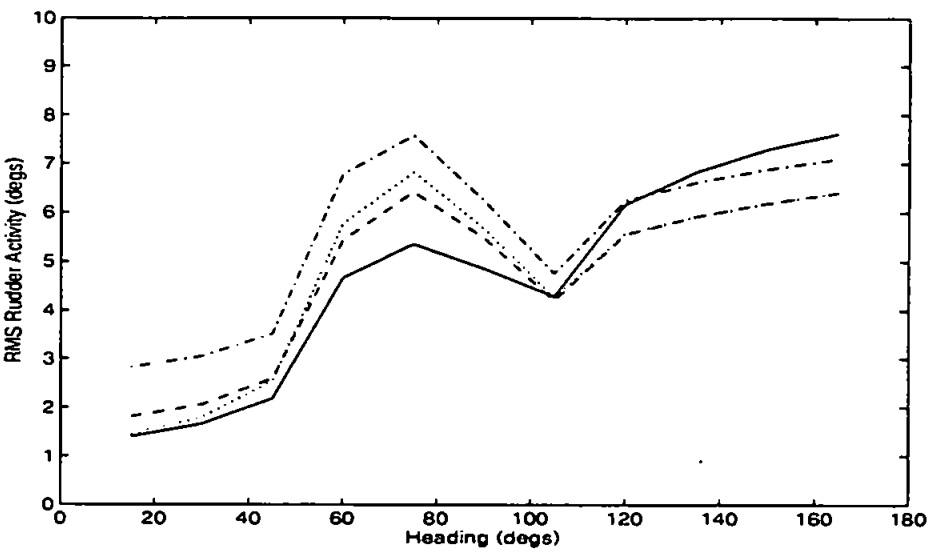

Figure G11 : Sea State 5

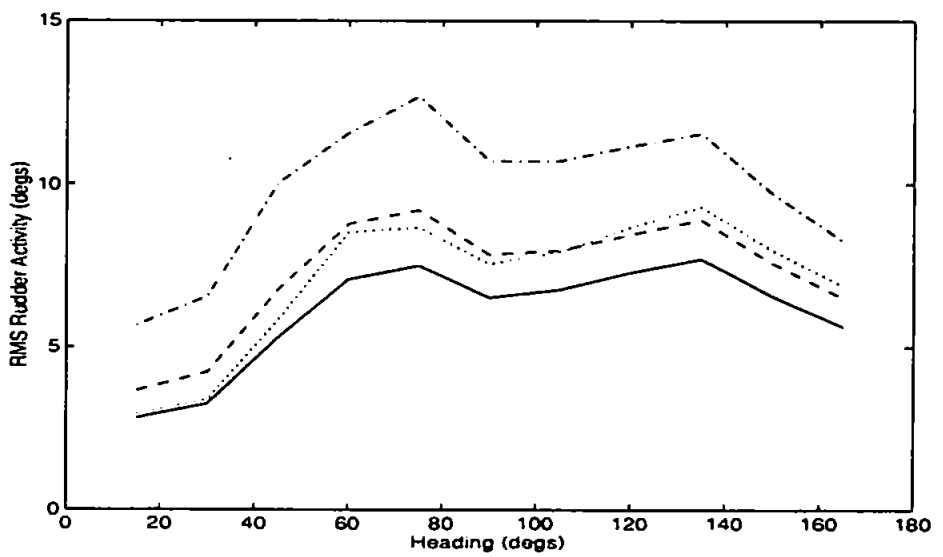

Figure G12 : Sea State 8

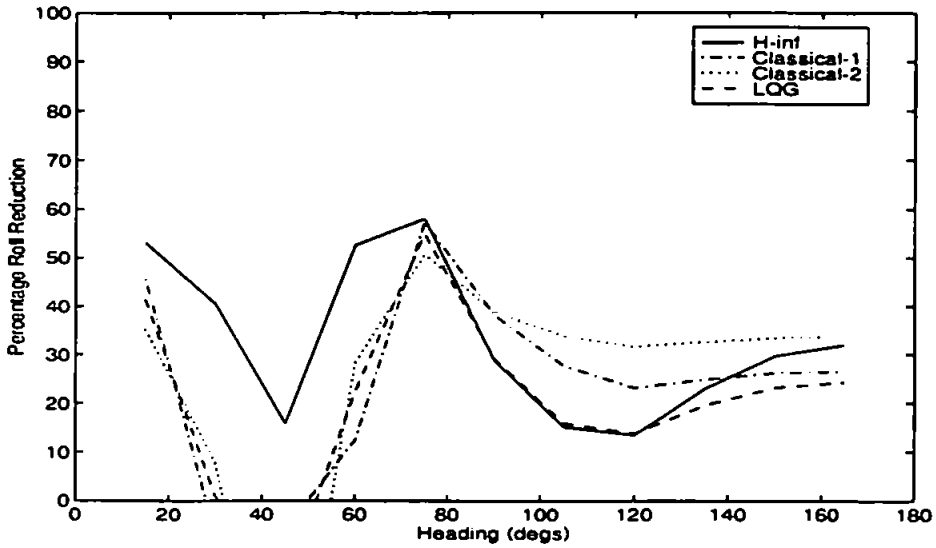

Figure G13 : Sea State 3

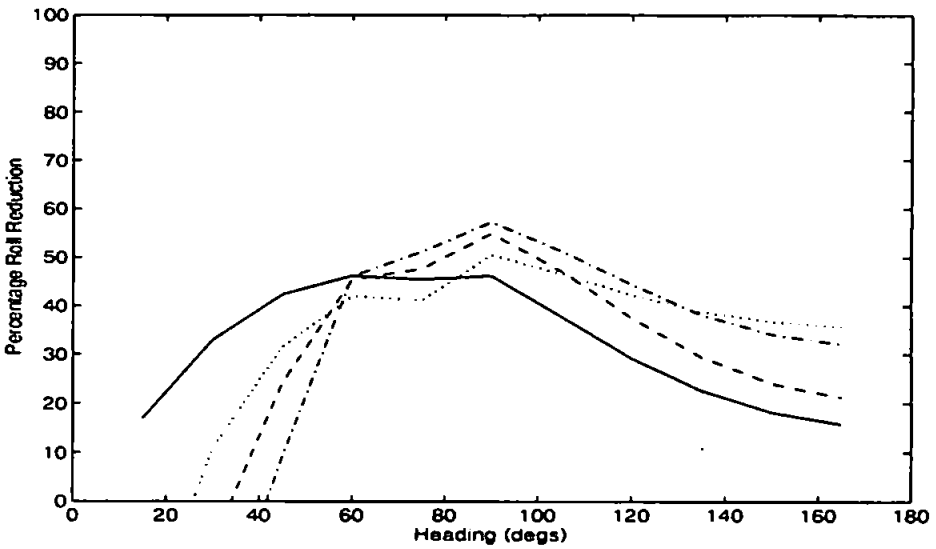

Figure G14 : Sea State 5

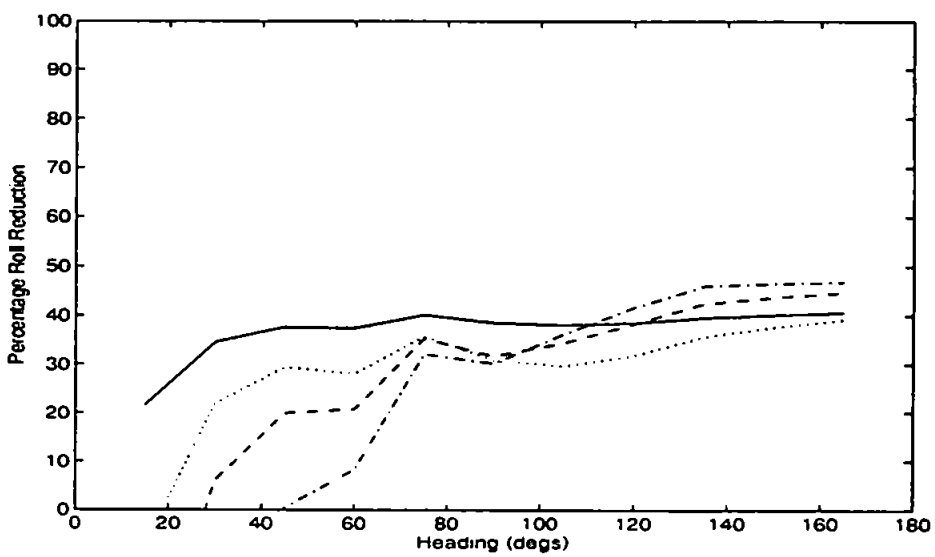

Figure G15 : Sea State 8

RRS Only - Ship speed 26 kts - RMS rudder activity

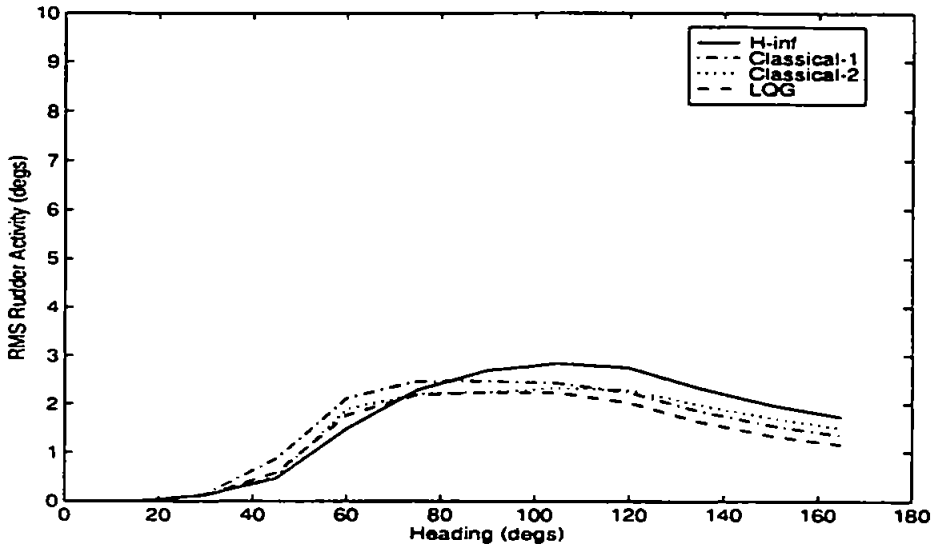

Figure G16 : Sea State 3

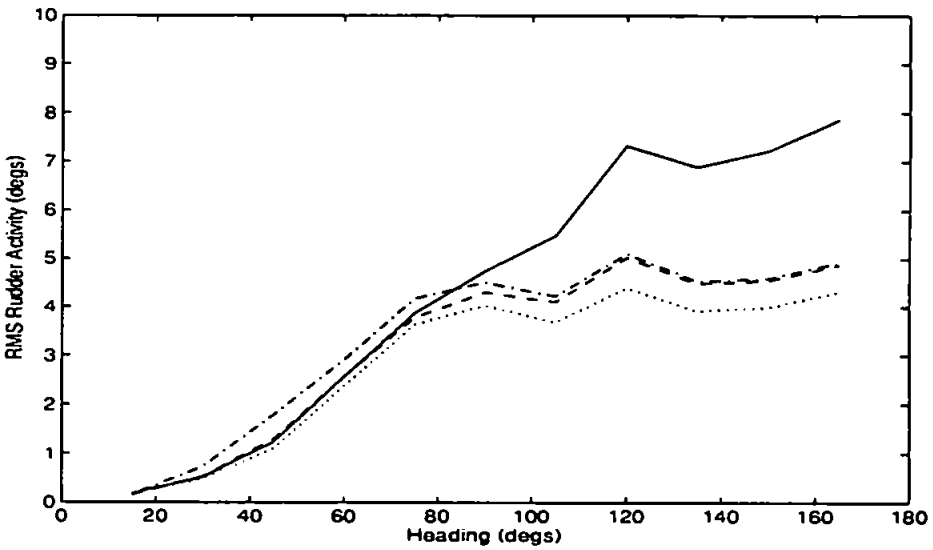

Figure G17 : Sea State 5

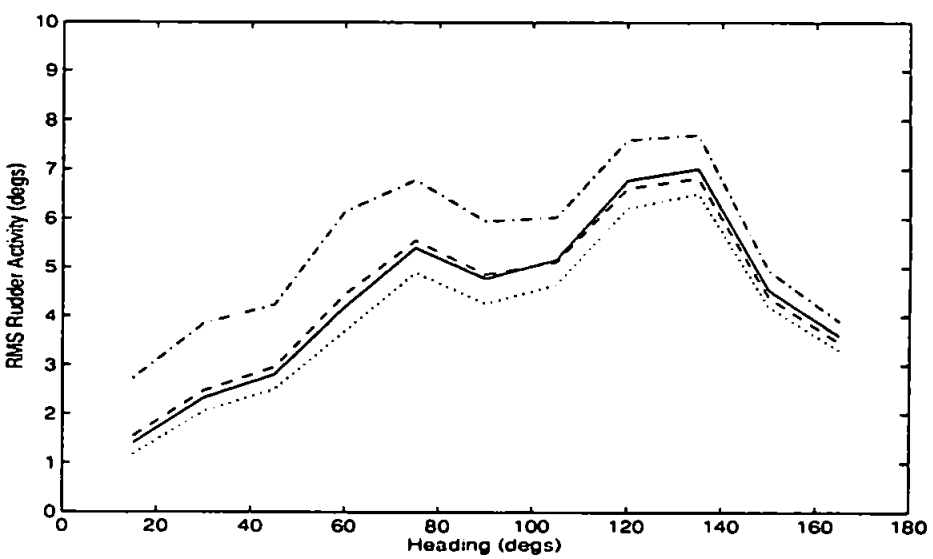

Figure G18 : Sea State 8

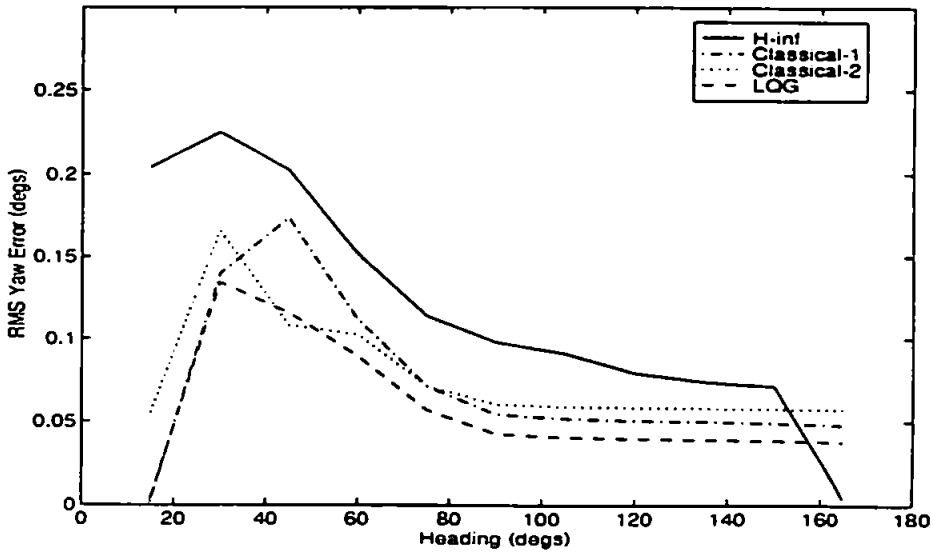

Figure G19 : Sea State 3

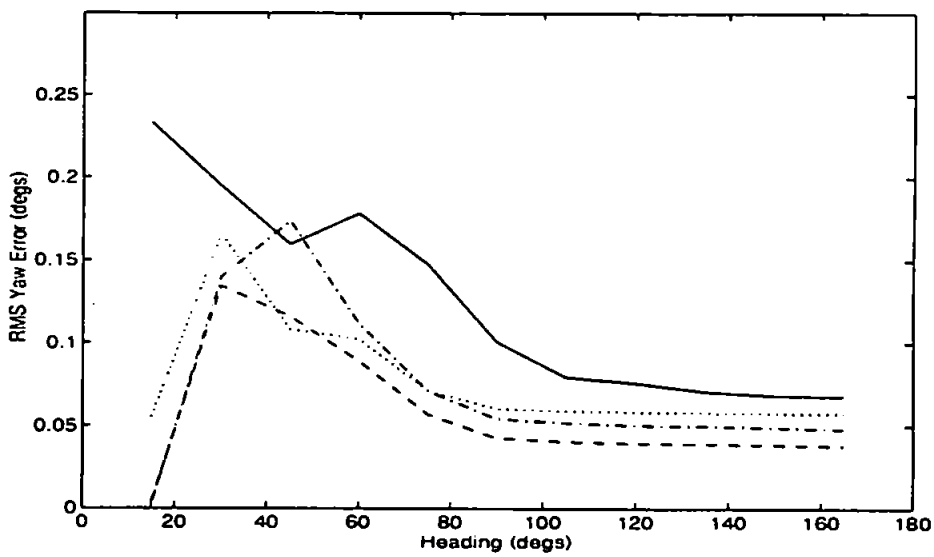

Figure G20 : Sea State 5

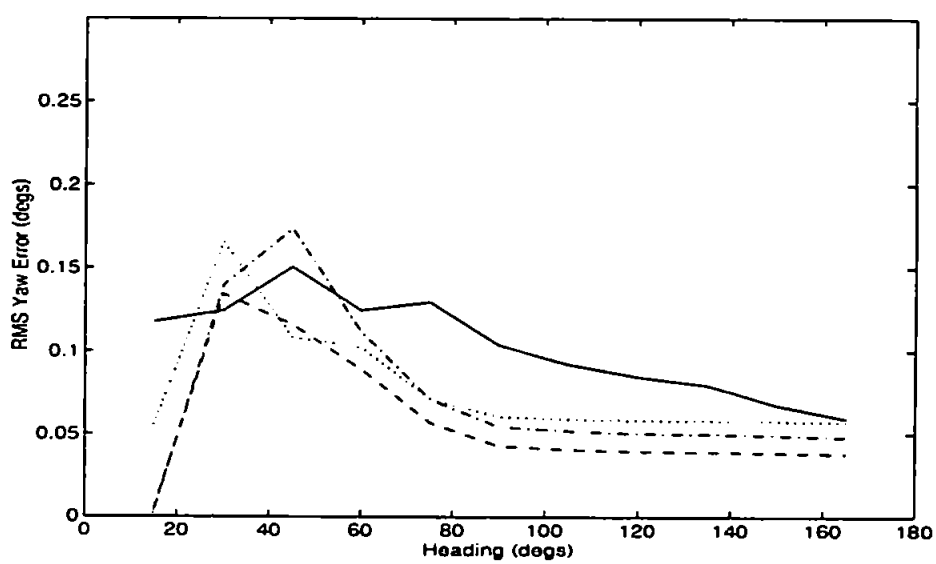

Figure G21 : Sea State 8

Fin Stabilisaion Only - Ship speed 12 kts - Percentage roll reduction graphs

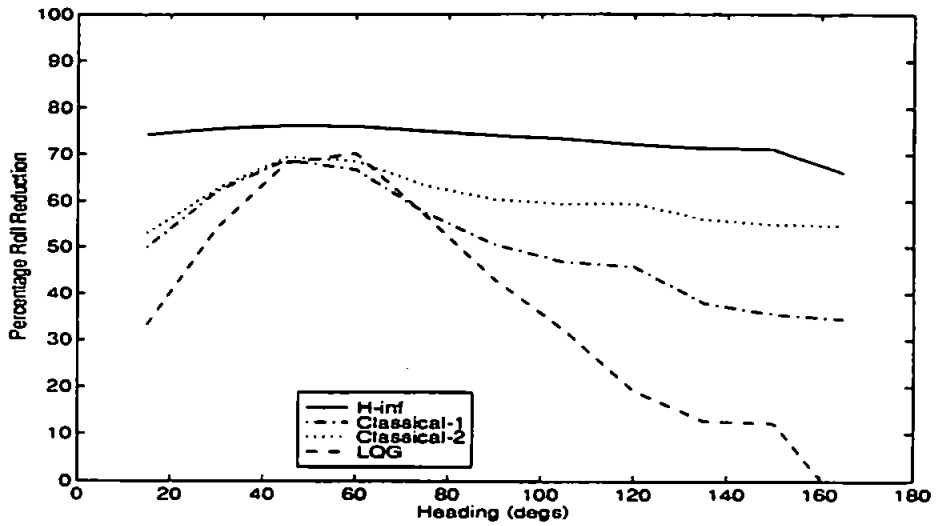

Figure G22 : Sea state 3

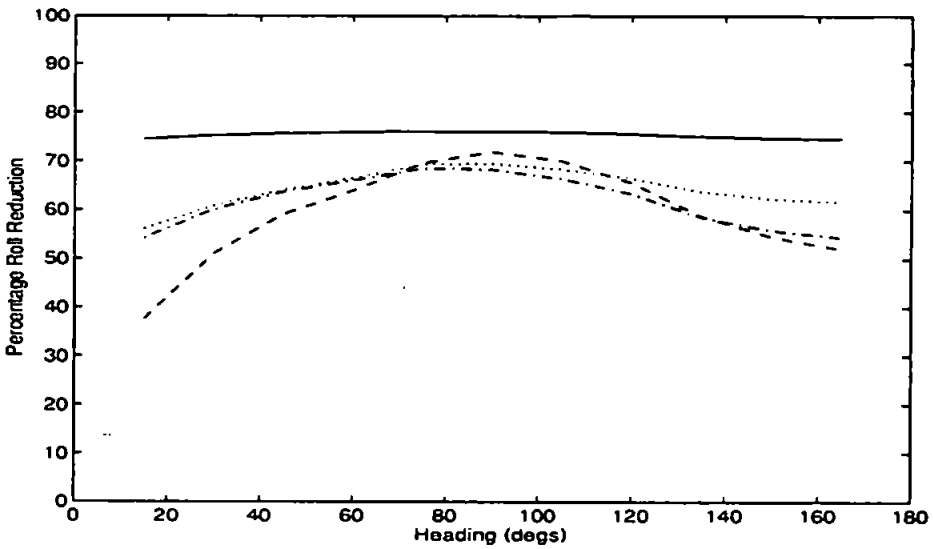

Figure G23 : Sea state 5

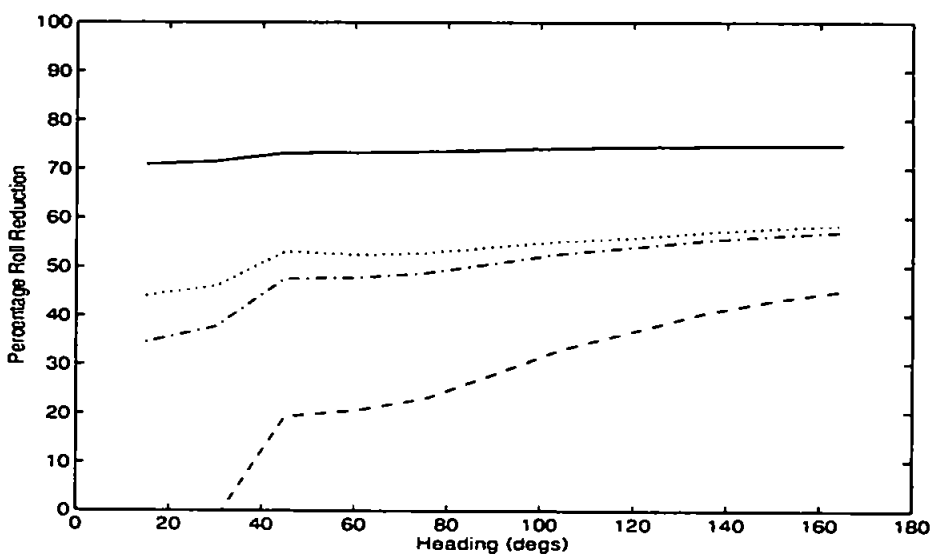

Figure G24 : Sea state 8

Fin Stabilisation Only - Ship speed 12 kts - RMS fin activity

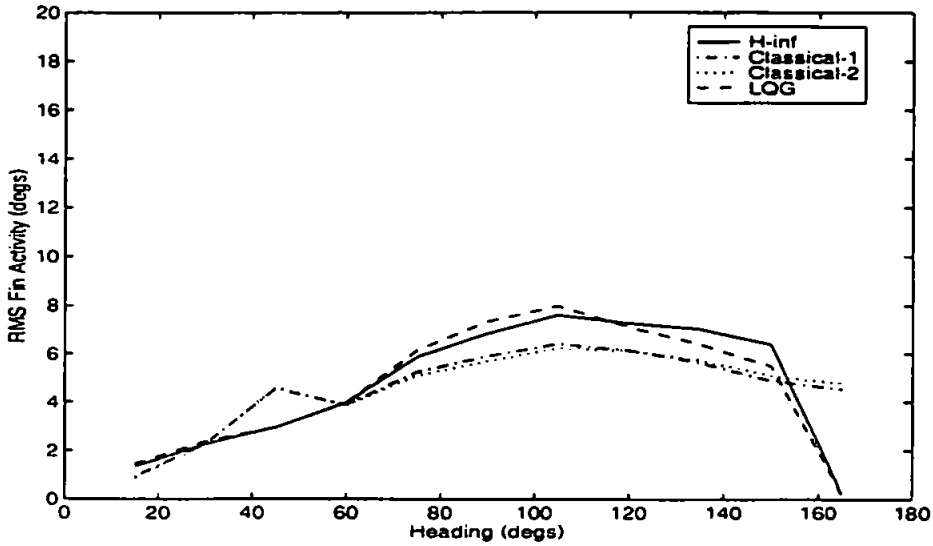

Figure G25 : Sea state 3

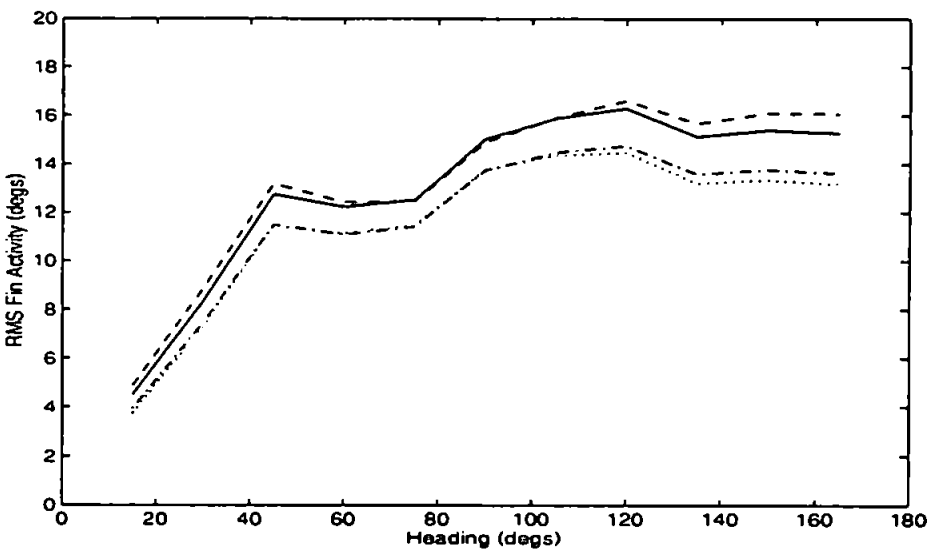

Figure G26 : Sea state 5

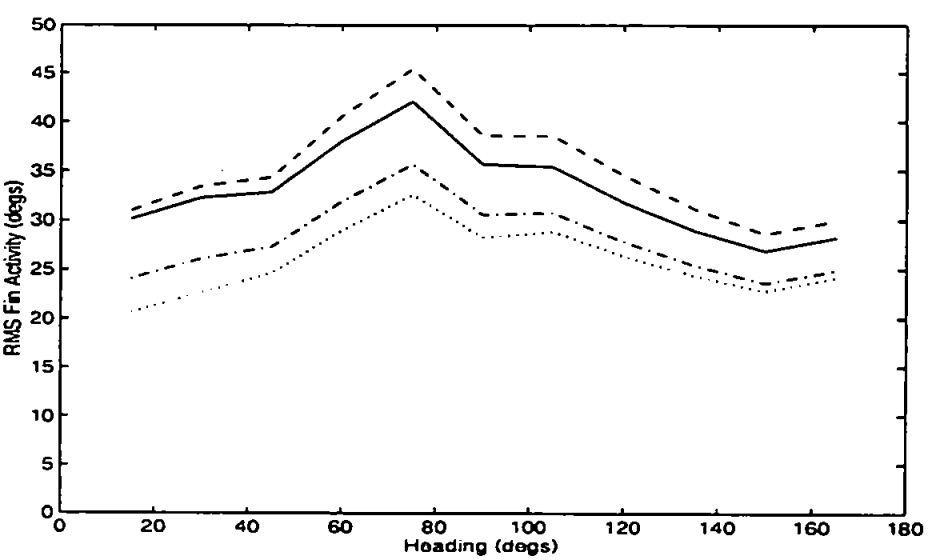

Figure G27 : Sea state 8

Fin Stabilisaion Only - Ship speed 18 kts - Percentage roll reduction graphs

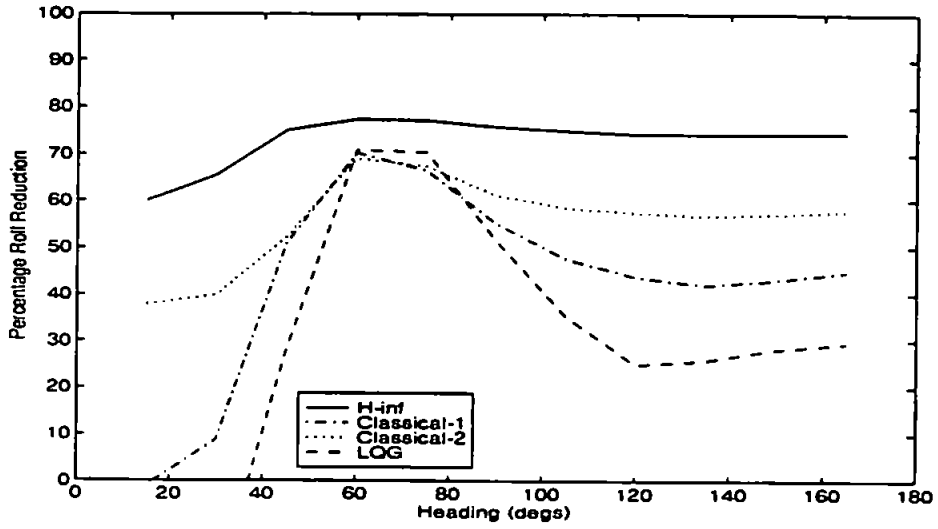

Figure G28 : Sea state 3

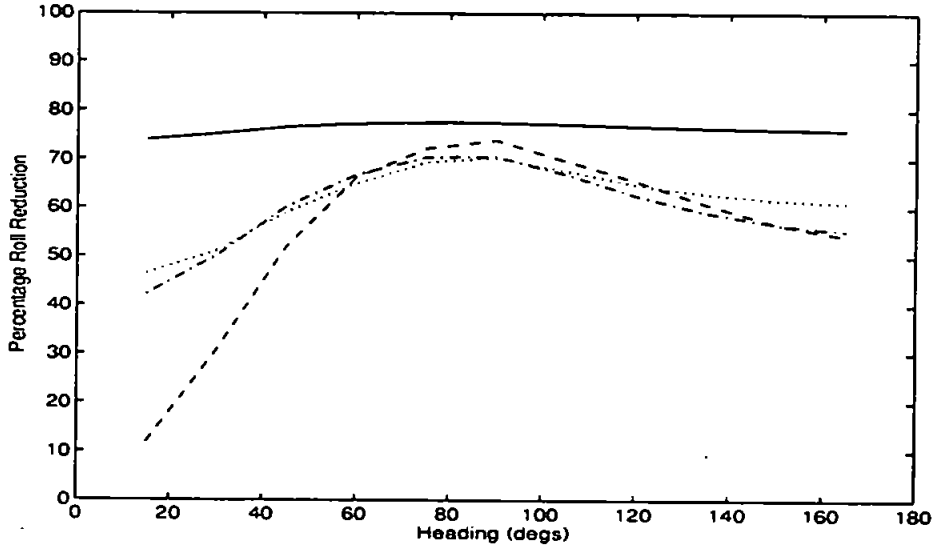

Figure G29 : Sea state 5

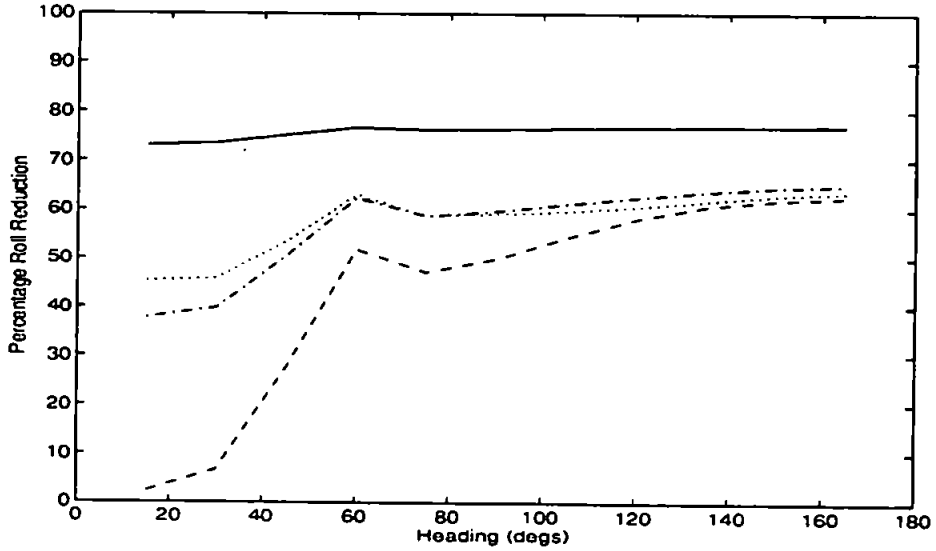

Figure G30 : Sea state 8

Fin Stabilisation Only - Ship speed 18 kts - RMS fin activity

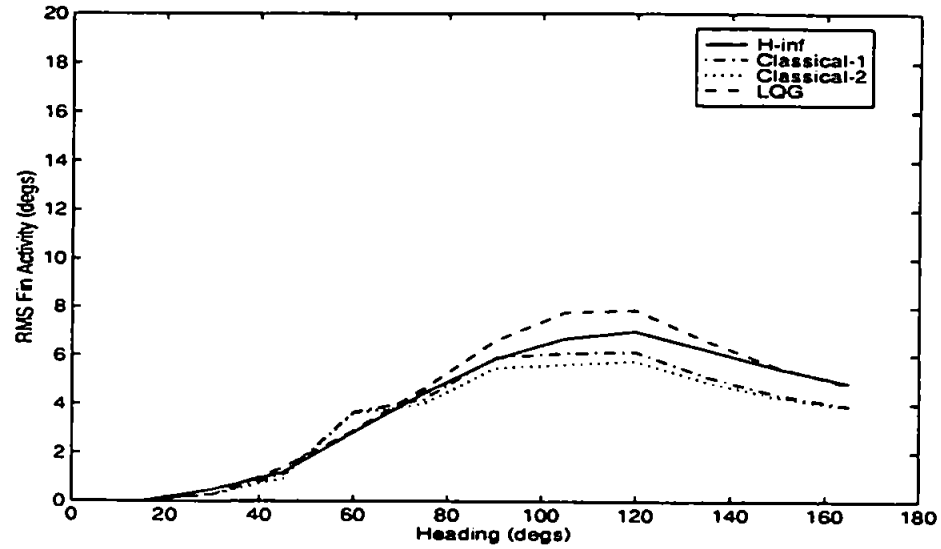

Figure G31 : Sea state 3

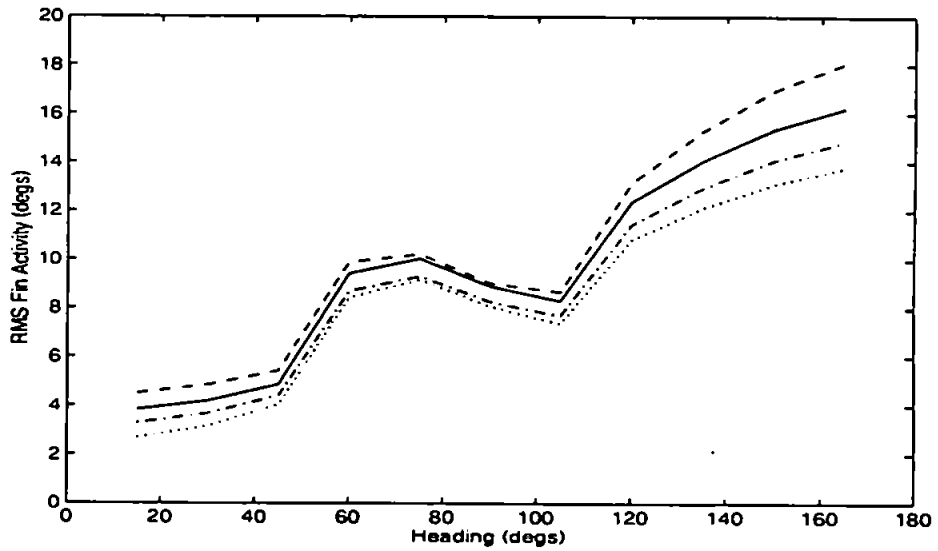

Figure G32 : Sea state 5

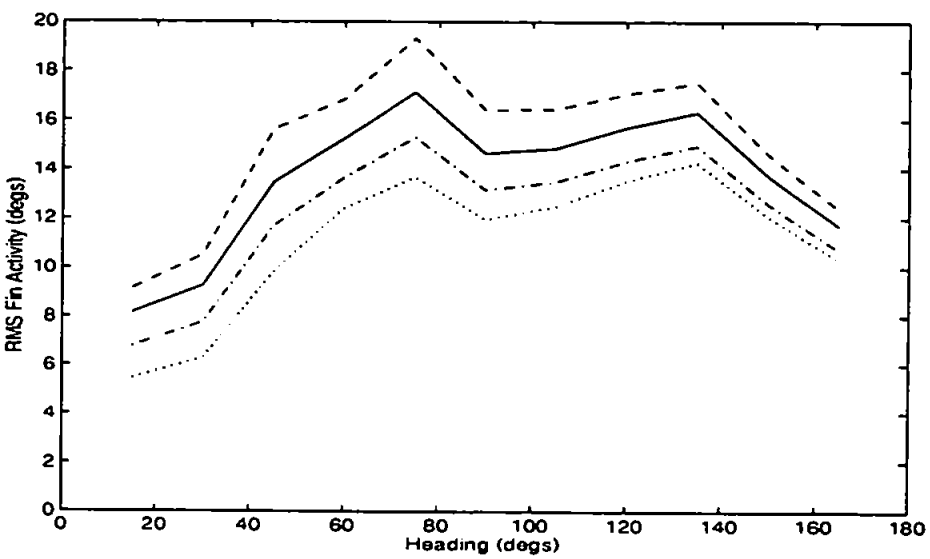

Figure G33 : Sea state 8

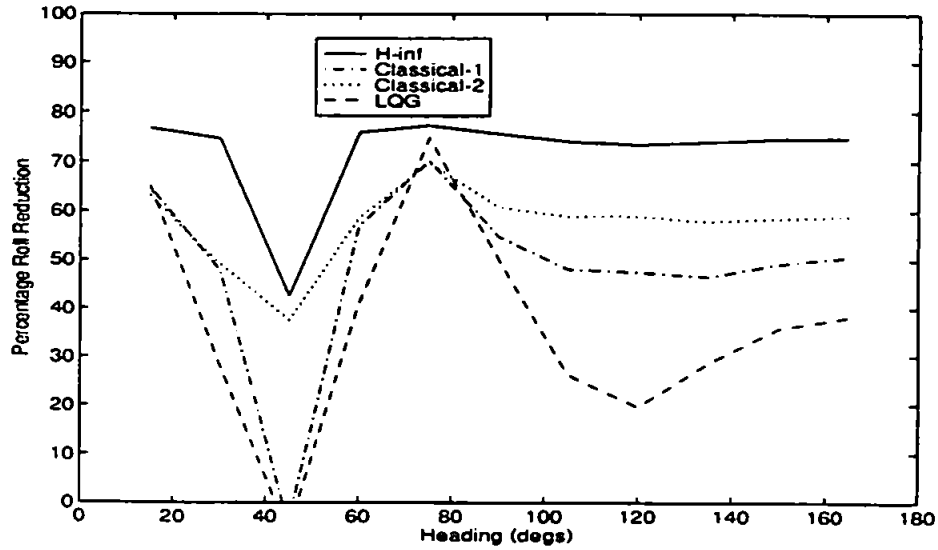

Figure G34 : Sea state 3

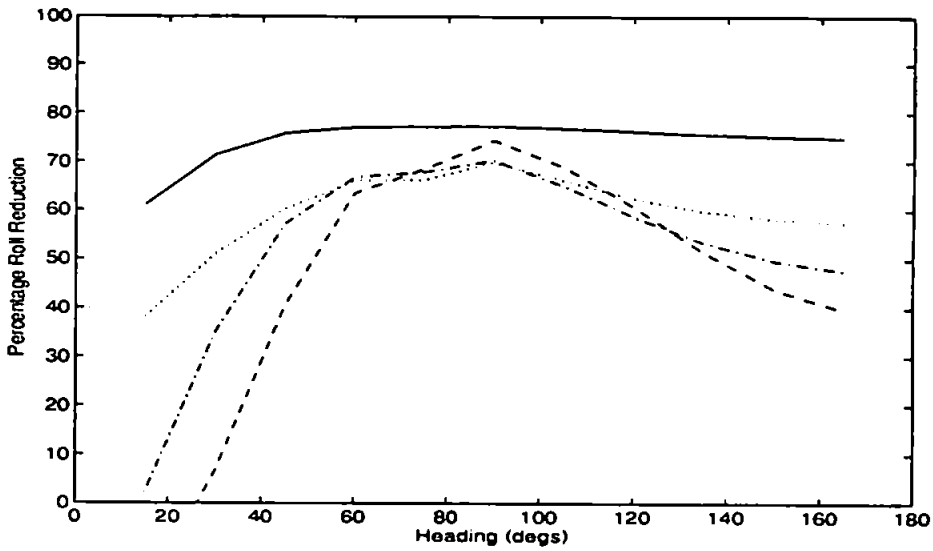

Figure G35 : Sea state 5

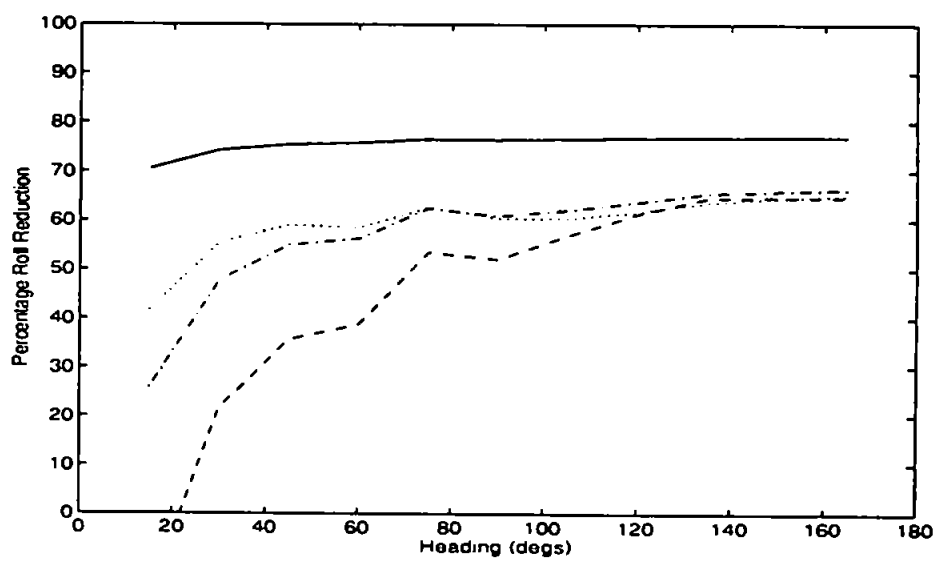

Figure G36 : Sea state 8

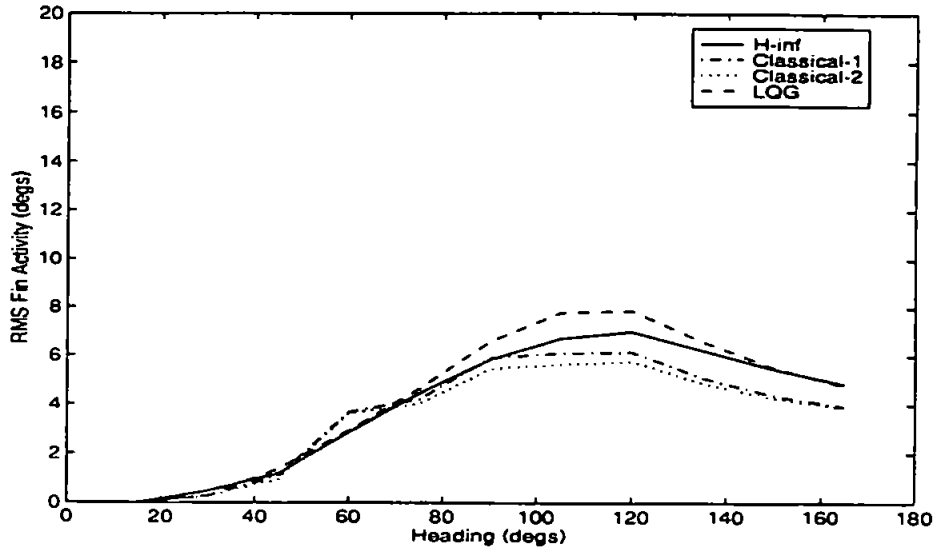

Figure G37 : Sea state 3

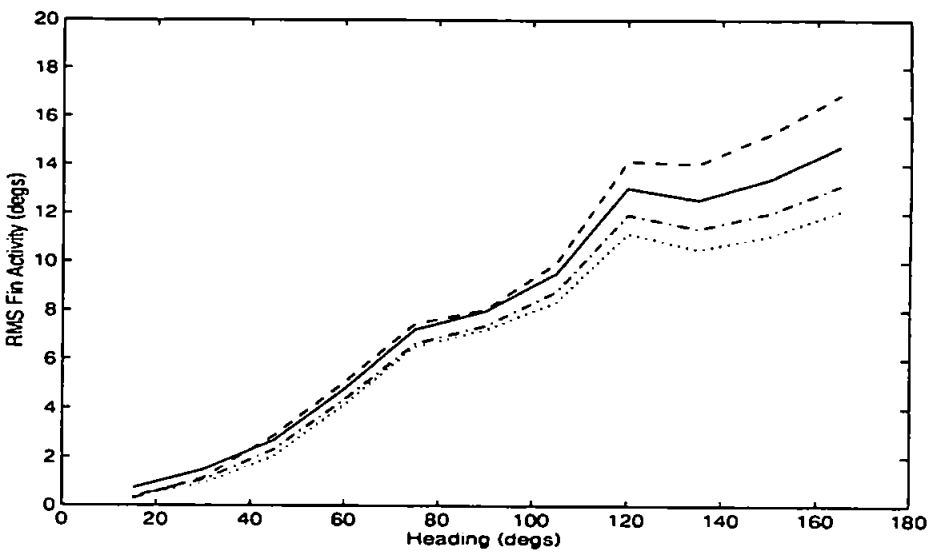

Figure G38 : Sea state 5

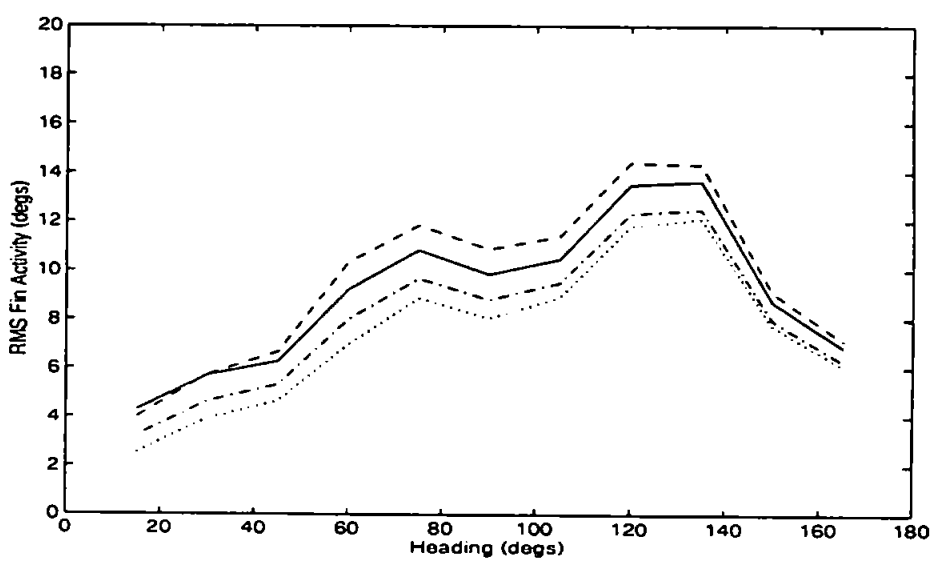

Figure G39 : Sea state 8

Fins and RRS - Ship speed 12 kts - Percentage roll reduction graphs

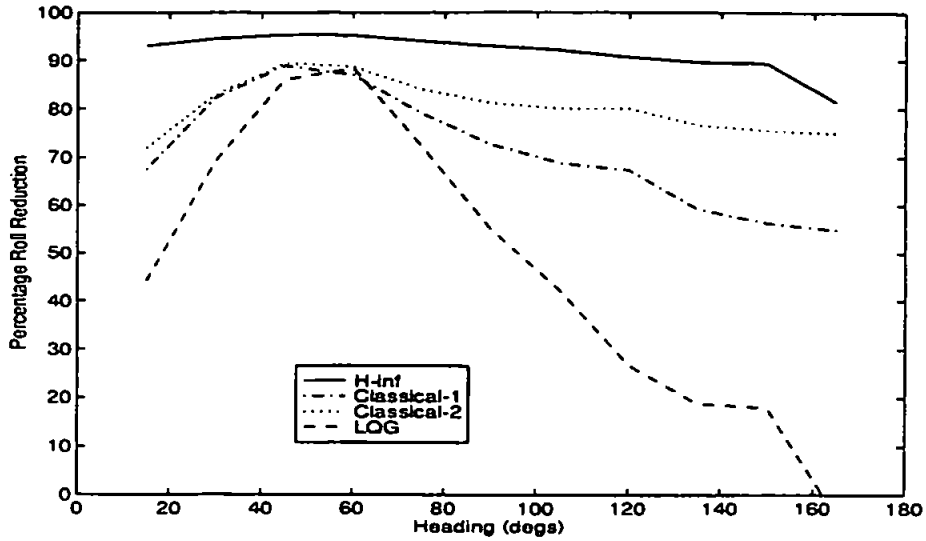

Figure G40 : Sea state 3

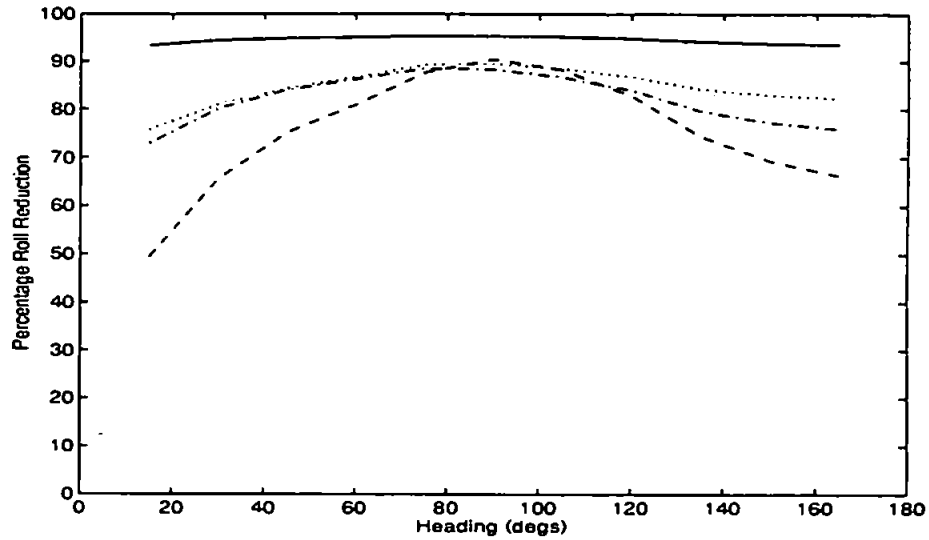

Figure G41 : Sea state 5

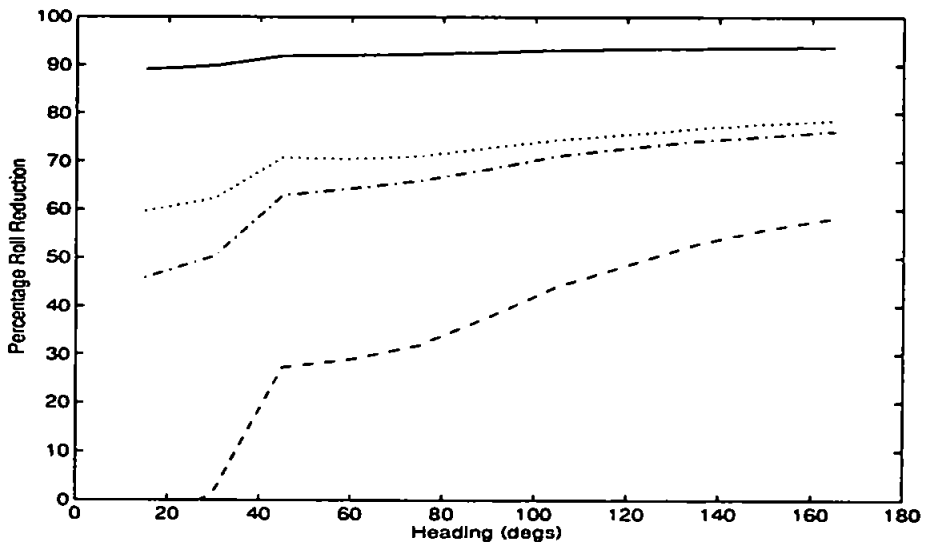

Figure G42 : Sea state 8

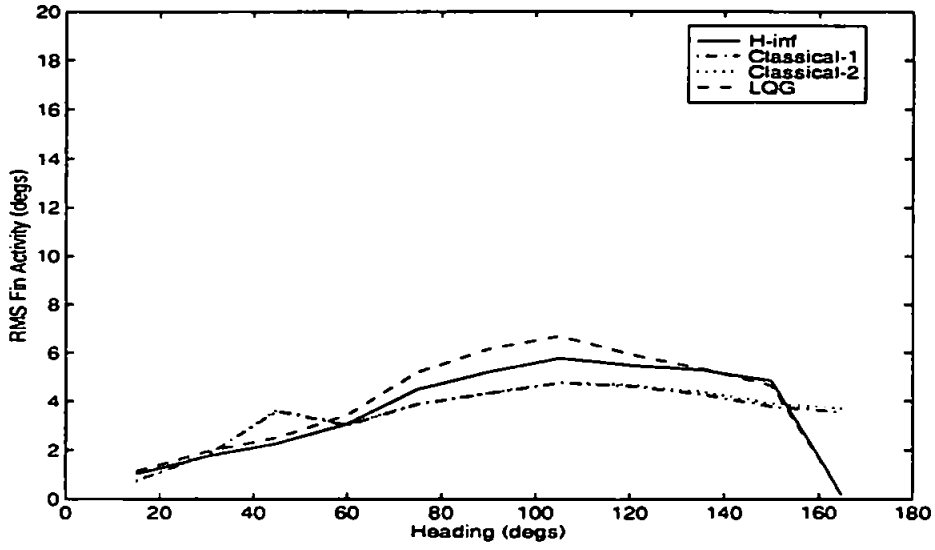

Figure G43 : Sea state 3

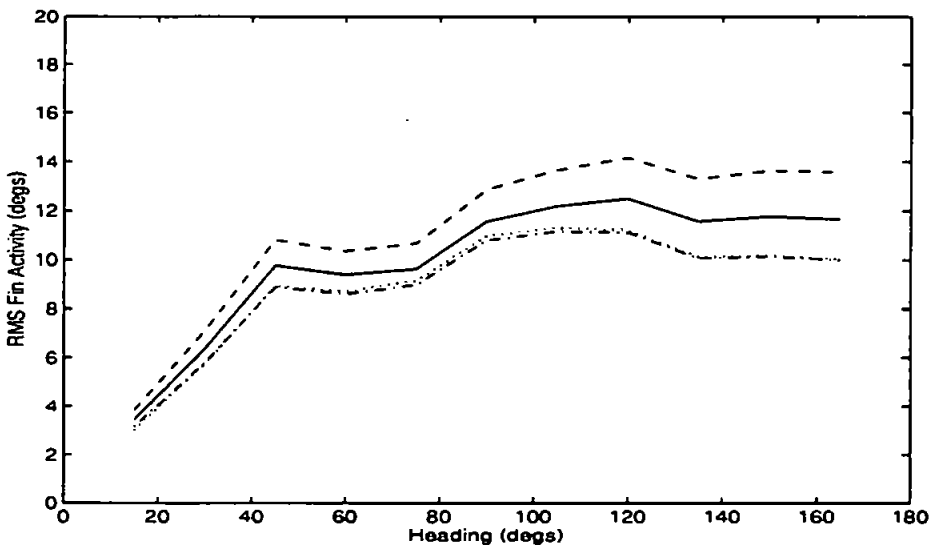

Figure G44 : Sea state 5

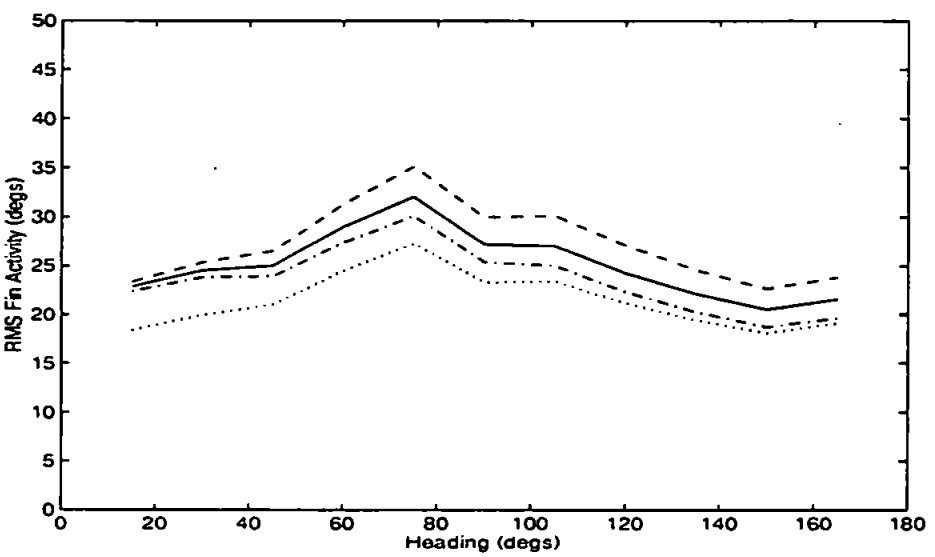

Figure G45 : Sea state 8

Fins and RRS - Ship speed 12 kts - RMS rudder activity

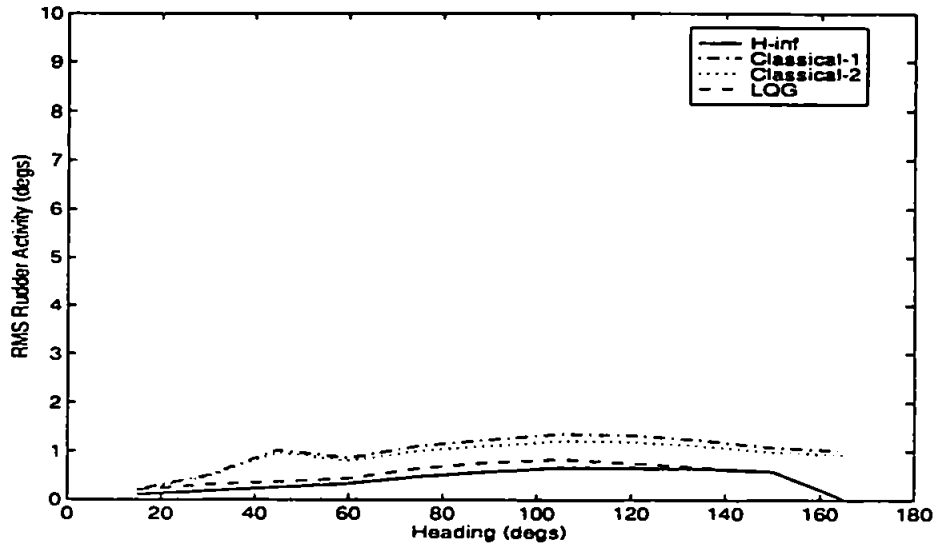

Figure G46 : Sea state 3

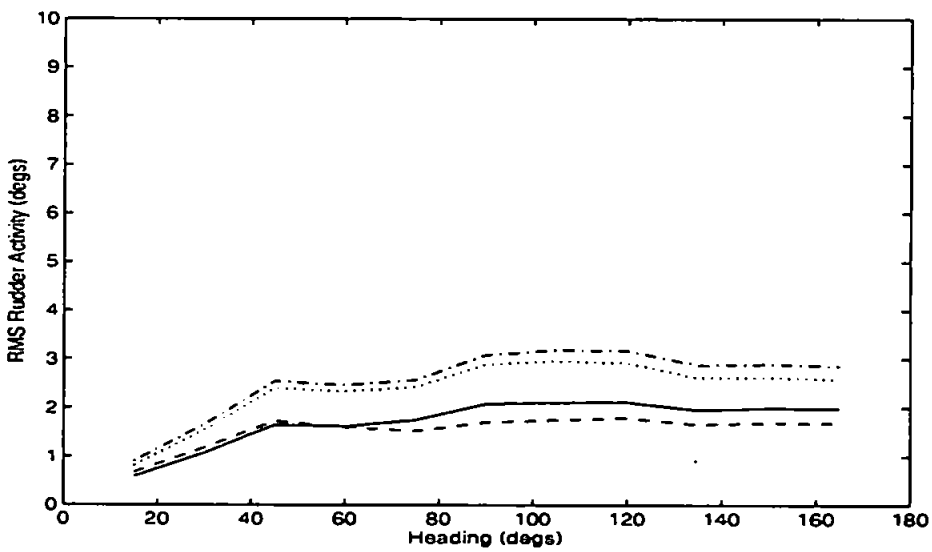

Figure G47 : Sea state 5

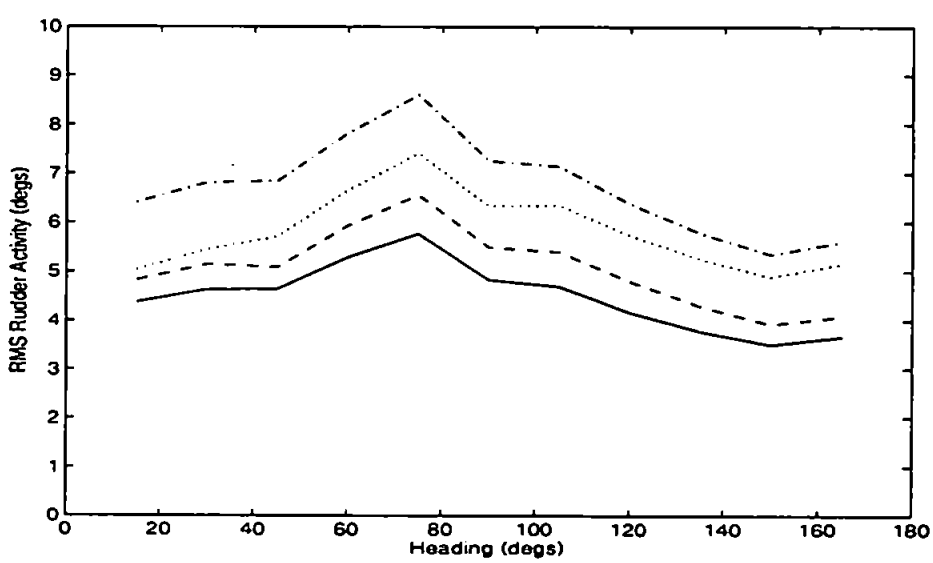

Figure G48 : Sea state 8

Fins and RRS - Ship speed 18 kts - Percentage roll reduction graphs

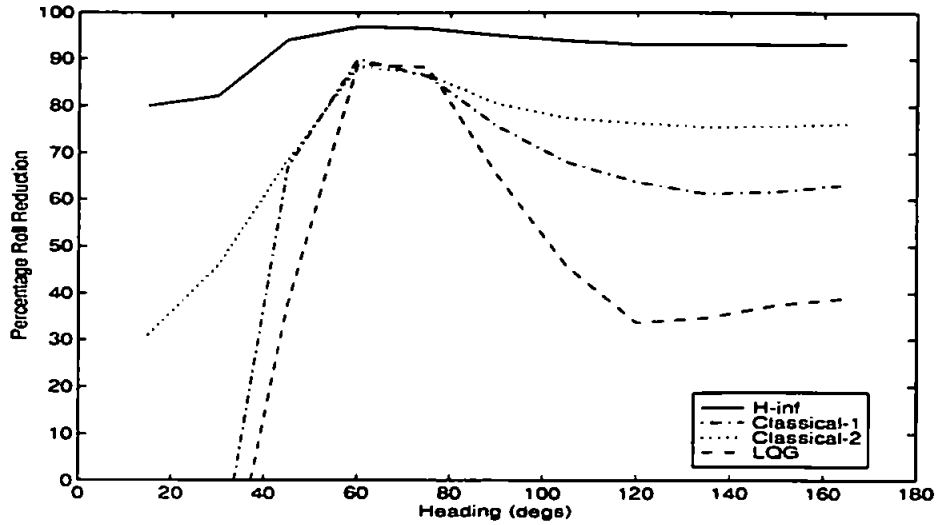

Figure G49 : Sea state 3

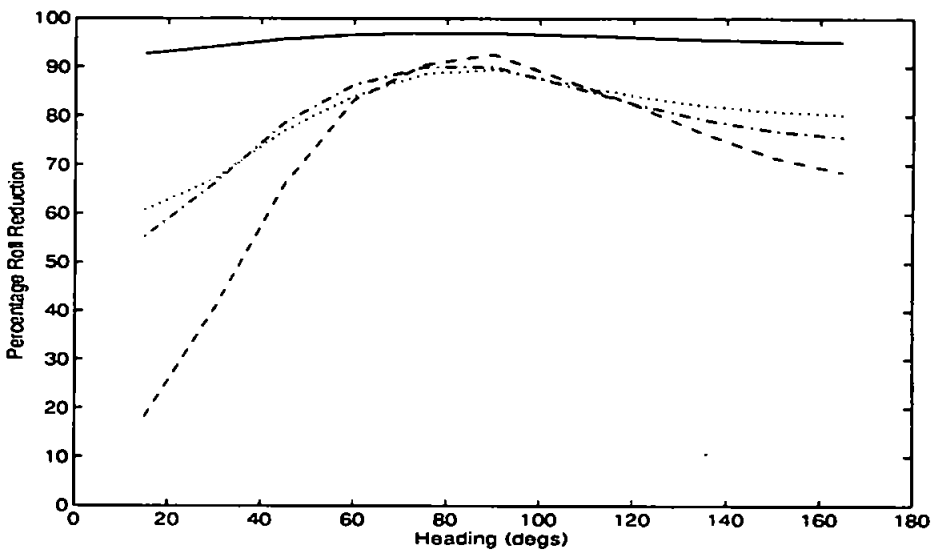

Figure G50 : Sea state 5

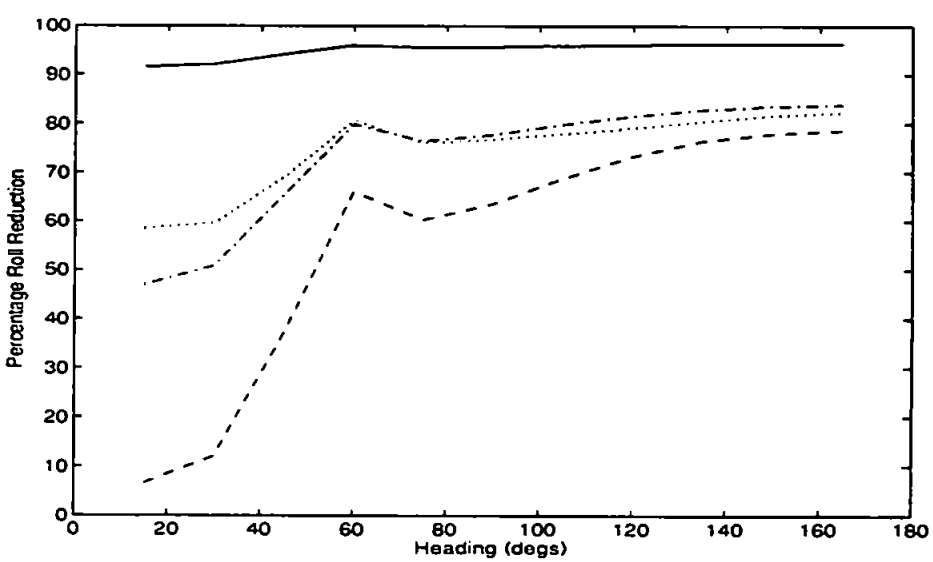

Figure G51 : Sea state 8

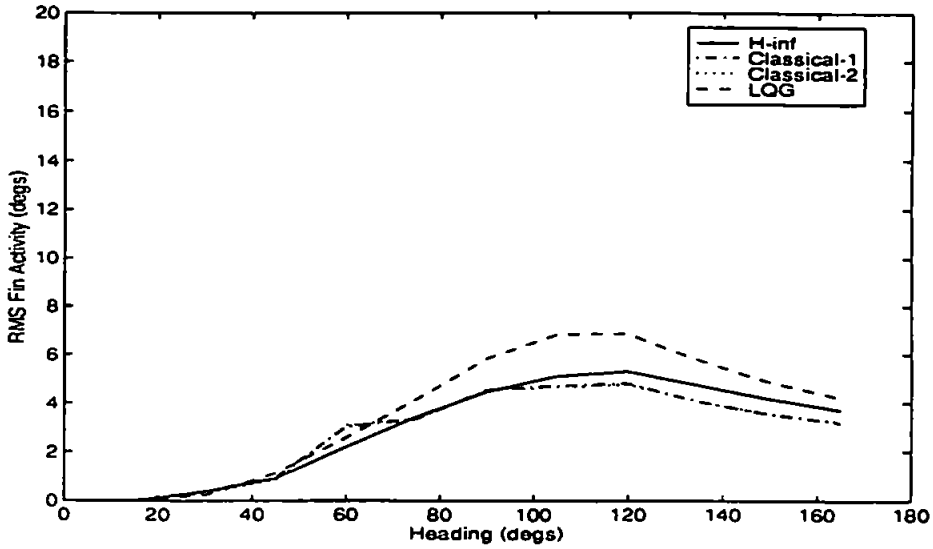

Figure G52 : Sea state 3

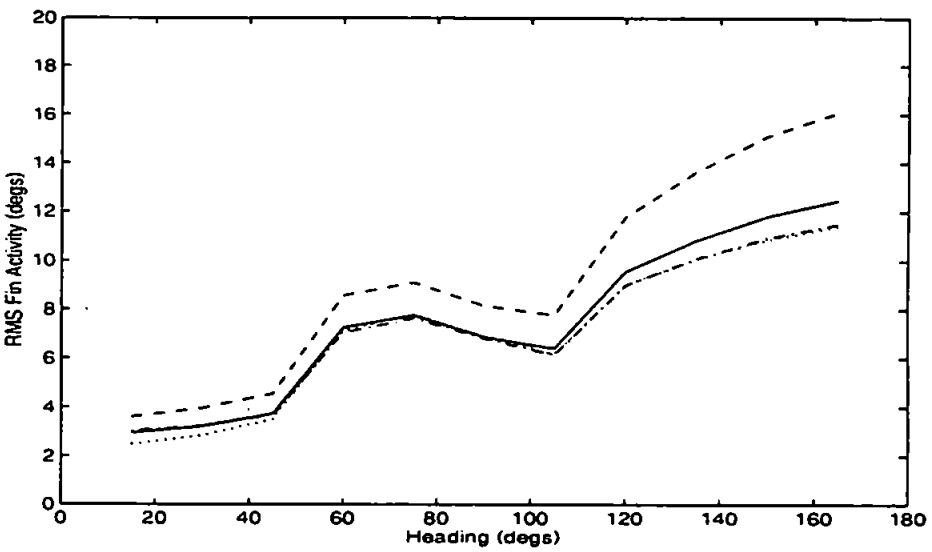

Figure G53 : Sea state 5

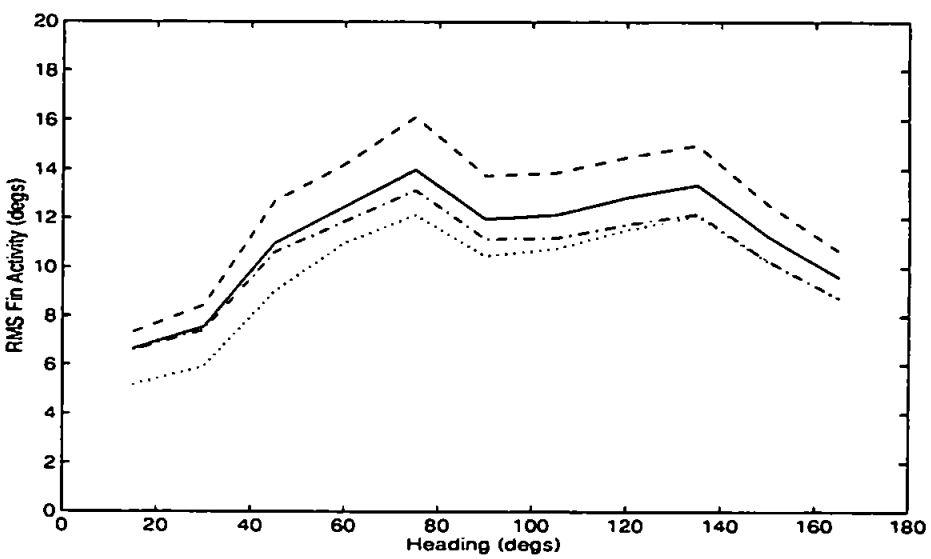

Figure G54 : Sea state 8

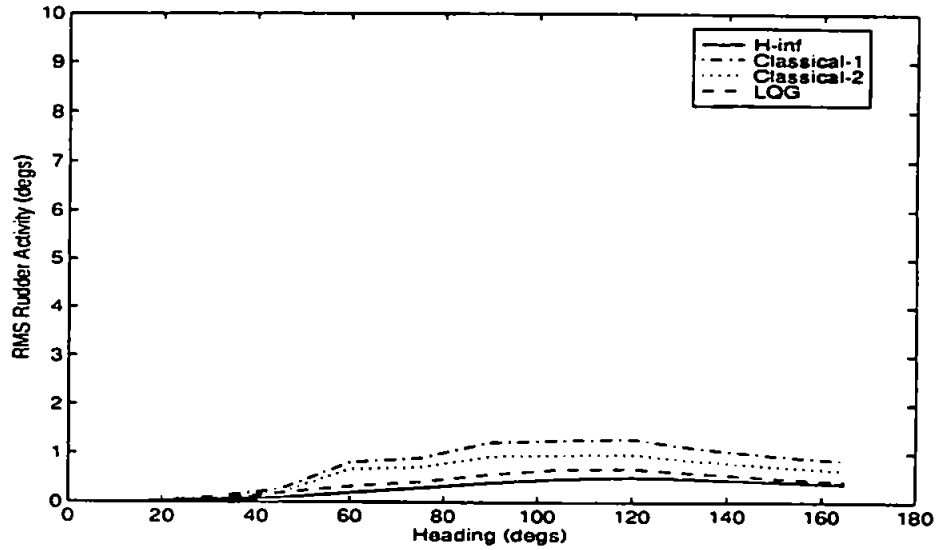

Figure G55 : Sea state 3

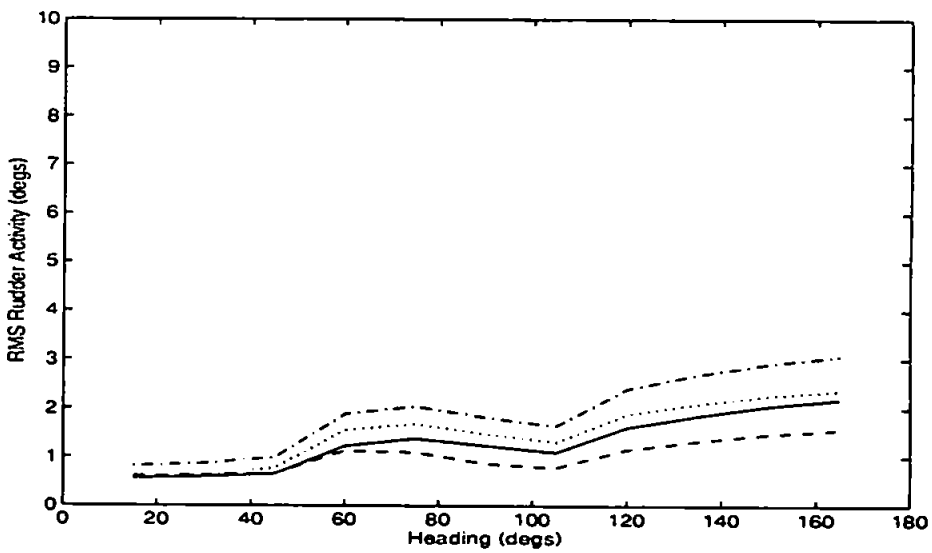

Figure G56 : Sea state 5

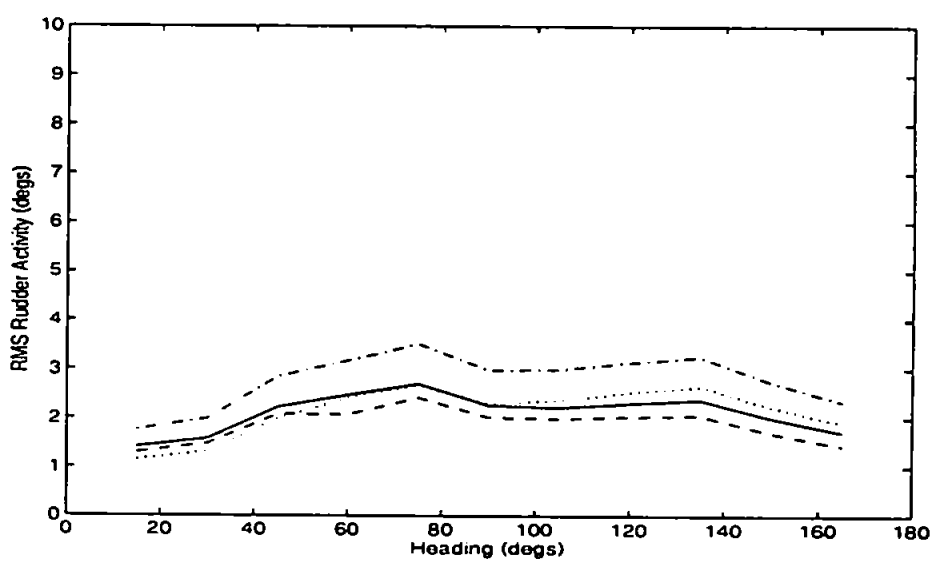

Figure G57 : Sea state 8

Fins and RRS - Ship speed 26 kts - Percentage roll reduction graphs

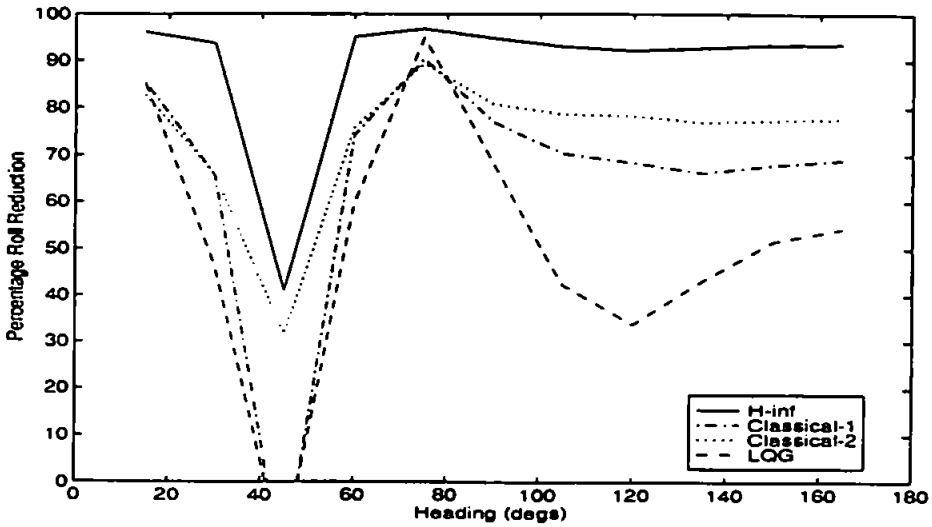

Figure G58 : Sea state 3

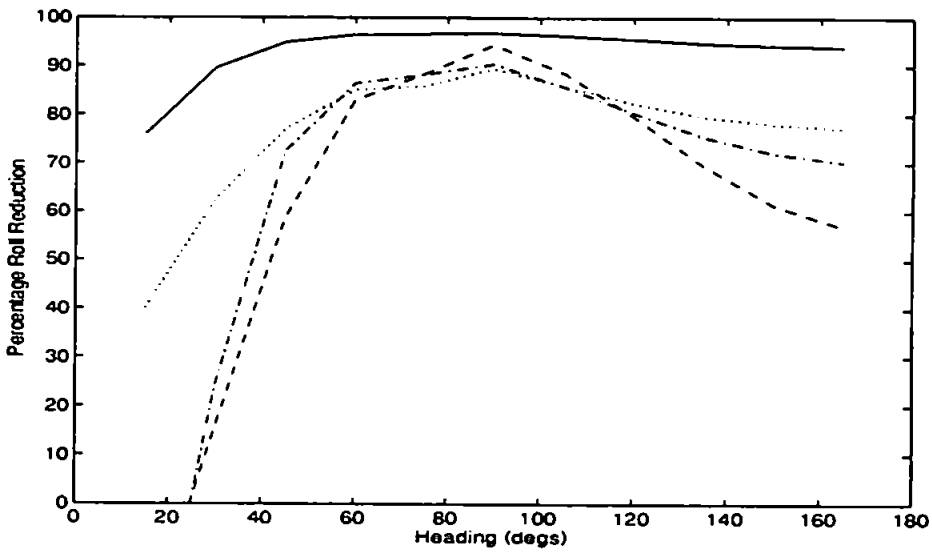

Figure G59 : Sea state 5

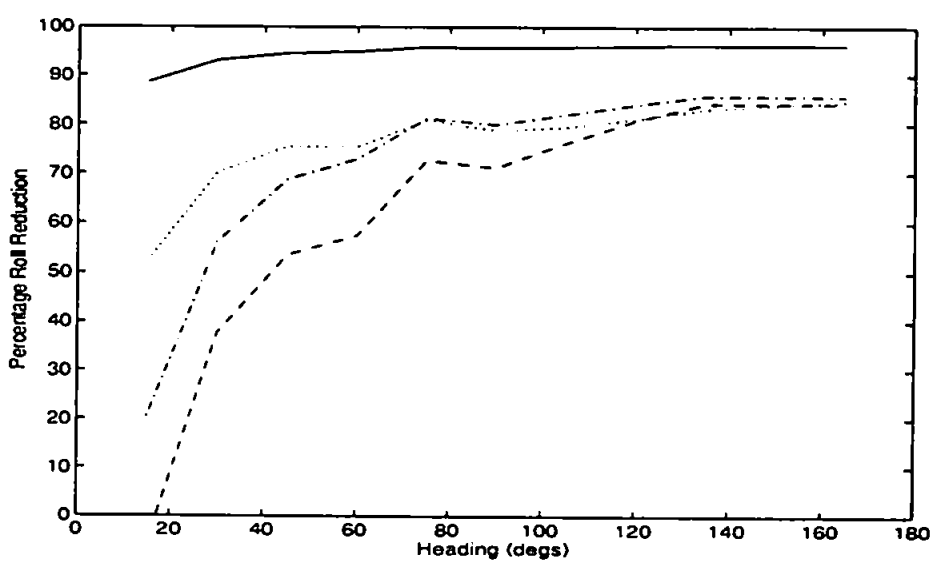

Figure G60 : Sea state 8

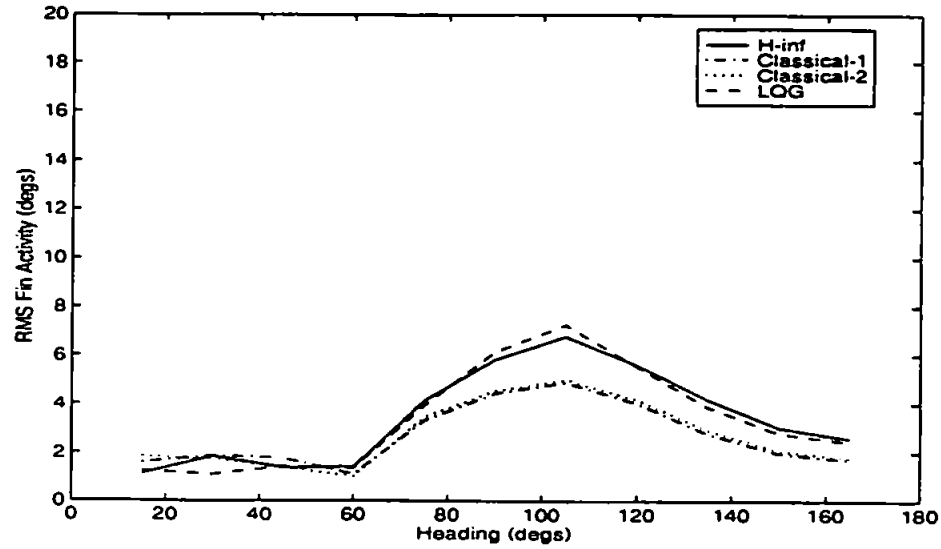

Figure G61 : Sea state 3

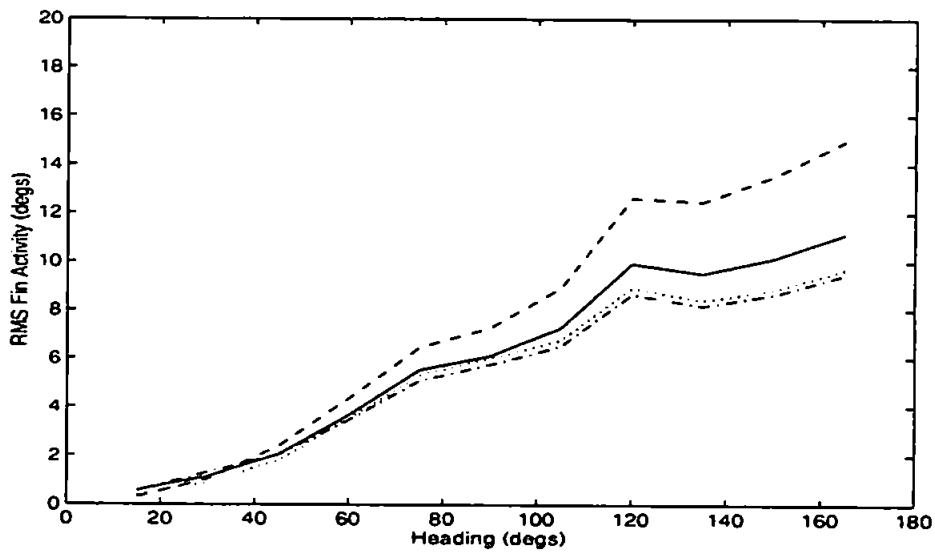

Figure G62 : Sea state 5

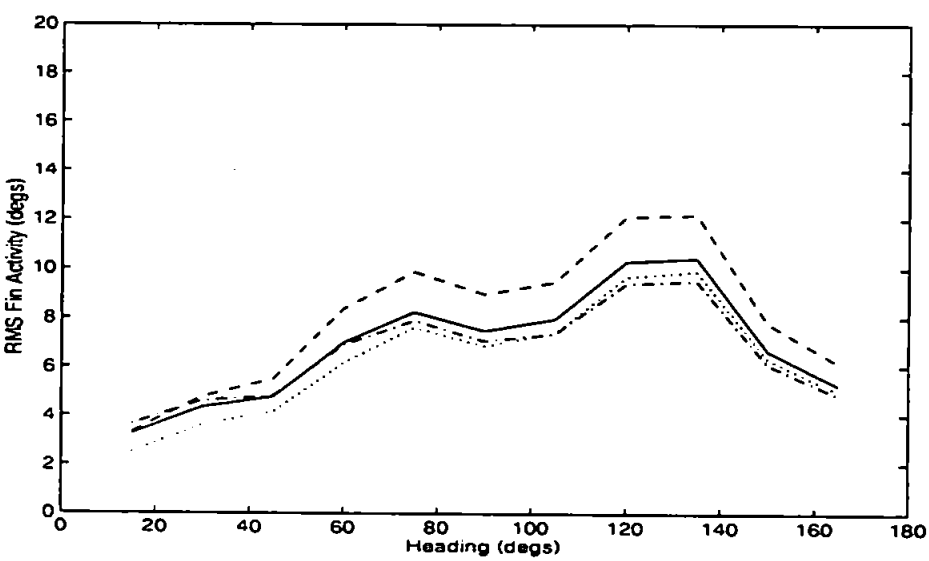

Figure G63 : Sea state 8

Fins and RRS - Ship speed 26 kts - RMS rudder activity

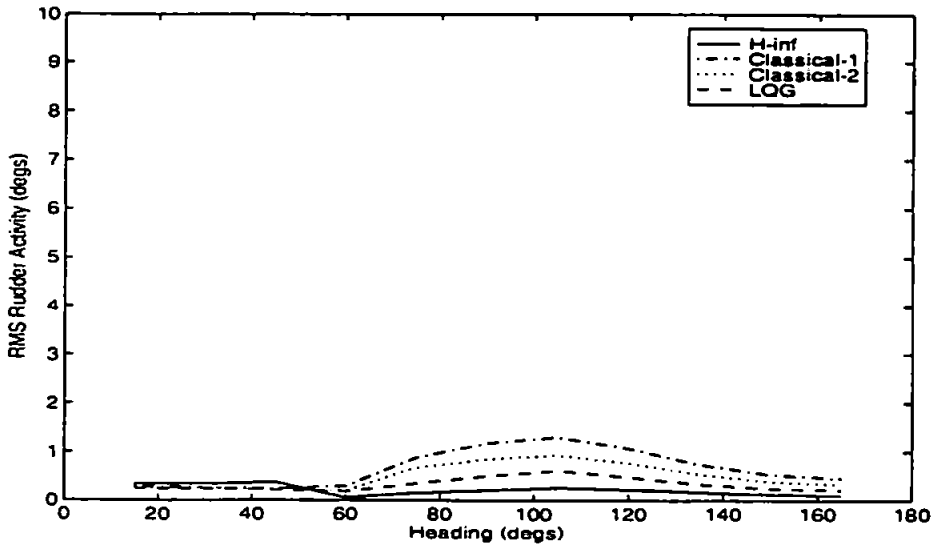

Figure G64 : Sea state 3

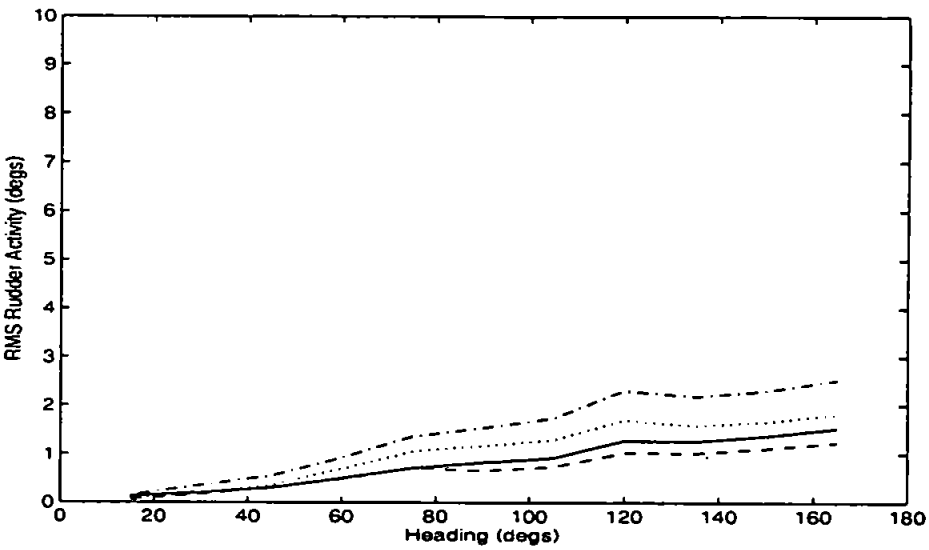

Figure G65 : Sea state 5

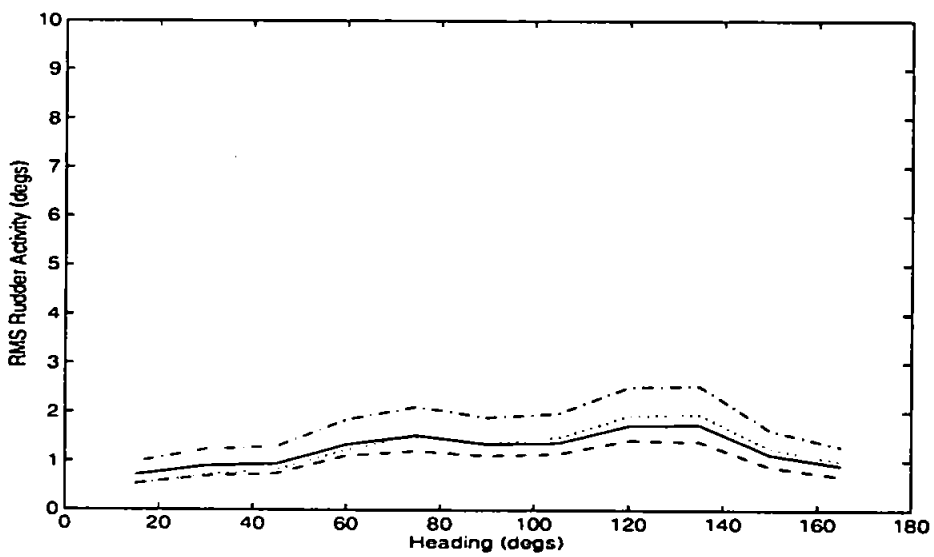

Figure G66 : Sea state 8

APPENDIX H - PROGRAM LISTING

```
//ASA Version of ALGO
//program ALGO.cpp

#include <dac.h>
#include <iostream.h>
#include <conio.h>
#include <iomanip.h>
#include <stdlib.h>
#include <math.h>
#include <fstream.h>
#include <string.h>
#include <stdio.h>

Dac env(HI);
AD ad(&env);
DA fin_da(&env,2), rud_da(&env,1);

int fin_info1[10], rud_info1[10];
int fin_rate_fb=0, rud_rate_fb=0;
float fin_info2[10], rud_info2[10];

float fin_num[12], rud_num[12], ap_num[12];
float fin_den[12], rud_den[12], ap_den[12];
float fin_x[12], rud_x[12], ap_x[12];
float fin_y[12], rud_y[12], ap_y[12];

float pc_fin=0, pc_rud=0, pc_ap=0;
float Ts=0.1, runT, speed;
float ip_data[12];
float roll_v2d=10, ccu_v2d=4, herror_v2d=4, asu_v2d=1/.148;

void fin_demand();
void rud_demand();
void ap_demand();
void readings();
void get_info();
void K_coeff();
void read_coeff();
void control();
void beep();


//////////////////TEMPORARAY GLOBALS
//FILE *roll, *ccu, *herror, *asu;


///////////////////////MAIN
main()
{  int i, cnt;


        fin_da.sendv(3.5); rud_da.sendv(2.5);
        for(i=0;i<=11;++i)
        {
                fin_den[i]=0; fin_num[i]=0; rud_den[i]=0; rud_num[i]=0;
                fin_x[i]=0; fin_y[i]=0; rud_x[i]=0; rud_y[i]=0;
                ip_data[i]=0;
        }
        for (i=0;i<10;++i)
        {
                fin_info1[i]=0;         fin_info2[i]=0;
                rud_info1[i]=0;         rud_info2[i]=0;
        }
        clrscr();
        cout<<"Please enter run time : "; cin>>runT;
        cout<<"Please enter ship speed : ";cin>>speed;

        clrscr();
        K_coeff();
        read_coeff();
        get_info();
        clrscr();
        control();
}
```

```
////////////////////////////CONTROL
void control()
{

        FILE *fin_memt, *rud_memt;

        Timer clk(&env,Ts);
        DA fin_da(&env,2), rud_da(&env,1);

        char fin_file[12], rud_file[12], key='1',g='n',tempc;
        int  rud_asa_pos=1, fin_asa_pos=1,i;
        float etime=0, fin_d2v=.25, rud_d2v=.148, pc_fin_out, pc_rud_out, speed_gain, max_fin;
        float rud_asa[6], rud_asa_data[201], fin_asa[6], fin_asa_data[201], temp_asa;
        float temp_rud;

        for (i=0;i<=6;++i) {rud_asa[i]=0; fin_asa[i]=0;}
        rud_asa[1]=1; fin_asa[1]=1;
        for (i=0;i<=200;++i) {rud_asa_data[i]=0; fin_asa_data[i]=0;}

        cout<<"\n\n\n Enter file name for fin data: "; cin >>fin_file;
        cout<<"\n Enter file name rudder data: "; cin >>rud_file;
/*
roll=fopen("roll","r");
ccu=fopen("ccu","r");
herror=fopen("herror","r");
asu=fopen("asu","r");
*/

        if (speed<5) speed_gain=0;
        else if ((speed>5) && (speed<15)) speed_gain=1;
        else speed_gain=225/(speed*speed);

        if (speed<=18) max_fin=28;
        else
        {
                max_fin=.0068*speed*speed*speed-.579*speed*speed+17.176*speed-161.5012;
                max_fin=28-max_fin;
        }


        clrscr();
        cout<<"\n\nThe pc generated fin demand signal has a speed gain of "<<speed_gain<<"\n";
        cout<<"..and the maximum excursion angle is "<<max_fin<<" degrees.";

        cout<<"\n\n\nDo you wish to graph data (y/n) : "; cin>>g;

Graf g1(TOP_THIRD,0,-20,60,20,"Time","Roll angle, Fin Motion (stbd)","ROLL MOTION",PAN,CLIP,GRID,""),
        g2(MIDDLE_THIRD,0,-30,60,30,"Time","CCU/PC_FIN","FIN DEMANDS",PAN,CLIP,GRID,""),
        g3(LOWER_THIRD,0,-15,60,15,"Time","ASU/PC_RUD","RUDDER DEMAND",PAN,CLIP,GRID,"");

        ofstream fin_mem("d:\\fin_temp");
        ofstream rud_mem("d:\\rud_temp");
        clk.startTimer();

        do
        {
                clk.tic(); etime=clk.getTime();

                fin_demand(); rud_demand();     ap_demand(); readings();

//Generate fin demand
                if (fin_info1[1])
                {
                        if (fin_info1[3] && (etime>fin_info2[2]))
                                pc_fin=fin_y[1]*fin_info2[3];
                        else if (fin_info1[2] && (etime>fin_info2[1]))
                                pc_fin=ip_data[2];
                        else if (fin_info1[4])
                                pc_fin=fin_info2[4]*sin(fin_info2[5]*etime);
                        else
                                pc_fin=fin_info2[6];
                }
                else
                        pc_fin=0;
                pc_fin=pc_fin*speed_gain;


                pc_rud=rud_y[1]*rud_info2[2];

////////////////////////////////Process the control signal pc_fin, pc_rud
```

```
temp_asa=rud_asa[4]*rud_asa[4];
rud_asa[2]=rud_asa[2]-rud_asa_data[rud_asa_pos]+temp_asa;
rud_asa[3]=sqrt(rud_asa[2]/200);
rud_asa_data[rud_asa_pos]=temp_asa;
rud_asa_pos++;
if (rud_asa_pos>200) rud_asa_pos=1;
rud_asa[5]=rud_asa[5]+Ts;
if(rud_asa[5]>20)
{
        if (rud_asa[3]>8.5)    rud_asa[1]=rud_asa[1]-0.2*rud_asa[1];
        else rud_asa[1]=rud_asa[1]+0.2*rud_asa[1];
        if (rud_asa[1]>1) rud_asa[1]=1;
        rud_asa[4]=pc_rud*rud_asa[1];
        rud_asa[5]=0;
}
else
{
        rud_asa[4]=pc_rud*rud_asa[1];
}
if (etime>rud_info2[5])
        pc_rud_out=rud_asa[4];
else
        pc_rud_out=pc_rud;

temp_asa=fin_asa[4]*fin_asa[4];
fin_asa[2]=fin_asa[2]-fin_asa_data[fin_asa_pos]+temp_asa;
fin_asa[3]=sqrt(fin_asa[2]/200);
fin_asa_data[fin_asa_pos]=temp_asa;
fin_asa_pos++;
if (fin_asa_pos>200) fin_asa_pos=1;
fin_asa[5]=fin_asa[5]+Ts;
if (fin_asa[5]>20)
{
        if (fin_asa[3]>29) fin_asa[1]=fin_asa[1]-0.2*fin_asa[1];
        else fin_asa[1]=fin_asa[1]+0.2*fin_asa[1];
        if (fin_asa[1]>1) fin_asa[1]=1;
        fin_asa[4]=pc_fin*fin_asa[1];
        fin_asa[5]=0;
}
else
{
        fin_asa[4]=pc_fin*fin_asa[1];
}
if (etime>fin_info2[7])
        pc_fin_out=fin_asa[4];
else
        pc_fin_out=pc_fin;

if (pc_rud_out>28)    pc_rud_out=28;
else if (pc_rud_out<-28) pc_rud_out=-28;
else ;

if (pc_fin_out>max_fin) pc_fin_out=max_fin;
else if (pc_fin_out<-max_fin) pc_fin_out=-max_fin;
else ;


//Generate rudder demand
if (rud_info1[1])
{
        if (rud_info1[2])
                pc_rud_out=ip_data[6];
        else if (rud_info1[3])
                pc_rud_out=ap_y[1]*rud_info2[4];
        else if (rud_info1[4])
        {
                if (etime>rud_info2[1])
                        pc_rud_out=ip_data[6]+pc_rud_out;
                else
                        pc_rud_out=ip_data[6];
        }
        else
        {
                if (etime>rud_info2[1])
                        pc_rud_out=pc_rud_out+ap_y[1]*rud_info2[4];
                else if (etime>rud_info2[3])
                        pc_rud_out=ap_y[1]*rud_info2[4];
                else
                        pc_rud_out=ip_data[6];
        }
}
```

```
                else
                        pc_rud_out=ip_data[6];


////////////////////////////////////////OUTPUT Signals, store and display


                rud_da.sendv((pc_rud_out*rud_d2v)/2+2.5);
                fin_da.sendv((pc_fin_out*fin_d2v)/2+3.5);

                fin_mem<<etime<<" "<<ip_data[1]<<" "<<ip_data[7]<<" "<<pc_fin<<" "<<pc_fin_out<<" "<<fin_asa[1]<<"
"<<ip_data[2]<<" "<<ip_data[3]<<" "<<ip_data[4]<<" "<<fin_y[1]<<"\n";
                rud_mem<<etime<<" "<<pc_rud<<" "<<pc_rud_out<<" "<<rud_asa[1]<<" "<<ip_data[5]<<" "<<ip_data[6]<<"
"<<(ap_y[1])<<" "<<(rud_y[1])<<"\n";

                if (g=='y')
                {
                        g1.plot(1,etime,ip_data[1]);
                        g1.plot(2,etime,ip_data[4]*4);
                        g2.plot(1,etime,ip_data[2]);
                        g2.plot(2,etime,pc_fin_out);
                        g3.plot(1,etime,ip_data[6]);
                        g3.plot(2,etime,pc_rud_out-ip_data[6]);
                }
                else
                {
                        gotoxy(5,5);
                        cout<<"Elapsed time = "<<etime<<"      "<<key<<"\n";
                        cout<<pc_fin_out<<"\n"<<pc_rud_out;
                }
                ip_data[9]=pc_fin;
                ip_data[10]=pc_rud;

                if (kbhit()) key=getch();
                if (clk.toc()==-1) beep();
        }while ((etime<runT) && (key != 'q'));

        pc_rud_out=0;           rud_da.sendv((pc_rud_out*rud_d2v)/2+2.5);
        pc_fin_out=0;           fin_da.sendv((pc_fin_out*fin_d2v)/2+3.5);
        beep();

        fin_mem.close();
        rud_mem.close();

//////////////////LOGGING DATA
        fin_memt=fopen("d:\\fin_temp","r");
        rud_memt=fopen("d:\\rud_temp","r");
        ofstream f_fin(fin_file);
        ofstream f_rud(rud_file);

        clrscr();
        cout<<"Just a moment...logging fin data";
        while (!feof(fin_memt))
        {
                tempc=fgetc(fin_memt);
                if (tempc!= EOF) f_fin<<tempc;
        }
        fclose(fin_memt);
        f_fin.close();

        cout<<"\nanother moment..logging rudder data";
        while (!feof(rud_memt))
        {
                tempc=fgetc(rud_memt);
                if (tempc!= EOF) f_rud<<tempc;
        }
        fclose(rud_memt);
        f_rud.close();
/*
        fclose(roll);
        fclose(ccu);
        fclose(herror);
        fclose(asu);
*/
}


////////////////////////////////////FIN DEMAND
void fin_demand()
{
        int n,nn;
```

```
        float numT, denT;

        for(n=11;n>1;--n) fin_x[n]=fin_x[n-1];

        if (fin_rate_fb) fin_x[1]=ip_data[7];
        else fin_x[1]=ip_data[1];
        numT=0;

        for(n=1;n<=11;++n) numT=numT+fin_x[n]*fin_num[n];

        for(n=11;n>1;--n) fin_y[n]=fin_y[n-1];
        denT=0;
        for(n=2;n<=11;++n) denT=denT+fin_y[n]*fin_den[n];
        fin_y[1]=numT-denT;
}

////////////////////////////RUD DEMAND
void rud_demand()
{
        int n,nn;
        float numT, denT;

        for(n=11;n>1;--n) rud_x[n]=rud_x[n-1];

        if (rud_rate_fb) rud_x[1]=ip_data[7];
        else rud_x[1]=ip_data[1];
        numT=0;

        for(n=1;n<=11;++n) numT=numT+rud_x[n]*rud_num[n];

        for(n=11;n>1;--n) rud_y[n]=rud_y[n-1];
        denT=0;
        for(n=2;n<=11;++n) denT=denT+rud_y[n]*rud_den[n];
        rud_y[1]=numT-denT;
}


////////////////////////////AP DEMAND
void ap_demand()
{
        int n,nn;
        float numT, denT;

        for(n=11;n>1;--n) ap_x[n]=ap_x[n-1];
        ap_x[1]=ip_data[5];
        numT=0;

        for(n=1;n<=11;++n) numT=numT+ap_x[n]*ap_num[n];

        for(n=11;n>1;--n) ap_y[n]=ap_y[n-1];
        denT=0;
        for(n=2;n<=11;++n) denT=denT+ap_y[n]*ap_den[n];
        ap_y[1]=numT-denT;

}


////////////////////////////READINGS
void readings()
{
        int i;

        for (i=1;i<=6; ++i)
        {
                ad.setchan(9+i);
                ip_data[i]=ad.readv();
        }
        ip_data[1]=ip_data[1]*roll_v2d;
        ip_data[2]=ip_data[2]*ccu_v2d;
        ip_data[5]=ip_data[5]*herror_v2d;
        ip_data[6]=ip_data[6]*asu_v2d;
/*
        fscanf(roll,"%f",&ip_data[1]);
        fscanf(ccu,"%f",&ip_data[2]);
        fscanf(herror,"%f",&ip_data[5]);
        fscanf(asu,"%f",&ip_data[6]);
*/
        ip_data[7]=(ip_data[1]-ip_data[8])/Ts;
        ip_data[8]=ip_data[1];
```

```
}


////////////////////////////CONTROLLER COEFFIECIENTS
void read_coeff()
{
        int i;
        FILE *file_ptr;
        float value, temp[23];


//Get the fin coeefiecients
        file_ptr=fopen("fin.k","r");
        i=0;
        while (!feof(file_ptr)){
                fscanf(file_ptr,"%f",&value);
                temp[i]=value;
                cout<<value<<"\n";
                ++i;
        }
        fclose(file_ptr);
        for(i=0;i<=10;++i)
                fin_num[i+1]=temp[i];
        for(i=11;i<=21;++i)
                fin_den[i-10]=temp[i];
        //Rate or angle feed back
        if (temp[22]>0)
                fin_rate_fb=1;

//Get the rudder controller coeefients
        file_ptr=fopen("rud.k","r");
        i=0;
        while (!feof(file_ptr)){
                fscanf(file_ptr,"%f",&value);
                temp[i]=value;
                cout<<value<<"\n";
                ++i;
        }
        fclose(file_ptr);
        for(i=0;i<=10;++i)
                rud_num[i+1]=temp[i];
        for(i=11;i<=21;++i)
                rud_den[i-10]=temp[i];
        if (temp[22]>0)
                rud_rate_fb=1;

//Get the autopilot controller coeefients
        file_ptr=fopen("ap.k","r");
        i=0;
        while (!feof(file_ptr)){
                fscanf(file_ptr,"%f",&value);
                temp[i]=value;
                cout<<value<<"\n";
                ++i;
        }
        fclose(file_ptr);
        for(i=0;i<=10;++i)
                ap_num[i+1]=temp[i];
        for(i=11;i<=21;++i)
                ap_den[i-10]=temp[i];
}


////////////////////////////////RUN TIME INFO
void get_info()
{
        char c;
        int p;

        clrscr();
        cout<<"********************* FIN INFORMATION ***************\n\n\n";
        cout<<"Do you wish fin stabilisation : (y/n) : "; cin>>c;
        if (c=='y')
                fin_info1[1]=1;
        else
                fin_info1[1]=0;

        if (fin_info1[1])
        {
```

```
		cout<<"\n\n1. CCU Controller alone \n";
		cout<<"2. PC based controller alone \n";
		cout<<"3. CCU and PC controller \n";
		cout<<"4. Sinusoid motion \n";
		cout<<"5. Constant d.c. level \n\n";
		cout<<"Enter : ";cin>>p;

		if (p==1)
		{
			fin_info1[2]=1;
			cout<<"\nEnter start time (secs) : "; cin>>fin_info2[1];
		}
		else if (p==2)
		{
			fin_info1[3]=1;
			cout<<"\nEnter start time (secs) : "; cin>>fin_info2[2];
			cout<<"...please enter gain for PC controller : ";cin>>fin_info2[3];
		}
		else if (p==3)
		{
			fin_info1[2]=1; fin_info1[3]=1;
			cout<<"\nEnter CCU start time (secs) : "; cin>>fin_info2[1];
			cout<<"\nEnter PC start time (secs) : "; cin>>fin_info2[2];
			cout<<"...please enter gain for PC controller : ";cin>>fin_info2[3];
		}
		else if (p==4)
		{
			fin_info1[4]=1;
			cout<<"\nEnter amplitude (degs) : ";cin>>fin_info2[4];
			cout<<"... and frequency (rad/s) : ";cin>>fin_info2[5];
		}
		else
		{
			fin_info1[5]=1;
			cout<<"\nEnter amplitude (degs) : ";cin>>fin_info2[6];
		}
		if (fin_info1[2]==1 && fin_info1[3]==0)
			cout<<"Saturation prevention NOT active";
		else
		{
			cout<<"\n\nImplement saturation prevention of servos after (secs) : ";
			cin>>fin_info2[7];
		}

		clrscr();
}

clrscr();
cout<<"********** RUDDER INFORMATION **********\n\n\n";
cout<<"Do you wish control of rudders (y/n) : ";cin>>c;
if (c=='y')
		rud_info1[1]=1;

if (rud_info1[1])
{
		cout<<"\n\n1. ASU Alone (default)";
		cout<<"\n2. PC autopilot ";
		cout<<"\n3. RRS + ASU";
		cout<<"\n4. RRS + PC autopilot";
		cout<<"\n\nEnter : ";cin>>p;
		if (p==1)
		{
			rud_info1[2]=1;
			cout<<"\nThe ASU will be on permanently ";
		}
		else if (p==2)
		{
			rud_info1[3]=1;
			cout<<"\nPlease enter autopilot gain : "; cin>>rud_info2[4];
		}
		else if (p==3)
		{
			rud_info1[4]=1;
			cout<<"\nRRS start time (secs) : "; cin>>rud_info2[1];
			cout<<"...enter gain : "; cin>>rud_info2[2];
			cout<<"\n\nThe ASU will remain active for entire sequence";
		}
		else if (p==4)
		{
			rud_info1[5]=1;
```

```
                        cout<<"\nPC autopilot must start before RRS";
                        cout<<"\nPC autopilot start time (secs) : "; cin>>rud_info2[3];
                        cout<<"...enter PC autopilot gain : "; cin>>rud_info2[4];
                        cout<<"\nRRS start time (secs) : "; cin>>rud_info2[1];
                        cout<<"...enter RRS gain : "; cin>>rud_info2[2];
                }
                if (rud_info1[2]==0)
                {
                        cout<<"\n\nActivate servo saturation prevention after (secs) : ";
                        cin>>rud_info2[5];
                }
        }

        clrscr();
        cout<<"***** SUMMARY *****";
        cout<<"-----------";
        cout<<"\n\n------FINS\n\n";
        if (fin_info1[1])
        {
                if (fin_info1[2] && fin_info1[3])
                {
                        printf("From 0 to %f secs NO stabilisation ",fin_info2[1]);
                        printf("\n...from %f to %f secs CCU only active ",fin_info2[1],fin_info2[2]);
                        printf("\n...from %f to %f secs pc fin stabilisation only",fin_info2[2],runT);
                        printf("\nPC gain is %f",fin_info2[3]);
                }
                else if (fin_info1[2])
                {
                        printf("No stabilisation from 0 to %f secs",fin_info2[1]);
                        printf("\n...CCU stabilisation alone active after %f secs",fin_info2[1]);
                }
                else if (fin_info1[3])
                {
                        printf("No stabilsation from 0 to %f secs ",fin_info2[2]);
                        printf("\n...PC active alone after %f secs with gain = %f",fin_info2[2],fin_info2[3]);
                }
                else if (fin_info1[4])
                        printf("Fin demand = %f*sin(%f t) degs",fin_info2[4],fin_info2[5]);
                else if (fin_info1[5])
                        printf("Fin demand = %f degs",fin_info2[6]);

                cout<<"\n\nSaturation prevention algorithm active after "<<fin_info2[7]<<" seconds.";
        }
        else
                cout << "NO FIN STABILISATION";

        cout<<"\n\n\n\n++++++++++RUDDERS\n\n";
        if (rud_info1[1])
        {
                if (rud_info1[2])
                        cout<<"ASU active from 0s to end of sequence ";
                else if (rud_info1[3])
                {
                        cout<<"PC Autopilot active from 0s with gain of ";
                        cout<<rud_info2[4];
                }
                else if (rud_info1[4])
                {
                        cout<<"ASU active from 0s to end of sequence ";
                        printf("\nRRS active after %f secs\n",rud_info2[1]);
                        printf("...with gain = %f",rud_info2[2]);
                }
                else
                {
                        printf("ASU active from 0 to %f secs",rud_info2[3]);
                        printf("\n...PC autopilot takes over at %f secs",rud_info2[3]);
                        printf("\n...at gain = %f",rud_info2[4]);
                        printf("\n\nRRS active from %f secs",rud_info2[1]);
                        printf("\n...with gain = %f",rud_info2[2]);
                }

                cout<<"\n\nSaturation algo active after "<<rud_info2[5]<<" seconds.";
        }
        else
                cout<<"ASU active by default\n";
        getch();
}

void beep()
{
        sound(500);
        delay(500);
```

```
        nosound();
}


//CHILDASA.cpp

///#include <dac.h>
#include <iostream.h>
#include <conio.h>
#include <iomanip.h>
#include <stdlib.h>
#include <math.h>
#include <fstream.h>
#include <string.h>
#include <stdio.h>


void K_coeff();

/*
main()
{
        K_coeff();
}
*/



////////////////////////////CONTROLLER COEFFIECIENTS
//File handeling program
void K_coeff()
{
        FILE *fin_ptr, *rud_ptr, *ap_ptr, *fin_store, *rud_store, *ap_store;
        int finK, rudK, apK;
        float value;

        cout<<"\n\nPlease enter FIN controller number : ";cin>>finK;
        cout<<"Please enter RUDDER controller number : ";cin>>rudK;
        cout<<"Please enter AUTOPILOT controller number : ";cin>>apK;

        if (finK==1) fin_ptr=fopen("fin1.k","r");
        else if (finK==2) fin_ptr=fopen("fin2.k","r");
        else if (finK==3) fin_ptr=fopen("fin3.k","r");
        else if (finK==4) fin_ptr=fopen("fin4.k","r");

        else if (finK==5) fin_ptr=fopen("fin5.k","r");
        else if (finK==6) fin_ptr=fopen("fin6.k","r");
        else if (finK==7) fin_ptr=fopen("fin7.k","r");
        else if (finK==8) fin_ptr=fopen("fin8.k","r");
        else if (finK==9) fin_ptr=fopen("fin9.k","r");
        else if (finK==10) fin_ptr=fopen("fin10.k","r");
        else if (finK==11) fin_ptr=fopen("fin11.k","r");
        else if (finK==12) fin_ptr=fopen("fin12.k","r");
        else if (finK==13) fin_ptr=fopen("fin13.k","r");
        else if (finK==14) fin_ptr=fopen("fin14.k","r");
        else if (finK==15) fin_ptr=fopen("fin15.k","r");
        else if (finK==16) fin_ptr=fopen("fin16.k","r");

        else fin_ptr=fopen("fin1.k","r");

        cout<<"\n\nfinK is "<<finK;
        fin_store=fopen("fin.k","w");
        while (!feof(fin_ptr)){
                fputc(fgetc(fin_ptr),fin_store);
        }
        fclose(fin_ptr);
        fclose(fin_store);

        if (rudK==1) rud_ptr=fopen("rud1.k","r");
        else if (rudK==2) rud_ptr=fopen("rud2.k","r");
        else if (rudK==3) rud_ptr=fopen("rud3.k","r");
        else if (rudK==4) rud_ptr=fopen("rud4.k","r");
        else if (rudK==5) rud_ptr=fopen("rud5.k","r");
        else if (rudK==6) rud_ptr=fopen("rud6.k","r");
        else if (rudK==7) rud_ptr=fopen("rud7.k","r");
        else if (rudK==8) rud_ptr=fopen("rud8.k","r");
        else if (rudK==9) rud_ptr=fopen("rud9.k","r");
        else if (rudK==10) rud_ptr=fopen("rud10.k","r");
        else if (rudK==11) rud_ptr=fopen("rud11.k","r");
        else if (rudK==12) rud_ptr=fopen("rud12.k","r");
```

```
else if (rudK==13) rud_ptr=fopen("rud13.k","r");
else if (rudK==14) rud_ptr=fopen("rud14.k","r");
else if (rudK==15) rud_ptr=fopen("rud15.k","r");
else if (rudK==16) rud_ptr=fopen("rud16.k","r");
else rud_ptr=fopen("rud1.k","r");

cout<<"\nrudK is "<<rudK;
rud_store=fopen("rud.k","w");
while (!feof(rud_ptr)){
        fputc(fgetc(rud_ptr),rud_store);

}
fclose(rud_ptr);
fclose(rud_store);

if (apK==1)             ap_ptr=fopen("ap1.k","r");
else if (apK==2) ap_ptr=fopen("ap2.k","r");
else if (apK==3) ap_ptr=fopen("ap3.k","r");
else if (apK==4) ap_ptr=fopen("ap4.k","r");
else ap_ptr=fopen("ap1.k","r");

cout<<"\napK is "<<apK;
ap_store=fopen("ap.k","w");
while (!feof(ap_ptr)){
        fputc(fgetc(ap_ptr),ap_store);
}
fclose(ap_ptr);
fclose(ap_store);

cout<<"\n\nLeaving CHILD.cPP";

}
```

APPENDIX I - PUBLISHED WORK

SEA-TRIAL EXPERIMENTAL RESULTS OF FIN/RUDDER ROLL STABILISATION

M.T. Sharif[1], G.N. Roberts[2], R. Sutton[3]

1. Royal Naval Engineering College, Plymouth, PL5 3AQ, U.K.
2. Gwent College of Higher Education, Newport, NP9 5XR, U.K.
3. University of Plymouth, Plymouth, PL4 8AA, U.K.

Abstract: This paper reports on full-scale roll stabilisation trials on board a frigate-size Royal Naval warship. The trials entailed comparing the efficacy of the fins functioning alone, with the combined effects of the fins and rudders operating in congress to reduce roll motions. The rudders were employed in a supplementary role and no mechanical modifications were made. To afford a comparison of the results the data acquired is presented in the RMS form.

Keywords: Fins, Rudders, Roll Stabilisation, Classical Control

1. INTRODUCTION

The roll stabilisation of ships when subject to the inclemencies of its operating environment has been an active area of research since the advent of large-scale shipping. A plethora of devices have been constructed and implemented with varying degrees of success. Perhaps the most propitious device has been the Brown Brother fin stabilisers. Recognising their advantages in ship operability, the Royal Navy as a matter of policy fits such equipment to all its warships of appropriate size.

Recent advances which have demonstrated the feasibility of utilising the rudder in roll stabilisation (RRS) (Cowley 1972; Amerongen 1987) has imparted an impetus to the Royal Navy to initiate research effort into this area, specifically, to examine the effectiveness of the rudders in a secondary stabilisation role to the fins.

Using the rudders exclusively in the stabilisation role would have detrimental repercussions on the rudder bearings and servomechanism due to the added motion. However, it is possible to circumvent the necessarily expensive costs of upgrading the rudder bearings and installing more powerful motors in the hydraulics if they are utilised as described. Hence, this route of enhanced stabilisation is expedient and most attractive to the Royal Navy. This paper reports on the first phase of sea trials conducted on board a frigate-size warship during 7-8th March 1994. The second section describes the linear mathematical models of the ship system on which depends the control theory to generate adequate controllers. Also, the physical constraints are described. The third section deals with the control theory adopted. Prior to going on board considerable technical preparations were made which are elaborated in section 4. Penultimately, trials conducted are detailed and results presented. Finally, some conclusions are drawn, with suggested recommendations.

2. SYSTEM MODELLING

Royal Naval frigates are, as mentioned, equipped with fin stabilisers. These are geometrically located in the plane of the centre of gravity (cog) of the ship when loaded under normal conditions. Thus, since moments act through the cog of any body, the fins can impart the maximum roll moment possible. The relative location of these is shown in Figure 1.

The synthesis of controllers for any system requires a linear mathematical representation of their associated dynamics. The initial effort is then to

acquire such models which accurately embody the physical behaviour of the plant.

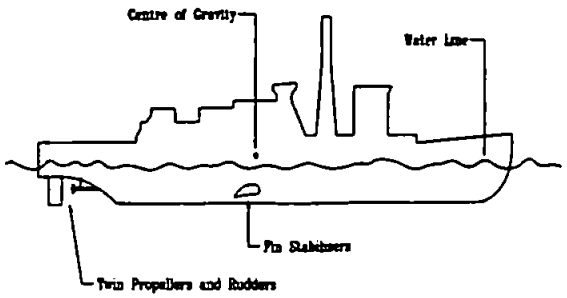

Fig 1. Location of fins and rudders

Figure 2 is a multivariable model of the ship system in terms of fin/rudder induced motions. The transfer functions which relate fin/rudder to ship motions are of interest only (g11(s) and g12(s)). These were derived from sea trials and successively refined over time. To ensure their reliability, comparisons were performed with the seakeeping prediction software at Haslar, U.K. This software has been developed utilising strip theory, and verified with extensive sea trials data. The results afforded a degree of confidence in the models which will be employed in subsequent controller design

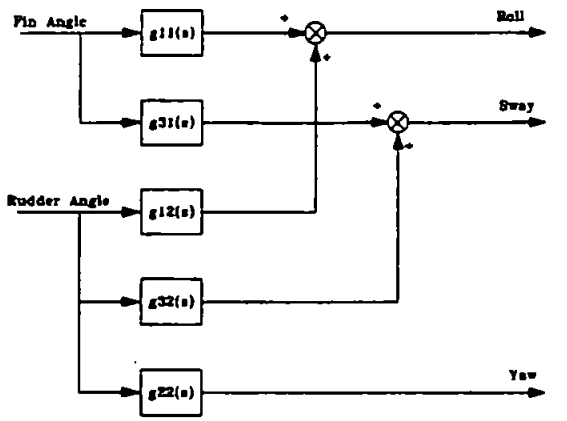

Fig. 2 Multivariable ship motion model

2.1 Stabilising fins

The fins act as actuators in the control loop; imparting a regulated moment about the ship's axis of roll in opposition to the sea-induced roll. Marshfield (1981) derives a simple second-order transfer function to model this roll (1).

$$g11(s) = \frac{k_{11}0.25}{s^2+2\zeta_\omega 0.5s+0.25} \qquad (1)$$

Here k_{11} represents the non-linear relationship between the moment generating effectiveness of the fins and ship speed. The damping ratio, ζ_ω, is derived empirically. The parameters were subsequently refined by Whalley (1981) and Roberts (1989).

2.2 Rudder dynamics

In ships of appropriate size a peculiar phenomenon is observed, namely that when the ship's rudder is 'put-over' the ship exhibits a proclivity to initially heel inwards. During this heel in the 'wrong' sense, no significant yaw motion occurs. Eventually the ship rolls outwards and the ship enters a steady-state turn. Such behaviour is illustrated by Figure 3 which shows the roll and yaw motions with the typical time scales involved. This ephemeral roll motion may be explained by hydrodynamic considerations detailed in (Rawson and Tupper, 1984).

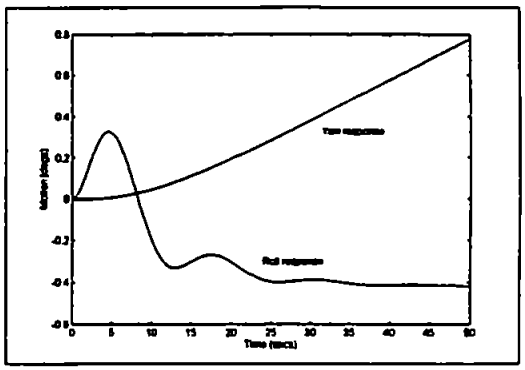

Fig. 3 Rudder-induced ship motion

In terms of roll stabilisation, several studies, for example (Amerongen, 1982) and (Katebi, 1978), have been conducted to establish the applicability of utilising the rudders exclusively in the stabilisation of ships. However, it is realised that this characteristic may rather be, harnessed in congress with the fin stabilisers to accrue greater roll stabilisation.

The transfer function is derived in a similar manner as previously (2)

$$g12(s) = \frac{k_{12}0.25(1-8.75s)}{(1+8.2s)(s^2+0.25s+0.25)} \qquad (2)$$

A non-minimum phase zero is incorporated to impart an initial inward heel to the model when simulated in the time domain. As before, k_{12} is a parameter to represent the non-linear behaviour of the rudder with ship speed.

Both models are now accurately represented by the mathematical models, particularly at a ship cruising speed of 18 knots. This is then the nominal model exploited for controller design.

2.3 Fin and rudder hydraulics

The effectiveness of roll stabilisation is completely dependent upon the servomechanism which activates the control surfaces.

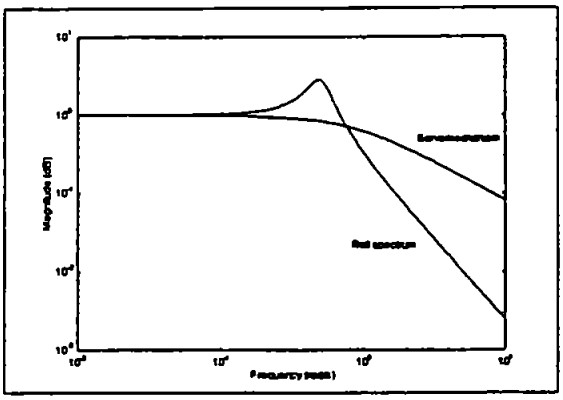

Fig. 4 Typical roll and servomechanism frequency response

This is illustrated in Figure 4, which shows a typical frequency response of ship roll and servomechanism. If the servomechanism frequency response encompasses the entire ship roll response then it will actively stabilise at all frequencies of motion. At the very minimum it should extend beyond the ship roll resonance peak, where sea-induced roll is amplified.

For both the fin and rudder hydraulics there are associated with their mechanics two non-linearities, which are modelled as shown in Figure 5.

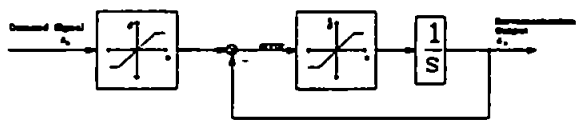

Fig. 5 Non-linear servomechanism model

The first saturation element models the maximum angles of excursion. For adequate stabilisation, the slew of the servomechanism is of paramount importance. This is non-linear to the extent that their maximum rate is restricted. This slew limitation is manifested by bandwidth consideration of the frequency response in Figure 4. The slew non-linearity is modelled by the second saturation element in the feedback loop. For the fins the maximum angle of excursion is $\pm 30^0$; for the rudders $\pm 28^0$. Slews of $\pm 30^0 s^{-1}$ and $\pm 6^0 s^{-1}$ for fins and rudders are representative of the Royal Navy vessels considered.

The servomechanisms are driven into saturation if either amplitude or frequency, or both components, of the control signal is excessively large. The consequence of this is that the bandwidth of the servomechanism reduces, further exacerbating the deficiency in slew. There are other detrimental repercussions to be considered: wear of the components increases, greatly reducing Mean Time Between Failure (MTBF), introduction of intolerable phase lags, precipitating system instability, generation of spurious frequency components, and most significantly, invalidation of linear control laws. Therefore, it is imperative that some contingency algorithm be available to avoid saturation.

It is possible to relate the RMS value to the bandwidth of the servomechanism. Therefore, a scheme is used which monitors this RMS level and alters the gain of the control signal such that the bandwidth remains above a predetermined value (Sharif, 1993).

2.4 Sea disturbance

Unstabilised roll motions on a ship are induced by the hydrodynamic interaction between the sea and the ship's hull. An adequate model representation of this 'noise' is required in order to ascertain the frequency and amplitude envelope of the perturbations the ship is likely to encounter in the environment. This information is used to design a controller which has appropriate sensitivity properties enabling it to reject the interference.

A representation of the sea spectrum may be well encapsulated by the Bretschneider model (3), where H is the significant wave height and T the modal period.

$$S(\omega) = \frac{691}{T^4\omega^5}\left[\frac{H_{\frac{1}{3}}}{2}\right]^2 \exp\left[\frac{-691}{T^4\omega^4}\right] \qquad (3)$$

This gives the spectrum of the sea and may be implemented in software for time simulation by passing white noise through a Laplace domain transfer function which approximates (3), the Bretschneider spectrum.

3. CONTROL STRATEGY

Having established reliable models for the pertinent constituents of the ship system, it is possible to proceed with the control design. As this paper reports the first phase of sea trials, the controllers tested were derived from well-promulgated control theory, namely classical control.

The configuration of the overall fins and rudder stabilisation loops are shown in Figure 6. Since there is no interference between rudder and fin loops, they

may be treated independently in the controller design. Furthermore, there is sufficient frequency separation between rudder-induced roll and yaw motions such that the effect of the rudder in its roll stabilisation role has a negligible detriment on yaw motions.

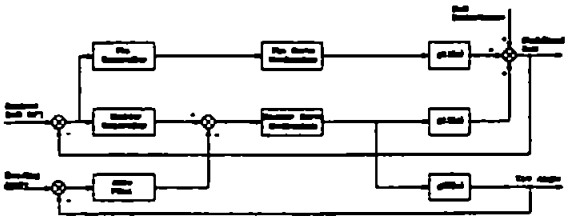

Fig. 6 Fin/rudder control configuration

The controller can exactly oppose the disturbance moment with the fin/rudder generated moment only at one frequency. This frequency location is chosen at the roll resonance of the ship. Therefore, the strategy is to ascertain the phase lag introduced by the fin/ship, or rudder/ship, interaction and the servomechanism and inject the phase advance of the same magnitude. Hence, the net phase will be zero between the control action and the ship motion and complete roll reduction will result at roll resonance.

However, at other frequency locations the roll reduction will be less than complete. Figure 7 illustrates the method of roll reduction. It is a Nyquist locus of the system. Considering the fin loop only, the same analysis follows for the rudder loop. The disturbance rejection transfer function is given by

$$\frac{\theta}{D} = \frac{1}{1+G_{cF}(s)g11(s)} \qquad (4)$$

It can be seen from (4), where D is the disturbance and θ the roll angle, and from Figure 7, that the system will accrue roll reduction provided that $|(1 + G_{cF}(j\omega)g11(j\omega)| < 1$, effectively at those frequencies where the locus lies outside the unit circle, centred at (-1,0). Amplification of roll will occur over the locus when it is inside unit circle.

For both the fin and rudder loops the following transfer function, (5) and (6) respectively, for the controllers will achieve the phase objectives as suggested by (Lloyd, 1974).

$$G_{cF}(s) = \frac{(k_{f1}s^2+k_{f2}s+k_{f3})k_{\phi}k_{\beta}}{0.003s^3+0.43s^2+0.43s+1} \qquad (5)$$

$$G_{cR}(s) = \frac{(k_{r1}s^2+k_{r2}s+k_{r3})k_{\eta}k_{\eta}}{0.05s^2+0.5s+1} \qquad (6)$$

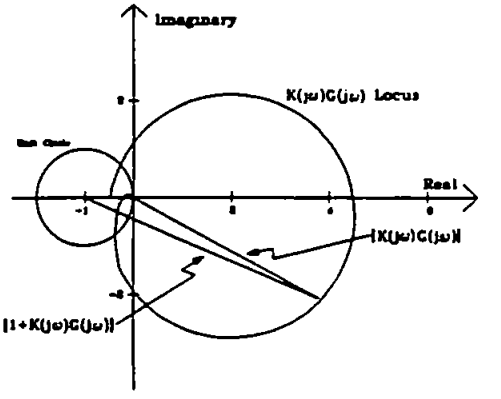

Fig. 7 Nyquist locus of ship stabilisation system

The parameters, k_{f1} etc and k_{r1} etc, may be selected by the designer to meet particular objectives in motion stabilisation. The remaining parameters, k_{ϕ} and k_{η}, are the ship's speed-dependent gains to account for non-linear hydrodynamic variations in fin and rudder performance. The parameters k_{β} and k_{η} dictate the amount of roll reduction achieved, given the constraints in terms of servomechanism saturation.

4. PREPARATION FOR THE SEA TRIALS

In order to record data and control the actuators, a considerable amount of preparation was required, in terms of not only the software and controller design, but also of the hardware implications necessary to interface with the fin and rudders, given the nature of the environment on board a warship.

4.1 Software development

To implement the controllers, they must be converted into a digital representation. Using a bilinear transformation technique difference equations for the controllers were derived and subsequently encoded into software routines in C++.

A prerequisite for this method is the consideration of the sampling time adherence to the Nyquist sampling criteria. The natural roll period of the ship is approximately 10.5 seconds. It was decided that a 0.5 second sampling period should not only provide an accurate reconstruction of the signals but also sufficient period for data storage, graphical display, and calculation for the next control output.

4.2 Interface to ship

It was imperative to interface with the ship's fin/rudders with the minimal of disruption to ship operations and machinery. A schematic of the wiring configuration is given in Figure 8.

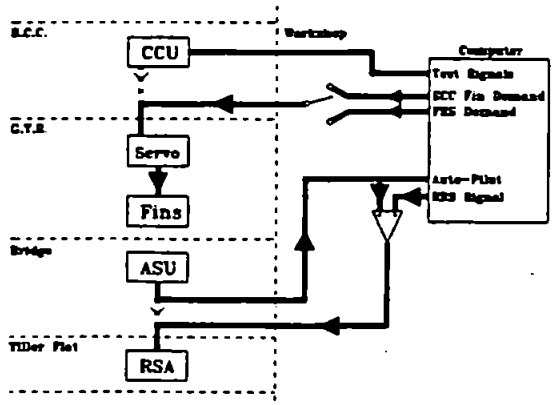

Fig. 8 Interconnection schematic

The computer was installed in the workshop. Normally the fins are controlled by the ship's Central Control Unit (CCU) located in the Ship Control Centre (SCC). The CCU provides demand signals to the servomechanisms situated in the Gas Turbine Room (GTR) and test outputs for the user. It was possible to disconnect this route and replace it with computer-generated signals, namely FRS mode. The configuration incorporates a safety feature, in that it is physically possible to revert to CCU control of the fins should a malfunction occur in the computer.

The signals required to be associated with the rudder loop are heading error and autopilot demand. The Auto Steering Unit (ASU), which is located at the bridge, furnishes both these signals. The connections between the bridge and the rudder servomechanism, in the tiller flat, were broken and re-routed via the workshop and computer. This necessitated the signals travelling approximately 50 metres one way without the aid of boosters. Fortunately, this did not prove to be a serious impediment to effective signal reception.

The autopilot signal is superimposed on the RRS signal lest interference occur with the direction of the ship. Therefore, when the RRS is not engaged, the autopilot is the default signal to the rudders. In this way both the fins and the rudder systems are completely controlled by the computer software.

5. RESULTS

A large number of individual trials were conducted with various controllers and the fin/rudder modes of operation. The fins and rudders were engaged with three different sequences, and repeated several times with an assortment of controllers. Each sequence had a duration of 400 seconds. The data was subsequently analysed and presented in terms of RMS values.

For the entire duration of the trials the sea remained at around state two. Unfortunately, such calm weather is not expedient for roll stabilisation trials. Typical roll motions which were experienced are shown in Figure 9.

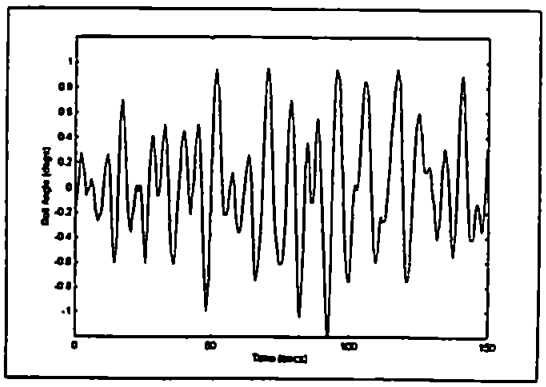

Fig. 9 Typical roll motions experienced

However, significant fin motion was observed indicative of stabilisation occurring, therefore, it was decided to proceed with the trials.

A summary of the fin/rudder configurations of operation are given in Table 1.

Table 1 Summary of modes of operation for trials.

Time	0-100 secs			100-400 secs		
Mode	CCU	FRS	RRS	CCU	FRS	RRS
Sqn 1	ON	OFF	OFF	OFF	OFF	ON
Sqn 2	ON	OFF	OFF	ON	OFF	ON
Sqn 3	ON	OFF	OFF	OFF	ON	ON

Results for sequence 1. This involved having the ship stabilised by the fins for the first 100 seconds using the CCU generated signal. After 100 seconds the RRS was engaged and the fins switched off and set to their neutral position. This would afford direct comparison of fin stabilisation with RRS.

Table 2 Typical results of sequence 1

RMS	Roll		Fin Activity		Rudder Motion		Heading Error	
Time	<100	>100	<100	>100	<100	>100	<100	>100
Run 1	0.19	0.19	0.94	0	0	2.39	8.21	10.4
Run 2	0.42	0.49	1.46	0	0	5.83	9.81	10.9

Two sets of runs are shown with sequence 1 in Table 2 for two different controllers. RMS statistics are collated for various relevant signals, before and after 100 seconds. It is seen that when the fins are switched off the roll value does not change significantly for either controller during RRS

operation. Also, the fins and rudder activity remain within acceptable bounds.

Results for sequence 2. This sequence will establish that employing the rudders in a supplementary role will result in enhanced levels of roll reduction. The trials entailed employing the CCU fin stabilisers during the entire 400 seconds test period. After 100s the RRS was engaged. The results are displayed in Table 3, for two typical runs.

For both controllers, when the rudders are engaged higher stabilisation levels are achieved, of approximately 25%. Note also that fin activity correspondingly diminishes as the rudders assist in generating the roll-correcting moments.

Table 3 Typical results of sequence 2

RMS	Roll		Fin Activity		Rudder Motion		Heading Error	
Time	<100	>100	<100	>100	<100	>100	<100	>100
Run 1	0.63	0.46	4.48	1.08	0	3.46	10.1	11.3
Run 2	0.61	0.45	4.17	1.01	0	3.13	10.3	10.8

Results for sequence 3. The final sequence entailed controlling both the rudders and fins from the computer. Therefore, the CCU signal was replaced by the computer signals after 100s. At the same time the rudders were engaged in the stabilisation mode. The resulting RMS values are shown in Table 4.

Table 4 Typical results of sequence 3

RMS	Roll		Fin Activity		Rudder Motion		Heading Error	
Time	<100	>100	<100	>100	<100	>100	<100	>100
Run 1	0.57	0.57	1.28	0.85	0	3.41	9.94	11
Run 2	0.58	0.54	1.3	0.77	0	2.99	10.8	11.1

When the computer controls both the fins and rudders the roll RMS exhibits a marginal improvement. As expected from previous results. The fin activity decreases due to RRS being operational.

6. CONCLUSIONS AND DISCUSSION

As mentioned earlier the sea state remained very low. Such comparatively small amplitudes of roll motion will not greatly exert the controllers. Therefore, their full effectiveness can not be appreciated. Furthermore, due to ship operations the speed remained at 12 knots, limiting the moment-generating capabilities of the actuators.

Despite these unsuitable environmental conditions, valuable conclusions can be derived from the data gathered. Sequence 1 manifests the similar effectiveness of the rudders with fins in roll stabilisation at low sea states. The trials vindicated the most important objective, that employing the rudders in a supplementary role with the fins enhances roll stabilisation, as can be demonstrated by the results from Sequence 2. Furthermore, the results compare favourably with the time simulation data generated at the design stage, affording considerable confidence in the mathematical models for future control design. Finally, the experience tested the reliability and versatility of all aspects of the software and hardware which was developed.

In conclusion, the sea trials gave encouraging results in utilising the rudders in a supplementary role to the fins, without any modifications to the machinery. It is envisaged that at higher sea states the saturation-prevention mechanism will realise its potential. The next phase of trials will examine other controllers which will be arrived at via different control theory, and the results will be presented.

REFERENCES

Amerongen, J. van. (1987) RRS: Controller Design and Experimental Results, *8th Ship Control Systems Symposium* pp1.128-1.142

Amerongen, J. van. (1982) Rudder Roll Stabilisation, *4th International Symposium on Ship Operation and Automation*, pp 43-50

Cowley, W.E. (1972) The Use of Rudder as Roll Stabiliser, *3th Ship Control Systems Symposium* Vol. C

Katebi, M.R. (1978) LQG Autopilot and RRS Control Systems, Design *8th Ship Control Systems Symposium* pp3.69-3.84

Lloyd, A.R.J.M. (1974) Roll Stabiliser Fins : A Design Procedure, *RINA Architects* Vol. 85 pp233-254

Marshfield, B. (1981) HMS **** Roll Stabilisation Trials, *Admiralty Marine Technology Establishment* R81012 (Restricted)

Rawson, K.J., E.C. Tupper (1984) *Basic Ship Theory*, Longman, Bath

Roberts, G.N. (1989 Ship Motion Control Using a Multivariable Approach, *PhD Thesis*, University of Wales

Sharif, M.T. (1993) Investigation of Bandwidth Dependency on RMS Values in Servomechanisms, R.N.E.C., *Internal Report* 93025 (Restricted)

Whalley, R., J.H. Westcott (1981) Ship Motion Control, *6th Ship Control Systems Symposium* ppH1.1-H1.16

Lateral Force Stabilisation : A Comparison of Controller Designs

by

M.T. Sharif*, G.N. Roberts*, S.A. French* R. Sutton**
* Royal Naval Engineering College, Manadon, Plymouth, U.K.
** University of Plymouth, Plymouth, U.K.

Nomenclature

$\eta_a = (a, \phi, \psi)$: *Angular motion (Roll Pitch Yaw)*

$\eta_T = (h_1, h_2, h_3)$: *Translatory Displacement of cg*

$x \in \mathbb{R}^{n \times n}$, $Q > 0 \in \mathbb{R}^{n \times n}$ $R \geq 0 \in \mathbb{R}^{m \times n}$

P = (x,y,z) : Position on Ship
D = (D_1, D_2, D_3) : Displacement (earth reference) of Point P
X : Cross-product
u : Control Effort, (optimal control)
y : Measured Signals (optimal control)
ω_n : Sea Disturbance Natural Frequency of Roll

1 Introduction

The ship's company of a modern warship may be seen as the metaphorical blood and heart of the machine. Indeed each individual member is a slave to the ship, catering to its essential requirements to ensure an optimal fighting capability. This symbiotic relationship is often disturbed by the prevailing forces of nature ie sea movement, wind and weather which buffet the ship in a seemingly unpredictable fashion. Thus creating a most hazardous environment for the crew. Subsequently degrading the performance of the human operators to such an extent that routine functions may have to be abandoned, commands to launch weapons may be impossible, rendering the fighting ship impotent.

In ships which have been stabilised for roll, experienced crew often report the "roughness" of the ship motion. This is taken to mean lateral acceleration being aggravated despite ameliorating the roll. It is increasingly recognised that the lateral motions of a ship are a greater impediment to effective crew performance rather than the pure roll alone. Monk [1] demonstrates that a human operator's ability to perform a task would be impaired by 20-30% under conditions of 6° RMS of roll, and would be impaired by 50% under 0.07g RMS lateral acceleration. Furthermore, he recommended that lateral accelerations should not to exceed $1.5 ms^{-2}$ at the bridge in order yield a satisfactory roll motion.

Over the course of time ship designers have sought to control the motions of a ship thereby restore that symbiotic

harmony. The devices employed to achieve this have been successful to varying degrees. Perhaps the most propitious in this respect have been active stabilisation fins. Such devices are fitted to all Royal Navy ships of appropriate size. The feasibility of utilizing the rudder in a similar function, rudder roll stabilisation (RRS), was recognised by Cowley [2,3] and Lloyd [4] amongst others. However, after the initial research further development was hampered due to stability problems. The baton of research effort was again taken up by Kallstrom, Van Amerongen and Klugt [5-13]. This effort culminated in a fully operational RRS system in the Royal Netherlands Navy. Albeit as a result of the control strategy pursued it necessitated extensive redesign and updating of hydraulic equipment to move the rudder faster.

This paper sets out to develop a novel approach to model the lateral accelerations of a ship in terms of transfer functions in the s-domain. Thus making them more amenable to control design. A classical and optimal control strategy is proposed to use existing rudder servo-mechanisms in order to implement lateral acceleration stabilisation.

2 Lateral Force Estimator (LFE)

2.1 Applicability

Over the last decade considerable research effort has been dissipated in designing controllers for roll stabilisation utilizing the rudder. The efficacy of one controller design over another is assessed by means of the resultant stabilised RMS roll motion in a particular sea state. As a technical criterion this is sufficient. However, no correlation is attempted between the roll stability of a ship and the performance of its crew. Intuitively one may suspect that the greater the roll stability so correspondingly should the crew performance increase approaching their optimal. This is not necessarily so.

The roll reduction criterion does not consider that a member of the crew encounters greater impedance in his task if he cannot maintain a grip on the surface of the vessel. Lose of grip is induced by acceleration of the ship in parallel with the ship deck, rather like having a rug pulled from under one's feet, thus necessitating the crew to seek a solid, fixed object to grasp least they should completely lose their balance. It then becomes extremely difficult to perform manual tasks when subject to these unpredictable motions. Such a motion is called Lateral Force Estimator (LFE).

This LFE induced degradation in crew performance would suggest a more meaningful criteria to assess ship motion stabilisation. Baitis [14] tentatively characterises these as Motion Induced Interruptions (MII), the likelihood of an interruption in a task due to accelerations parallel to the deck. Attention is drawn to the fact that MII differs from Motion Sickness Incidence (MSI) in that these are derived from motions normal to the deck. In ref [15] Baitis continues this

line of research. More recently Monk [16] makes an exhaustive examination into the impact of LFE on crew performance in several classes of ship and under varying environmental conditions. Graham [17] has countenanced the same scenario from a rigorous and detailed mathematical approach.

Despite this intellectual effort to understand and collate the varying aspects of the interaction between human performance and LFE very little effort has been made to attempt a controller design for the fin/rudder to alleviate LFEs. Tang [18,19] made a feasibility study using the fins and the rudder respectively for LFE stabilisation. However, the simulation studies employed existing RRS controllers and simulations using a ship motion prediction software which is written in terms of strip theory. Unfortunately, these types of simulation model are not easily accessible to control design in terms of bandwidth and robustness margins.

2.2 The Theory

LFE is a vector summation of earth referenced and lateral acceleration in the plane of the deck (due to wave induced lateral accelerations) and a roll angle induced lateral acceleration. It should be noted that the LFE is only a valid estimator of MII under conditions in which the vertical accelerations are negligible. This condition is necessary to distinguish it from lateral accelerations.

An initial attempt was made by Bell [20] to stabilise a motion similar to LFE; the apparent vertical. This is the earth referenced roll motion due to sway, which is analogous to swinging a ship as a pendulum. However, he concluded that it was not practical to stabilise such a motion.

Consider figure 1 which shows the earth and ship referenced accelerations.

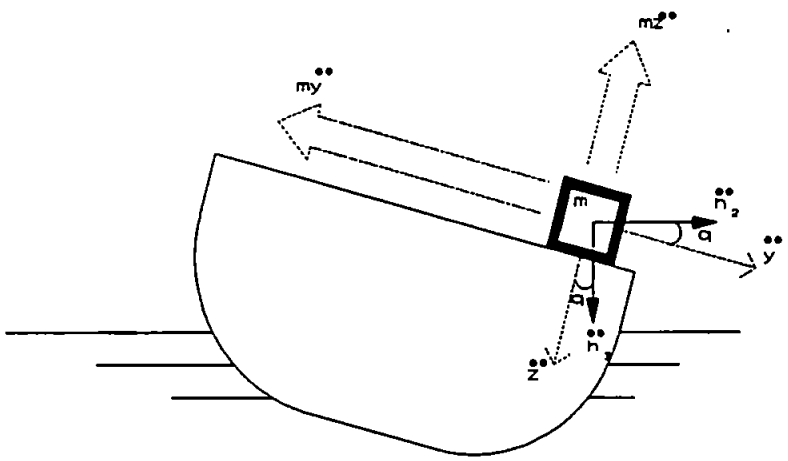

Figure 1 Accelerations Acting Parallel to Ship Deck

In general

$$D=\eta_T+\eta_a XP$$

$$D_2=h_2+x\psi-za \qquad \text{+ve to starboard}$$

With reference to figure 1 resolving the acceleration parallel to the deck

$$\ddot{y}=\ddot{h}_2\cos(a)+\ddot{h}_3\sin(a) \tag{1}$$

The total apparent force experienced by mass m, parallel to deck, given that it is subject to gravitational forces resolved to the normal and parallel to deck :

$$m\ddot{y}-mg\sin(a) \quad port \tag{2}$$

Hence, apparent acceleration :

$$\begin{aligned}\ddot{h}_{A2}&=\ddot{y}-g\sin(a)\\&=\ddot{h}_2\cos(a)+\ddot{h}_3\sin(a)-g\sin(a)\end{aligned}$$

And for small amplitude motions

$$\ddot{h}_{A2}=\ddot{h}_2-ga \tag{3}$$

Hence

$$\ddot{h}_{A2}=\ddot{h}_2+x\ddot{\psi}-z\ddot{a}-ga \tag{4}$$

In this study only one point is considered which is at the main deck above the centre of gravity (cg). Therefore, the ψ term may be ignored leaving the sway and roll induced lateral accelerations.

2.3 Mathematical Modelling

2.3.1 Sea Disturbance Model

The external disturbance on the ship: winds, which induces waves and the sea current, must be modelled in order to assess the efficacy of any controller in computer simulations. A steady state wind or current would cause a permanent list to the ship which cannot be corrected by RRS. Therefore the only disturbance modelled is the sea waves.

It is possible to describe the waves as a frequency spectrum shaped to emulate what the ship would perceive at

various headings. A Bretschneider sea spectrum is used and described by :

$$S(\omega) = \frac{691}{(T^4\omega^5)}\left[\frac{H_{\frac{1}{3}}}{2}\right]^2 \exp\left(-\frac{691}{T^4\omega^4}\right) \quad m^2 s$$

Such a frequency spectrum is well represented by a second order filter of the form

$$H(s) = \frac{k_s\omega_n^2}{s^2 + 2z_n\omega_n s + \omega_n^2}$$

The input to the filter being white noise. The natural frequency of oscillation, ω_n is varied in accordance with the encounter frequency. The damping ratio z_n and k_s are also changed to meet the changing RMS motion values with increasing sea states. In this study sea state five is used throughout as a disturbance. Not only will this afford a robust test of the controllers but also Monk [16] suggests that this is where most LFE occurs.

A similar transfer function model was developed from unstabilised ship roll data provided by the Defence Research Agency at Haslar and from published results in [24].

2.3.2 Ship Dynamics

The multivariable ship model is shown in figure 2. It can be seen that the rudder and the fins give rise to sway and roll motions [4].

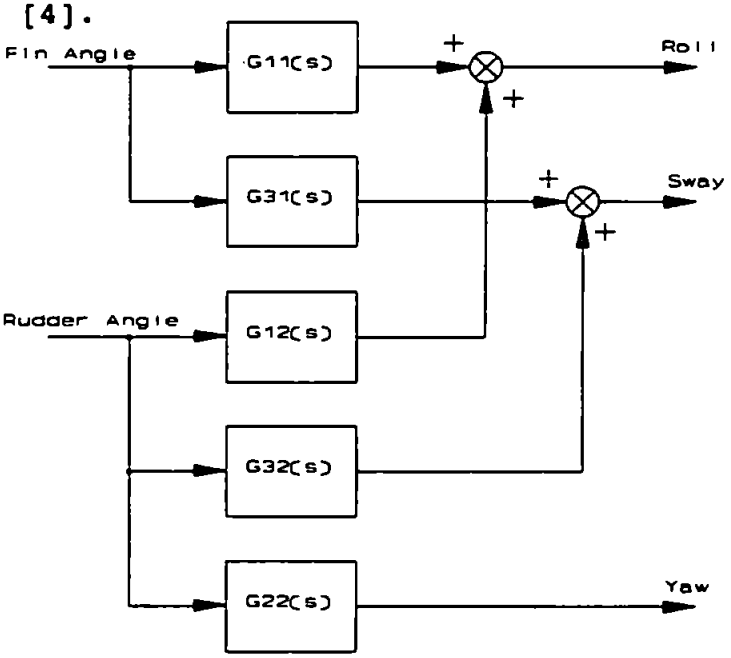

Figure 2 Multivariable Ship Motion Model

The fin/roll (G11(s)), rudder/roll (G12(s)) and rudder/yaw (G22(s)) transfer functions were derived by heuristic iterations and are well documented in literature [13,23,25]. Using data furnished by DRA Haslar from forced fin and rudder roll trials a rudder/sway (G32(s)) transfer function was established. However, owing to significant interaction between sway and roll in the forced fin roll responses, it was not possible to ascertain any reliable transfer function for G31(s). Therefore only the rudder will be employed in subsequent controller design. The results of the transfer functions correlated well with the data documented in reference [13]. It must be noted that the transfer functions are for a frigate size ship travelling at 18 knots.

The LFE signal is a vector summation of three constituent parts as given in equation (4). When combining these the phase relations between them are imperative. Their relative phases are documented in [23] "...sway leads wave phase by 90° and as ω tends to zero, sway amplitude tends to wave amplitude". Also a similar assertion is found in [20] "...addition is subject [roll plus sway acceleration] to a phase correction of 90°."

Adhering to these promulgations the constituent blocks for the LFE signal are now constructed. Figure 3 shows the schematic to generate the LFE signal.

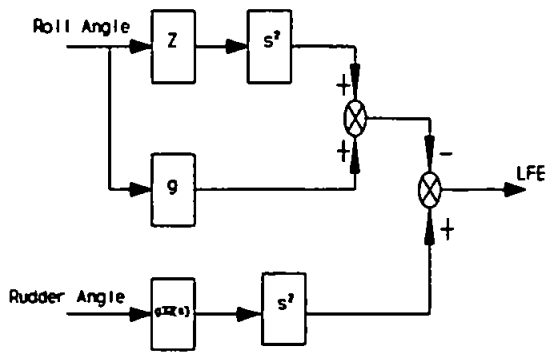

Figure 3 : LFE Components

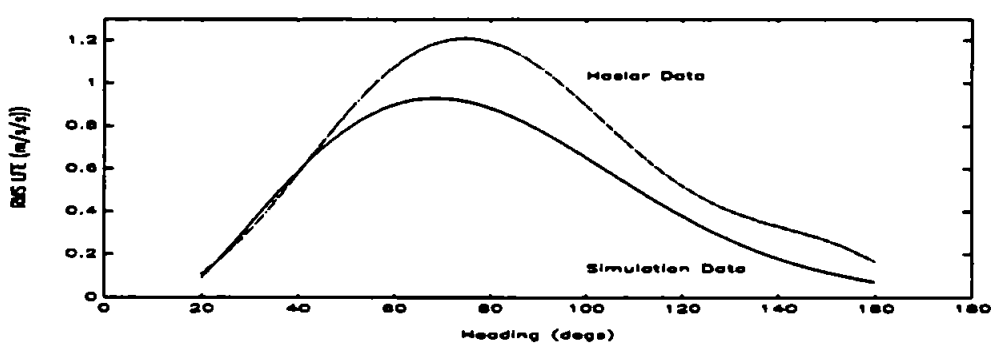

Figure 4 LFE Comparison

Examining the phase relationships between sway and roll shows tenuous adherence to the conditions above. However, upon simulations at various headings for the unstabilised case gave acceptable approximations to the LFE results published in reference [18,19] and with DRA Haslar data as shown in Figure 4. Although the LFE simulation signal is consistently underestimated a gain term could be added at the output to rectify this.

2.3.3 Rudder Servo-Mechanism

The efficacy of RRS is dependent upon the bandwidth of the rudder servo-mechanism. If the bandwidth is less than the frequency range of ship roll then the rudder will be at best impotent at roll reduction or at worst will aggravate roll further.

The servo-mechanism has two non-linearities which are the maximum excursion angle for the rudder and a maximum rate at which it can move. A representative rate limit is $6°s^{-1}$ for Royal Navy warships. Figure 5 shows the manner in which the servo mechanism is modelled.

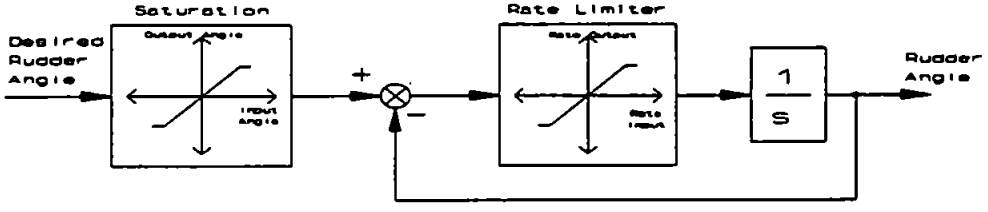

Figure 5 Model of a Non-Linear Rudder Servo-Mechanism

In reference [25] the RMS input signal to such a servo-mechanism was related to its bandwidth. If the RMS value is retarded below 5° then the servo-mechanism exhibits satisfactory bandwidth characteristics. In all subsequent controller design this criterion is adhered.

3. Controller Design and Simulation Results

3.1 Classical Controller

In reference [4] Lloyd postulates a method of designing a controller for fin roll stabilisation based on phase lead compensators which concentrates control action at one frequency point. By adjusting a gain the level of roll reduction is controlled and thereby saturation of rudder servo-mechanism prevented. By following a similar approach Roberts and Braham [26] proposed several RRS controllers of the form below.

$$\frac{Rudder\,Demand}{Unstabilised\,Roll} = \frac{as^2+bs+c}{k_1s^2+k_2s+k_3} \qquad (5)$$

Initially the impact of the RRS controller on LFE is examined. Figure 6 shows the arrangement of the simulations.

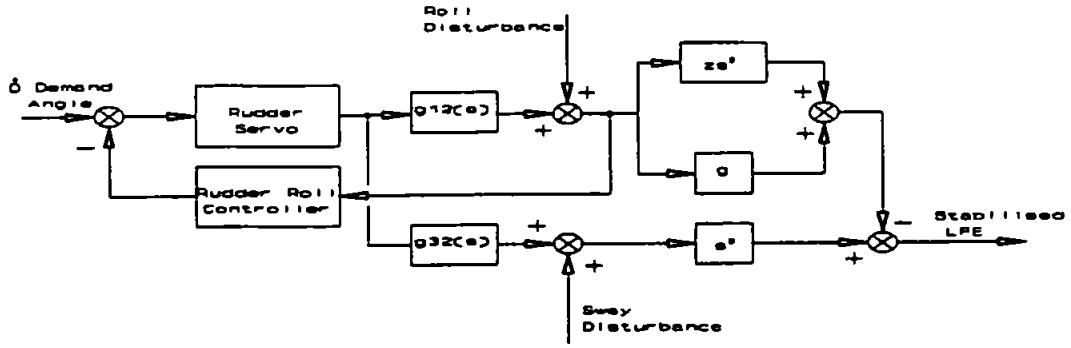

Figure 6 RRS Controller and LFE Signal

The RRS controller is 'tuned' around ship roll resonance. From the results in the Appendix, Figures A1a adequate roll reduction is achieved but Figure A1b shows poor LFE reduction and amplification at headings above 80°. Since LFE is an acceleration signal then the 'a' term of (5) is increased. From Figure A2a and A2b roll has worsened but LFE reduction is achieved over all the headings. If the RRS is 'tuned' to a lower frequency it is evident that not a great deal of improvement results, see Figures A3a and A3b.

It is evident that LFE stabilisation using the RRS controller is not a viable approach. The LFE signal is now directly fed to the RRS controller. The combinations of parameters 'a,b,c' in equation (5) is arranged such that 'a' (acceleration term) is large. Roll stabilisation occurs (Figure A4a) but LFE is amplified (Figure A4b).

Following the recommendations in [18,19] the LFE controller is 'tuned' to a low frequency and the RRS controller is implemented in parallel. Figure 7 shows the arrangement.

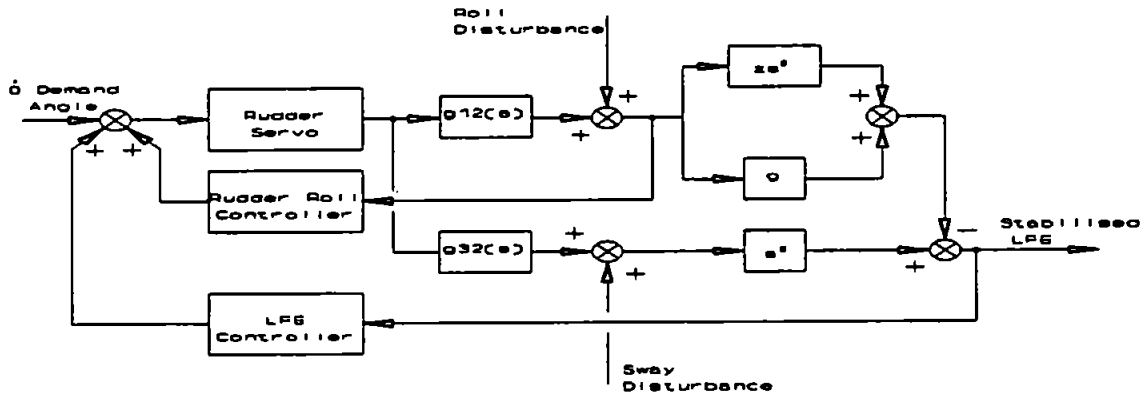

Figure 7 : RRS and LFE Controllers Acting

This configuration accrues by far the best results in roll and LFE reduction, Figures A7a and A7b.

3.2 Optimal Controller

The classical type controller showed mixed and variable results, due to the conflicting demands of the frequency range. Using the same models already developed a much more mechanical and acquiescent design procedure is provided by pursuing an optimal control strategy.

A state-space description of the process is set up. And the subsequent performance of the controller may be configured such that more emphasis is placed on either roll or LFE reduction. This is achieved by changing the weightings with respect to each other in a cost function. A cost function is of the form

$$J = \int_0^{\infty} uQu^T + yRy^T \, dt$$

The integral is minimised according to the values in R and Q. Thus by altering Q the control effort is at a higher premium thereby avoiding saturation of the rudder servo-mechanism. By altering values in Q comparative to each other, emphasis is placed on either roll or LFE.

The optimal feedback matrix requires that all the states be directly accessible. However, in reality only the measured roll and LFE signals are available which themselves may be corrupted by noise. Using a optimal estimator, such as a Kalman filter, (dual of the optimal control problem), it is possible to reconstruct all the states from the measurements. This was adopted to the simulations to achieve some degree of a realistic scenario. Further details of this optimal control theory may be found in [27].

Turning to the simulation results displayed in Figures A6-A8 in the Appendix.

From Figure A6a it is clearly demonstrates that considerable roll reduction is achieved as roll weighting is increased, the only limiting factor being the servo-mechanism. The subsequent LFE reduction increases due to the sway term in the LFE signal increasing as a result of increasing rudder activity.

Figures A7a and A7b show the roll and LFE respectively when the LFE weighting only is increased. Substantial LFE reduction is achieved. Although roll reduction is achieved the levels are not the same as above. Rather it ostensibly appears that any roll reduction is a by-product of LFE.

As an analogy with the classical case when two controllers are employed, one for RRS and the other for LFE stabilisation so both weightings are varied in congress. The subsequent roll and LFE are shown in Figures A8a and A8b respectively. These demonstrate rather vividly the dependence of LFE due to its roll component on roll minimisation. In the

same figures graphs 'a' show when roll weighting is comparatively large. Up to 60% roll reduction is achieved in the entire heading envelope, whilst giving modest LFE reduction. Graphs 'b', shows best LFE reduction. However, roll reduction has greatly decreased due to the controller applying the effort at a different frequency range. It is noted that LFE reduction achieved is only 10-30% better. Finally graphs 'c' are recorded when the LFE and roll weightings are both large. Whilst at this configuration roll reduction is a marginal maximum, due to increased rudder activity aggravating the sway, LFE levels have increased.

4 Discussion and Conclusions

This study attempted to construct a time simulation of the LFE in terms of s-domain transfer functions. Such a description of the system rather than multivariable differential equations of motion is very amenable to control design.

Two types of controller were implemented. The optimal controller out performed the classical one consistently. In designing the classical controller the nature of the LFE signal was not fully appreciated. As such the conflicting demands at best produced modest LFE reduction or could, indeed, exacerbate the accelerations.

Careful examination of equation (4) manifests the complex nature of the LFE.

Firstly consider the roll constituent of the LFE. As position of the LFE is moved higher than the cg such that it equals the value of gravitational acceleration the roll induced component of the LFE is minimised due to the antiphase addition. Moving beyond and higher still, then the roll acceleration term of the LFE will tend to dominate.

Now consider the effects of frequency variation. The double differentiation of a sinusoid is given by :

$$\ddot{y} = -k\omega^2 \sin(\omega t) \qquad (6)$$

Starting with the input roll frequency being less than one then the roll acceleration term will never exceed the $g\theta$ term. If the input roll frequency exceeds unity then from equation (6) it is seen that the magnitude is the constant, k, times the square of the frequency. Clearly this term will now render the $z\ddot{\theta}$ negligible.

The sway component of the LFE amplifies its complexity. A frequency response of the rudder/sway (G32(s)) is shown in Figure 8.

For RRS the controller operates at relatively high frequencies. From Figure 8 at such frequencies the sway acceleration signal is amplified exacerbating the LFE. This graph seems to vindicate recommendation made by 18,19], at the expense of increased roll.

As demonstrated by even this limited study stabilising

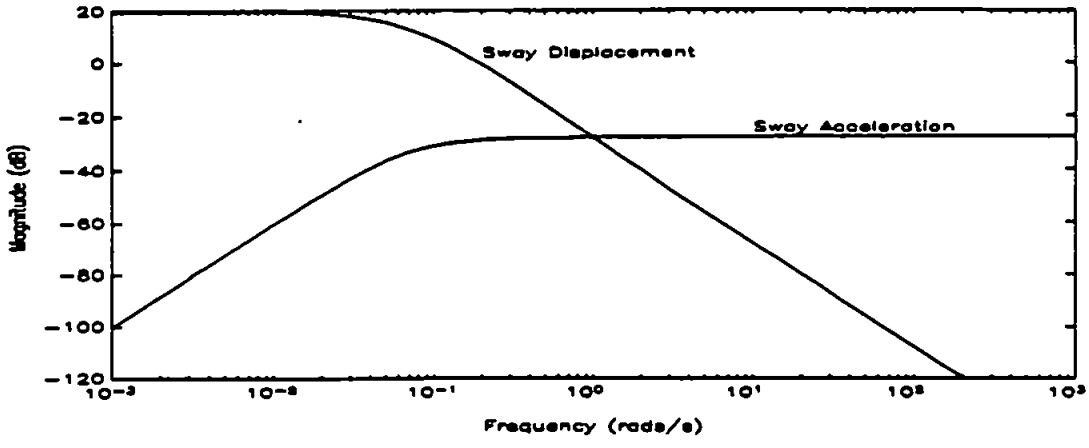

Figure 8 : Rudder/Sway Frequency Response

for LFE is not a simple matter. If it were possible to measure the constituent signals of the LFE then perhaps independent controllers may be implemented. Unfortunately, the LFE signal is a combination of other signals. As such a controller perhaps may be able to alleviate either LFE or roll depending on what the operating requirements may be. However, that would be possible for only very limited environmental conditions. An adaptive scheme should be pursued not only to deal with the changing dimensions within the LFE but also the inclement nature of the environment.

In conclusion, the three major components of LFE due to their dependence on ship motion (magnitude and frequency), sea state, position of the LFE and that the LFE is a vector combination then one must proceed with caution in order to design and implement a LFE stabilisation controller.

References

[1] Monk K "A Warship Roll Criteria" *Royal Institution of Naval Architects* 1987 pp219-240

[2] Cowley W.E and Lambert T.H."The Use of the Rudder a Roll Stabilisers" *3rd Ship Control Systems Symposium,* vol C, 1972

[3] Cowely W.E."Development of an Autopilot to Control Yaw and Roll" *The Naval Architect* 1972 January

[4] Lloyd A.R.J.M. "Roll Stabilisation by Rudder" *4th Ship Control Systems Symposium* vol.2 Netherlands 1975 pp214-242

[5] Kallström C.G. "Control of Yaw and Roll by a Rudder/Fin Stabilisation System" *6th Ship Control Systems Symposium* vol.2 Ottowa 1981

[6] Kallström C.G. "Roll Reduction by Rudder Control" *SNAME Spring Meeting STAR Symposium* Pittsburg 1988

[7] Kallström C.G. and Shultz W.P. "An Integrated Rudder Control System for Roll Damping and Course Maintenance" *9th Ship Control Systems Symposium* Vol.3 Maryland 1990

[8] Van Amerongen J. and Van Cappelle J.C."Mathematical Modelling for Rudder Roll Stabilisation" *6th Ship Control Systems Symposium,* Vol 1 Ottawa 1981

[9] Van Amerongen J. and Van Nauta Lemke H.R., "Rudder Roll Stabilisation" *Proceedings of Fourth International Symposium on Ship Operation Automation,* Vol.10, Genoa,1983 pp43-50

[10] Van Amerongen J., Van Nauta Lemke H.R., Van der Klugt P.G.M "Roll Stabilisation of Ship by Means of the Rudder" *Proceedings of 3rd Workshop AAST,* USA, 1983 pp19-26

[11] Van Amerongen J., Van der Klugt P.G.M., Piedders J.B.M., "Model Test and Full-Scale Trials with a Rudder Roll Stabilisation System" *7th Ship Control System Symposium,* Vol 1 UK 1984 pp95-114

[12] Van der Klugt P. "Rudder Roll Stabilisation : The Dutch Solution" *Naval Engineers Journal,* May 1990, pp83-92

[13] Van der Klugt P. "Rudder Roll Stabilisation" *PhD Thesis* Delft University of Technology 1987

[14] Baitis A.E. "RRS for Coast Guard Cutter Frigates" *Naval Engineers Journal* May 1983 pp267-282

[15] Baitis A.E. "Human Factors Considerations Applied to Operation of the FFG-8 and Lamps MK-II" *Naval Engineers Journal* May 1984 pp191-199

[16] Monk K "A Warship Roll Criteria" *RINA* Oct. 1987 pp219-240

[17] Graham R. "Motion Induced Interruptions as Ship Operability Criteria" *Naval Engineers Journal* March 1990 pp65-71

[18] Tang A, and Wilson P.A. "Lateral Force Estimator Stabilisation" *Control Applications in Marine Systems* Genoa April 1992 pp141-149

[19] Tang A., and Wilson P.A. "LFE Stabilisation Using Rudder" *Manoeuvring and Control of Marine Craft* July 1992 pp379-392

[20] Bell J. "Stabilisation to the Apparent Vertical-Measurement of Sway" *Transactions of RINA* vol.107 1965 pp257-264

[21] Roberts G.N, and Towill D.R. "Multivariable Control of Warship Manoeuvring" *Proc. 10th IFAC World Congress* vol.6 pp220-225 March 1987

[22] Whalley R, Westcott J. H. "Ship Motion Control" *6th Ship*

Control Systems Symposium vol.3 Ottawa 1981 ppH1-1 - pH1-16

[23] Schmitke R.T. "Ship Sway Roll and Yaw in Oblique Seas" *Transactions of SNAME* vol.86 1978 pp206-216

[24] Lloyd A.R.J.M. "Motions of Steered Model Warship in Oblique Wave" *RINA* vol.132 1990 pp78-98

[25] Sharif M.T. "Frequency Response of Rudder Servo-Mechanism" *Technical Report RR-92028* Control Engineering Dept., Royal Naval Engineering College 1992

[26] Roberts G.N. and Braham S.W. "Warship Roll Stabilisaiton Using Integrated Control of Rudder and Fins" *9th Ship Control Systems Symposium,* vol 1, pp234-248

[27] Kwakernaak H. and Sivan R. "Linear Optimal Control Systems" John Wiley & Son 1972

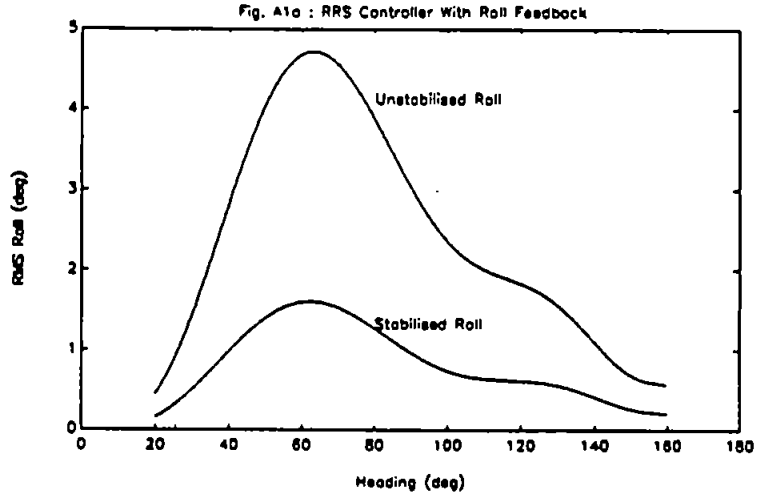
Fig. A1a : RRS Controller With Roll Feedback
Unstabilised Roll
Stabilised Roll
RMS Roll (deg)
Heading (deg)
0
1
2
3
4
5
0
20
40
60
80
100
120
140
160
180

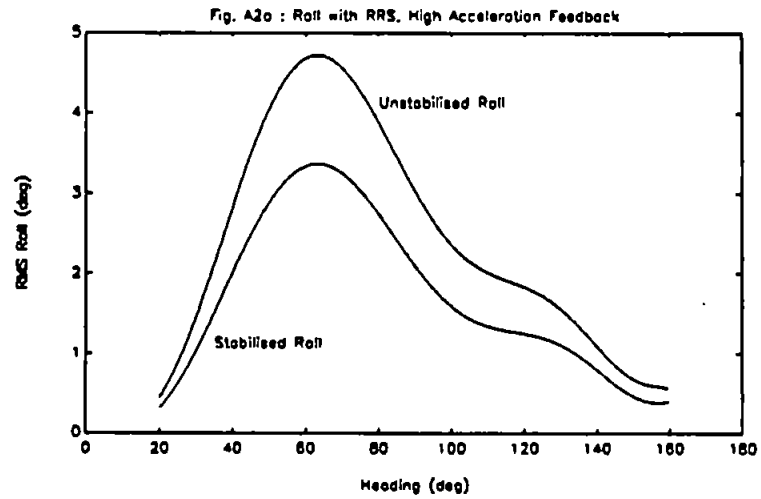
Fig. A2a : Roll with RRS, High Acceleration Feedback
Unstabilised Roll
Stabilised Roll
RMS Roll (deg)
Heading (deg)
0
1
2
3
4
5
0
20
40
60
80
100
120
140
160
180

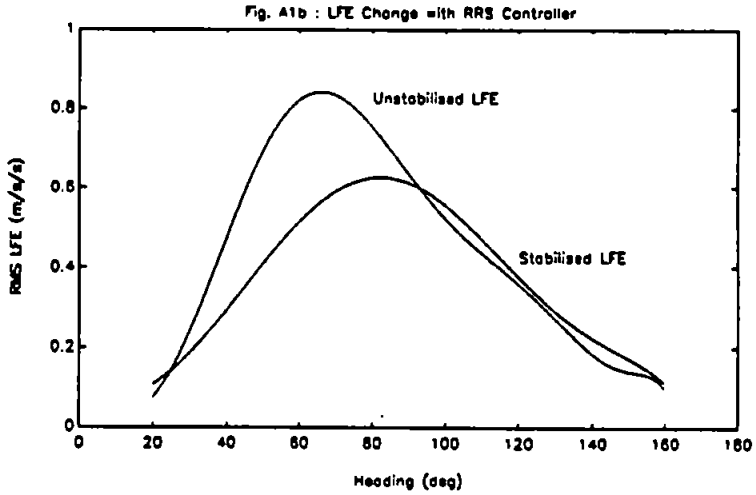
Fig. A1b : LFE Change with RRS Controller
Unstabilised LFE
Stabilised LFE
RMS LFE (m/s/s)
Heading (deg)
0
0.2
0.4
0.6
0.8
1
0
20
40
60
80
100
120
140
160
180

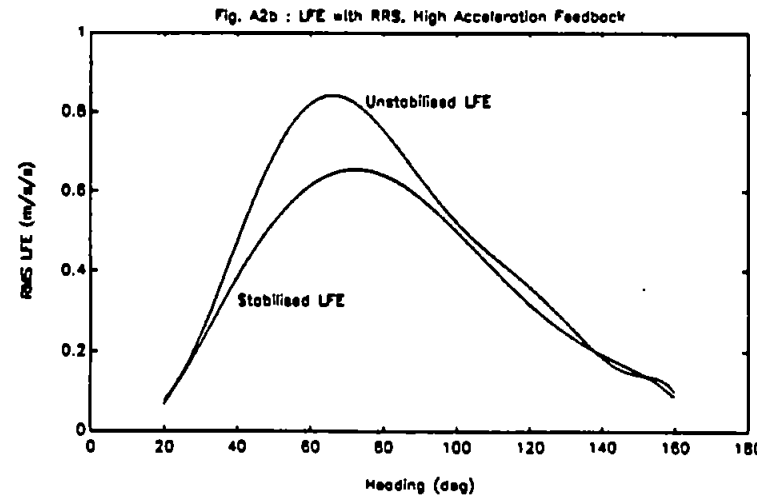
Fig. A2b : LFE with RRS, High Acceleration Feedback
Unstabilised LFE
Stabilised LFE
RMS LFE (m/s/s)
Heading (deg)
0
0.2
0.4
0.6
0.8
1
0
20
40
60
80
100
120
140
160
180

Fig. A3a : Roll with RRS Tuned below Roll Resonance Frequency

Fig. A3b : LFE with RRS Tuned below Roll Resonance Frequency

Fig. A4a : Roll with LFE Controller (High Acceleration Term)

Fig. A4b : LFE with LFE Controller (High Acceleration Term)

Fig. A5a : Roll with LFE and RRS Controllers

Fig. A5b : LFE with LFE and RRS Controllers

Fig. A6a : Roll Change with Variation in Roll Weighting

Fig. A6b : LFE Change with Variation in Roll Weighting

Fig. A7a : Roll Change with Variation in LFE Weighting

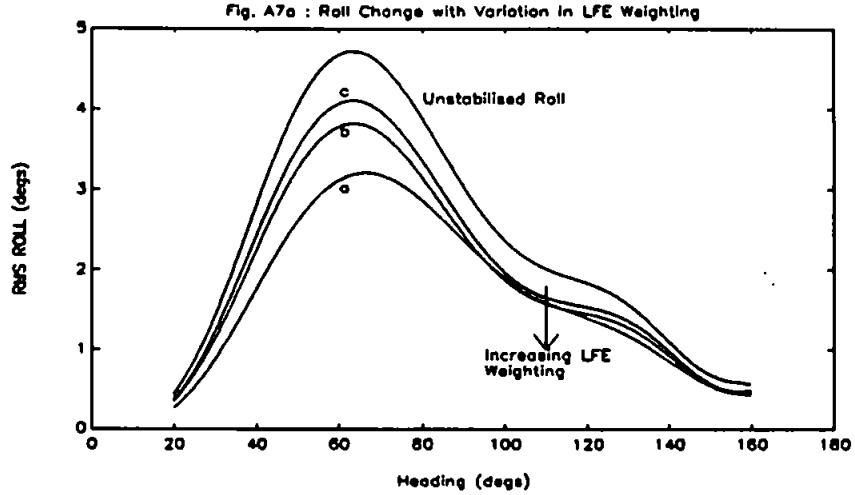

Fig. A8a : Roll due to Variation in LFE and Roll Weightings

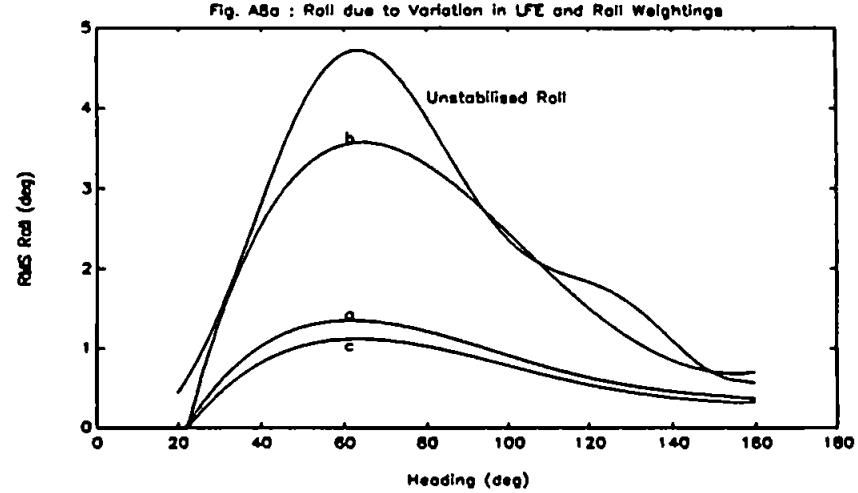

Fig. A7b : LFE Change with Variation in LFE Weighting

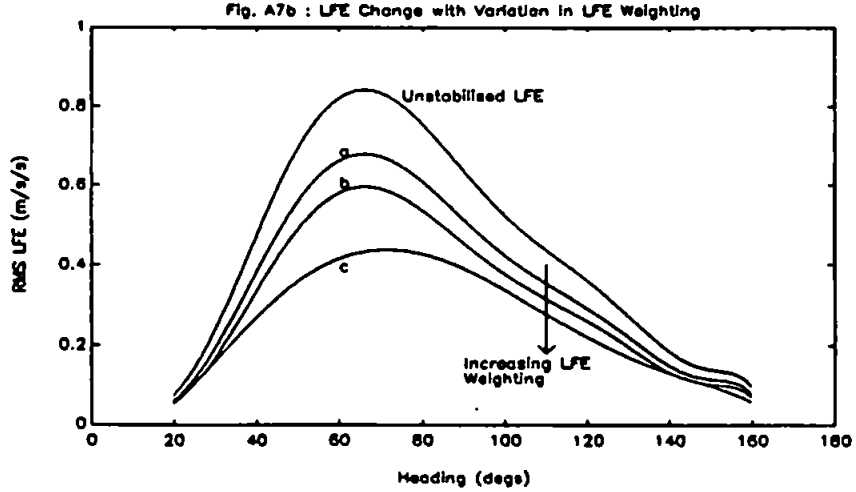

Fig. A8b : LFE due to Variation in LFE and Roll Weightings

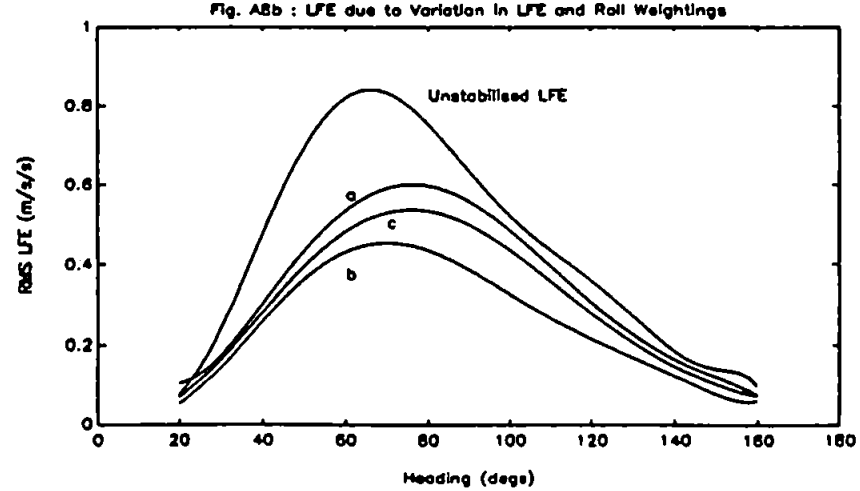

INTEGRATED ROBUST SHIP ROLL STABILISATION

M.T. Sharif†, G.N. Roberts‡, R. Sutton‡

† Royal Naval Engineering College, U.K.
‡ University of Plymouth, U.K

INTRODUCTION

The pernicious consequences of roll motions have a profound effect on the operational effectiveness of all types of ships. In warships the motions may be serious enough to curtail helicopter excursions from the deck, and degrade performance of the weapons systems and radars. Thus rendering the warship impotent to perform its designated role. For ships in general, roll motions may reduce personnel to simply hanging on to a fixed object to maintain balance, cargo may be disturbed, interruptions to machinery may occur and these motions may greatly agitate passengers. All these factors act in conglomeration to produce an inherent degradation in ship operability.

Many devices have been invented and implemented to ameliorate the roll motion. However, few devices have perhaps had the same impact on roll stabilisation as the active fin stabilisation system. These have been studied in rigorous detail [1-4].

Although active fin stabilisation systems had been developed and utilised as early as the second world war, it was not until 1956 that the Royal Navy formally adopted the resolution to equip all new vessels with these devices as a matter of course. With the advent of the helicopter bearing warships in the 1950's, and development of sophisticated weapons systems and radars the decision was judicious.

It has been observed in ships, of appropriate size, that when the rudder is 'put-over' the ship initially heels inwards before attaining the steady state outward heel angle as it enters the turn [5]. Furthermore, this initial roll angle occurs before the ship enters into any yaw motion. Suggesting that the characteristic ephemeral rudder induced roll may be used in congress with the fins to enhance roll stabilisation without significant interference to the heading angles. This potential has been recognised and studies conducted to assess its feasibility [6-10].

To date, generally, the implementation of this strategy has been to the exclusion of fin stabilisers. The Royal Navy is actively pursuing techniques to utilise both control surfaces given the limited capability of the rudder actuators. In order that implementation would require alteration of the software only to drive the rudder and no expensive upgrading of machinery.

Much research effort has been dissipated on the design of the controllers. This endeavour has in the main employed the 'classical' technique approach. The strategy being to inject phase advance around the roll resonance peak. This procedure 'optimises' the controller against only one set of environmental disturbances. However, the warship operating environment is broad. The sea state can change from dead calm to gale force, the effectiveness of the control surfaces are dependent upon the ship speed and parameters in the transfer functions must change to reflect this, the sea encounter frequency varies widely, low frequencies having a destabilising effect, and there is general uncertainty in the transfer function models. Thus the warship's roll stabilisation controllers may be countenanced with disturbances very different from the ones for which they were designed.

The H∞ optimisation offers a technique to design a controller which not only encompasses these variations but also accounts for robust stability and guaranteed levels of performance, analogous to disturbance rejection.

In this paper H∞-synthesis is utilised to design a fin/rudder controller given appropriate weightings. The system is decomposed into its fractional representation in order to assess whether robust stability and performance criteria are attained.

SYSTEM MODELS

Multivariable Ship Model

Figure 1 shows the multivariable ship model. The fin to roll and rudder to roll transfer functions, g11(s) and g12(s) are of interest. As indicated earlier and from vicarious experience [4] it is assumed that there is negligible yaw motions induced by the rudder action.

As with any control design procedure an initial estimate of the dynamics of the plant are imperative. Facilitation in the controller synthesis is proportional to the accuracy and reliability of the transfer functions. A comparison was performed for g11(s) and g12(s) with sea keeping prediction software at DRA Haslar, which uses strip theory results and has been verified by extensive full scale trials. This showed good correlation between the RMS values produced in spite of the frequency dependent hydrodynamic coefficients. There is to an extent now some confidence in the validity of the transfer functions.

Control Surfaces

Stabilising fins. The fin/roll transfer function was derived from sea trials by Marshfield [11] and given as a simple second order system (1).

$$g11(s) = \frac{k_{11}0.25}{s^2 + 2\zeta_s 0.5 s + 0.25} \qquad (1)$$

Here k_{11} represents the non-linearity in fin moment generation due to ship speed and ζ_s is the ship damping ratio. It is known that the damping ratio, ζ_s, is a non-linear function of ship speed and encounter frequency [12].

The RMS values at various combinations of speed and encounter frequency for g11(s) were compared with data supplied by DRA Haslar. An empirical relationship between damping ratio and heading is derived as shown in figure 2 to yield close correlation with DRA Haslar data.

Rudder to Roll Dynamics. From the same source the rudder to roll transfer function is derived, for a frigate size warship (2).

$$g12(s) = \frac{k_{12}0.25(1-4.5s)}{(1+8.2s)(s^2+0.25s+0.25)} \qquad (2)$$

Again the parameter k_{12} represents rudder effectiveness at various ship speeds. The degree of variation of the other parameters in (1) and (2) is not known.

Both these transfer functions, (1) and (2), have been subsequently refined by Roberts and WHalley [13,14], such that the dynamics are well known at 18kts. This is the nominal ship model exploited in the controller synthesis.

Sea Disturbance

Ideally the roll angle of the ship should remain at 0°. However, hydrodynamic interaction between the hull and the sea induce undesired perturbations in six degrees of freedom, one of these is the roll motion. The severity of the roll motions depending on the wave height and encounter frequency. Fortunately, the sea spectrum is well defined by a Bretschneider spectrum (3), where H is the significant wave amplitude and T the wave period.

$$S(\omega) = \frac{691}{T^4\omega^5}\left[\frac{H_{\frac{1}{3}}}{2}\right]^2 \exp\left(-\frac{691}{T^4\omega^4}\right) \quad m^2s \qquad (3)$$

A transfer function representation of the Bretschneider spectrum may be generated by (4) with white noise as the input.

$$D(s) = \frac{k_d\omega_d^2}{s^2+2z_d\omega_d s+\omega_d^2} \qquad (4)$$

Here ω_d represents the encounter frequency, z_d the damping ration and k_d a gain factor to account for the wave height. All these parameters were empirically chosen to closely relate to data furnished by DRA Haslar.

Fin and Rudder Actuators

The fin and rudder actuator hydraulics have associated with them two non-linearities as shown by figure 3. These limitations are the maximum excursion angles and rate limits. The rudder angle being $\pm 30°$, slew at $\pm 6°s^{-1}$ and the fin angle $\pm 30°$ and slew at $\pm 29°s^{-1}$. These are incorporated in simulation the studies which were subsequently conducted.

To be effective as roll stabilisers the actuators' bandwidths must extend beyond the roll resonance frequency of the ship. From [15] it is known that the bandwidth of a servo-mechanism is dependent upon the RMS level of the demand signal. Therefore, this should be monitored in simulations.

Furthermore, from these considerations it is apparent [16] that the rudder efficacy in roll stabilisation will not be as great as the fins and hence act in a secondary role. This adheres to the Royal Navy objectives of harnessing the existing rudder capability by retro fit of controllers rather than embarking upon expensive refits.

Control Arrangement

Figure 4 shows the feedback arrangement of the stabilisation system. A similar scheme described by Grimble in [17] would suggest that there is cross coupling between rudder and fin actions. However, provided that the minimum aim is attained, viz. roll is not amplified by the control surfaces, it may be assumed that such cross coupling does not exist. Furthermore, in [17] it appears that the addition of a fin moment with a rudder induced roll angle is being proposed. These two signals represent incompatible physical quantities and are not subject to algebraic manipulation. Thus their addition is considered to be spurious.

The manner in which the solution is sought is suggested naturally by figure 4 ie the two loops are treated independently, thereby greatly simplifying the problem.

H∞ SYNTHESIS

The method adopted to synthesis the controllers for the fin/rudder loops is via H∞ synthesis. This is essentially a search procedure to seek a controller, if one exists, such that the closed loop system adheres to a specified stability and robust performance criteria [18]. The optimisation procedure attempts to satisfy the stability conditions postulated by the small gain theorem viz. a feedback loop composed of stable operators is assured stability given that their operator gains have a product less than unity. Thus H∞ synthesis endeavours to minimise the maximum singular values. The problem definition is briefly outlined here.

Let

$$T = GK(I+GK)^{-1} \qquad (5)$$

$$S = (I+GK)^{-1} \qquad (6)$$

$$C = K(I+KG)^{-1} \qquad (7)$$

Here K, denotes the controller, G the open loop plant, T complimentary sensitivity function, S the output sensitivity function, and C the control sensitivity.

Consider figure 5 where u are the control signals, v represent disturbance and noise inputs, y physical quantities, e error signals, and x and z are uncertainty input/outputs. P is the nominal plant and Δ, block diagonal uncertainty representation. P may be partitioned as shown below :

$$P = \begin{bmatrix} P_{11} & P_{12} \\ P_{21} & P_{22} \end{bmatrix} \qquad (8)$$

Ignoring the effects of the uncertainty block, Δ, for the moment, then let M denote the closed loop function mapping v to e. This is known as a lower linear fractional transformation (9) with inputs $(v,u)^T$ and outputs $(x,y)^T$ and embodies the closed loop characteristic of the system.

$$M = P_{11} + P_{12}K(I-P_{22}K)^{-1}P_{21} = F_l(P,K) \qquad (9)$$

The H∞ optimisation problem is then to minimise (9) by seeking over all controllers which will both stabilise the closed loop plant and is realisable i.e. proper. The cost functions can being defined, given the contingencies of the engineering and performance implications

idiosyncratic to an particular application, by frequency dependent weightings transfer functions.

The sensitivity weighting is constructed such that the resulting controller minimises sea disturbance and satisfies the norm (10)

$$||\gamma W_p S||_\infty \leq 1 \qquad (10)$$

Robust stability is guaranteed, to multiplicative perturbations, Δ by the complimentary sensitivity function and weighting, W_Δ if the norm (11) is adhered.

$$||\gamma W_\Delta T||_\infty < 1 \qquad (11)$$

In order to restrain the actuators from encroaching into their non-linear regions, a similar inequality constraint imposed with a weighting, W_c, will accomplish this objective (12).

$$||\gamma W_c C||_\infty \leq 1 \qquad (12)$$

The augmented plant may be written as (13) whose parameters corresponds with (8). Where γ is a scalar search variable.

$$G_{AUG} = \begin{bmatrix} \begin{pmatrix} \gamma W_p \\ 0 \\ 0 \end{pmatrix} & \begin{pmatrix} -\gamma W_p G \\ \gamma W_c \\ \gamma W_\Delta G \end{pmatrix} \\ I & -G \end{bmatrix} \qquad (13)$$

Analysis of the robust margins are calculated such that the Δ structure has one scaler block. In this manner the effects of the uncertainty due to W_Δ may be assessed. The benefits accrued by setting up the structure of the problem as shown in figure 5, and thereby affording a fractional representation, is that by considering the maximum singular values of the appropriate entries of the matrix a measure of stability and robustness will become evident.

Given that an H∞ controller, or indeed any other controller, has been synthesised then by consideration of figure 5, if the controller, K, is absorbed into the plant, P, the following may be stated (14)

$$\begin{bmatrix} x \\ e \end{bmatrix} = Q \begin{bmatrix} z \\ v \end{bmatrix} = \begin{bmatrix} Q_{11} & Q_{12} \\ Q_{21} & Q_{22} \end{bmatrix} \begin{bmatrix} z \\ v \end{bmatrix} \qquad (14)$$

It is apparent [18] that, given the orientation of the signals, Q_{11} is associated with internal stability to any uncertainty. Therefore to guarantee robust stability it is sufficient, provided that Δ is normalised by absorbing the factors into the P structure, to ensure that condition (15) is adhered.

$$||Q_{11}||_\infty < 1 \qquad (15)$$

Similarly, the performance issue is associated with the output signal, e and exogenous disturbances, v. The matrix element mapping these is Q_{22}. The performance specification may the be stated to be (16)

$$||Q_{22}||_\infty < 1 \qquad (16)$$

We now proceed to define the cost functions.

SELECTION OF WEIGHTINGS

Sensitivity Weighting. The sensitivity is a measure of the systems ability to reject sea disturbances. Efficacious performance from the H∞ controller will depend on judicious construction of this weight. Grimble, [17], gives guidance to these ends. However, a few modifications are made.

The sensitivity weight implemented (17) is such that it encompass the likely region where sea disturbances will occur - a v-shape notch filter, with its peak around the ship roll resonance frequency. The gain magnitude is made relatively large here but constant at higher frequencies. This has the effect of reducing controller overshoot.

$$W_p(s) = \frac{0.0664s^2 + 8s + 0.016}{4s^2 + s + 1} \qquad (17)$$

Complimentary Sensitivity Weight. H∞ control necessitates descriptions of systems in a linear fashion. Unfortunately, the vagaries of the real world mean that a considerable amount of information must be discarded due this restriction. The complimentary sensitivity function is a device used to encapsulate this uncertainty naturally inherent in the transfer functions.

Around roll resonance confidence of the model is greatest, outwith this region uncertainty exists in such places as frequency dependent hydrodynamic coefficients, actuator non-linearities, speed dependent gains, and other factors which cannot be depicted by linear transfer functions. This renders the closed loop system susceptible to instability. Therefore the shape of weight is constructed in (18) to reflect these limitations.

$$W_\Delta = \frac{4s^2 + 4s + 1}{0.04s^2 + 40s + 0.01} \qquad (18)$$

Control Sensitivity Weight. As mentioned earlier, these depict restrictions in actuator demand signals in the H∞ synthesis. Since the rudder has much greater engineering constraints, it is given a relatively larger weight, $W_{\sigma r}$, than the fin control weight $W_{\sigma f}$ (19). Furthermore, from the slew rates of the actuators it is realised that the upper bound of the rudder must be restricted to prevent the rudder saturating.

$$W_{\sigma r} = \frac{3.33s^2 + 3.7s + 1}{3.33s^2 + 5000s + 1} \qquad W_{\sigma f} = \frac{12.5s^2 + 20.6s + 1}{12.5s^2 + 500s + 1} \qquad (19)$$

The weights are shown in figure 6.

RESULTS

The Controllers. The γ values achieved for the rudder and fin loops are 0.63 and 0.59 respectively. Frequency plots of the controllers are shown in figure 7. On examination the magnitude of $K_r(s)$ appears alarmingly large. However, the peak occurs well away from the region where most control action is applied, i.e. the roll resonance peak, and is of little significance as demonstrated in the sensitivity plot of figure 8. The peak occurring at the corresponding 100 rads^{-1} as in figure 7.

A possible explanation for this large peak in the fin is by making an analogy with classical controllers. Here the desired phase advance can be applied only at one location; the resonance peak. It appears that the H∞ controller attempts to impart phase advance over a much broader

frequency region. This is achieved by zeros in the controller resulting in the gain slope over the frequency of stabilisation.

To an extent the rudder controller behaves in the same manner but has lower magnitude. This is achieved by the cost weighting, W_u and the fact that the relatively smaller phase advance magnitude is required due to the non-minimum phase nature of g12(s).

Time Simulations. These are performed with the non-linearities incorporated. The disturbance signals represent sea states 3,5, and 8 which have significant wave heights of 0.88m, 3.25m, and 11.5m and modal periods of 5.79s, 9.7s and 18s respectively. As expected, from figure 9, the stabilisation achieved is significant. At best between 70 and 90 percent reduction is accrued. However, degradation occurs at off-beam seas where the stabilisation accrues is in the range of 55 to 70 percent.

Assessing the RMS values of the control signals driving the fin/rudder actuators is more significant than the actual movement since it gives an indication of saturation, detrimental to actuator bandwidths. The RMS values appear to be satisfactory, figures 10 and 11, although acceptable levels of saturation are inevitable.

Performance and Robust Analysis

Robustness. Figure 12 shows the stability to the weighting function W_Δ which is essentially a singular value plot of condition (15). It is seen that, from the small gain theorem, that the system is robust to this specification (18). The maximum values are 0.59 and 0.63 for the fin and rudder loops respectively. Thus it may be stated that W_Δ may increase by 1.7 and 1.6 times before the fin and rudder loops, respectively, are countenance by instability.

Performance. The nominal performance to the specified weights is given by the $\max(\sigma(Q_{22}))$. These are shown in figure 13. As anticipated these are achieved with large margins. The maximum values are 0.58 and 0.25 yielding sufficient margins before performance degradation occurs.

CONCLUSIONS

Employing the rudder and fins actuators in harmony is a feasible solution to roll stabilisation. The performance and robustness levels may defined by the weighting functions. Optimising the H∞ norm in a minimal sense guarantees that the objectives were attained. By defining the linear fractional representations it was possible to assess the robustness and performance behaviour of the system.

The design procedure considered the case of uncertainty due to W_Δ. A progression would be to harness the potential of μ-analysis to assess these bounds in the presence of real parameter variations, i.e. structured perturbations, together with W_Δ by the pertinent construction of the Δ block.

Therefore, it is envisaged that by examining the hydrodynamic coefficients in the equations of motion for the ship and other sources of uncertainty, as outlined above, the perturbations may be ascertained in a detailed manner. Further investigation is anticipated whether μ may be employed in an iterative sequence to generate the H∞ controller.

REFERENCES

[1] Lloyd,A.R.J.M., "Hydrodynamic Performance of Roll Stabiliser Fins" 3rd Ship Control Systems Symp. vol. C 1972

[2] Lloyd,A.R.J.M.,"Roll Stabiliser Fins : A Design Procedure" RINA 1974 pp233-254

[3] Allan,J.J.,"Rolling and its Stabilisation by Active Fins" INA vol87 1945 pp123-135

[4] Cowley,W.E., "The Use of Rudder as Roll Stabiliser" 3rd Ship Control Systems Symp. vol C 1972

[5] Rawson, Tupper "Basic Ship Theory" Longman 1984

[6] Cowley,W.E. & Lambert,T.H.,"The Use of Rudder as a Roll Stabiliser" 3rd Ship Control Systems Symp. 1972 vol C

[7] Katebi,M.R., et al "LQG Autopilot and RRS Control Systems Design" 8th Ship Control Systems Symp. 1978 pp3.69-3.84

[8] Amerongen,J.van,"RRS:Controller Design and Experimental Results" 8th Ship Control Systems Symp. 1987 pp1.128-1.142

[9] Amerongen,J.van,"Rudder Roll Stabilisation" 4th Intl. Symp. on Ship Operation and Automation 1982 pp43-50

[10] Roberts,G.N. & Braham,S.W.,"A Design Study on the Control of Warship Rolling Motion Using Rudder and Stabilising Fins" IEE Control Conf. '91 pp838-843

[11] Marshfield,B,"HMS **** Roll Stabilisation Trials" AMTE(H) /R81012 (Restricted)

[12] Yoji,H,"Prediction of Ship Roll Damping" Univ. of Michigan C. of NA & ME Sept. 1981

[13] Roberts,G.N.,"Ship Motion Control Using a Multivariable Approach" PhD Thesis, Univ. of Wales 1989

[14] Whalley,R.,Wescott,J.H.,"Ship Motion Control",6th Ship Control Systems Symp. 1981 ppH1.1-H1.16

[15] Sharif,M.T.,"Frequency Response of a Rudder Servo Mechanism" RNEC Technical Report RR92028 Oct. 1992

[16] Powell,D.C.,"Rudder Roll Stabilisation : A Critical Review" 9th Ship Control Systems Symp. 1990 pp2.245-2.263

[17] Grimble,M, et al"H∞ Based Ship Fin/Rudder Roll Stabilisation Design" 10th Ship Control Systems Symp. 1993 pp5.225-5.265

[18] Maceijowski,J.M.,"Multivariable Feedback Design" Addison-Wesley 1989

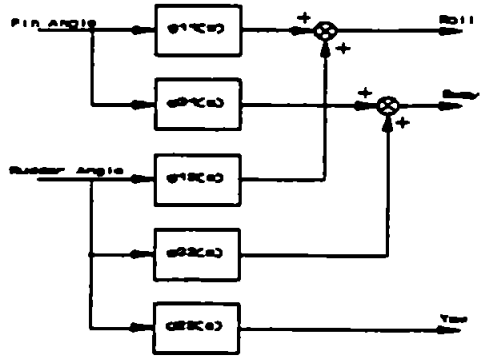

Figure 1 : Multivariable Ship Model

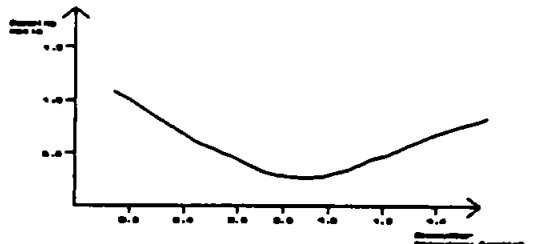

Figure 2 : Variation of Ship Damping Ratio

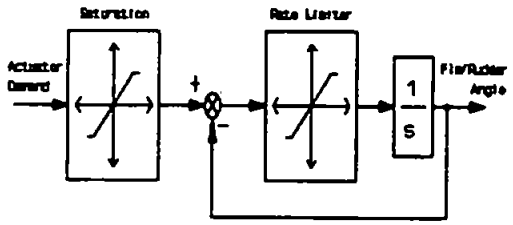

Figure 3 : Servo-Mechanism Models

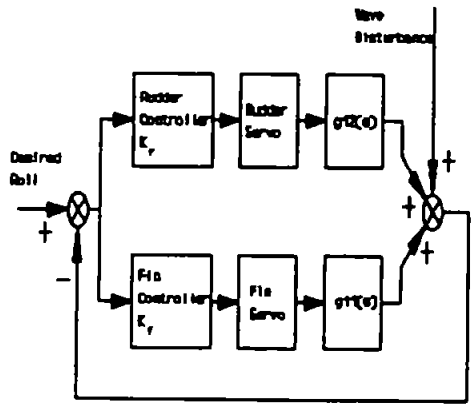

Figure 4 : Roll Stabilisation Arrangement

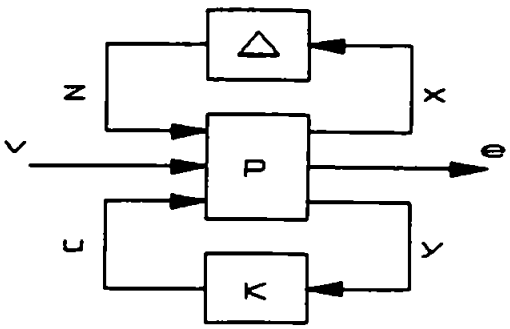

Figure 5 : Perturbation and Controller Feedback Representation

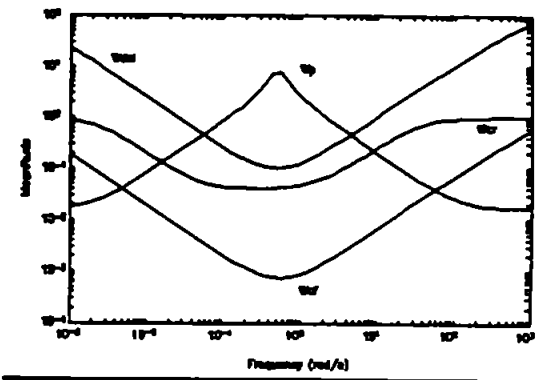

Figure 6 : Frequency Plots of Weighting Functions

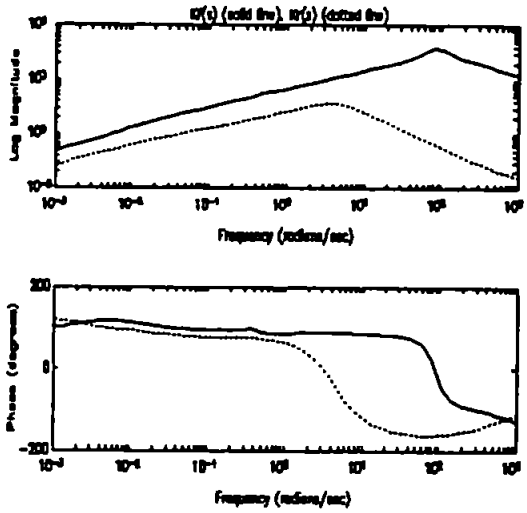

Figure 7 : Frequency Plots of Controllers

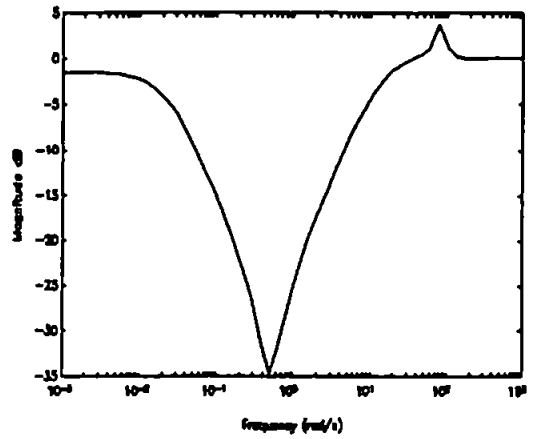

Figure 8 : Sensitivity Function

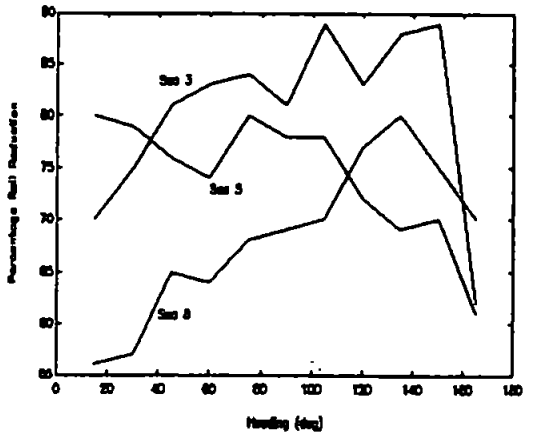

Figure 9 : Fin/Rudder Stabilisation Roll Reduction

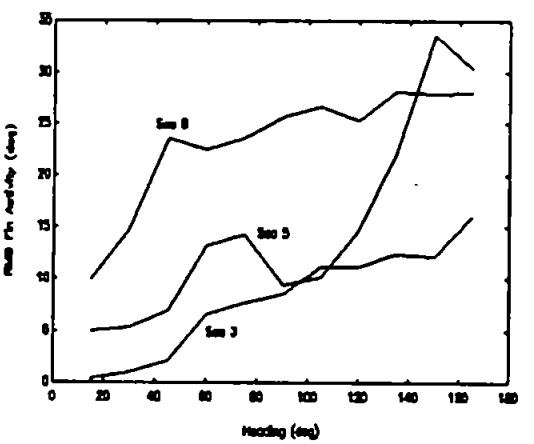

Figure 10 : RMS Fin Activity

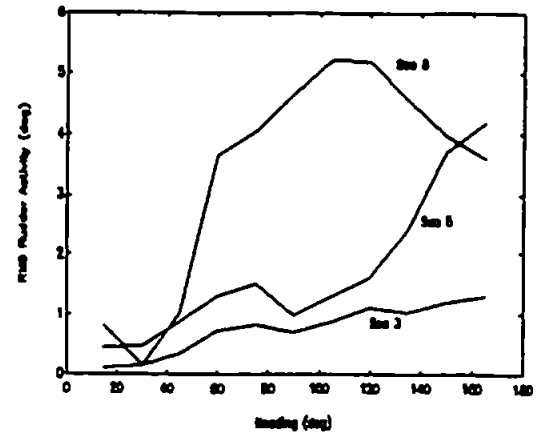

Figure 11 : RMS Rudder Activity

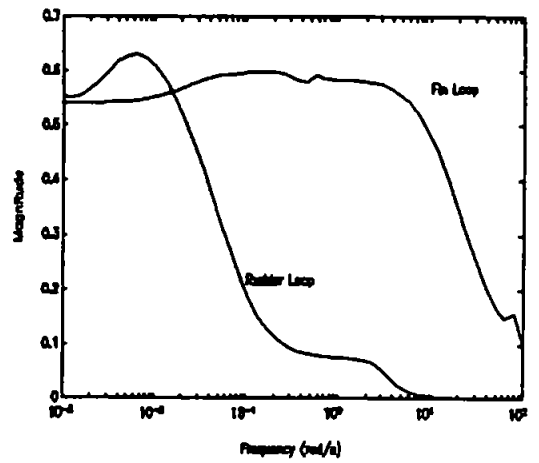

Figure 12 : Maximum Singular Value for Stability Robustness

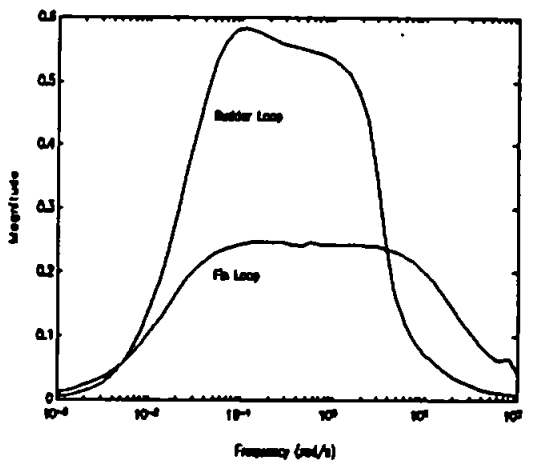

Figure 13 : Maximum Singular Value Plots for Performance

ROBUST FIN/RUDDER SHIP ROLL STABILISATION

M.T. Sharif[1], G.N. Roberts[2], R. Sutton[3]

1. Royal Naval Engineering College, U.K.
2. Gwent College of Higher Education, Newport, U.K.
3. University of Plymouth, U.K

Abstract

In ship operations the consequences of roll motions can seriously degrade the performance of mechanical and personnel effectiveness. Stabilising fins are used to alleviate these problems. Recently rudders, which have been extensively modified, have been used exclusively to stabilise roll. This paper examines the H_∞ and μ-synthesis technique to design controllers for existing fin and rudders.

1. Introduction

The pernicious consequences of roll motions have a profound effect on the operational effectiveness of all types of ships. In warships the motions may be serious enough to curtail helicopter excursions from the deck, and degrade performance of the weapons systems and radars. Thus rendering the warship impotent to perform its designated roll. For ships in general, roll motions may reduce personnel to simply hanging on to a fixed object to maintain balance, cargo may be disturbed, interruptions to machinery may occur and these motions may greatly agitate passengers. All these factors act in conglomeration to produce an inherent degradation in ship operability.

Many devices have been invented and implemented to ameliorate the roll motion. However, few devices have perhaps had the same impact on roll stabilisation as the active fin stabilisation system [1].

Although active fin stabilisation systems had been developed and utilised as early as the second world war, it was not until 1956 that the Royal Navy formally adopted the resolution to equip all new vessels with these devices as a matter of course. With the advent of the helicopter bearing warships in the 1950's, and development of sophisticated weapons systems and radars the decision was judicious.

It has been observed in ships, of appropriate size, that when the rudder is 'put-over' the ship initially heels inwards before attaining the steady state outward heel angle as it enters the turn [2]. Furthermore, this initial roll angle occurs before the ship enters into any yaw motion. Suggesting that the characteristic ephemeral rudder induced roll may be used in congress with the fins to enhance roll stabilisation without significant interference to the heading angles. This potential has been recognised and studies conducted to assess its feasibility [3].

To date, generally, the implementation of this strategy has been to the exclusion of fin stabilisers. The Royal Navy is actively pursuing techniques to utilise both control surfaces given the limited capability of the rudder actuators. In order that implementation would require alteration of the software only to drive the rudder and no expensive upgrading of machinery.

Much research effort has been dissipated on the design of the controllers. This endeavour has in the main employed the 'classical' technique approach. The strategy being to inject phase advance around the roll resonance peak. This procedure 'optimises' the controller against only one set of environmental disturbances. However, the warship operating environment is broad. The sea state can change from dead calm to gale force, the effectiveness of the control surfaces are dependent upon the ship speed and parameters in the transfer functions must change to reflect this, the sea encounter frequency varies widely, low frequencies having a destabilising effect, and there is general uncertainty in the transfer function models. Thus the warship's roll stabilisation controllers may be countenanced with disturbances very different from the ones for which they were designed.

H∞ and the μ-synthesis offers a technique to design a controller which not only encompasses these variations in disturbance but also accounts for robust stability and robust performance.

In this paper μ-synthesis is utilised to design a fin/rudder controller given appropriate weightings. The μ-analysis is performed to assess robust stability and performance against model perturbations.

2. System Models

Multivariable Ship Model

Figure 1 shows the multivariable ship model. The fin to roll and rudder to roll transfer functions, g11(s) and g12(s) are of interest. As indicated earlier and from vicarious experience [4] it is assumed that there is negligible yaw motions induced by the rudder action.

As with any control design procedure an initial estimate of the dynamics of the plant are imperative. Facilitation in the controller synthesis is proportional to the accuracy and reliability of the transfer functions. A comparison was performed for g11(s) and g12(s) with sea keeping prediction software at DRA Haslar. Which uses strip theory results and has been verified by extensive full scale trials. This showed good correlation between the RMS values produced in spite of the frequency dependent hydrodynamic coefficients. There is to an extent now some confidence in the validity of the transfer functions.

Control Surfaces

Stabilising fins. The fin/roll transfer function was derived from sea trials by Marshfield [5] and given as a simple second order system (1).

$$g11(s) = \frac{k_{11}0.25}{s^2 + 2\zeta_s 0.5s + 0.25} \qquad (1)$$

Here k_{11} represents the non-linearity in fin moment generation due to ship speed and ζ_s is the ship damping ratio. It is known that the damping ratio, ζ_s, is a non-linear function of ship speed and encounter frequency [6].

The RMS values at various combinations of speed and encounter frequency for g11(s) were compared with data supplied by DRA Haslar. An empirical relationship between damping ratio and heading is derived as shown in figure 2 to yield close correlation with DRA Haslar data.

Rudder to Roll Dynamics.

From the same source the rudder to roll transfer function is derived, for a frigate size warship (2).

$$g12(s) = \frac{k_{12}0.25(1-4.5s)}{(1+8.2s)(s^2+0.25s+0.25)} \qquad (2)$$

Again the parameter k_{12} represents rudder effectiveness at various ship speeds. The degree of variation of the other parameters in (1) and (2) is not known.

Both these transfer functions, (1) and (2), have been subsequently refined by Whalley and Roberts [7,8], such that the dynamics are well known at 18kts. This is the nominal ship model exploited in the controller synthesis.

Sea Disturbance

Ideally the roll angle of the ship should remain at 0°. However, hydrodynamic interaction between the hull and the sea induce undesired perturbations in six degrees of freedom, one of these is the roll motion. The severity of the roll motions depending on the wave height and encounter frequency. Fortunately, the sea spectrum is well defined by a Bretschneider spectrum (3), where H is the significant wave amplitude and T the wave period.

$$S(\omega) = \frac{691}{T^4\omega^5}\left[\frac{H_{\frac{1}{3}}}{2}\right]^2 \exp\left(-\frac{691}{T^4\omega^4}\right) \quad m^2s \qquad (3)$$

A transfer function representation of the Bretschneider spectrum may be generated by (4) with white noise as the input.

$$D(s) = \frac{k_d\omega_d^2}{s^2 + 2z_d\omega_d s + \omega_d^2} \qquad (4)$$

Here ω_d represents the encounter frequency, z_d the damping ration and k_d a gain factor to account for the wave height. All these parameters were empirically chosen to closely relate to data furnished by DRA Haslar.

Fin and Rudder Actuators

The fin and rudder actuator hydraulics have associated with them two non-linearities as shown by figure 3. These limitations are the maximum excursion angles and rate limits. The rudder angle being ±30°, slew at $\pm 6°s^{-1}$ and the fin angle ±30° and slew at $\pm 29°s^{-1}$. These are incorporated in simulation the studies.

To be effective as roll stabilisers the actuators' bandwidths must extend beyond the roll resonance frequency of the ship. From [9] it is known that the bandwidth of a servo-mechanism is dependent upon the RMS level of the demand signal. Therefore, this should be monitored in simulations.

Furthermore, from these considerations it is apparent that the rudder efficacy in roll stabilisation will not be as great as the fins and hence act in a secondary role. This adheres to the Royal Navy objectives of harnessing the existing rudder capability by retro fit of controllers rather than embarking upon expensive refits.

3. Control Arrangement

Figure 4 shows the feedback arrangement of the stabilisation system. A similar scheme described by Grimble in [10] would suggest that there is cross coupling between rudder and fin actions. However, provided that the minimum aim is attained, viz. roll is not amplified, it may be assumed that such cross coupling does not exist. Furthermore, in [10] the addition of a fin moment with a rudder induced roll angle is spurious.

The manner in which the solution is sought is suggested naturally by figure 4 ie the two loops are treated independently, thereby greatly simplifying the problem.

4. μ SYNTHESIS

The method adopted to synthesis the controllers for the fin/rudder loops is via μ synthesis. This is essentially an iterative procedure for design of an H∞ controller, if one exists, such that the closed loop system adheres to a specified stability and robust performance criteria [11,12]. The theory is briefly outlined here.

Let

$$T = GK(I+GK)^{-1} \qquad (5)$$

$$S = (I+GK)^{-1} \qquad (6)$$

$$C = K(I+KG)^{-1} \qquad (7)$$

Here K, denotes the controller, G the open loop plant, T complimentary sensitivity function, S the output sensitivity function, and C the control sensitivity.

Consider figure 5 where u are the control signals, v represent disturbance and noise inputs, y physical quantities, e error signals, and x and z are uncertainty input/outputs. P is the nominal plant and Δ, block diagonal uncertainty representation.

P may be partitioned as shown below :

$$P = \begin{bmatrix} P_{11} & P_{12} \\ P_{21} & P_{22} \end{bmatrix} \tag{8}$$

Then let M denote the closed loop function mapping v to e, which is known as a lower linear fractional transformation (9).

$$M = P_{11} + P_{12}K(I - P_{22}K)^{-1}P_{21} = F_l(P,K) \tag{9}$$

The H∞ optimisation problem is then to minimise (9) over all stabilising and realisable controllers. The constraints being defined, dependent upon the engineering and performance ramifications, can be represented by weightings.

The sensitivity weighting is constructed such that the resulting controller minimises sea disturbance and satisfies the norm (10)

$$\|\gamma W_p S\|_\infty \le 1 \tag{10}$$

Robust stability is guaranteed, to multiplicative perturbations, Δ by the complimentary sensitivity function and weighting, W_Δ if the norm (11) is adhered.

$$\|\gamma W_\Delta T\|_\infty < 1 \tag{11}$$

In order to restrain the actuators from encroaching into their non-linear regions, a similar inequality constraint imposed with a weighting, W_c, will accomplish this objective (12).

$$\|\gamma W_c C\|_\infty \le 1 \tag{12}$$

The augmented plant may be written as (13) whose parameters corresponds with (8). Where γ is a scalar search variable.

$$G_{AUG} = \begin{bmatrix} \begin{pmatrix} \gamma W_p \\ 0 \end{pmatrix} & \begin{pmatrix} -\gamma W_p G \\ \gamma W_c \end{pmatrix} \\ \begin{pmatrix} 0 \\ I \end{pmatrix} & \begin{pmatrix} \gamma W_\Delta G \\ -G \end{pmatrix} \end{bmatrix} \tag{13}$$

In μ analysis the robust margins are calculated such that they reflect both structured and unstructured perturbations which are configured in Δ. This information excludes any perturbations which are physically impossible thus yielding less conservative safety margins, than for example the rather arbitrary 'gain margin' quoted in classical control design. As a trade-off the robust margin accrued through Δ may be transferred to the performance of the system. μ analysis may also be used to assess the degradation of disturbance rejection in the face of perturbations Δ.

Consider figure 5 if the controller, K, is absorbed into the plant, P, then the following may be stated (14)

$$\begin{bmatrix} e \\ x \end{bmatrix} = Q \begin{bmatrix} v \\ z \end{bmatrix} = \begin{bmatrix} Q_{11} & Q_{12} \\ Q_{21} & Q_{22} \end{bmatrix} \begin{bmatrix} v \\ z \end{bmatrix} \tag{14}$$

It is apparent [11] that Q_{11} is associated with internal stability to perturbations. Therefore to guarantee robust stability it is sufficient, provided, $\|\Delta\|_\infty < 1$, to ensure that (15).

$$\|Q_{11}\|_\infty < 1 \tag{15}$$

However, a stable permissable block diagonal perturbation, Δ, destabilises the plant if

$$\det[I - Q_{11}(j\omega)\Delta(j\omega)] = 0 \tag{16}$$

Therefore, it is possible to define μ (17),[12], σ being the singular value.

$$\mu(Q_{11}(j\omega)) = \frac{1}{\min(\bar{\sigma}(\Delta(j\omega)), \det(I - Q_{11}(j\omega)\Delta(j\omega)) = 0)} \tag{17}$$

Let

$$\underline{U} = diag(U_1, U_2, \ldots, U_n) \; ; \quad U_i \times U_i = I \tag{18}$$

and

$$\underline{D} = diag(D_1, \ldots D_n, d_1 I, \ldots d_n I) \; ; \; D_i \in C^{r_i \times r_i} \; ; \; d_i \in R \tag{19}$$

such that the sets match the structure of Δ. Then the bounds, where ρ, is the spectral radius, may be shown (20).

$$\rho(UQ) \le \mu(Q) \le \bar{\sigma}(DQD^{-1}) \tag{20}$$

The approach to calculate μ is to find D which minimises $\bar{\sigma}(DQD^{-1})$ and is convex in D.

For robust performance in the presence of structured perturbations, Δ, from (14) and figure 5, the controller absorbed into P, the condition is (21). This is the upper linear fractional transformation, $F_u(Q,\Delta)$.

$$\|Q_{22} + Q_{21}\Delta(I - Q_{11}\Delta)^{-1}Q_{12}\|_\infty < 1 \tag{21}$$

H∞ and μ analysis may be used in following manner :

- Perform H∞ optimisation to yield controller, K
- Perform μ analysis on closed loop system with K, to obtain optimum D-scale matrices.
- Incorporate D scales into structure and resynthesis H∞ controller.

In this manner a controller, if one exists, is generated which adheres to specified robust stability and performance criteria.

5. Selection of Weightings

Sensitivity Weighting.
The sensitivity is a measure of the systems ability to reject sea

disturbances. Efficacious performance from the H∞ controller will depend on judicious construction of this weight. Grimble, [20], gives guidance to these ends. However, a few modifications are made.

The sensitivity weight implemented (23) is such that it encompass the likely region where sea disturbances will occur - a v-shape notch filter. The gain magnitude is made relatively large here but constant at higher frequencies. This has the effect of reducing controller overshoot.

$$W_p(s) = \frac{0.0664s^2 + 8s + 0.016}{4s^2 + s + 1} \qquad (23)$$

Complimentary Sensitivity Weight.
This encapsulates uncertainty contained in the transfer functions. Around roll resonance confidence is greatest, outwith this region uncertainty exists in such places as frequency dependent hydrodynamic coefficients, actuator non-linearities, and speed dependent gains. This renders the closed loop system susceptible to instability. Therefore the weight is constructed in (24) to reflect this.

$$W_\Delta = \frac{4s^2 + 4s + 1}{0.04s^2 + 40s + 0.01} \qquad (24)$$

Control Sensitivity Weight.
As mentioned, these depict restrictions in actuator demand signals in the H∞ synthesis. Since the rudder has much greater engineering constraints, it is given a relatively larger weight, W_{cr}, than the fin control weight W_{cf} (25).

$$W_{cr} = \frac{3.33s^2 + 3.7s + 1}{3.33s^2 + 5000s + 1} \qquad W_{cf} = \frac{12.5s^2 + 20.6s + 1}{12.5s^2 + 500s + 1} \qquad (25)$$

6. Results

The Controllers.
The γ values achieved for the rudder and fin loops are 0.63 and 0.59 respectively. Frequency plots of the controllers are shown in figure 6. On examination the magnitude of $K_r(s)$ appears alarmingly large. However, the peak occurs well away from the region where most control action is applied, i.e. the roll resonance peak, and is of little significance as demonstrated in the sensitivity plot of figure 7. The peak occurring at the corresponding 100 rads^{-1} as in figure 6.

A possible explanation for this large peak in the fin is by making an analogy with classical controllers. Here the desired phase advance can be applied only at one location; the resonance peak. It appears that the H∞ controller attempts to impart phase advance over a much broader frequency region. This is achieved by zeros in the controller resulting in the gain slope over the frequency of stabilisation.

To an extent the rudder controller behaves in the same manner but has lower magnitude. Achieved by the cost weighting and the fact that the less phase advance is required due to the non-minimum phase nature of g12(s).

Time Simulations.
These are performed with the non-linearities incorporated. The disturbance signals represent sea states 3,5, and 8 which have significant wave heights of 0.88m, 3.25m, and 11.5m and modal periods of 5.79s, 9.7s and 18s respectively. As expected, from figure 8, the stabilisation achieved is significant. At best between 70 and 90 percent. With degradation occurring off-beam seas where the stabilisation accrues is in the range of 55 to 70 percent.

Assessing the RMS values of the control signals driving the fin/rudder actuators is more significant than the actual movement since it gives an indication of saturation, detrimental to actuator banwidths. The RMS values appear to be satisfactory, figures 9 and 10, although acceptable levels of saturation are inevitable.

7. μ Analysis

Using the numerical algorithms encoded into Matlab® software the μ analysis is performed.

Robustness.
Figure 11 shows the nominal stability to the weighting function W_Δ which is essentially a singular value plot of condition (15). It is seen that, from the small gain theorem, that the system is robust to this specification (24).

It is known that the k_{t1}, k_{t2}, and the damping ratio vary with the ship speed. Justifiably it is assumed that the ship resonance frequency is constant. This uncertainty is implemented as the structured perturbations in Δ. Using the condition from (16), it is apparent from figure 12 that the μ calculation gives a values of 4.09 and 1.05. Implying that robust stability is preserved provided that $\|\Delta\|_\infty < .25$ and $< .95$ for the rudder and fin loops. Therefore, parameters must be reduced by these percentages to adhere to robust stability.

Performance. The nominal performance to the specified weights is given by the $\max(\sigma(Q_{22}))$. These are shown in figure 13. As anticipated these are achieved with large margins.

An assessment is now made whether the performance will be maintained when the system is subject to the structured perturbations given by Δ above. The μ calculation evaluates the condition (21) at each frequency point. The results are displayed in graph 14. There exists a perturbation such that $\|F_u(Q,\Delta)\|_\infty > 4.33$ and > 1.64 for the rudder and fin loops respectively. Therefore, it is manifest that robust performance will be accomplished given that $\Delta < 0.23$ and $\Delta < 0.61$ for the rudder and fin loops.

8. Conclusions

Employing the rudder and fins actuators in harmony is a feasible solution to roll stabilisation. The performance and robustness levels may defined by the weighting functions. Optimising the H∞ norm in a minimal sense guarantees that the objectives were attained. It was possible to define the likely perturbations such that μ-analysis may be performed to assess whether the system will remain robust in stability and performance.

It is envisaged that by examining the hydrodynamic coefficients and equations of motion for the ship any further sources of

uncertainty may be ascertained. The D-K iteration method may then be used in designing a controller which will be robust to these specifications.

Sea trials are planned aboard a frigate size warship in the near future to expose the controllers to the harsh realities of the real world.

9. Refrences

[1] Lloyd,A.R.J.M., "Hydrodynamic Performance of Roll Stabiliser Fins" 3rd Ship Control Systems Symp. vol. C 1972

[2] Rawson, Tupper "Basic Ship Theory" Longman 1984

[3] Cowler,W.E., "The Use of Rudder as Roll Stabiliser" 3rd Ship Control Systems Symp. vol C 1972

[4] Amerongen,J.van,"RRS:Controller Design and Experimental Results" 8th Ship Control Systems Symp. 1987 pp1.128-1.142

[5] Marshfield,B,"HMS **** Roll Stabilisation Trials" AMTE(H) #R81012 (Restricted)

[6] Yoji,H,"Prediction of Ship Roll Damping" Univ. of Michigan C, of NA & ME Sept. 1981

[7] Roberts,G.N.,"Ship Motion Control Using a Multivariable Approach" PhD Thesis, Univ. of Wales 1989

[8] Whalley,R.,Westcott,J.H.,"Ship Motion Control",6th Ship Control Systems Symp. 1981 ppH1.1-H1.16

[9] Sharif,M.T.,"Frequency Response of a Rudder Servo Mechanism" RNEC Technical Report RR92028

[10] Grimble,M, et al"H∞ Based Ship Fin/Rudder Roll Stabilisation Design" 10th Ship Control Systems Symp. 1993 pp5.225-5.265

[11]Maceijowski,J.M.,"Multivariable Feedback Design" Addison-Wesley 1989

[12] Doyle,J.C., et al,"Performance and Robustness Analysis for Structured Uncertainty" Proc. IEEE Conf. Decision & Control 1982 pp629-636

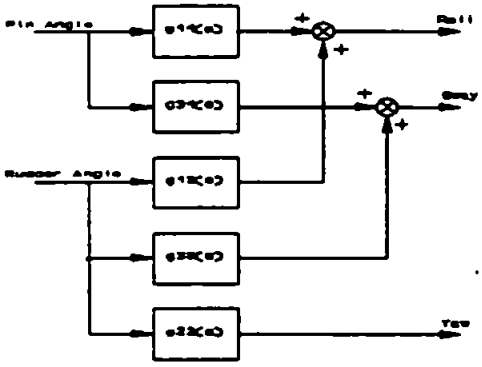

Figure 1 : Multivariable Ship Model

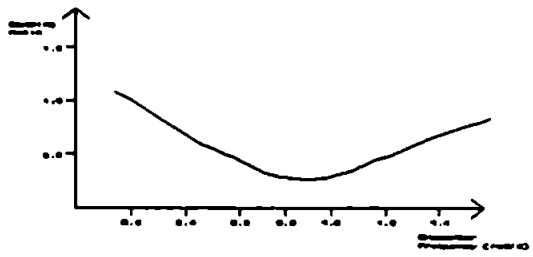

Figure 2 : Variation of Ship Damping Ratio

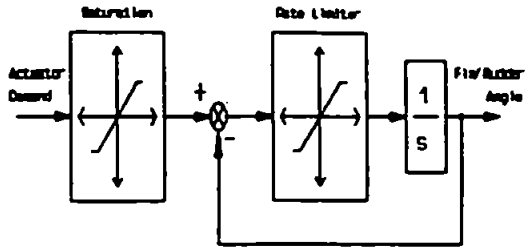

Figure 3 : Servo-Mechanism Models

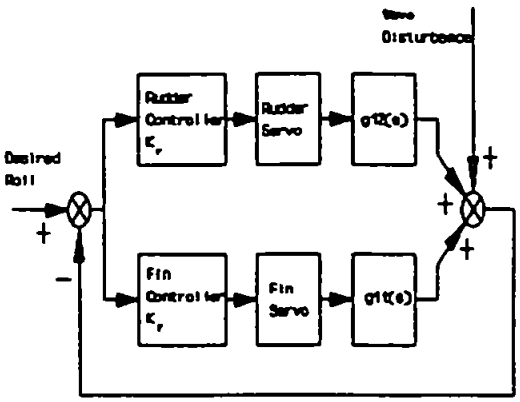

Figure 4 : Roll Stabilisation Arrangement

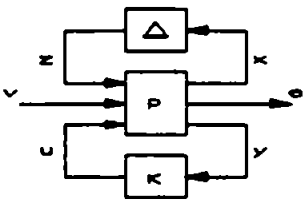

Figure 5 : Perturbation and Controller Feedback Representation

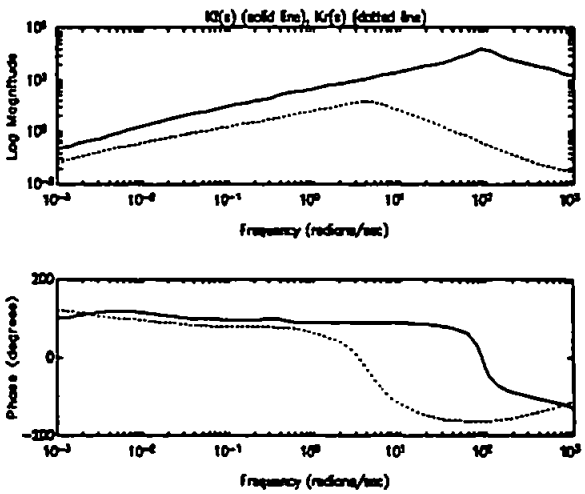

Figure 6 : Frequency Plot of Controllers

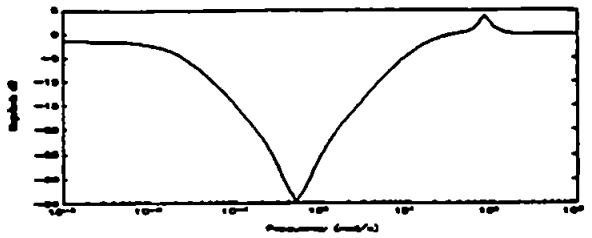

Figure 7 : Fin/Control Sensitivity Function

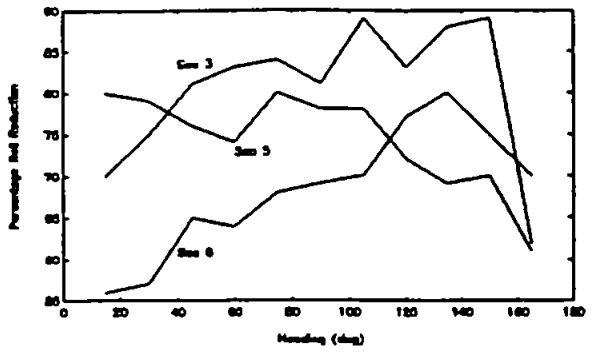

Figure 8 : Fin/Rudder Stabilisation Roll Reduction

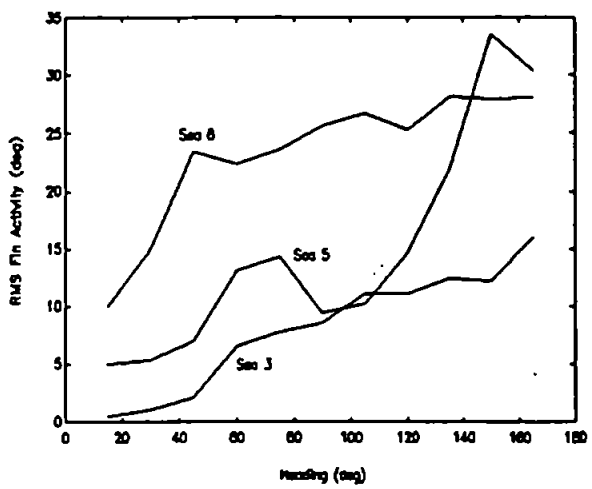

Figure 9 : RMS Fin Activity

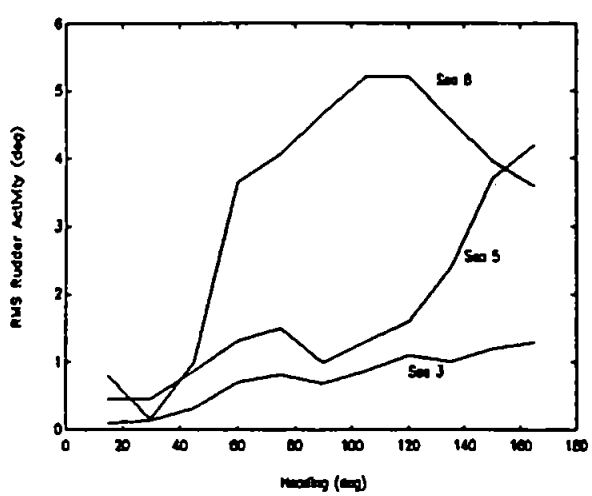

Figure 10 : RMS Rudder Activity

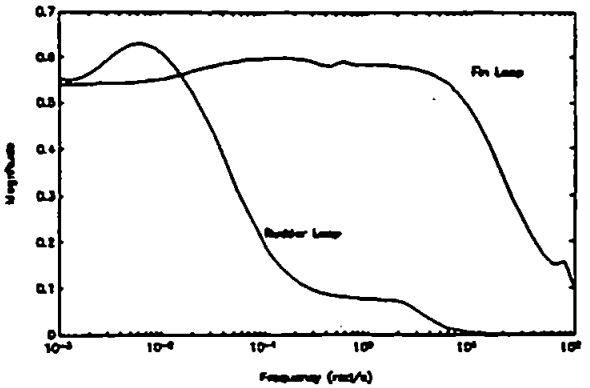

Figure 11 : Nominal Stability

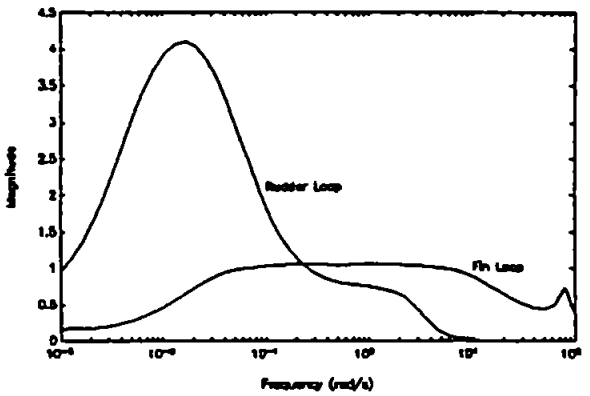

Figure 12 : Robust Stability

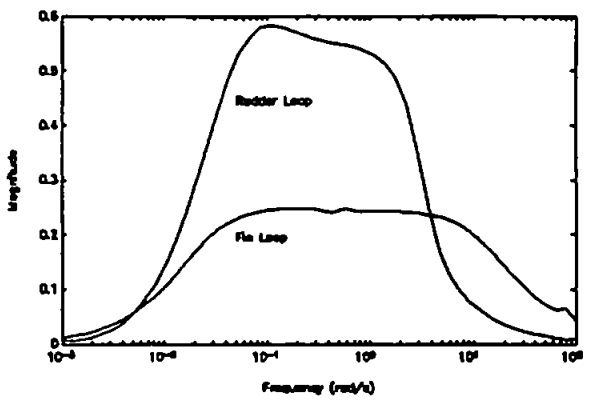

Figure 13 : Nominal Performance

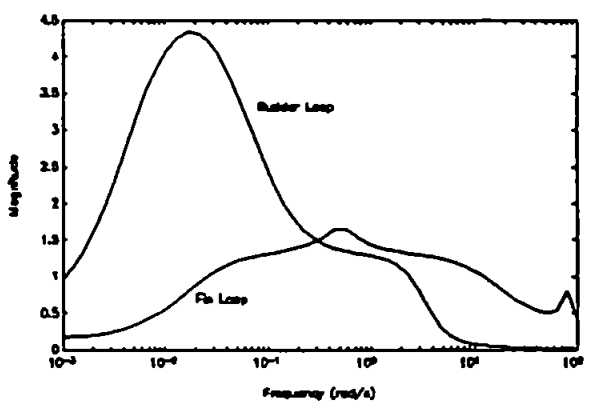

Figure 14 : Robust Performance

Full Scale Experimental Results of Fin/Rudder Roll Stabilisation

M.T. Sharif[1]
G.N. Roberts[2]
R. Sutton[3]

1. Royal Naval Engineering College, Plymouth PL5 3AQ, U.K.
2. Gwent College of Higer Education, Newport NP9 5XR, U.K.
3. University of Plymouth, Plymouth PL4 8AA, U.K.

ABSTRACT

This paper reports the results from full scale roll stabilisation trials on board a frigate size Royal Naval warship. The trials entailed comparing the efficacy of the fins functioning alone with the combined effects of the fins and rudders working in congress to reduce roll motions. The rudders were employed in a supplementary role and no mechanical modifications were made. To afford a comparison of the results the data acquired is presented in the RMS form.

Keywords: Fins, Rudders, Roll Stabilisation, Classical Control

1. INTRODUCTION

The roll stabilisation of ships when subject to the inclemencies of its operating environment has been an active area of research since the advent of large scale shipping. A plethora of devices have been constructed and implemented with varying degrees of success. Perhaps the most propitious device has been the Brown Brother's fin stabilisers. Recognising their advantages in ship operability the Royal Navy as a matter of policy fits such equipment to all its warships of appropriate size.

Recent advances which have demonstrated the feasibility of utilising the rudder in roll stabilisation [1,2] (RRS) has imparted an impetus to the Royal Navy to initiate research effort into this area. Specifically to examine the effectiveness of the rudders in a secondary stabilisation role to the fins.

Using the rudders exclusively in the stabilisation role would have detrimental repercussions on the rudder bearings and the servo-mechanism due to the added motion. However, it is possible to circumvent the necessarily expensive costs of upgrading the bearings and installing more powerful motors if the rudders are utilised as described. Hence, this route of enhanced stabilisation is expedient and most attractive to the Royal Navy.

This paper reports on the first phase of sea trials conducted on board a frigate size warship during March 7-8th 1994. The second section describes the linear mathematical models of the ship system on which depends the control theory to generate adequate controllers. Also the physical constraints are described. The third section deals with the control theory adopted. Prior to going on board considerable technical preparations were made which are elaborated in section four. Penultimately, trials conducted are detailed and results presented. Finally, some conclusions are drawn with suggested recommendations.

2. MODELLING

The synthesis of the controllers for any system requires linear mathematical representation of their associated dynamics. The initial effort is then to acquire such models which accurately embody the physical behaviour of the plant.

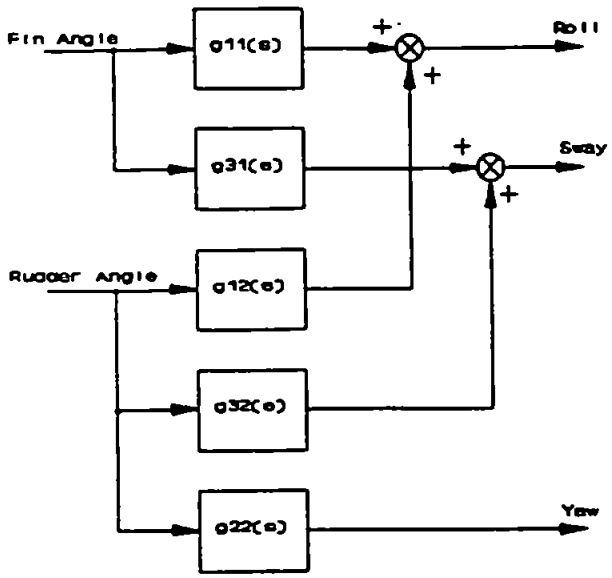

Figure 1 : Multivariable Ship Motion Model

Figure 1 is a multivariable model of the ship system in terms of the fin/rudder induced motions. The transfer functions which relate fin/rudder motion to roll are of interest only (g11(s) and g12(s)). These were derived from sea trials and successively refined over time. To ensure their reliability a comparison was performed with the seakeeping prediction software at Haslar. This software has been developed utilising strip theory and verified with extensive sea trials data. The results afforded a degree of confidence in the models which will be employed in subsequent controller design.

2.1 Stabilising Fins

The fins act as actuators in the control loop: imparting a regulated moment about the ship's axis of roll in opposition to the sea induced roll. Marshfield [3] derives a simple second order transfer function to model this roll (1).

$$g11(s) = \frac{k_{11}0.25}{s^2+2\zeta_s 0.5 s+0.25} \qquad (1)$$

Here k_{11} represents the non-linear relationship between the effectiveness of the fins and ship speed. The damping ratio, ζ_s, is derived empirically. The parameters were subsequently refined by Roberts and Whalley [4,5].

2.2 Rudder Dynamics

In ships of appropriate size a peculiar phenomena is observed, namely that when the ship's rudder is 'put-over' the ship exhibits a proclivity to initially heel inwards. During this heel in the 'wrong' sense no significant yaw motion occurs. Eventually the ship heels outwards and the ship enters a steady state turn. Such behaviour is illustrated by Figure 2. Which shows the roll and yaw motions with the typical time scales involved. This ephemeral roll motion may be explained by hydrodynamic considerations [6].

However, in terms of roll stabilisation it is realised that this characteristic may be harnessed in congress with the fin stabilisers to accrue greater roll stabilisation. Several studies [7,8] have been conducted to establish the applicability of the rudder acting alone in the stabilisation of ships.

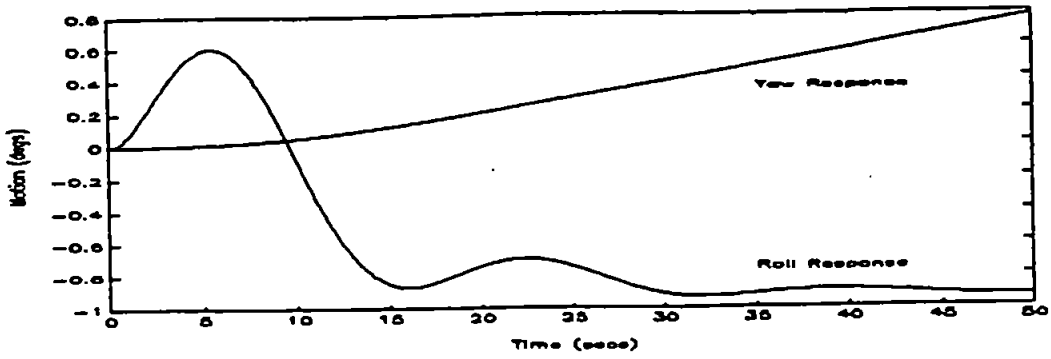

Figure 2 : Rudder Induced Ship Motion

The transfer function is derived in a similar manner as previously (2)

$$g12(s) = \frac{k_{12}0.25\,(1-4.5s)}{(1+8.2s)\,(s^2+0.25s+0.25)} \qquad (2)$$

A non-minimum phase zero is incorporated to impart an initial inward heel to the model when simulated in the time domain. As before k_{12} is a parameter used to represent non-linear behaviour of the rudder with ship speed.

Both models are now accurately represented by the mathematical models particularly at a ship cruising speed of 18 knots. This is then the nominal model exploited for controller design.

2.3 Fin and Rudder Hydraulics

The effectiveness of roll stabilisation is completely dependent upon the servo-mechanism which activates the control surfaces. This is illustrated in Figure 3.

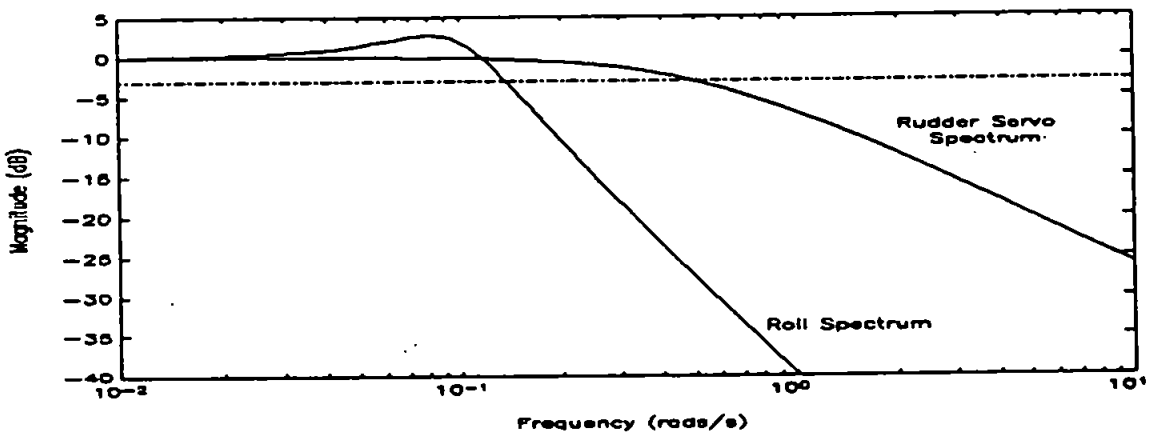

Figure 3 : Typical Roll and Servo-Mechanism Frequency Response

Which shows a typical frequency response of ship roll and servo-mechanism. If the servo-mechanism frequency response encompasses the entire ship roll response then it will actively stabilise at all frequencies of motion. At the very minimum it should extend beyond the ship roll resonance peak, where sea induced roll is amplified.

For both the fin/rudder hydraulics there are associated with their mechanics two non-linearities which

are modelled as shown in Figure 4.

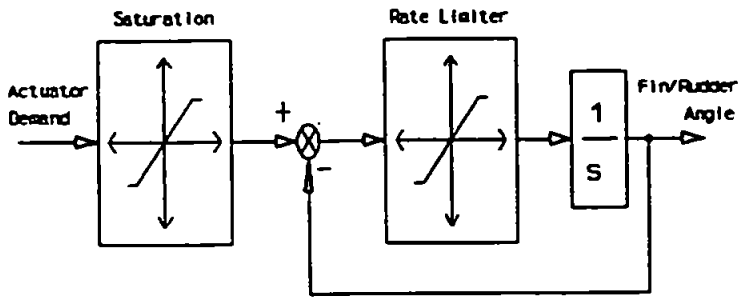

Figure 4 : Non-Linear Servo-Mechanism Model

This first saturation element models the maximum angles of excursion. For adequate stabilisation the slew of the servo-mechanism is of paramount importance. This is non-linear to the extent that their maximum rate is restricted. Which is manifest by the frequency response (Figure 3). This non-linearity is modelled by the saturation element in the feedback loop.

For the fins the maximum angle of excursion is $\mp 30°$, for the rudders $\mp 28°$. Slews of $\mp 30°s^{-1}$ and $\mp 6°s^{-1}$ for fins and rudder are representative of Royal Navy vessels.

Considering the behaviour of the servo-mechanism when they are driven into saturation. This occurs if either the amplitude or frequency of the control signal is sufficiently large. A consequence of this is that the bandwidth of the servo-mechanism reduces further exacerbating the deficiency in slew. It is possible to relate the RMS value of the control signal to the bandwidth of the servo-mechanism. Therefore, a scheme is used which monitors this RMS level and alters the gain of the control signal such that the bandwidth remains above a predetermined value [9].

2.4 Sea Disturbance

Unstabilised roll motions on a ship are caused by the hydrodynamic interaction between the sea and the ship's hull. An adequate model representation of this 'noise' is required in order to ascertain the frequency and magnitude envelope of perturbations the ship is likely to countenance in the environment. This information is used to design a controller which has appropriate sensitivity properties enabling it to reject this interference.

A representation of the sea spectrum may be well encapsulated by the Bretschneider model (3). Where H is the significant wave height and T the wave period.

$$S(\omega) = \frac{691}{T^4 \omega^5}\left[\frac{H_{\frac{1}{3}}}{2}\right]^2 \exp\left[\frac{-691}{T^4 \omega^4}\right] \qquad (3)$$

This gives the spectrum of the sea and may be implemented in software for time simulations by passing white noise through a Laplace domain transfer function which approximates (3), the Bretschneider spectrum.

3 CONTROL STRATEGY

Having established reliable models for the pertinent constituents of the ship system it is possible to

proceed with the control design. As this paper reports the first phase of sea trials the controllers tested were derived from well promulgated control theory namely classical control.

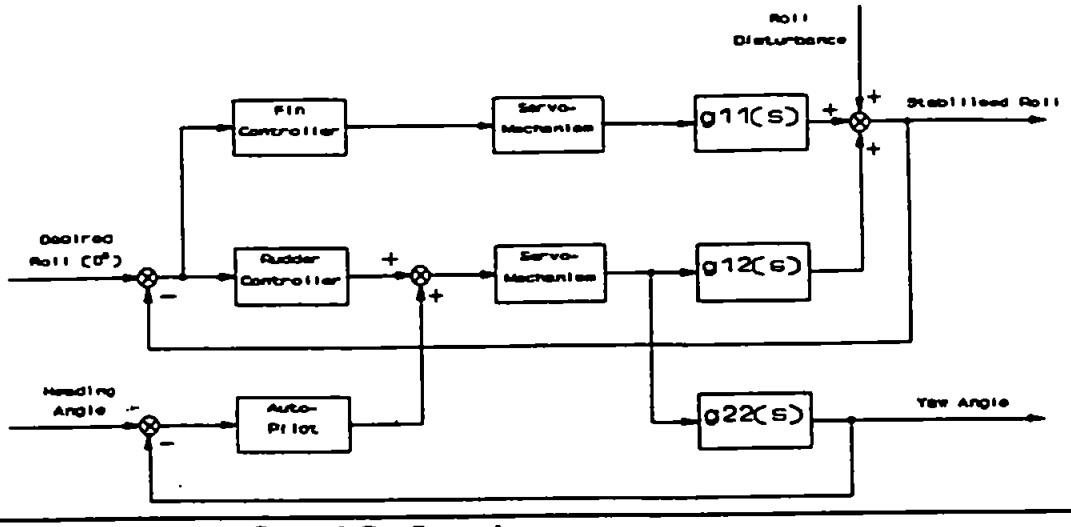

Figure 5 : Fin/Rudder Control Configuration

The configuration of the overall fins and rudder stabilisation loops are shown in Figure 5. Since there is no interference between the rudder and fin loops they maybe treated independently in the controller design. Furthermore, there is sufficient frequency separation between rudder induced roll and yaw motions such that the effect of the rudder in its roll stabilisation role has negligible detriment on yaw motion.

The controller can exactly oppose the disturbance moment with the fin/rudder generated moment only at one frequency due to phase lags introduced by the fin/ship interaction and servo-mechanism. This frequency location is chosen at the roll resonance of the ship. Therefore, the strategy is to ascertain the phase lag introduced by the ship/sea disturbance and servo-mechanism, and arrange the controller to inject phase advance at that point. Hence, the net phase will be zero and complete roll reduction will result at roll resonance.

However, at other frequency locations the roll reduction will be less than complete. Figure 6 illustrates the method of roll reduction. It is a Nyquist locus of the system. Consider the fin loop only, the same analysis follows for the rudder loop, the disturbance rejection transfer function is given by the following (4).

$$\frac{\theta}{D}(s) = \frac{1}{1 + G_{cp}(s)\, g11(s)} \qquad (4)$$

It can be seen from (4), where D is sea disrturbance and θ the roll angle, and Figure 6 that the system will accrue roll reduction provided $|(1 + G_{cp}(s)\, g11(s))|$ is less than unity, effectively at those frequencies where locus lies outside the unit circle, centred at (-1,0). Amplification of roll will occur over the locus when it is inside the unit circle.

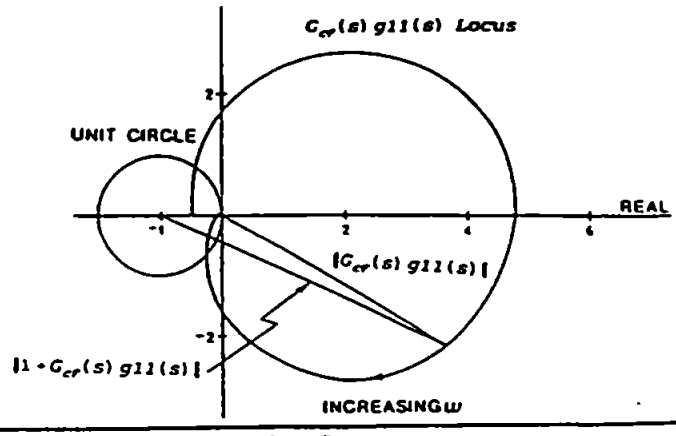

Figure 6 : Nyquist Locus of Ship Stabilisation System

For both fin and rudder the following transfer functions, (5) and (6) respectively, for the controllers will achieve the phase objectives as suggested by Lloyd [10].

$$G_{cF}(s) = \frac{(k_{f1}s^2 + k_{f2}s + k_{f3})\,k_{fg}k_{fs}}{0.003s^3 + 0.043s^2 + .43s + 1} \qquad (5)$$

$$G_{cR} = \frac{(k_{r1}s^2 + k_{r2}s + k_{r3})\,k_{rg}k_{rs}}{0.05s^2 + 0.5s + 1} \qquad (6)$$

The parameters, k_{f1} etc and k_{r1} etc, may be selected by the designer to meet particular objectives in motion stabilisation. The remaining parameters, k_{fs} and k_{rs}, are the ship speed dependent gains to account for non-linear hydrodynamic variations in fin and rudder performance. The parameters k_{fg} and k_{rg} dictate the amount of roll reduction achieved given the constraints in terms of servo-mechanism saturation.

4 SEA TRIALS PREPARATION

In order to record data and control the fin/rudder actuators a considerable amount of preparation was required. Not only in terms of software and controller design but also the hardware implications necessary to interface with the fins and rudders given the nature of the environment.

4.1 Software Development

To implement the controllers they must be converted into a digital representation. Using the bilinear transformation technique a difference equation for the controllers was derived. And subsequently encoded into a software routine in C.

A prerequisite for this method is the consideration of the sampling time and adherence to the Nyquist sampling criteria. The natural roll period of the ship is some 10.5 secs. It was decided that 0.5 sec sampling period should not only provide an accurate reconstruction of the signals but also sufficient period for data storage, graphical display, and calculation for the next control output.

4.2 Interface to Ship

It was imperative to interface with the ship's fin/rudders with the minimal of disruption to ship operations and machinery. A schematic of the wiring configuration is given at Figure 8.

The computer was set up in the workshop. Normally the fins are controlled by the ship's Central Control Unit (CCU) located in the Ship Control Centre (SCC). The CCU provides demand signals to the servo-mechanisms situated in the Gas Turbine Room (GTR) and test outputs for the user. It was possible to disconnect this route and replace it with the computer generated signals. The configuration incorporates a safety feature in that it is physically possible to revert to CCU control of the fins should a malfunction occur in the computer.

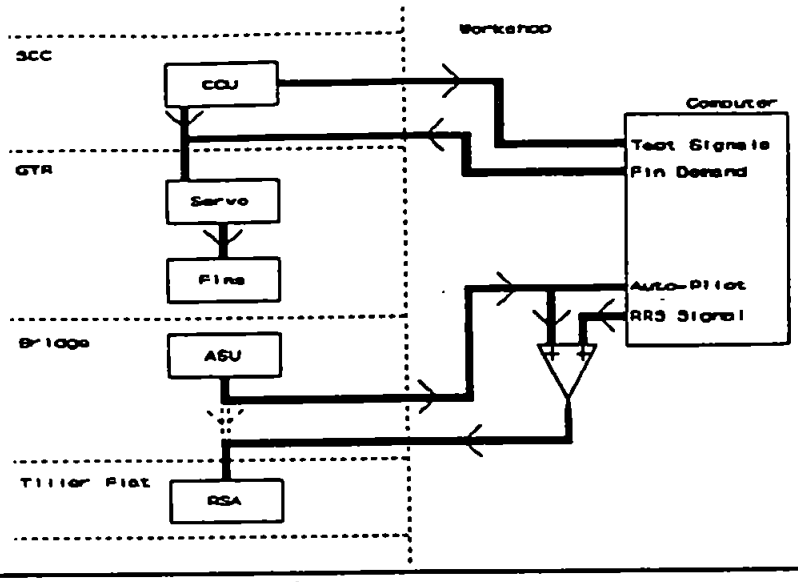

Figure 7 : Interconnections Schematic

The signals required associated with the rudder loops is the heading error and autopilot. The Auto Steering Unit (ASU), which is located at the bridge, furnishes both these signals. The connections between the bridge and the rudder servo-mechanisms, in the tiller flat, was broken and re-routed via the workshop and computer. This necessitated the signals travelling approximately 50 metres one way without the aid of boosters. Fortunately, this did not prove to be a serious impediment to effective signal reception.

The autopilot signal is superimposed on the RRS signal lest interference occurs with the direction of the ship. Therefore, when the RRS was not engaged the autopilot is the default signal to the rudders. In this way both the fins and rudder systems are completely controlled by the computer software.

5 Results

A large number of individual trials were conducted with various controllers and fin/rudder modes of operation. The fins and rudders were engaged with three different sequences and repeated several time with an assortment of controllers. Each sequence was for a duration of 400 seconds. The data was subsequently analysed and presented in terms of RMS values.

For the entire duration of the trials the sea remained at around state two. Unfortunately, such calm weather is not expedient for roll stabilisation trials. Typical roll motions which were experienced are shown in Figure 9.

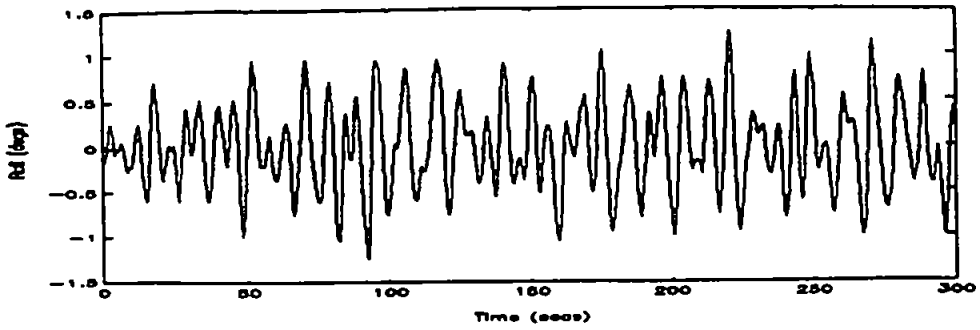

Figure 8 : Typical Roll Motions Experienced

Sequence 1 involved having the ship stabilised by fins for the first 100 seconds using the CCU generated signal. After 100 seconds the RRS was engaged and the fins switched off and set to their neutral position. This would afford a direct comparison of fin stabilisation with RRS.

Table 1 : Results of Sequence 1

Run	Roll RMS (°)		Fin Activity RMS (°)		RRS Activity RMS (°)		Heading Error RMS (°)	
	< 100s	> 100s	< 100s	> 100s	< 100s	> 100s	< 100s	> 100s
1	0.19	0.19	0.94	0	0	2.39	8.21	10.44
2	0.42	0.49	1.46	0	0	5.83	9.81	10.99

Two sets of runs are shown with sequence 1 in Table 1 for two controllers. RMS statistics are collated for various relevant signals before and after 100 seconds. It is seen that when the fins are switched off the roll value does not change significantly for either controller during RRS operation. Also the fins and rudder activity remain within acceptable bounds.

Sequence 2. This sequence will establish that employing the rudders in a supplementary role will accrue enhanced levels of roll reduction. The trial entailed employing the CCU fin stabilisers during the entire 400s test period. After 100s the RRS is engaged. The results are displayed in Table 2 for two typical runs.

Table 2 : Results of Sequence 2

Run	Roll RMS (°)		Fin Activity RMS (°)		RRS Activity RMS (°)		Heading Error RMS (°)	
	< 100s	> 100s	< 100s	> 100s	< 100s	> 100s	< 100s	> 100s
1	0.63	0.46	4.48	1.08	0	3.46	10.04	11.33
2	0.61	0.45	4.17	1.01	0	3.13	10.39	10.88

For both controllers, when the rudders are engaged better stabilisation is achieved approximately 25%. Note also that fin activity correspondingly diminishes as the rudders assist in generating the roll correcting moments.

Sequence 3 entailed controlling both the fins and rudders from the computer. As such the CCU signal

was replaced by the computer signals after 100s. At the same time the rudders were engaged. The resulting values of RMS are shown in Table 3.

Table 3 : Results of Sequence 3

Run	Roll RMS (°)		Fin Activity RMS (°)		RRS Activity RMS (°)		Heading Error RMS (°)	
	< 100s	> 100s	< 100s	> 100s	< 100s	> 100s	< 100s	> 100s
1	0.57	0.57	1.28	0.85	0	3.41	9.94	11.01
2	0.58	0.54	1.30	0.77	0	2.99	10.83	11.14

When the computer controls the fins and rudders the roll RMS exhibits a marginal improvement. As expected from previous results the fin activity decreases due to RRS being operational.

6 Conclusions and Discussion

As mentioned earlier the sea state remained very low. Such comparatively small amplitudes of motion will not greatly exert the controllers. Therefore, their full effectiveness cannot be appreciated. Furthermore, due to ship operations the speed remained at 12 knots. Limiting the moment generating capabilities of the actuators.

Despite these unsuitable environmental conditions valuable conclusions can be derived from the data gathered. Sequence 1 manifests the similar effectiveness of the rudders with fins in roll stabilisation at low sea states. The trials vindicated the most important objective that employing the rudders in a supplementary role with the fins enhances roll stabilisation. As can be demonstrated by the results from Sequence 2. Furthermore, the results compare favourably with the time simulation data generated at the design stage. Affording considerable confidence in the mathematical models for future control design. Finally, the experience tested the reliability and versatility of all aspects of the software and hardware which was developed.

In conclusion, the sea trials gave encouraging results in utilising the rudders in a supplementary role to the fins, without any modifications to the machinery. It is envisaged that at higher sea states the saturation prevention mechanism will realise its potential. The next phase of trials will examine other controllers which were arrived at via different control theory and the results will be presented.

7 REFERENCES

[1] Cowley, W.E. 1972 "The Use of Rudder as Roll Stabiliser" 3rd Ship Control Sys. Symp. vol.C

[2] Amerongen, J. van 1987 "RRS : Controller Design and Experimental Results" 8th Ship Control Sys. Symp. pp1.128-1.142

[3] Marshfield, B. 1981 "HMS **** Roll Stabilisation Trials" AMTE(H) R81012 (Restricted)

[4] Roberts, G.N. 1989 "Ship Motion Control Using a Multivariable Approach" PhD Thesis Uni. of Wales

[5] Whalley R.,Westcott J.H., 1981 "Ship Motion Control" 6th Ship Sys. Symp. ppH1.1-H1.16

[6] Rawson, Tupper 1984 "Basic Ship Theory" Longman

[7] Amerongen J. van. 1982 "Rudder Roll Stabilisation" 4th Intl. Symp. on Ship Operation and Automation pp43-50

[8] Katebi M.R. et al 1978 "LQG Autopilot and RRS Control Systems Design" 8th Ship Control Sys. Symp. pp3.69-3.84

[9] Sharif M.T., Roberts G.N. 1993 "Investigation of Bandwidth Dependency on RMS Values in Servo-Mechanisms" Internal Report, RNEC

[10] Lloyd A.R.J.M. 1974 "Roll stabiliser Fins : A Design Procedure" RINA pp233-254

FINAL EXPERIMENTAL RESULTS OF FULL SCALE FIN/RUDDER ROLL STABILISATION SEA TRIALS

M.T. Sharif*, G.N. Roberts**, R. Sutton***

* *Royal Naval Engineering College Manadon, Plymouth, PL5 3AQ, U.K.*
** *Gwent College of Higher Education, Newport, NP9 5XR, U.K.*
*** *University of Plymouth, Plymouth, PL4 8AA, U.K.*

Abstract. The consequences of roll motions in ship operations can seriously degrade the performance of mechanical and personnel effectiveness. In order to alleviate roll motions many ships are equipped with fin stabilisers. Rudders can also generate roll motions which can be harnessed to function in congress with the fins to accrue enhanced levels of stabilisation. However, in existing ships their contribution to roll stabilisation, without extensive modification to the rudder assembly and power plant, has never been fully realised on account of their limited slew rates. This paper reports on the final phase of full-scale sea trials conducted utilising the existing rudders and fins on board a frigate size warship where various control strategies were employed.

Key Words. Fin/Rudders, Roll Stabilisation, Robust Control

1. INTRODUCTION

The pernicious consequences of roll motions have a profound effective on all types of ships. Many devices have been invented and implemented to ameliorate the roll motion. However, few devices have perhaps had the same impact on roll stabilisation as the active fin stabilisation system (Lloyd, 1972). Around the 1950's the Royal Navy formally adopted the resolution to equip all new vessels with these devices as a matter of course. With the advent of the helicopter bearing warships and development of sophisticated weapons systems and radars the decision was judicious.

It has been observed in ships, of appropriate size, that when the rudder is 'put-over' the ship initially heels inwards before attaining the steady state outward heel angle as it enters the turn (Rawson and Tupper, 1984). Furthermore, this initial roll angle occurs before the ship enters into any yaw motion. Suggesting that the characteristic ephemeral rudder induced roll may be used in congress with the fins to enhance roll stabilisation without significant interference to the heading angles, Rudder Roll Stabilisation (RRS). This potential has been recognised and studies conducted to assess its feasibility (Cowley, 1972).

To date, generally, the implementation of the RRS strategy has been to render the fin stabilisers obsolete, (Amerongen *et al*, 1987 and Kallstrom and Schultz, 1990). Since the rudders' slew rate is invariably insufficient, the practice, (Klugt, 1990), is to upgrade the rudder assemblies and associated peripherals. The corollary envisaged, is not that this will accrue greater levels of roll stabilisation than the fins alone, but to eliminate the self generated noise produced by the fins which is detrimental to effective sonar operations, and realise the expected cost benefits.

For existing frigates the fins must be retained and to utilise the rudders, without any mechanical modifications. This has provoked the Royal Navy to actively pursue a 'something-for-nothing' technique to utilise both control surfaces despite the limited capability of the rudders in the RRS mode. It affords the advantage that the necessary expenses incurred in improving the rudder servomechanism and assemblies can be avoided. Therefore, there will be three modes of operation; fins alone, limited stabilisation with rudders alone, and both fins and rudders. In the latter mode, since some stabilisation would be performed by the rudders it will reduce fin activity and hence sonar noise,

and enhance the roll amelioration than is possible with either actuating controller engaged alone

The aims of the project and this phase of the series of sea-trials are summarised;

- To ascertain the feasibility of utilising the rudders in congress with the fins.
- Assessment of increase in roll stabilisation with both fins and rudders engaged in stabilisation mode.
- Examine the levels of roll stabilisation with fins and rudders engaged individually, with existing controllers and latest robust design techniques.
- Assessment of existing fin controllers and RRS augmented autopilot, with the latest control technology.

The remainder of this paper is organised as follows: the second section describes the linear mathematical models of ship system and control strategy. Section 3 is a concise overview of the control theory utilised to synthesis the controller and weight selection procedure. Prior to conducting the trials the technical preparations made are briefly outlined. The penultimate section details the trials configurations and the associated results are presented, together with simulation statistics. Finally some inferences are derived with suggested recommendations.

2. SYSTEM MODELLING

The ship system is a complex multivariable system but can be simplified if the equations of motion are derived from first principles, separated into lateral and vertical plane motions and assume that no coupling exists between these two classes (Abkowitz, 1972). However, sway, yaw and roll motions have influence on the motions amongst themselves. Such a complex model, which encompasses detailed knowledge of the hydrodynamic parameters and functions in multi-degree-of-freedom mode would be invaluable for simulation and predictions purposes. However, this is type of representation is usually not amenable to control design and a simplified approach is pursued. Each aspect of the system is now considered.

2.1 Stabilising Fins

The fins act as actuators in the regulation mode; imparting a hydrodynamicaly generated roll moment about the ship's axis of roll, and provided the controller has been designed correctly, it will oppose the sea induced roll. For control purposes the fin induced roll of the ship must be considered as a single degree of freedom.

The following transfer function is derived with the relevant coefficients supplied from sea trials data by (Whalley and Westcott, 1981 and Roberts 1989), and where g11(s) will be placed in the multivariable context, k_{11} is a speed dependent gain term to encapsulate the increasing moment generating capacity of the fins with ship speed, and ζ_s is the damping ratio, ϕ, the roll and α, fin angles.

$$\frac{\phi(s)}{\alpha(s)} = g11(s) = \frac{k_{11}\omega_n^2}{s^2 + 2\zeta_s\omega_n s + \omega_n^2} \qquad (1)$$

The fins will not induce any yaw motions on account of their longitudinal centre of roll moment being located very close to the plane of the centre of gravity (CoG). Marshfield (1981) made some fin-induced sway motion measurements on a frigate size warship. He reports insignificant sway generated by the fins. Of course the extent depends on the dihedral angle of the fins (Lloyd, 1989).

2.2 Rudder Dynamics

The dynamics of the ship are such that the rudders can be utilised for both course-keeping, which has been well promulgated in literature, and roll stabilisation. In its latter role the rudder employs the peculiar characteristic, that when the rudder is first 'put-over' the ship develops a transitory inward heel which appears to be in the wrong sense before attaining the steady-state outward heel. The salient characteristic in this analysis is that minimal yaw motion has occurred. This is indicative of frequency separation between the roll and yaw channels as shown in Figure 1.

Therefore, utilising the rudders for roll stabilisation, will not have a detrimental effect on the yaw of the ship Although Blanke and Christensen (1993) and Broome (1979) suggest that this yaw/roll coupling is significant, real sea trials experience has shown that appropriate filters can be installed as a contingency against this scenario, (Amerongen, *et al* 1987).

The transfer function which replicates this rudder/roll behaviour is derived from full-scale sea trials (2), where k_{12} is analogous to k_{11},

$$\frac{\phi(s)}{\delta(s)} = g12(s) = \frac{k_{12}\omega_n^2(1-4.5s)}{(1+8.2s)(s^2+2\zeta_s\omega_n s+\omega_n^2)} \quad (2)$$

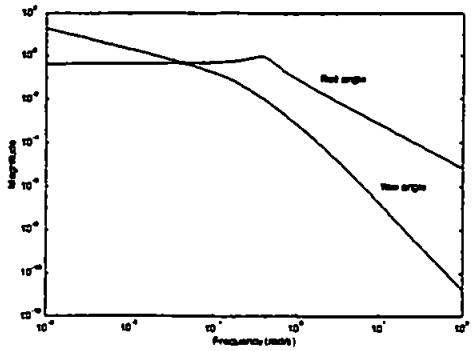

Figure 1 :Typical roll and yaw spectrums

2.3 Servomechanism Modelling

Since the main objective of this project is to utilise the existing rudders, it may be judicious to examine their servomechanisms' capabilities to perform in their new role. Their effectiveness in roll stabilisation is dependent upon the servomechanism which activates the control surfaces. This is illustrated in Figure 2 which shows a typical frequency response of ship roll and rudder servomechanism. If the its frequency spectrum encompasses the ship's entire roll spectrum then it will actively stabilise at all frequencies of motion. At the very minimum it should extend beyond the ship roll resonance peak, where sea induced roll is amplified.

The non-linear model of the servomechanism is presented, and is similar to various other researchers, showing only the slew rate section. For adequate stabilisation the slew rate of the servomechanisms is of paramount importance. It is non-linear to the extent that their maximum rates are restricted. Slew rates of $30°s^{-1}$ and $6°s^{-1}$ for fins and rudders respectively are representative of Royal Navy vessels considered, therefore the fins are considered imminently adequate.

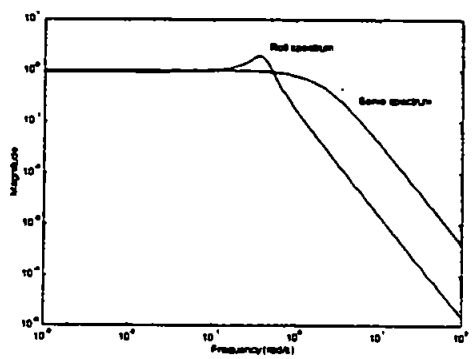

Figure 2 : Typical roll and servo. spectrums

2.4 Sea Disturbances

In the simulations conducted the sea was modelled as recommended by the 10th ITTC, the Bretschneider whose power spectral density is given by (3), where, T significant wave period H significant wave height,

$$S(\omega) = \frac{172.8H^2}{T^4\omega^5}\exp\left(-\frac{691}{T^4\omega^4}\right) \quad (3)$$

A time series of this may be approximated by injecting white noise, $\eta(t)$, through the solution of the differential equation, (4), and adjusting the tuning coefficients β, h and ω_p, in order to match (3).

$$h\omega_p\dot{d}(t) = \ddot{\eta}(t) + \beta\dot{\eta}(t) + \omega_p\eta(t) \quad (4)$$

2.5 Control Configuration

Taking the factors discussed in sections 2.1 and 2.2 into consideration a scheme for the fin/rudder stabilisation loop transpires, as shown in Figure 3.

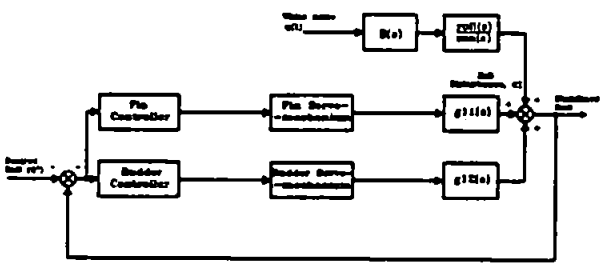

Figure 3 : Control Strategy

This suggests a natural strategy to synthesis the controller, by considering the fin and rudder loops independently. (Grimble *et al*, 1993) favours a MISO approach.

3. CONTROLLER SYNTHESIS

3.1 Classical Control

This type of controller was utilised in the initial series of sea-trials, (Sharif *et al*, 1994) and is reiterated here for information.

Consider the fin loop only, the same analysis follows for the rudder loop, the disturbance rejection transfer function is given by the following (5), where $G_{CF}(s)$ is the fin controller,

$$\frac{\phi(s)}{\alpha(s)} = \frac{1}{1+G_{CF}(s)g11(s)} \quad (5)$$

From (5), and in conjunction with Figure 4, it can be seen that the system will accrue roll reduction provided $|(1+G_{CF}(j\omega)g11(j\omega)| > 1$. Effectively at those frequencies where the locus lies outside the unit circle, centred at (-1,0). Considering the regions where the locus lies inside the unit circle, the converse is true; roll amplification will occur. The locus is arranged such that its constituent frequencies coincide at the region where the sea induced roll disturbance does not exist.

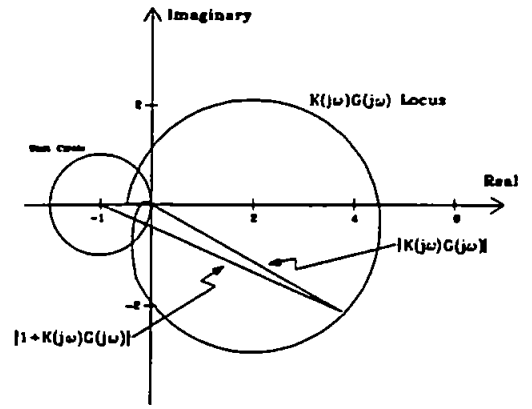

Figure 4 : Nyquist locus of ship roll

For both fins and rudders the following type of controllers, (6) and (7) respectively, will achieve the phase objectives.

$$G_{CF}(s) = \frac{(k_{fa}s^2 + k_{fv}s + k_f)k_{fg}k_{fu}}{0.003s^3 + 0.043s^2 + 0.43s + 1} \quad (6)$$

$$G_{CR} = \frac{(k_{ra}s^2 + k_{rv}s + k_r)k_{rg}}{0.05s^2 + 0.5s + 1} \quad (7)$$

The coefficients of (6) and (7), may be selected by the designer to meet particular objectives in motion stabilisation. The fin parameter, k_{fu}, is the ship speed dependent gain to account for increasing levels of performance of the fins. The parameters k_{ra} and k_{rv} dictate the amount of roll reduction achieved given the constraints in terms of servomechanism saturation and stability margins.

3.2 Optimal Control

Again the performance of the optimal controllers was investigated in Sharif *et al* (1994) and is briefly mentioned. This control strategy relies on optimising a output cost function of the form (8). The control objectives are embodied in the cost function in terms of the state weightings Q and R. Where Q is the relative control weight dictating servomechanism action, and R is the relative importance attached to achieving acceptable levels of stabilisation.

$$J = \int_0^{\infty} uQu^T + yRy^T \, dt \quad (8)$$

Optimal control synthesis requires that the states of the process to be completely accessible. However, if this is not possible, then an estimation of the process is constructed in order to extract the desired information. This is achieved by a Kalman filter which is an optimal estimator to white noise. Since the sea, is a not a white noise process the estimation can be considerably diverge from the true values. Various configurations of the state-space model and relative weightings were used to synthesis the controllers.

3.3 Robust Control

The warship operation environment is varied; the ship speed is never constant, the sea state alters, the encounter frequency changes, a swell may develop, winds may increase, loading conditions change for every voyage, and the mathematical models are inherently uncertain. Classical and optimal type controllers are designed around a specific set of environmental conditions, the performance degrading as these factors change.

Robust control addresses these problems. It guarantees, given actuator limitations, a minimum level of performance and stability for a specified operation envelope; not only in terms of disturbances which impinge on the system but also those due to uncertainties produced by the inadequacies of the linear mathematical representations of the ship system. This method is embodied by the μ-synthesis procedure. Essentially, an iterative process for the design of H_∞ controllers such that the closed loop adheres to the specified performance and stability criteria. The main aim of the sea trials described was to assess the performance of such controllers and their development is discussed in greater detail.

Let T, the complimentary sensitivity, S the sensitivity and C the control sensitivity, be defined as, where G is the plant and K, controller,

$$T = GK(I + GK)^{-1} \quad (9)$$

$$S = (I + GK)^{-1} \quad (10)$$

$$C = K(I + KG)^{-1} \quad (11)$$

Figure 5 depicts the schematic control scheme where u is the control signal, v represents disturbance and noise inputs, y physical quantities, e error signals, and x and z

are uncertainty inputs/outputs. P is the nominal plant and Δ the block diagonal representations of uncertainty; environmental and mathematical.

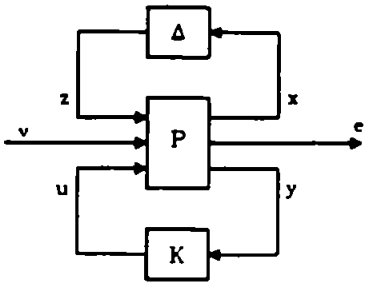

Figure 5 : Controller structure

If P is partitioned as shown in (12)

$$P = \begin{bmatrix} P_{11} & P_{12} \\ P_{21} & P_{22} \end{bmatrix} \tag{12}$$

Then let M denote the closed loop function mapping v to e, this is known as the lower fractional transformation (13).

$$M = P_{11} + P_{12}K(I - P_{22}K)^{-1}P_{21} = F_l(P,K) \tag{13}$$

The H_∞ optimisation problem is then to minimise (13) over all stabilising and realisable controllers. The constraints being defined, dependent upon engineering constraints, by weighting functions (Maceijowski, 1989). Provided that the following H_∞-norm inequalities are satisfied then robust stability and performance are assured, here γ is a search variable the weightings W will be discussed in the next section.

$$\|\gamma W_p S\|_\infty < 1 \tag{14}$$
$$\|\gamma W_\Delta T\|_\infty < 1 \tag{15}$$
$$\|\gamma W_c C\|_\infty < 1 \tag{16}$$

Using the structured singular value, μ, approach, (Doyle, 1982), a less conservative measure of robustness may be calculated. If the controller, K, is absorbed into the plant, P and provided Δ has a block diagonal structure and is normalised then partitioning,

$$\begin{pmatrix} e \\ x \end{pmatrix} = Q \begin{pmatrix} v \\ z \end{pmatrix} = \begin{bmatrix} Q_{11} & Q_{12} \\ Q_{21} & Q_{22} \end{bmatrix} \begin{pmatrix} v \\ z \end{pmatrix} \tag{17}$$

then for robustness the μ is defined as (18) and must remain less than unity.

$$\mu(Q_{11}(j\omega)) = \frac{1}{\min(\bar{\sigma}(\Delta(j\omega)), \det(I - Q_{11}(j\omega)\Delta(j\omega)) = 0)} \tag{18}$$

3.3.1 Selection of the Weights

Sensitivity Weight (W_p): The disturbance rejection transfer function, S, is the measure of a systems ability to reject exogenous environmental disturbances, in this case output, disturbance. The relevant weight, W_p, for inequality (14), should reflect the frequency locations where the desired disturbance attenuation is to occur, a guidance to these ends is given by Grimble (1993).

Considering, that the sea disturbance is given by a Bretschneider sea spectrum (3). This suggests that the weighting W_p, be constructed such that it encompasses the spectrum where environmental disturbances will occur. Therefore, the shape of the W_p will resemble a band-pass filter centred around the predominant frequency of the prevailing sea state, as shown by (19) and (20) for the fin and rudder loops respectively.

$$W_{pf}(s) = \frac{22s}{0.36s^2 + 1.3s + 1} \tag{19}$$

$$W_{pr}(s) = \frac{3.62s}{0.36^2 + 2s + 1} \tag{20}$$

The spectral spread of the filter is such that it will not evoke the servomechanism to respond to high frequency disturbances, crucial to prevent saturation of the rudders. Also, the demanded disturbance attenuation from the rudder is significantly less than the fins, to reflect their comparative capabilities.

Complimentary Sensitivity Weight (W_Δ): This weight encapsulates the uncertainty contained in the mathematical models. It may be stated that the ship dynamics are accurately modelled around the roll resonance frequency. However, at the higher and lower frequency regions uncertainty exists to a larger extent such as; hydrodynamic frequency depend parameters, actuator non-linearities and speed dependent gains. This renders the closed loop system susceptible to instability.

The weight, W_Δ, is constructed to reflect this. It has comparatively less magnitude around the roll resonance but the weight increases as the frequency increases (21).

$$W_\Delta(s) = \frac{120s^2 + 36s + 43}{s^2 + 3s + 0.036} \tag{21}$$

Control Sensitivity Weights (W_c): These weights, more explicitly, depict the restrictions on regions of operation of the servomechanisms. Since, the rudder servomechanisms has greater functional constraints, its weight is proportionally greater than the fins. The weights are shaped as a band stop filter centred around the region of greatest roll. The rudder control weight is

order to avoid frequency saturation. The weights are shown in (22) and (23) for the fins and rudders respectively.

$$W_{cf}(s) = \frac{5s^2 + 50.1s + 1}{5s^2 + 100000s + 1} \qquad (22)$$

$$W_{cr}(s) = \frac{5s^2 + 6.5s + 1}{5s^2 + 1800s + 1} \qquad (23)$$

The Controllers: With the given weights, the software routines within Matlab®, were utilised in order to arrive at the controllers. Figure 6 and 7 shows the various functions lying below their respective weightings and μ, is less than unity indicative of robust stability and performance for both the fin and rudder loops respectively. Figure 8 displays the frequency response of the controllers. It is seen that the fin controller exhibits a great deal more alacrity than the rudders as would be expected.

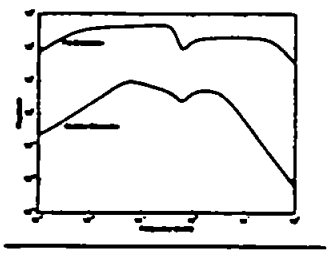

Figure 8 : Frequency response of controllers

4. PREPARATION for the SEA TRIALS

In order to record data and control the fin/rudder actuators a considerable amount of preparation was required. Not only in terms of software and controller design but also the hardware implications necessary to interface with the fins and rudders given the nature of the environment on board a warship. Details of this procedure was given in Sharif *et al* (1994) during the first phase of sea trials. The interface schematic is shown for information only in Figure 9.

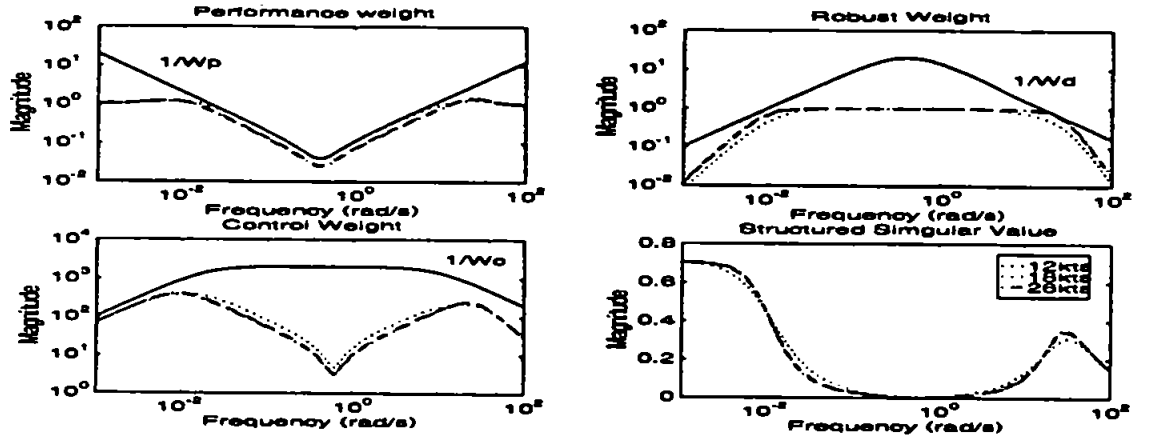

Figure 6 : Fin controller criteria

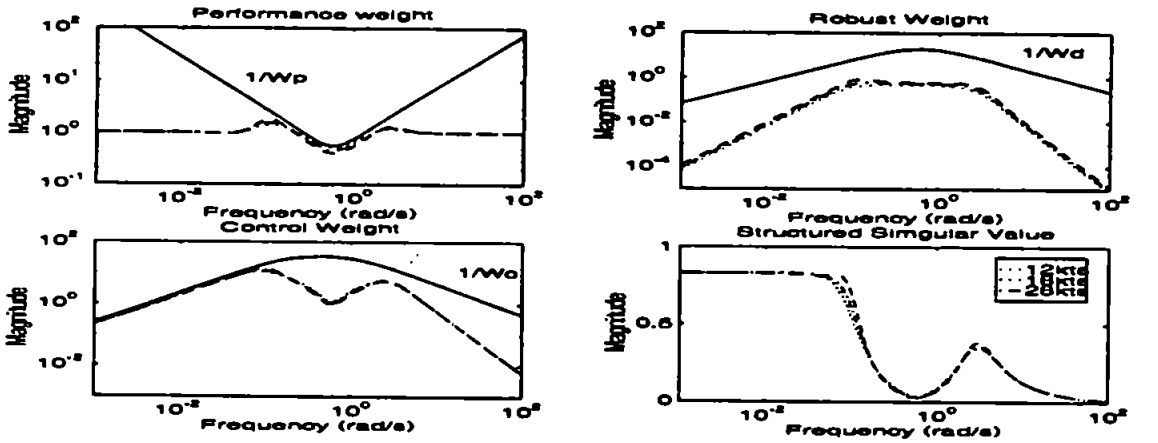

Figure 7 : Rudder controller criteria

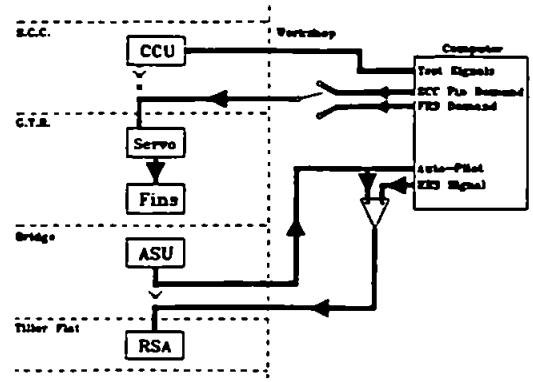

Figure 9 : Interconnections scheme

5. RESULTS

A large number of individual trials were conducted with various controllers and modes of fin/rudder operation. The fins and rudders were engaged with two different sequences; namely rudders alone and fins with rudder stabilisation. Each sequence was for a duration of 420 seconds.

For the entire duration of the trials the sea remained at around state two-three and at predominantly beam seas. Unfortunately, such calm weather is not expedient for roll stabilisation trials and any conclusions derived must be tenuous at best. Typical roll motions which were experienced are shown in Figure 10. The data was subsequently analysed and presented in terms of RMS values and significant heights. It was also decided to conduct a parallel simulations study using the PAT91 sea-keeping software at DRA Haslar.

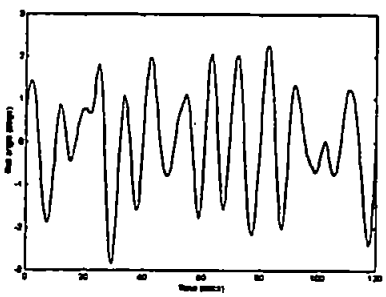

Figure 10 : Typical roll motions experienced

5.1 Rudder Roll Stabilisation

In this sequence of trials the ship was stabilised using the fins for the first 120 seconds. The fins were then switched off and the rudder stabilisation activated. Table 1 shows the typical RMS roll and controller demand values. The last column shows the corresponding values using the PAT91.

Table 1: Results for sequence one

Model	Sea Trials								PAT91	
RMS	Roll RMS		Fin Demand		Rudder Demand		Heading Error		Roll	Rudder
Time (s)	<120	>120	<120	>120	<120	>120	<120	>120	n/a	n/a
Classical	0.7	0.6	8	0	2.9	2.71	0.26	0.18	0.5	3.7
LQG	0.31	0.41	4	0	3.78	4.24	0.28	0.26	0.33	4.1
	1.12	1.61	10.5	0	4.09	6.11	0.27	0.28	1.4	5.8

These are the typical values obtained with each type of controller. The fin controller employed in this case was the one currently fitted on board the ship. Before the RRS is implemented the RMS of the rudder is that of the autopilot and thereafter of the two signals summed.

The PAT91 roll and rudder demand results are with the RRS permanently engaged. They correlate well with the experimental values. The rudder is relatively less effective in terms of its moment generating capability as compared with the fins, subsequently the marginal increase in RMS roll, in all cases, may be indicative of this feature.

5.2 Fin Stabilisation and RRS Active

The primary aim of this project was to ascertain the efficacy of the rudders as secondary stabilisers. To these ends the next sequence of trials were performed with the fins permanently engaged and controlled by the CCU signals. The rudders were activated for stabilisation after 120 seconds.

The results are shown at Table 2 again with the PAT91 predicted RMS values. As expected, since a portion of the stabilisation is performed by the rudders, roll and fin activity both diminish, with the H_∞ controller consistently yielding better results.

Table 2: Results for sequence two

Model	Sea Trials								PAT91	
RRS	Roll RMS		Fin Demand		Rudder Demand		Heading Error		Roll	Rudder
Time (s)	<120	>120	<120	>120	<120	>120	<120	>120	n/a	n/a
Classical	0.59	0.52	7.4	6.3	1.88	2.5	0.44	0.42	0.17	2.59
LQG	0.75	0.45	7.58	5.8	3.3	4.8	0.39	0.35	0.6	4.1
H_∞	1.78	0.48	9.92	5.21	1.47	4.69	0.35	0.35	0.8	4.5

Comparing the trials data with the PAT91 simulations, Table 2 shows the predictions to be accurate given the relatively small magnitudes of motion. The trials' sea states and pertinent conditions were emulated on PAT91 using a conjectured CCU fin controller which replicates

similar levels of stabilisation as demonstrated by the trials data. Again, in the PAT91 simulations, the H_∞ controllers consistently performed well in changing sea conditions as compared with other controllers.

At the outset it was envisaged that the stabilisation of the ship via fins and rudders will be controlled completely from the computer generated demand signals, permitting extensive comparison of various controllers in fin alone stabilisation mode to be performed. Unfortunately, the sea conditions did not permit this.

6. DISCUSSION and CONCLUSIONS

As mentioned earlier the sea state remained very low through-out the trials. Such comparatively small amplitudes of motion did not greatly exert the controllers and therefore, their full effectiveness cannot be appreciated. Furthermore, due to ship operations the speed remained at 12-16 knots, limiting the moment generating capabilities of the actuators.

Despite these unsuitable environmental conditions valuable conclusions can be derived from the trials data acquired. Sequence 1 manifests the similar effectiveness of the rudders with the fins in roll stabilisation at low sea states. The trials vindicated the most important objective, that of employing the rudders in a supplementary role with the fins enhances roll stabilisation, as can be demonstrated by the results from Sequence 2 and Table 2.

The trials results compare favourably with the time simulation data generated at the design stage, affording considerable confidence in the mathematical models for future control design and the numerical integration routines embedded in the simulations software. Comparing the simulations with the real data there is evidence that the robust type controllers yield greater roll amelioration.

The PAT91 sea-keeping program verified the sea trials results and the time simulations. They indicate that the potential for using the rudders in concert with the fins as stabilisers is yet to be realised. Again the robust type controller gives the best performance.

7. REFERENCES

Abkowitz, M.A. (1972) *Stability and Motion Control of Ocean Vehicles.* MIT Press

Amerongen, J. van, P.G.M. van der Klugt, J.B.M. Pieffers, (1987) *Rudder Roll Stabilisation-Controller Design and Experimental Results.* 8th Ship Control Systems Symposium, The Hague, Vol. 2

Blanke, M., A.C. Christensen (1993) *Rudder-Roll Damping Autopilot Robustness to Sway-Yaw-Roll Couplings.* 10th SCSS, Ottawa

Broome, D.R. (1979) *An Integrated Ship Control System for CS Manchester Challenge.* Royal Institute of Naval Architects

Cowley, W.E., (1972) *The Use of Rudder as Roll Stabiliser* 3rd SCSS, Bath

Doyle, J.C. (1982) *Performance and Robustness Analysis for Structured Uncertainty.* Proc IEEE Conf. Decision and Control

Grimble, M.J., M.R. Katebi, Y. Zhang (1993) *H_∞ Based Ship Fin-Rudder Roll Stabilisation Design.* 10th SCSS, Ottawa Vol. 5

Kallstrom, C.G., W.L. Schultz, (1990) *An Integrated Control System for Roll Damping and Course Maintenance.* 9th SCSS, Bethesda, Vol. 3

Klugt, P.G.M. van der, (1990) *ASSA: The RRS Autopilot for Dutch M-Class.* 9th SCSS, Bethesda, Vol. 2

Lloyd, A.R.J.M. (1972) *Hydrodynamic Performance of Roll Stabiliser Fins.* 3rd SCSS, Bath

Lloyd, A.R.J.M. (1989) *Sea-keeping: Ship Behaviour in Rough Weather.* Ellis Horwood

Maceijowski, J.M. (1989) *Multivariable Feedback Design.* Addison-Wesley

Marshfield, W.B. (1981) *HMS ****** Roll Stabiliser Trials* DRA Haslar Report No. AMTE(H), R81012, Restricted

Rawson, K.J., E.C. Tupper, (1984) *Basic Ship Theory.* Longman

Roberts, G.N. (1989) *Ship Motion Control Using a Multivarible Approach.* PhD Thesis, University of Wales

Sharif, M.T., G.N. Roberts, R. Sutton Full-Scale Experimental Results of Fin/Rudder Roll Stabilisation, MCMC'94, Southampton

Whalley, R., J.W. Westcott (1981) *Ship Motion Control.* 6th SCSS, The Hague, Vol. H

8. ACKNOWLEDGEMENTS

The authors wish to express their gratitude to the MoD (ES251) for their continual support and encouragement on this project. The facilities made available and advise given by DRA Haslar, and in particular from Paul Crossland, were greatly appreciated.